UNIVERSIDADE DE LISBOA

INSTITUTO SUPERIOR TÉCNICO

Strategies to improve the drug release performance of hydrogels for therapeutic soft contact lenses

Patrizia Paradiso

Supervisor:	Doctor Ana Paula Valagão Amadeu do Serro
Co-supervisors:	Doctor Benilde de Jesus Vieira Saramago
	Doctor Rogério Anacleto Cordeiro Colaço

Thesis approved in public session to obtain the PhD Degree in Materials Engineering

Jury final classification: Pass with Distinction

Jury

Chairperson: Chairman of the IST Scientific Board

Members of the Committee:

Doctor Anuj Chauhan

Doctor Ana Isabel Henriques Dias Fernandes Pinto

Doctor Benilde de Jesus Vieira Saramago

Doctor Maria de Fátima Reis Vaz

Doctor Ana Paula Valagão Amadeu do Serro

Doctor António Jorge Rebelo Ferreira Guiomar

2015

UNIVERSIDADE DE LISBOA

INSTITUTO SUPERIOR TÉCNICO

Strategies to improve the drug release performance of hydrogels for therapeutic soft contact lenses

Patrizia Paradiso

Supervisor: Doctor Ana Paula Valagão Amadeu do Serro

Co-supervisors: Doctor Benilde de Jesus Vieira Saramago

Doctor Rogério Anacleto Cordeiro Colaço

Thesis approved in public session to obtain the PhD Degree in Materials Engineering

Jury final classification: Pass with Distinction

Jury

Chairperson: Chairman of the IST Scientific Board

Members of the Committee:

Doctor Anuj Chauhan, Professor, University of Florida, USA

Doctor Ana Isabel Henriques Dias Fernandes Pinto, Associate Professor, Instituto Superior de Ciência da Saúde Egas Moniz

Doctor Benilde de Jesus Vieira Saramago, Associate Professor, Instituto Superior Técnico da Universidade de Lisboa

Doctor Maria de Fátima Reis Vaz, Assistant Professor (with habilitation), Instituto Superior Técnico da Universidade de Lisboa

Doctor Ana Paula Valagão Amadeu do Serro, invited Assistant Professor, Instituto Superior Técnico da Universidade de Lisboa

Doctor António Jorge Rebelo Ferreira Guiomar, Assistant Researcher, Faculdade de Ciência e Tecnologia da Universidade de Coimbra

Funding Institutions: Fundação para a Ciência e a Tecnologia

2015

To my mom and dad

ABSTRACT

Ophthalmic drugs are often delivered via eye drops. However, these conventional ocular formulations show low bioavailability and may lead to drug wastage and side effects.

In the last few years soft contact lenses (SCLs) have attracted the researchers' interest as ideal platforms for controlled delivery of numerous drugs to the anterior part of the eye.

The present thesis focuses on the investigation and characterization of the release performance of two drugs, levofloxacin (LVF) and chlorhexidine (CHX), from two types of SCLs in-house materials, HEMA/PVP and TRIS/NVP/HEMA, and from two types of commercial silicone SCLs (ACUVUE® TrueEye and ACUVUE® OASYS).

To increase the drug release duration, different approaches were explored, namely: surface crosslinking, plasma treatment, vitamin E incorporation, liposomes-based coating and the potential of embedding drug loaded nanoparticles into the hydrogels. Furthermore, for some drug release experiments, two different types of hydrodynamic conditions were tested: static sink conditions and flow conditions.

Results show that both in-house hydrogels formulations revealed adequate properties to be used as ophthalmic materials and to release LVF and CHX as daily SCLs. Significant differences were found between experiments in static and hydrodynamic conditions. A simple mathematical model was also used as a first approach to predict the release performance in the human eye.

The most promising systems studied were obtained by vitamin E incorporation. Commercial SCLs demonstrated to be capable to deliver the considered drugs and maintain their concentrations in the tear film within the therapeutic window of several days. In detail, with the presence of 20% in weight of vitamin E, the release times of LVF from ACUVUE® TrueEye™ and from ACUVUE OASYS® exhibit a 3 and 6-fold increase, respectively, reaching 100 hours and 50 hours release, while for CHX the increase is 2.5 and 10-fold, respectively, to 130 hours and 170 hours.

RESUMO

Os fármacos oftálmicos são geralmente administrados na forma de colírios. No entanto, estas formulações convencionais apresentam baixa biodisponibilidade e podem levar a efeitos colaterais.

Nos últimos anos, as lentes de contacto (LdCs) têm atraído o interesse dos investigadores como veículos de libertação controlada de diferentes fármacos para a parte anterior do olho.

A presente tese centra-se na investigação e caracterização do desempenho de libertação de dois fármacos, levofloxacina (LVF) e clorexidina (CHX), a partir de dois tipos de materiais utilizados em LdCs preparados no laboratório, HEMA / PVP e TRIS/NVP/HEMA, e de dois tipos de LdC comerciais à base de silicone (ACUVUE® TrueEye e ACUVUE® Oasys).

Diferentes abordagens foram exploradas para aumentar o tempo de libertação dos fármacos, tais como: *crosslinking* superficial, tratamento com plasma, incorporação de vitamina E, revestimento superficial com lipossomas e incorporação nos hidrogéis de nanopartículas contendo fármaco. Em algumas experiências de libertação de fármaco, dois tipos diferentes de condições hidrodinâmicas foram testadas: condições estáticas e de fluxo.

Os resultados mostram que ambos os materiais produzidos em laboratório são adequados para serem utilizados em LdCs, em particular, em dispositivos diários para veiculação de LVF e CHX. Observaram-se diferenças significativas entre os resultados em condições estáticas e de fluxo. Utilizou-se também um modelo matemático como primeira aproximação para prever o desempenho das LdCs.

Os sistemas estudados mais promissores foram obtidos por incorporação de vitamina E. As LdCs comerciais testadas demonstraram a capacidade de libertar os fármacos, mantendo as respectivas concentrações no fluido lacrimal dentro da janela terapêutica durante vários dias: com a presença de 20% em peso de vitamina E, os tempos de libertação de LVF de Acuvue TrueEye ™ e Acuvue OASYS® aumentam 3 e 6 vezes, respectivamente, atingindo 100 horas e 50 horas, enquanto os tempos de libertação de CHX aumentam 2,5 e 10 vezes, respectivamente, para 130 horas e 170 horas.

KEYWORDS

HYDROGELS
SOFT CONTACT LENSES
DRUG DELIVERY SYSTEMS
LEVOFLOXACIN
CHLORHEXIDINE
MATHEMATICAL MODELLING
MICROFLUIDIC CELL

PALAVRAS CHAVE

HIDROGÉIS
LENTES DE CONTACTO
LIBERTAÇÃO CONTROLADA DE FARMACOS
LEVOFLOXACINA
CLOREXIDINA
MODELAÇÃO MATEMATICA
VITAMINA E

ACKNOWLEDGEMENTS

First and foremost, I would like to express my forever gratitude to my supervisor Professor Ana Paula Serro, and to my co-supervisors Professor Benilde Saramago and Professor Rogerio Colaço. I thank them for all the guidance and support throughout this work and along the past years. They taught me the importance of keeping motivated and efficient on my work, and to respond to fails and to improve, and most important, they contributed significantly to my growth as a researcher and as a person, each of them in a peculiar way.

I would like to thank Fundação para a Ciência e Tecnologia for the fundamental financial support to this Ph.D program with Ref. SFRH/BD/71990/2010 and for the funding through the PEst-OE/QUI/UI0100/2011, the Luso-German Integrated Actions 2012 ref.ª: A-29/12, the M-ERA.NET/0005/2012 and the UID/QUI/00100/2013 projects.

I recognize that this research would not have been possible without some important collaboration. I wish to extend many thanks to Professor José Luis Mata for all the help in the construction of custom equipment and for his daily smile, and to Professor Anabela Fernandes for her kindness. I am grateful to Professor Miguel Rodrigues from IST for his guidance and support during the supercritical fluids enhance atomization experiments, to Professor Virginia Chu from INESC Microsistemas e Nanotecnologias, whose collaboration made the plasma experiments possible and to Professor António Pedro Alves de Matos, from the Curry Cabral Hospital, who performed the microbiological assays against *A. castelanii*. I thank Professor Luis Santos from IST, who performed the raman spectroscopy and ellipsometry measurements, and was always helpful and kind to me. Special thanks goes to Professor Anuj Chauhan, from the Chemical Engineer Department at the University of Florida for welcoming me in his friendly group and for providing me with direction, technical support and to have represented a mentor to me during the months spent at UF. I would like to express my sincere thanks to Professor Ana Isabel Fernandes from Instituto Superior de Ciências da Saúde Egas Moniz, for her critical comments and suggestions during this thesis work. I also thank Professor Rumen Krastev and Simona Margutti, from the Biomaterial team at Natural and Medical Sciences Institute (NMI) at the University of Tübingen, Professor Antonio Maçanita from IST and Professor Maria Guilhermina Moutinho from Instituto

Superior de Ciências da Saúde Egas Moniz for their collaboration and for having allowed me to have access to their lab and facilities.

I would like to acknowledge all my lab colleagues, especially Raquel, Bruno, Andreia and José for their help, good mood and companionship.

I am truly grateful to Filipe and to all my friends, too many to enumerate, not only to the ones in Lisbon, who represent my family here, but also to the others scattered around the world. I am grateful for you being next to me always.

Last, but not least, I would like to dedicate this thesis to my family. Words cannot describe my everlasting gratefulness to my parents; they represent my source of strength and my example of integrity. They taught me to stay positive since, whatever it happens, life goes on.

Index

LIST OF FIGURES

LIST OF TABLES

LIST OF ABBREVIATIONS

1VI	1-vinylimidazonle
4VI	4-vinylimidazole
AA	Acrylic acid
AIBN	2,2′-azobis(2-methylpropionitrile)
AM	Acrylamide
APMA	N-(3-aminopropyl) methacrylamide
AFM	Atomic force microscopy
AMA	Alkyl methacrylate
BMA	Butyl methacrylate
CAC	Benzyldimenthylhexadecylammonium chloride
CAN-BD	Carbon dioxide assisted nebulization
CD	Cyclodextrin
CF	Carboxyfluorescein
CHOL	Cholesterol
CHX	Chlorhexidine diacetate
CMA	Cyclohexyl methacrylate
CyA	Cyanuric acid
DMPC	1,2-Dimyristoyl-sn-glycero-3-phosphocholine
EGDMA	Ethylene glycol dimethacrylate
EVA	Poly(ethylene-co-vinyl acetate)
DAA	Diacetone, acrylamide
DD	Distilled and deionized

DEAA	N, N-diethylacrylamide
DEAM	2-(diethylamino) ethyl methacrylate
DLS	Dynamic light scattering
DMA	*n*,*n*-dimethyl acrylamide
DMMA	*n*,*n*-dimethylacrylamide
DMPC	Dimyristoylphosphatidylcholine
DMSA	2,3-dimercaptosuccinic acid
EEMA	Ethoxyethyl methacrylate
EWC	Equilibrium water content
FDA	Food and Drug Administration
FTIR	Fourier transform infrared spectroscopy
GMA	Glyceryl methacrylate
GTA	Glutaraldehyde
GUV	Gigant unilamellar vescicle
HEAA	N-hydroxyethyl acrylamide
HEMA	Hydroxyethyl methacrylate
HEPES	N-(2-hydroxyethyl) piperazine-N′-(2-ethanesulfonic acid)
HP50	Hydroxy propyl methyl cellulose phthalate, grade 50
HPMCP	Hydroxy propyl methyl cellulose phthalate
HPLC	High-performance liquid chromatography
IBM	Isobornyl methacrylate
IST	Instituto Superior Técnico
LVF	Levofloxacin
LUV	Large unilamellar vesicles

MAA	Methacrylic acid
MAPTAC	Methacrylamine propyltrimethylammonium chloride
MIC	Minimal inhibitory concentration
MLV	Multilamellar vescicles
MPDMS	Monofunctional polydimethylsiloxane
MPTS:	(3-mercaptopropyl)trimethoxysilane
MMA	Methyl-methacrylate
MHRA	Medicine and Healthcare Products Regulatory Agency
MOEP	Methacryloyloxyethyl phosphate
NCVE	N-carboxyvinyl ester
NVP	N-vinyl pyrrolidone
PAH	poly(allylamine hydrochloride)
PBVC	Poly(dimethysiloxy) di (silylbutanol) bis (vinyl carbamate)
PCL	Polycaprolactone
PDMS	Polydimethyl siloxane
PEG	Polyethylene glycol
PHEMA	poly(hydroxyethyl methacrylate)
PGT	Propoxylated glyceryl triacrylate
PEI	Polyethylenimine
PGSS	Particles generation from gas saturated solutions
PLGA	Poly(lactic-co-glycolic) acid
PLTF	Pre lens tear film
PMMA	Polymethylmethacrylate
PoLTF	Post lens tear film

PRK	Photorefractive keratectomy
PSS	Poly(sodium 4-styrene-sulfonate)
PVP	Poly- vinyl pyrrolidone
PYG	Peptone Yeast extract Glucose
QCM	Quartz Crystal Microbalance
R18	Octadecyl rhodamine B chloride
RESS	Rapid expansion of supercritical solutions
SAA	Supercritical fluids assisted atomization
SAS	Supercritical antisolvent precipitation
SC	Swelling capacity
SCF	Super critical fluid
SCL	Soft contact lens
SEA	Super critical fluid enhanced atomization
SEM	Scanning electron microscopy
SIA	Siloxanyl acrylate
SIMA	Siloxanyl methacrylate
STP	Standard temperature and pressure
TPVC	Tris-(trimethyl siloxysilyl) propylvinyl carbamate
TRIS	3-tris(trimethylsilyloxy)silylpropyl 2-methylprop-2-enoate
USAN	United States Adopted Names
UV	Ultraviolet
UVB	Ultraviolet B
VA	Vinyl acetate
VMA	N-vinyl-N-methylacetamide

LIST OF SYMBOLS

A	Area
C	Concentration
D_{eff}	Effective diffusivity
Dk	Oxygen permeability
Dk/h	Oxygen transmissibility
f	Fraction of drug release
F	Rate of ion transport
h	Gel thickness
I_0	Incident light intensity
I	Transmitted light intensity
K	Partition coefficient
k_1	First order release rate constant
k_0	Zero order release rate constant
k_H	Higuchi dissolution rate constant
k_{KP}	Peppas Korsmeyer release rate constant
M	Amount of mass released
n	Diffusion exponent
Q	Fractional drug release
$\dot{q}$	Drug release rate
Ra	Average roughness
R_r	Tear volume fraction renovated at each minute
t	Time
Tm	Temperature of the gel to liquid crystalline phase transition

%T	Transmittance
V	Volume
V_t	Tear volume
W or w	Weight
γ_{LV}	Liquid–vapor interfacial energy
γ_{SL}	Solid-liquid interfacial energy
γ_{SV}	Solid-vapour interfacial energy
Θ_W	Water contact angle

1 State of The Art

Table of contents

1.1 Contact lenses: a challenge for ocular drug delivery

The external eye structure is constituted by the eyelids and surrounding tissues, conjunctiva, lacrimal apparatus, cornea, and anterior chamber. Despite being easily accessible from the exterior, it is one of the most elaborate structures in the human body. Its complexity, together with the high resistance to the permeation of drugs and other foreign substances, make it a difficult target organ for drug delivery, representing a challenge for pharmacologists and drug delivery scientists.

Nowadays eye diseases are treated, in 90% of the cases, through the use of topical eye drops in form of solution or suspensions [1]. Eye drops instillations are well accepted by patients due to the cost-effectiveness and to the easy application; however, these conventional ocular formulations show low bioavailability due to physiological and anatomical constraints of the eye. Only a small fraction of the administered dose is absorbed (<5%) [2] due to: the continuous tear dilution [3, 4], dispersion and drainage during blinking and tearing reflex [1, 3], and due to the non-specific absorption [3, 5]. Given the limited tear volume capacity of the eye, ≈7 μL [6], a large part of the drug dose (25 μL per drop) is squeezed out immediately after the eye drop is instilled. Additionally, after instillation, the drainage of the tear increases [2], taking 5-10 minutes, to reset the volume to the normal physiological conditions [7, 8]. As a result of the tear drainage, part of the drug is absorbed into the systemic circulation directly in the local blood capillaries of the conjunctival sac or in the nasal cavity [9], reaching all major organs, with eventual side effects [10]. Furthermore, another fraction of the drug instilled is absorbed by the conjunctiva which has a larger area and higher permeability than the cornea [11, 12]. High drug loss and poor cornea's absorption result in multiple dosing and extended eye drops therapies. The high instillation frequency reduces the patient compliance and, furthermore, may lead to drug overdosing [13].

Taking into consideration the referred facts, one may conclude that eye drops do not represent the ideal solution for ophthalmic drug delivery. Several strategies have been employed to overcome some of the drawbacks described, namely: high viscosity formulations, polymeric gels, mucoadhesive and in situ forming gels, biodegradable or

non-degradable inserts [2, 5, 14, 15]. However, none of those approaches has shown sufficient improvements in bioavailability, or revealed to be patient friendly as the eye drops solution, which continues to be the most popular, if not the exclusive, way of treatment of the anterior eye.

Though, the investigation of the enormous potential of controlled release systems for ophthalmic drugs continues being explored. Controlled drug release permits to obtain a more effective drug therapy and to better safeguard drug efficacy, compared to conventional drug formulations. Namely, it allows the drug to overcome eventual physiological barriers, and avoids the undesirable elimination of the drug before reaching the target, increasing the drug bioavailability. It permits to deliver the drug to the target diminishing drug absorption into the blood stream, reducing therefore the risks of side effects. Furthermore, controlled drug delivery improves patient compliance, specifically, by decreasing or abolishing the frequency of drug administration, and consequently avoiding variability in drug concentration in the body, which may be due to overdosing or lacking of dosing by the patient.

New ophthalmic drug delivery vehicles have been investigated, aiming at the design of a product which is, at the same time, capable to perform drug controlled release, without affecting vision and eye functions (blinking and tearing), and whose production must be cost effective and approved by regulatory terms. Within this context, soft contact lenses (SCLs) have emerged as a valid option for drug delivery to the anterior chamber of the eye.

SCLs are made of biocompatible materials, are already in use by patients and have been approved by the Food and Drug Administration (FDA), in the USA [16], and by the Medicine and Healthcare Products Regolatory Agency (MHRA) in Europe [17]. Although misuses of contact lenses such as lack of hygiene and/or sleeping with the lenses are considered the major risk factor of eye pathologies, such as keratitis [18], SCLs may also be used as ophthalmic bandages to protect the ulcerous cornea from external agents and from rubbing due to blinking [19-25].

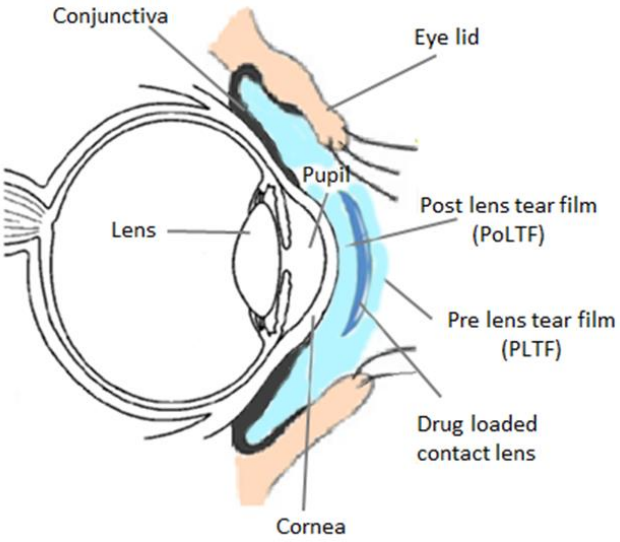

Figure 1.1 Schematic representation of a drug loaded contact lenses inserted in the eye. The principal component of the human eye are shown . Adapted from [18]

Furthermore, drug-loaded SCLs, see Figure 1.1, may have a continuous therapeutic effect if providing a sustained drug release. When a drug loaded contact lens is placed on the eye, the drug diffuses through the lens matrix, and enters the PoLTF (post lens tear film), where drug molecules, thanks to the presence of the lens, will have a longer residence time compared to the case of topical application as drops [5, 19, 20].

This longer residence time in the eye surface will reduce the drug inflow into the nasolacrimal sac, reducing the systemic drug absorption and eventual side effects, as mentioned before. There is another advantage on using contact lenses as drug vehicles: the diffusion of the drug molecules through the lens matrix is slower compared to that in aqueous solution, and that would potentially permit a continuous drug release from the contact lens. For these reasons, drug eluting contact lenses would allow, ideally, to maintain the drug concentration in the PoLTF in a therapeutic window, i.e. higher than the efficacy threshold and lower than the toxic limit of the drug. The ideal performance of a drug eluting SCL is schematically compared to the eye drops therapy in Figure 1.2.

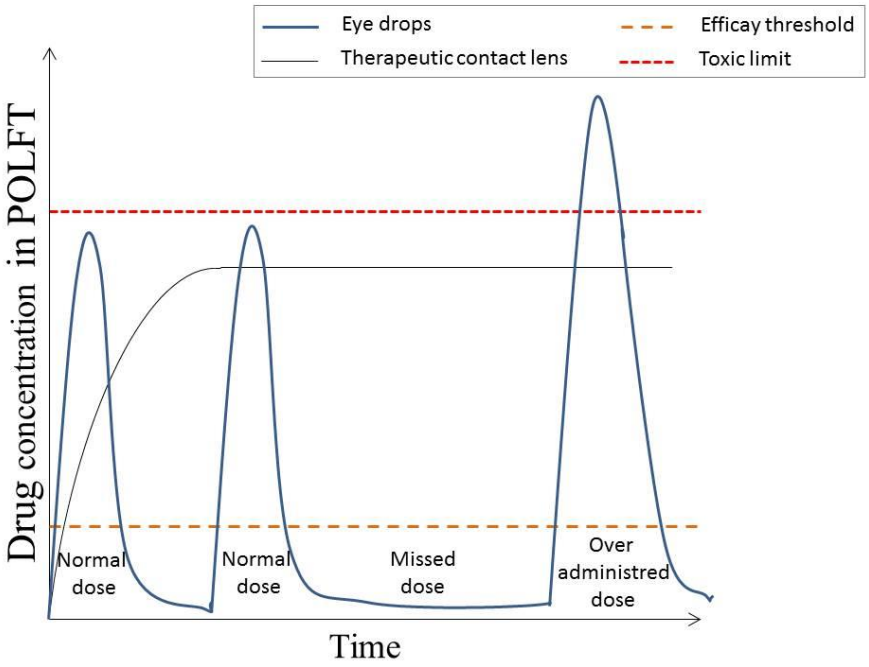

Figure 1.2: Graphical representation of the drug concentration in the PoLFT in the case of eye drop instillation and of therapeutic contact lens use.

Despite the clear positive impact in the ophthalmologic therapeutic field and their incredible potential, drug eluting SCLs are still not available in the market.

To respond to this necessity, the present work is focused on the development and characterization of specially conceived contact lenses for controlled ocular drug delivery.

Conventional and silicone materials for SCLs were compared and characterized and their potential as drug delivery systems was investigated, under different conditions and strategies (viz. plasma treatment, vitamin E absorption, liposome coatings). Furthermore several attempts to simulate the *in vivo* conditions were performed, namely a mathematical model was conceived, and drug release tests were performed under physiological hydrodynamic conditions and, in another set of experiment, under the eyeblinking movement conditions.

Despite the paramount importance of the development of adequate ocular drug delivery systems, this field of research has never been explored before at Instituto Superior Tecnico (IST), in Lisbon. Therefore, the extensive knowledge obtained in the

development of this work (preparation of hydrogels, drug quantifications methods, coatings assembly, blinking simulator, etc), contributed, not only to increase the knowledge of SCLs as platforms for ocular drug delivery, but also to lay the foundations of research projects at IST, which, meanwhile, resulted in several ongoing MSc thesis and two new PhD Thesis.

1.2 Soft contact lenses

In this section a brief historic overview over contact lenses will be given, followed by the description of the essential properties needed for a SCL material. Finally, hydrogel materials used for soft contact lenses will be presented.

1.2.1 The origins of contact lenses

The idea of contact lenses came from the famous Italian architect, mathematician, and inventor Leonardo da Vinci in 1508 [21]. One century after, the French philosopher and mathematician René Descartes in 1636, and the English scientist Thomas Young in 1801 [21], remarked this conjecture. But it was not until 1887 that the first glass contact lenses were created and fitted by the German physician Adolf Eugéne Fick [21]. These glass lenses were fabricated and successfully tested *in vivo* on rabbits, on the physician himself and on a small group of volunteers [21]. These lenses were made of glass and covered the entire front surface of the eye, including the conjunctiva, therefore they could be tolerated for only a few hours and failed to gain widespread use.

In 1936, polymethylmethacrylate (PMMA), was introduced as a material for rigid contact lenses by the American optometrist, William Feinbloom [21]. PMMA lenses were not well accepted in the market because of their lack of comfort. One important disadvantage of these rigid lenses was that no oxygen was transmitted through the lenses to the conjunctiva and cornea, which can cause a number of adverse clinical effects, such as corneal edema [22], limbal hyperæmia [23] and endothelial blebs [24]. These conditions tend to be reversible, but non-reversible complications, such as corneal vascularization, polymegethism and pleomorphism, may also occur.

The development of the first soft hydrogel contact lenses was made by the Czech Professor Otto Wichterle in 1961 [21]. SCLs represented the first successful clinical application of hydrogel polymers, and remain today one of the most important hydrogel uses [16]. Professor Wichterle was investigating the synthesis of a new material that could be used for implantation into the human body: poly(hydroxyethyl methacrylate) (PHEMA). Thanks to the introduction of this new material, soft contact lenses were soon accepted and prescribed due to their immediate comfort.

PHEMA lenses were first distributed in western Europe in 1962, but they only become popular in 1971 when, after the license being bought by Bausch and Lomb (B&L), they were approved by the FDA under the name of Polymacon. Soon, after the commercial introduction in 1971 of PHEMA, a wide range of new hydrogel polymers were introduced [21]. A lot of effort has been made since then in order to find the best material which complied with the properties needed for a contact lens hydrogel, namely a superior oxygen permeability.

In 1998, an important development was the launch of the first silicone hydrogel in the market by Ciba Vision in Mexico. These new material added the benefits of silicone, which decreased the risks of hypoxia-related complications due to its extremely high oxygen permeability, to the comfort and clinical performance of the conventional hydrogel that had been used for the previous 30 years [21].

1.2.2 Relevant properties of materials for SCLs

In order to be suitable as SCL materials, hydrogels should not interfere with the user's visual performances, and, at the same time, they should ensure the comfort and the maintenance of the normal ocular physiology of the user. For these reasons, SCLs materials are subject to a series of restrictions on what concerns some of their properties.

Here below the most significant contact lens material properties will be described.

1.2.2.1 Biocompatibility

The most important property that a material is required to possess in order to be used as SCLs is biocompatibility.

A biocompatible material is a material free of toxicity and of injurious effects, which does not cause an immune response in the host biological system [25]. Moreover, biomaterials for SCLs use must have very specific characteristics to mimic the ocular surface and allow structuring the tear film similarly to what is observed *in vivo*, viz. transparency, wettability, and ion and oxygen transmissibility, which all together guarantee the biocompatility of the lenses [25].

1.2.2.2 Optical transparency

SCL materials must be transparent in the visible light range (λ= 400-700 nm), to permit the passage of the light to the cornea. A material is defined as transparent when, not only lets the light pass through it, as the translucent materials, but permits to see through it too.

The optical transparency performance is described as the transmittance (T%), namely the percentage of visible light transmitted through the material, and is expressed as [26]:

$$\%T = 100\ x\ \frac{I}{I_0}$$ **Equation 1.1**

Where I_0 and I represent the intensity respectively of the incident light and of the transmitted light (see Figure 1.3).

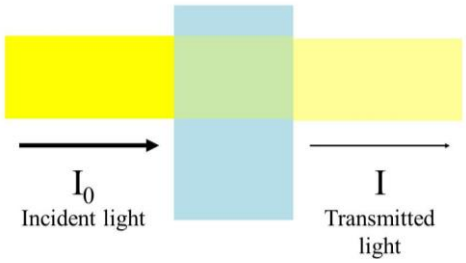

Figure 1.3 Schematic representation of light transmission through a material.

Hydrogels used as SCL materials, must present values of transmittance in the visible part of the spectrum higher than 90% [16].

One of the causes of poor transparency in a hydrogel is the micro-phase separation of the monomers within the matrix. This happens when hydrophobic and hydrophilic monomers are mixed, as in the case of silicone hydrogels. The loss of transparency can be avoided controlling the micro-phase dimension, in order to keep it below the wavelength of light [16].

1.2.2.3 Water Content

A polymer hydrogel is characterized by its capacity of swelling without dissolving, when water or other solvent enter the polymer matrix [27].

The equilibrium water content (EWC) of the hydrogel is a significant characteristic of the material and is defined as [16]:

$$EWC = \frac{Weight\ of\ water\ in\ hydrated\ polymer}{Total\ weight\ of\ hydrated\ polymer}\ x\ 100 \qquad \textbf{Equation 1.2}$$

Water has a major role in SCLs, namely, it acts as a plasticizer [28], affecting the mechanical properties of the gel and its dimensional stability [29], and supports oxygen and ions transport inside the matrix, which are essential processes for the clinical safety and for the comfort of the user [30]. Furthermore the EWC, together with the wettability and the electrostatic charge of the material, are directly involved in the biodeposition of lipid, protein and bacteria [31] on the contact lens surface.

The FDA divided soft contact lenses materials in 4 groups (See Table 1.1) according to their EWC and electrostatic charge [32]:

Table 1.1: FDA classification system for soft contact lens materials.

Category FDA	Water content	Electrostatic charge
Group I	Low water content (<50%)	nonionic
Group II	High water content (>50%)	nonionic
Group III	Low water content (<50%)	ionic
Group IV	High water content (>50%)	ionic

The relationship between comfort and EWC was explored by Efron *et al.* [33] and Young [34]. In both studies, lenses with low (38%), medium (55%) and high (70%) EWC were tested *in vivo*, concluding that the most comfortable, were the ones with the low EWC.

Conventional hydrogel materials present a higher range of EWC (30-73%), compared to silicone hydrogels (24-58%). Specific EWC values of commercial contact lenses made of conventional hydrogel and silicone hydrogels will be respectively reported in section 1.2.3 (Hydrogel materials for soft contact lenses), in Table 1.2 and Table 1.3.

1.2.2.4 Wettability

The human eye is a complex structure, and inside this structure, the presence of tears is fundamental. Tears ensure some important vital functions, namely the nutrients allocation to the eye tissues and the lubrication and protection of the ocular surface [6]. Furthermore they maintain the optical clarity, and together with the blinking action, are responsible for the elimination of the waste, i.e. dust or lashes [6]. For these reasons it is necessary to maintain a stable and uniform tear film over the SCLs. To make this possible the wettability of the hydrogel material is an essential property.

Wettability is the ability of a liquid to spread over a surface, and it is based on equilibrium of the solid–liquid–vapor triple-phase contact line. The most common way to measure the wettability is the direct contact angle measurement, from which the surface energy of the solid may be estimated [35]. Two types of techniques can be used: the sessile drop and the captive bubble methods [35], both schematized in Figure 1.4.

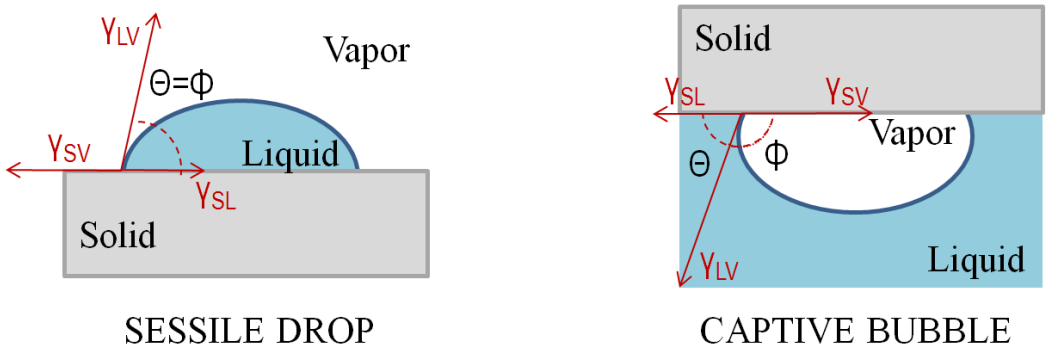

Figure 1.4: Schematic representation of the sessile drop and captive bubble method of goniometric analysis. In the case of the sessile drop the contact angle and the meniscus angle are coincident, while in the captive bubble method the contact angle is the supplementary angle of the meniscus angle.

The advantage of the captive bubble method is that the sample can be maintained hydrated, which, in the case of hydrogels, is a fundamental detail to better simulate the *in vivo* conditions during the measurement.

The contact angle value (θ) depends on the properties of the solid- liquid-vapor system, and in the case of a rigid and flat surface is defined by the Young equation [36]:

$$\gamma_{LV} \cos\theta = \gamma_{SV} - \gamma_{SL} \qquad \textbf{Equation 1.3}$$

where γ_{LV}, γ_{SV}, γ_{SL} represent respectively the liquid–vapor, solid-vapor and solid-liquid interfacial energies. The wettability increases with the decrease of the contact angle.

In the case of the contact lenses, high wettability results in a good stability of the tear film and on its spreading over the lens surface. A poor wettability means heterogeneity in the tear film that may cause scattering of the light and consequent interference with light transmission, reducing the lenses optical performance. Moreover, the wettability of the material is directly related to the lubricity of the lens and to the comfort of the user. An hydrophobic lens would affect the quality of the pre lens tear film (PLTF) (the tear film between the lens and the eyelid), in terms of increasing friction during blinking and creating the undesirable dry eye feeling.

Conventional hydrogel materials are characterized by lower contact angles, compared to the ones of silicone hydrogels. This is due to the hydrophobic monomers present in

silicone hydrogels composition. To overcome the hydrophobicity of the silicone hydrogels, two main strategies have been used along the years, namely plasma treatments, and the use of internal wetting agent [29].

1.2.2.5 Oxygen Permeability

Human cornea owes its transparency to its avascularity, being one of the few tissues in the human body lacking of blood vessels. This avascularity implies that the oxygen supply to the tissues comes in most part from the atmosphere, and, in a smaller part, from the aqueous humor and limbal vasculature [37]. For this reason, oxygen permeability represents a key property of SCL materials.

Low oxygen permeability of the SCL materials would impede oxygen supply to the cornea, giving the risk of hypoxia, and consequent pathologies, like, for example, cornea edema, papillary conjunctivitis, and most serious microbial keratitis [38].

Oxygen permeability is characteristic of the material and is described as Dk, where D is the oxygen diffusivity in the material, and k is the oxygen solubility. The Dk unit is barrer, which is a non-SI unit and is defined as follows [16]:

$$Dk\ unit, Barrer = \frac{[cm \cdot cm^3(O_2) at\ STP] \cdot 10^{-11}}{[\sec \cdot\ cm^2 \cdot mm\ Hg]}$$ **Equation 1.4**

Where cm refers to the thickness of the material, cm^3 to the volume of oxygen at standard temperature and pressure (STP) conditions, namely 0 ºC and 1 atm (101 325 Pa), cm^2 to the area of the lens, and mmHg to the partial pressure of oxygen.

Since the oxygen supply depends not only on the oxygen permeability of the SCL, but also on the SCL thickness (h), commercial contact lenses are often described by their oxygen transmissibility, Dk/h [16].

The minimum oxygen permeability required to maintain ocular health and avoid anoxia throughout the entire cornea, is 35 Barrer, for the open eye, and 125 Barrer, for the closed eye [39].

In conventional hydrogel materials, the monomers used are mostly impermeable to oxygen, and oxygen is transmitted mainly through water, giving a direct relationship between oxygen permeability and EWC, as described by the formula proposed by Morgan and Efron [40]:

$$Dk = 1.67e^{0.0397\mathrm{EWC}} \qquad \textbf{Equation 1.5}$$

In silicone hydrogel materials, the oxygen is primarily transmitted through the siloxane-containing components which have a higher permeability to oxygen than water, resulting in a strong increase of the oxygen permeability of these materials in comparison with the conventional hydrogels [41].

Figure 1.5 shows that in conventional hydrogels Dk increases with the increase of EWC, while in silicone hydrogels Dk decreases as EWC increases, being EWC inversely proportional to the silicone content of the material.

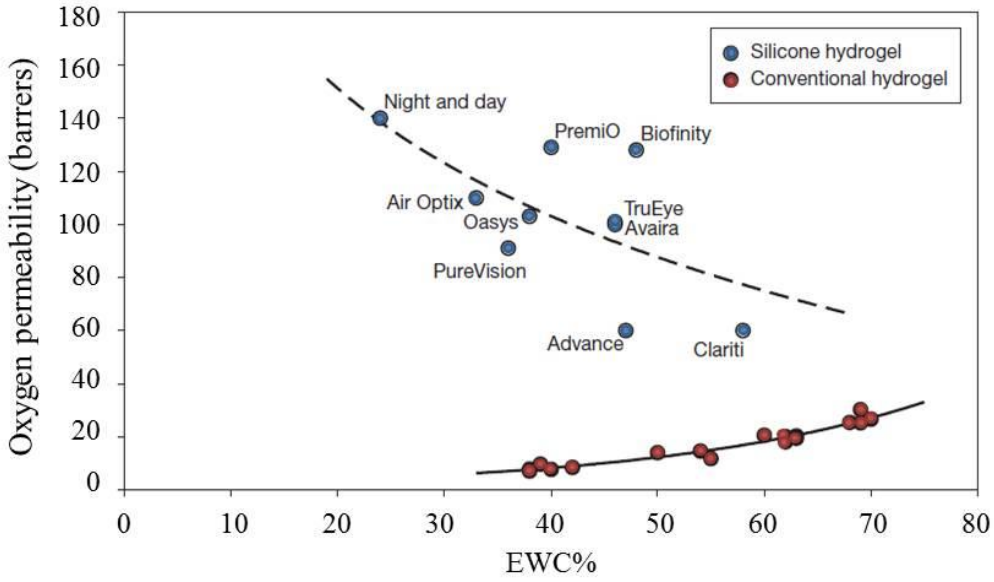

Figure 1.5: Relationship between water content and oxygen permeability for conventional hydrogels and silicone hydrogels. Adapted from [16].

Silicone contact lenses permit an oxygen supply to the cornea comparable with the physiological one [42], and for this reason they can be used as extended wear SCLs, being approved for continuous wear up to 30 days.

1.2.2.6 Ion Permeability

Sodium ion permeability of SCL materials is a critical parameter for the on-eye lens movement [43]. This movement ensures the presence of a hydrodynamic boundary layer in the PoLFT that avoids hydrophobic binding between the lens and the cornea [44], permitting the tear film to turn over and the waste to be removed [45]. Cerretani *et al.* recently proposed a biophysical mechanism consistent with the claimed need for the critical ion permeability [46]. The minimum value of ion diffusion coefficient required for SCL materials is 2.5×10^{-8} cm^2/s [47].

Silicone hydrogels present higher sodium ion permeability than conventional hydrogels with the same EWC. This may be attributed to the fact that silicone hydrogels present heterogeneous bi-phasic regions where the polymer and aqueous domains form phase separated regions, originating more effective channels which enhance ion permeability [43].

1.2.2.7 Refractive Index

SCL materials are desired to present refractive index similar to the one of the cornea (1.37) [16]. In conventional hydrogels, the refractive index has a linear dependence with the EWC, namely, it increases from 1.37–1.38 for hydrogel with 75% of EWC to 1.46–1.48 for hydrogels with 20% of EWC [16]. Silicone hydrogels do not follow this behavior, due to the different materials they are made of [16].

1.2.2.8 Mechanical Properties

Mechanical properties are important factors in the design and quality control of SCL materials. The most important mechanical property is the tensile elastic modulus which determines the stiffness of the lens.

The lens stiffness influences its fitting to the cornea and, consequently, the visual performance, the durability and the handling of the lens.

Comfort can best be achieved from a low modulus, flexible contact lens that would easily locate over the cornea, having a minimal interaction with the eyelids during blinking. However, a high degree of flexibility can be a disadvantage when trying to achieve optimum vision which is ensured by an increase in modulus: that means a decrease of initial comfort and can lead to mechanically induced pathology [29]. A balance between user comfort and visual performance is essential to be achieved.

Conventional hydrogel materials, thanks to the higher EWC, present a lower tensile modulus than silicone hydrogels [16]. Silicone hydrogels, thanks to the higher tensile modulus, are of easy handling and are more resistant to rupture than conventional hydrogels. This reason, together with the higher oxygen permeability, previously reported, makes silicone SCLs suitable for extended wear, while conventional hydrogel remain the best and the most used material for daily disposable lenses.

1.2.2.9 Electrostatic charge

Soft contact lenses materials can be ionic or non-ionic, depending on the nature of the monomers used in the polymerization. The charge of the polymeric matrix influences the water content of the hydrogel, namely, ionic monomers will increase the water uptake, since water is a polar molecule [48]. Furthermore, electrostatic charges are linked to protein adhesion, such as albumin, lysozyme and lactoferrin [49]. Lysozyme is the principal protein in the human tear film, with a low molecular weight and a positive charge, which easily interacts with the common negative charge of the ionic contact lenses. It was shown that the amount of protein absorbed *in vivo*, is proportional to the ionic character of the polymer [48].

Table 1.1 reports the FDA classification for soft contact lens materials, according to the electrostatic charge.

1.2.2.10 Friction properties

Surface lubricity of the SCL represents an important property to take in consideration when evaluating a SCLs material, since it is closely related to the lens comfort.

People blink 15-20 times per minute in a relaxed state, this frequency can drop to 3 times per minute if the subject is paying attention to something, i.e. reading a book, and can increase if the subject is under pressure [50].

During blinking the eyelid slides over the eye, for this reason it is of fundamental importance that, when wearing SCLs, friction between the anterior lens surface and the under-surface of the eyelid is avoided in order to preserve a smooth feeling.

Friction is the force opposing the movement between two surfaces in contact and it is estimated through friction coefficient (μ) measurements. Two common methods to measure the friction coefficient are microtribology [51] and atomic force microscopy (AFM) [52].

During blinking the eyelid is estimated to cause a pressure that ranges from 3.5 to 4.0 kPa, with average speed of around 12 cm/s [53]. Friction experiments need to be performed under parameters that are as close as possible to the real ones in order to obtain representative friction coefficient values. Sawyer *et al*. investigated the tribological properties of hydrogels measuring the friction coefficient through microtribometer [51]. They concluded that low tensile modulus and high water content hydrogels present lower friction coefficient [51]. In a more recent work, Tosatti *et al.* measured the friction coefficient of several commercial SCLs confirming that silicone hydrogels present slightly higher friction coefficients (0.02-0.6) compared to the ones of conventional hydrogels (0.02-0.45), and underlined the importance of the presence of the monomer polyvinylpyrrolidone (PVP) to decrease the friction coefficients. This matter will be better discussed in Section 1.2.3.1.

1.2.3 Hydrogel materials for soft contact lenses

Hydrogel polymers are three-dimensional networks of homopolymers and copolymers, cross-linked together [54]. As mentioned in the properties section, hydrogels are characterized by their capability to absorb large amounts of water without being dissolved. This is possible thanks to the presence of hydrophilic functional groups, which bond with water molecules, and to the chemical and physical cross linking, which ensures physical stability [54].

Hydrogels in the dehydrated state behave as solid and brittle materials, due to the proximity of the polymer chains which interact among themselves. When hydrogels hydrate, fluid enters the chains and causes pressure inside the chains which allows the network to swell, absorbing water and increasing the volume. When the swelling equilibrium is reached, the polymers chains are fully extended and the physical structure is ensured by the crosslinking (See Figure 1.6).

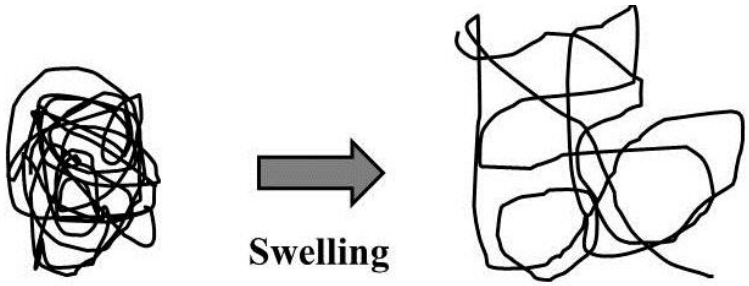

Figure 1.6: Swelling of an hydrogel, from dehydrated to hydrated state.

Usually, SCLs hydrogel materials are divided into two main groups, based on their oxygen permeability: conventional hydrogel materials (with low Dk) and silicone-based hydrogels (with high Dk) [55].

1.2.3.1 Conventional hydrogel materials

Methacrylates, together with acrylates, represent the most important classes of conventional hydrogels materials for SCLs [56]. The most common and representative methacrylate is PHEMA (Figure 1.7), which was the pioneer monomer material in the SCL hydrogels.

PHEMA is a homopolymer obtained by polymerizing the hydrophilic HEMA monomers with a cross linker, e.g. ethylene glycol dimethacrylate (EGDMA), (Figure 1.7). It is characterized by a low EWC of 38% and a consequent low oxygen permeability (9 barrer) [16], which is also due to the impermeability to oxygen of the polymer itself.

In order to increase the EWC of PHEMA hydrogel, copolymerization with other monomers has been tested. One of the first monomers used in the copolymerization of

PHEMA was with *n*-vinyl pyrrolidone (NVP) (Figure 1.7). NVP is a strongly hydrophilic nonionic lactam, whose hydrophilicity is due to the polar amide group (N-C=O). NVP is called a "super absorber" thanks to its capacity of absorbing several times its weight in water [57] and, thus, it is usually copolymerized with HEMA and methyl-methacrylate (MMA) (Figure 1.7).

MMA is the material of which rigid contact lenses are made of. It is a hydrophobic monomer and it is often used in SCLs to increase the mechanical strength of the polymers. It is interesting to highlight that, despite the hydrophobic character of MMA, when MMA and NVP are copolymerized, a material with a EWC higher than HEMA/NVP (up to the 60-85% of water) is obtained [16].

Other monomers used to increase EWC are: methacrylic acid (MAA), and *n*,*n*-dimethyl acrylamide (DMA) (Figure 1.7). MAA is highly hydrophilic and gives a ionic character to the hydrogel [58]. The addition of 1.5-2.5% of MAA to PHEMA results into a polymer with a EWC of 50-60% [16]. DMA, is considered a "super absorbent" monomer and it is characterized by an excellent hydrolytic stability [57].

Glyceryl methacrylate (GMA) (see Figure 1.7) is also used to produce conventional hydrogel contact lenses. This monomer is more hydrophilic than HEMA, and it has been copolymerized with MAA and HEMA [16]

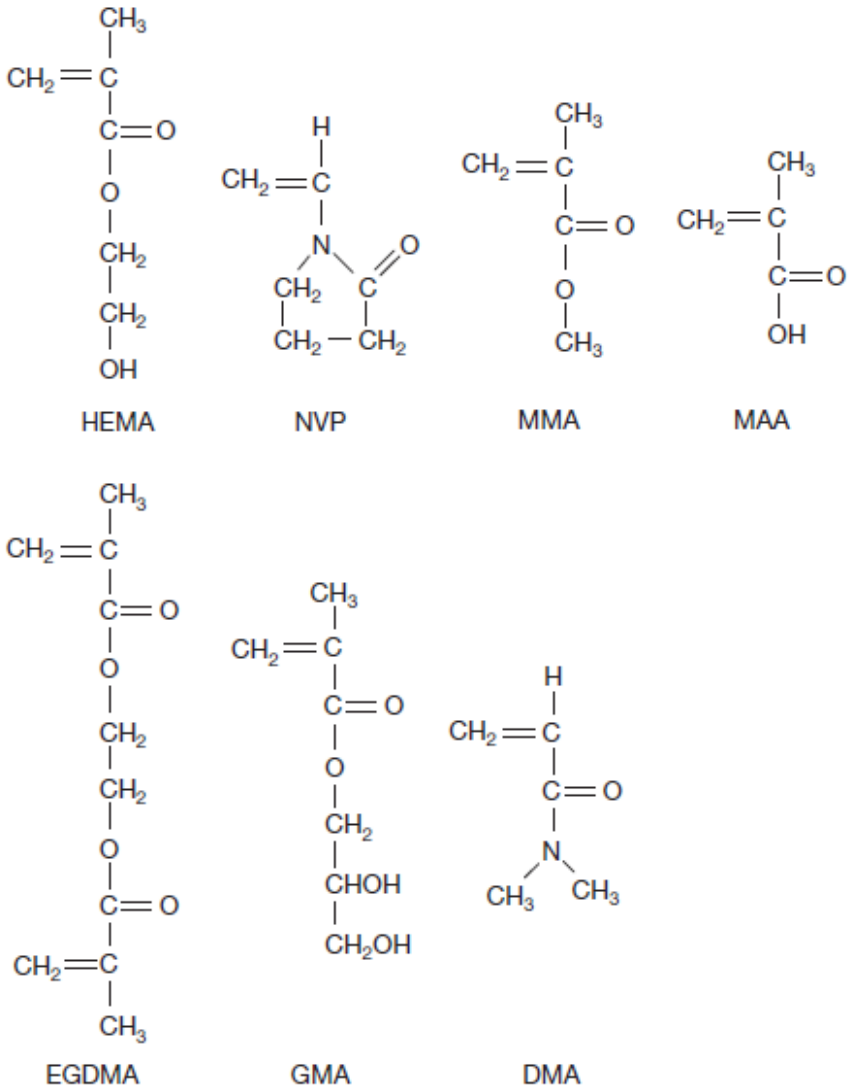

Figure 1.7: Molecular structures of the main components of SCLs hydrogel materials: hydroxyethyl methacrylate (HEMA); *n*-vinyl pyrrolidone (NVP); methyl methacrylate (MMA); methacrylic acid (MAA); ethylene glycol dimethacrylate (EGDMA); glyceryl methacrylate (GMA); *n,n*-dimethyl acrylamide (DMA) [25].

In 1981, an attempt to obtain an extended wear conventional hydrogel contact lens was made, creating a HEMA/NVP/MAA lens, whose water content reached 71%, increasing the oxygen permeability. Even though the Dk was high, these lenses were not considered suitable for monthly use, being restricted to weekly use by the FDA [16]. Furthermore, lenses with a high EWC had a series of disadvantages, such as an increased tendency to the biofouling and dehydration and are fragile due to the low tensile modulus.

Table 1.2, reports the currently available conventional hydrogel commercial contact lenses, together with the respective composition, FDA group and EWC.

Table 1.2: Currently available conventional hydrogel contact lenses. Adapted from [25].

Name	Manufacturer	Principal components	EWC %	USAN[a] nomenclature	FDA group
Biomedics 38	Coopervision	HEMA	38	Polymacon	I
CD	Ultra Vision	HEMA	38	Polymacon	I
Cibasoft	CIBA Vision	HEMA	38	Tefilcon-A	I
Classic	CIBA vision	HEMA, NVP, MMA	43	Tetrafilcon-A	I
CSI	CIBA vision	GMA, MMA	38	Crofilcon-A	I
Durasoft	CIBA vision	HEMA, EEMA[b], MAA	30	Phemfilcon-A	I
Frequency 38	CooperVision	HEMA	38	Polymacon	I
Hydron z4/z6	CooperVision	HEMA	38	Polymacon	I
Ultra Vision 38	Ultra Visiojn	HEMA	38	Polymacon	I
Medalist 38	Bausch & Lomb	HEMA	38	Polymacon	I
Menicon Soft	Menicon	HEMA, VA[b], PMA[b]	30	Mafilcon-A	I
Omega 38	Ultra Vision	HEMA	38	Polymacon	I
Optima 38	Bausch & Lomb	HEMA	38	Polymacon	I
Sauflon 38	Sauflon	HEMA	38	Polymacon	I
Seelite 38	Coopervision	HEMA	38	Polymacon	I
SeeQuence	Bausch & Lomb	HEMA	38	Polymacon	I
Soflens 38	Bausch & Lomb	HEMA	38	Polymacon	I
Softspin	Bausch & Lomb	HEMA	38	Polymacon	I
Actisoft 60	Coopervision	GMA[b]	60	Hioxifilcon-A	II
Excelens	CIBA Vision	PVA[b], MMA	64	Atlafilcon	II
ES 70	Coopervision	AMA, NVP	70	-	II
Focus Dailies	CIBA Vision	PVA	69	Nefilcon-A	II
Gentle Touch	CIBA Vision	MMA, DMA	65	Netrafilcon-A	II
Igel 67	Ultra Vision Optics	MMA, NVP, CMA[b]	67	Xylofilcon-A	II
Omniflex	Coopervision	MMA, NVP	70	Lidofilcon-A	II
Medalist 66	Bausch & Lomb	HEMA, NVP	66	Alphafilcon-A	II
Permaflex	CIBA Vision	MMA, NVP	74	Surfilcon-A	II
Precivion UV	CIBA Vision	MMA,NVP	74	Vasurfilcon-A	II
Proclear	Coopervision	HEMA, PC[b]-HEMA	62	Omafilcon-A	II
Rythmic	Coopervision	MMA, NVP	73	Lidofilcon	II

Name	Manufacturer	Principal components	EWC %	USAN nomenclature	FDA group
Sauflon-55	Sauflon	HEMA,NVP	55	-	II
Soflens One Day	Bausch & Lomb	HEMA, NVP	65	Hilafilcon-A	II
Soflens 66	Bausch & Lomb	HEMA, NVP	66	Alphafilcon-A	II
Accusoft	Ophthalmos	HEMA, PVP, MAA	47	Droxifilcon-A	III
Comfort Flex	Capital Contact Lens	HEMA, BMA[b], MAA	43	Deltafilcon-A	III
Durasoft 2	CIBA Vision	HEMA, EEMA, MAA	38	Phemefilcon-A	III
Soft Mate II	CIBA Vision	HEMA, DAA[b], MAA	45	Bufilcon-A	III
Acuvue	Johnson & Johnson	HEMA, MAA	58	Etafilcon-A	IV
Durasoft 3	CIBA Vision	HEMA, EEMA, MAA	55	Phemefilcon-A	IV
Focus 1-2 Week	CIBA Vision	HEMA, PVP, MAA	55	Vifilcon-A	IV
Focus Monthly	CIBA Vision	HEMA, PVP, MAA	55	Vifilcon-A	IV
Frequency 55	Coopervision	HEMA, MAA	55	Methafilcon-A	IV
Hydrasoft	Coopervision	HEMA, MAA	55	Methafilcon-A	IV
Hydrocurve II/3	CIBA Vision	HEMA, DAA, MAA	55	Bufilcon-A	IV
1 Day Acuvue	Johnson & Johnson	HEMA, MAA	58	Etafilcon-A	IV
Permalens	CIBA Vision	HEMA, NVP, MAA	71	Perfilcon-A	IV
Softcon	CIBA Vision	HEMA, PVP, MAA	55	Vifilcon-A	IV
Surevue	Johnson & Johnson	HEMA, MAA	58	Etafilcon-A	IV
Ultraflex 55	Coopervision	HEMA, MAA	55	Ocufilcon-A	IV

a: USAN stands for United States Adopted Names (USAN), and is the American denomination of SCLs, referring to the chemical composition of the material. In this study materials will be called by their chemical name.
b: butyl methacrylate (BMA); alkyl methacrylate (AMA); cyclohexyl methacrylate (CMA); ethoxyethyl methacrylate (EEMA); diacetone acrylamide (DAA); glyceryl methacrylate (GMA); vinyl acetate (VA).

In this work the hydrogel composition HEMA/PVP was selected as object of study. These monomers were chosen for their importance in the range of the conventional materials. In Chapter 2, the main properties of this material will be studied together with the drug release performances for two drugs, levofloxacin, and chlorhexidine. Further investigations and characterization of HEMA/PVP will be presented in Chapter 3 and Chapter 5, where the effect of plasma treatment and of liposome coating on the performance of drug-loaded hydrogels will be addressed, respectively.

1.2.3.2 Silicone hydrogel materials

Researchers understood that the increase of EWC was not enough to reach values of oxygen permeability adequate for the extended wear of lenses without having clinical complications, and moved their attention to the search of a new material highly permeable to oxygen: silicone. In silicone hydrogels the oxygen is transmitted through the silicone component of the lens material, resulting in a dramatic increase in the oxygen permeability of the materials [41]. The first material used was polydimethyl siloxane (PDMS) (Figure 1.8), which, despite its high oxygen permeability (600 barrers), did not have success into the commercial lenses field due to high discomfort in the users caused by its hydrophobicity [16].

The first successful siloxane-based contact lens was made of a material 3-tris(trimethylsilyloxy)silylpropyl 2-methylprop-2-enoate (TRIS) (Figure 1.8), where the mechanical properties of MMA where joined to the oxygen permeability of a siloxane rubber [16].

This silicone material had low surface-free energy and poor wettability. For these reasons, since 1970, the target of the researchers was to combine the properties of high oxygen permeable silicone materials to the ones of conventional hydrophilic materials, to obtain a material that is, at the same time, oxygen permeable and comfortable. The biggest challenge in this idea was to find a way to overcome the immiscibility of the hydrophobic and the hydrophilic phases [16].

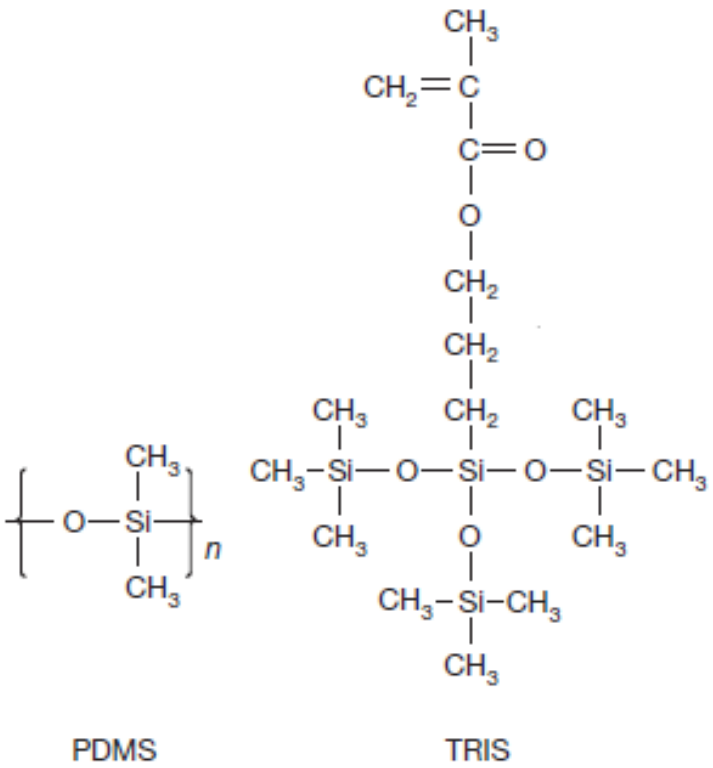

Figure 1.8 Molecular structures of the main siloxane components of soft contact lenses hydrogel materials: polydimethyl siloxane (PDMS); 3-tris(trimethylsilyloxy)silylpropyl 2-methylprop-2-enoate (TRIS). Adapted from [25].

The presence of polar groups in the TRIS structure has allowed the addition of different compounds in order to optimize the silicone hydrogels properties [16, 59-61].

Despite the copolymerization with conventional monomers, most part of silicone hydrogel contact lenses would still be unsuitable for use without a surface treatment, due to their intrinsic hydrophobicity. Different techniques are used to overcome this problem, the most common are the gas plasma techniques and the physical coating that modify the surface without changing the bulk properties [55]. Another approach is the use of wetting agents such as NVP and DMA, which result in an improvement of the wettability and in the increase the EWC [16]. This type of lenses is often characterized by a biphasic silicone, in which the silicone-containing phase is responsible for the oxygen transport, while the hydrophilic phase, allows the ions transport [55].Table 1.3 reports silicone hydrogels commercial contact lenses, together with the respective composition, FDA group and EWC.

Table 1.3 Currently available silicone hydrogel contact lenses. Adapted from [16].

Name	Manufacturer	Principal components	EWC %	USAN nomenclature	FDA group
Focus Night & Day	CIBA Vision	DMA, TRIS, siloxane	24	Lotrafilcon-A	I
AirOptix	CIBA Vision	DMA, TRIS, siloxane	33	Lotrafilcon-B	I
Acuvue Oasys	Johnson & Johnson	mPDMS[a], DMA, HEMA	38	Senofilcon-A	I
Acuvue Advance	Johnson & Johnson	mPDMS, DMA, HEMA, siloxane, PVP	47	Galyfilcon-A	I
Acuvue TruEye	Johnson & Johnson	MPDMS, DMA, HEMA, siloxane	46	Narafilcon-B	I
Avaira	Coopervision	NVP, VMA[a], IBM[a]	46	Enfilcon-A	I
Biofinity	Coopervision	NVP, VMA, IBM	48	Comfilcon-A	I
PremiO	Menicon	SIMA[a], SIA[a], DMA, pyrrolidone derivative	40	Asmofilcon-A	I
Claritin	Sauflon	Not disclosed	58	-	II
PureVision	Bausch & Lomb	NVP, TPVC[a], NCVE[a], PBVC	36	Balafilcon-A	III

a: Monofunctional polydimethylsiloxane (MPDMS); tris-(trimethyl siloxysilyl) propylvinyl carbamate (TPVC); N-carboxyvinyl ester (NCVE); poly(dimethysiloxy) di (silylbutanol) bis (vinyl carbamate) (PBVC); N-vinyl-N-methylacetamide (VMA); isobornyl methacrylate (IBM); siloxanyl methacrylate (SIMA); siloxanyl acrylate (SIA).

In this work the hydrogel composition TRIS/NVP/HEMA was selected as silicone hydrogel material. The polymer composition was decided according to the intrinsic importance of these monomers within the silicone hydrogels.

TRIS/NVP/HEMA will be studied and characterized, together with HEMA/PVP in Chapters 2 and 3. Chapter 4, reports the characterization and drug release investigation of two commercial silicone hydrogels: Acuvue TruEye®, and Acuvue Oasys®, both produced by Johnson & Johnson (see Table 1.3).

1.3 Ophthalmic drugs of interest for controlled release

As stated in Section 1.1, eye drops instillation, despite its low bioavailability, still represents today the most prescribed treatment of ocular pathologies. However, there are cases where it becomes particularly difficult to correctly comply with eye drops therapy, due to the high frequency of the drops instillation required in the posology, and controlled drug release through contact lenses become a palpable necessity.

Some of the more evident cases in which a controlled drug vehicle would be advantageous and would represent an improvement in quality of daily life of the users, are: post-eye-surgery therapy, ocular cystinosys, glaucoma and eye keratitis treatments.

Millions of people every year undergo laser surgery in order to correct myopia, hypermetropia, and astigmatism and to clear cataract. Laser vision correction technique, including Lasik (Laser-Assisted in situ Keratomileusis) and PRK (photorefractive keratectomy), is nowadays one of the most common laser based techniques [62]. After surgery, patients are given a postoperative eye drops therapy [63] namely: antibiotics (viz. ciprofloxacin, tobramycin, gentamicin, levofloxacin, ofloxacin and moxifloxacin), anti-inflammatories (viz. dicloflenac, dexamethasone and flurbiprofen) and anesthetics (viz. tetracaine, lidocaine and pubivocaine).

During the first days after the surgery, these therapies present frequent dosage requirements that may easily interfere with the patient daily activities and furthermore, may easily lead to overdose or lack of dosage. For example, tetracaine, together with tobramycin, should be applied every 2 hours for the first 72 hours after PRK surgery, including the nights [64]. Another example of post-surgery therapy is the instillation of dicoflenac, together with gentamicin, 4 times a day [65].

Cystinosis is a chronic metabolic disease that can affect the eye, causing the formation and accumulation of crystals in the ocular tissues, with consequent irreversible damage to the eye [66]. This disease is treated with cysteamine, with an intense eye drops therapy. Studies reported that cysteamine therapy is only effective if administered hourly while

awake, otherwise the benefits of the therapy would be compromised and the disease would progress [67].

Glaucoma represents a series of ocular disorders which lead to the damage of the ocular nerve [68]. Every year, glaucoma affects over 60 million people, being the second largest cause of blindness after cataract [69]. It is a progressive disease whose principle risk factors are: high blood pressure, diabetes and age - it affects usually people over 60 years old [70]. Its therapy consists in the topical administration of timolol, a beta blocker that acts diminishing the hypertension in the eye, and that needs to be instilled one to several times a day [69]. Due to the age of the patients, the correct administration of the eye drops, namely the correct placement of the eye drop onto the eye, the exact number of doses and the constant time interval between the doses, becomes a challenge, suggesting timolol as another drug of interest for ophthalmic drug control investigation.

Ocular keratitis is a common inflammation of the cornea that causes pain, light sensitivity and reduces vision. If associated to infection it can be, in severe cases, a potentially blinding condition [71], representing nowadays one of the principal causes of corneal opacification [72], which is world-wide, one of the most common cause of legal blindness after cataracts [72]. Among all ocular keratitis cases, approximately 50% are infectious, of which 80% are bacterial [73]. Millions of people all over the world are affected by bacterial keratitis and might be subject to devastating visual disability, the bigger impact happening in the countries of the South-east Asia region [74]. Infections are largely due to Gram-positive *S. aureus*, *S. epidermidis*, and different *Streptococcus* and *Bacillus* spp., but also Gram-negative bacteria such as *P. aeruginosa*, *S. marcescens*, *Moraxella lacunata*, *Microbacterium liquefaciens*, and *H. influenza* [75]. Among those microorganisms, *Staphylococcus aureus* and *Pseudomonas aeruginosa* are described as being the principal isolates in microbial keratitis [72, 76, 77].

Bacterial keratitis are characterized by a rapid progression that may lead to corneal destruction within the first 24–48 hours [75]. For this reason, an immediate diagnosis and treatment are imperative to avoid irreversible damages to the eyes structures, such as corneal scarring or perforation. The initial treatment of these pathologies consists in the topical administration of eye drops containing the ophthalmic antibiotic, such as aminoglycosides, fluoroquinolones and macrolides. Appendix A reports the list of the

ophthalmic antibiotics approved by the FDA, and listed by Provider Synergies, L.L.C, USA [78].

Due to the relative low cost and commercial availability, fluoroquinolones are the broad spectrum antibiotics most widely used for ocular infections and perioperative prophylaxis in ophthalmic surgery [79]. Fluoroquinolones are divided into "generations". The most recent commercially available is the 4th generation, which includes moxifloxacin and gatifloxacin, both characterized by an excellent aqueous penetration [80], and higher activity against *S. aureus* compared to the previous fluoroquinolone generations [81]. Within the 3rd generation, levofloxacin (LVF) is one the most common drugs for the therapy and prophylaxis of eye infections caused by *S. aureus* and *P. aeuriginosa* [82, 83], and is often prescribed to patients undergoing cataract surgery [84]. For these reasons LVF was chosen as the drug of study in the present work (See section 1.3.1).

Less common, but as dangerous as bacterial keratitis, are fungal and *Acanthamoeba* keratitis, whose immediate diagnosis and treatment with intense eye drops therapy are crucial for the eye healing.

Fungal keratitis have a higher incidence in third world humid tropical environmental countries [85], and, if not treated, it may lead to the perforation of the cornea and evisceration or enucleation of the eye [86]. The treatment usually consists in the topical administration of antifungal, namely: fluconazole, econazole, miconazole, natamycin, terbinafine and naftifine [87].

Acanthamoeba keratitis is a serious infection of the cornea caused by the amoebic parasite *Acanthamoeba.* This parasite can exist in the pathogenic trophozoite form or in the metabolically dormant form of cyst, and can be found in soil and fresh water [88]. This type of keratitis is often related to the use of soft contact lenses, in particular, as consequence of the incorrect use of tap water to rinse the lenses [89], and it is often reported in the third world, due to the poor hygiene conditions [90].

The antibacterial and antiseptic chlorhexidine is reported to be effective both against fungal [85] and *Acanthamoeba* keratitis [90-92], and it is also reported to be active against *S. aureus* [85]. Thanks to its low cost and high stability [93], this drug has a

huge potential to fight cornea infections in the third world, and, consequently, was chosen as the second drug of interest in this study (see section 1.3.2).

1.3.1 Levofloxacin

Levofloxacin, whose molecular formula is $C_{18}H_{20}FN_3O_4$, (see Figure 1.9), has molecular weight of 370.4 Da, and a physical appearance of a yellowish white to yellow powder. The molecule possesses an intermediate lipophilic character and its zwitterionic form predominates in water at physiological pH [94].

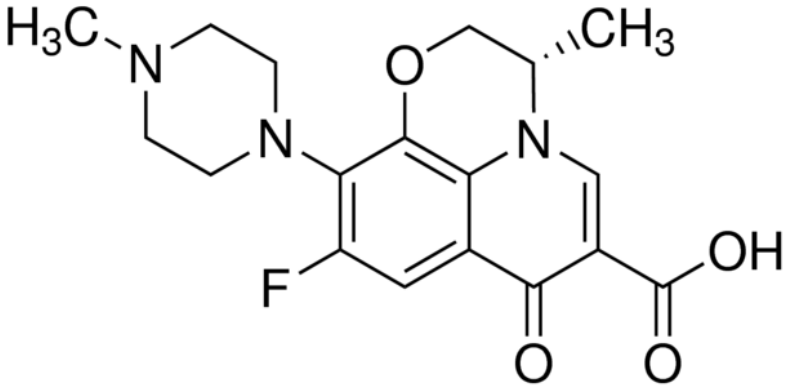

Figure 1.9 Molecular structure of Levofloxacin.

For ophthalmologic use, LVF is commercially available in the form of the colyrium QUIXIN® (0.5%), prescribed to treat bacterial conjunctivitis and keratitis, and as the collyrium IQUIX (1.5%), to treat corneal ulcers (See Appendix A).

The frequency of QUIXIN® drops application depends upon the severity of the infection. A typical therapy consists in the application of 1-2 drops every 2 hours on the first two days of treatment, not exceeding 8 times a day, followed by 1-2 drops, every 4 hours till complete 7 days, not exceeding 4 times a day [95]. The intense eye drops therapy and the risk of side effects due to overdose and systemic absorption which may lead to cornea and systemic toxicity (hepatotoxicity, nephrotoxicity, and neurotovixicity) [96-98], further justifies the choice of levofloxacin as drug of study.

1.3.2 Chlorhexidine

Chlorhexidine, whose molecular formula is $C_{22}H_{30}Cl_2N_{10,}$ has molecular weight of 505.4 Da, and presents low solubility in water [99] (See Table 1.4).

Table 1.4: Solubility of Chlorhexidine salts in water at 20ºC, adapted from [99].

Salts	Solubility (%W/V)
Chlorhexidine base	0.08
Diacetate	1.90
Dihydrochloride	0.06
Digluconate	>50

Chlorhexidine is a strong base and antiseptic which is used as pharmaceutical product in its more stable forms of salts e.g., the dihydrochloride, diacetate, and digluconate [100]. However, at physiological pH the salts dissociate and the cationic chlorhexidine ion is released.

The most popular salt is the digluconate, due to its higher water solubility [99]; however, in this study the diacetate chlorhexidine monohydrate will be investigated, due to its high availability and low cost.

Chlorhexidine diacetate (CHX), whose molecular formula is $C_{22}H_{30}Cl_2N_{10}*2C_2H_4O_2$ (see Figure 1.13), has molecular weight of 625.55 Da and a physical appearance of a white or almost white microcrystalline powder.

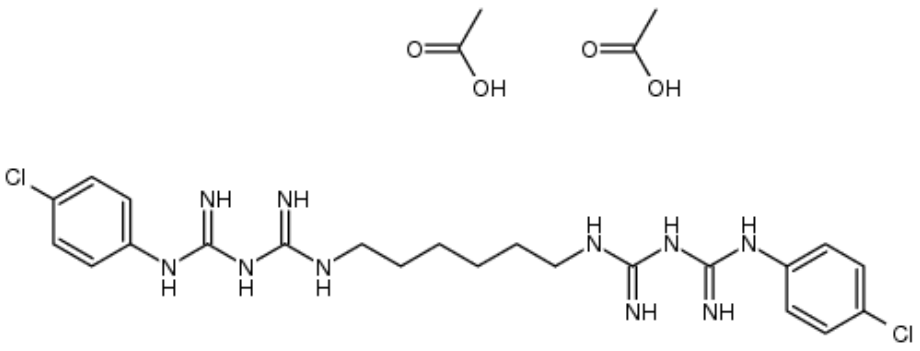

Figure 1.10 Molecular structure of chlorhexidine diacetate.

Even though chlorhexidine is reported to have high level of toxicity, studies conveyed its safety into the eye at concentrations up to 0.2% [99], while exposure to topical solution of 4% CHX would cause eye irritation and corneal edema [101].

Within the author knowledge, there are no chlorhexidine commercial collyriums to this date, however clinical use of CHX 0.02% eye drops are reported to treat infective keratitis [102] and *Acanthamoeba* keratits [103-105]. Rahman *et al*. reports the investigation of the treatment of fungal keratitis through the instillation of CHX 0.2% [85].

The therapy always involves the frequent instillation of drops for a prolonged time. Typically, the patient will instill one drop half hourly for the first 3 hours, then 1 hourly for 2 days, 2 hourly for 5 days, and 3 hourly for 2 weeks - a total of 3 weeks treatment [85].

1.4 Drug delivery by contact lenses

In the following sections, research in ocular drug delivery by contact lenses is reviewed, emphasizing the advantages and limitations of various methods attempted to improve drug release profiles. Primary approach relied on loading the drug into the contact lenses by soaking the hydrogels in a drug solution; more recently, different and more complex technologies were developed in order to improve the drug release kinetics.

1.4.1 Soaking of unmodified lenses in drug solution

Otto Wichterle, the inventor of soft, water-permeable contact lenses, was the first to envision SCLs as a vehicle for drug delivery [106]. Early attempts to transform SCLs into drug release vehicles relied on a very simple approach: soaking the commercial contact lenses in drug solution for long periods of time and then inserting the lenses into the eye. In 1970, Waltam *et al.* performed a preliminary *in vivo* study on rabbits, loading fluorescein solution (0.01%) into two types of commercial lenses, Bionite and Soflens, both hydrophilic materials. The presoaked lenses resulted in a 4-fold increase in drug concentration in the PoLTF, compared to a topical eye drops application posology, of one drop every 30 minutes, using the same concentration of fluorescein

[107]. In 1975, Hillman *et al.* tested pilocarpine-eluting lenses for the treatment of glaucoma. The human clinical response to intensive eye drops therapy of 4% pilocarpine solution (1 or 2 drops every 5 minutes for 30 minutes, then every 15 minutes for 90 minutes) was compared to the wearing of Sauflon lenses soaked in 1% pilocarpine solution. Presoaked contact lenses outperformed the eye drop therapy, demonstrating the higher bioavailability of pilocarpine delivered by contact lenses when compared to eye drops [108]. Since that time, researchers have tested many hydrogels materials and drugs *in vitro* and *in vivo* to better understand the mechanisms of drug release from soaked contact lenses. Drugs studied included: dexamethasone phosphate [109], antibiotics (chloromycetin, gentamicin, and carbenicillin) [110], gentamicin, kanamycin, tobramycin, ciprofloxacin, and floxacin [111], in humans; lomefloxacin in rabbits [111]; timolol [112], dexamethasone [113], cromolyn sodium, ketotifen fumarate, ketorolac tromethamine and dexamethasone sodium phosphate [114] *in vitro*.

Although this research stretches back decades, no commercial products have been released to the market so far. The main reason relies on the short duration of drug release from the unmodified commercial contact lenses. Within the several drug/lens combinations studied, the total release duration takes from few minutes to several hours. Although this represents an improvement over eye drop performances, it has not been sufficient to convince pharmaceutical companies to adopt this ocular drug delivery platform. To overcome the lack of this type of products in the ophthalmological therapeutic arsenal, several clinicians prescribe the application of eye-drops in association with the use of SCLs. This improves the drugs permeation and absorption through the cornea but still requires the patient's compliance and ability to self-administer the medicine.

In Chapter 2, the drug soaking approach has been investigated on the two types of hydrogels used in commercial SCLs: conventional hydrogels, and silicone hydrogels.

1.4.2 Molecular imprinted contact lenses

Molecular imprinting permits to improve the loading capacity of the drug in the hydrogel, increasing the partitioning of a solute into the matrix of the gel. This method was originally designed for highly crosslinked plastics, to remove specific molecules out of solutions [115]. Giving the not highly cross-linked nature of hydrogels, the

adaptation of this technique to SCLs is not straight forward. The idea behind this technique is to create cavities in the SCLs matrix with high affinity to specific drug molecules.

Figure 1.11 shows a schematic representation of the imprinting steps [116]. All the components (drug template that will create the cavities, functional monomers, crosslinker, and initiator), get self-assembled into the prepolymerization complex through covalent and non-covalent bounds. The polymerization occurs by crosslinking, which is activated by UV light or heat and the desired arrangement is obtained. The unreacted monomers and the template are extracted in order to create drug-recognizing cavities that have high affinity towards the template drug molecules. Once the cavities are formed, the drug molecules are reloaded into the polymer by soaking in an aqueous solution. During the drug release process, firstly the unbound drug molecules diffuse out of the lens, consequently the bound drug desorbs to maintain equilibrium inside the matrix and finally diffuses to the exterior [116-119].

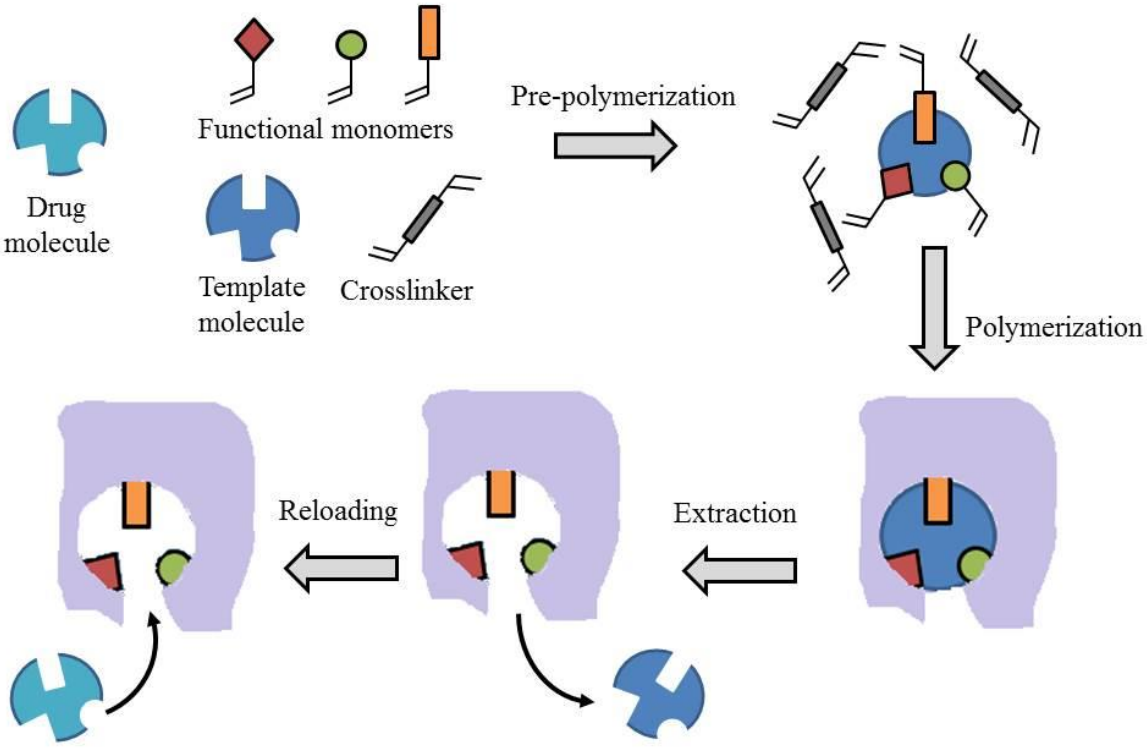

Figure 1.11 Schematic representation of molecular imprinting process

The key factors in these processes are the functional monomers which have to be compatible with the lens composition requirements to ensure e.g. biocompatibility, transparency, adequate mechanical properties. Furthermore, the monomers have to exhibit a strong affinity to the template drug, through hydrogen bond, hydrophobic or ionic interactions [116]. Based on this criteria, acrylic acid (AA), acrylamide (AM), methacrylic acid, methyl methacrylate and N-vinyl pyrrolidone have been studied as functional monomers in *in vitro* tests for the release of different molecules [120-125]. The importance of the ratios functional monomer/template and functional monomer/cross linker have been proved [126].

Timolol, the glaucoma treatment drug, is the most commonly studied drug in the molecular imprinted approach [123, 126-129]. In their experiments, Hiratani and Lorenzo obtained an increased loading capacity of the imprinted lenses of 3-fold, compared to the non-imprinted [123]. Alvarez Lorenzo *et al.* increased 300 times the antibiotic norfloxacin loading capacity of a PHEMA hydrogels [122]. Byrne *et al.* studied the antiallergenic ketotifen fumarate release from imprinted gels, and obtained a 6-fold increase in the loading amount, utilizing 4 functional monomers [121]. All those drugs are small molecules, in the range of 300-500 Dalton. However, other research groups have been trying to imprint larger molecules. Namely, Ali and Byrne designed a daily disposable contact lens that releases the comfort agent hyaluronic acid (1.2 million Dalton) [120], and White *et al.*, designed a silicone hydrogel capable to release another comfort agent, hydroxypropyl methylcellulose, along 50 days, thanks to the molecular imprinting method. [125].

Table 1.5 presents a summary of the recent studies on imprinted drug eluting contact lenses, including the experimental details.

Table 1.5: Summary of studies with molecular imprinted hydrogels used in drug delivery for contact lenses. Adapted from [130].

Principal monomer	Functional monomers	Drugs (template molecules)	Comments	Reference
HEMA	MAA, MMA*	Timolol	The drug capacity of the imprinted hydrogel increased 3-fold. Timolol released for more than 12 hours. Gel thickness was 0.7 mm	[131]
DEAA*	MAA	Timolol	The influence of the crosslinker, EGDMA concentration (10 to 280 mM) was studied.. Imprinted hydrogels (>80 mM EGDMA) presented a 10 fold higher loading drug capacity and were able to prolong timolol release, in 0.9% NaCl aqueous solution, for more than 24 h. Gel thickness was 0.3 mm.	[123]
DEAA, HEMA, SiMA*/DMAA* (50:50 v/v), MMA/DMAA (50:40 v/v)	MAA	Timolol	The influence of the composition of soft contact lenses on the molecular imprinted hydrogels was studied. The values of diffusion coefficients confirmed that timolol molecules move out easily from hydrophilic networks that present low affinity for the drug; i.e.MMA/DMAA and SiMA/DMAA lenses. Gel thickness was 0.3 mm.	[127]
DEAA	MAA	Timolol	*In vivo* study on rabbit of timolol imprinted soft contact lenses. The drug capacity of the imprinted lenses increased 1.6-fold, and the time release was twice longer than the non-imprinted lenses. Gel thickness was 0.08 mm.	[128]
DMAA/TRIS* (50:50 v/v)	MAA	Timolol	Influence of the ratio MAA/timolo (M/T) on the release performance was studied. M/T in the range 16-32 had drug diffusion coefficients two orders of magnitude lower than those of non-imprinted hydrogels. Gel thickness was 0.3 mm.	[126]
HEMA	AA, VP*	Norfloxacin	Influence of the M/T, AA/drug= 3 and 4, had the best release profiles (at least 24 hours) and a 2-fold increment of the loading capacity.	[122]
HEMA	VP, APMA*	Ibuprofen, diclofenac	The drug capacity of the imprinted hydrogel increased 10-fold, but less than 10% of the loaded drugs were able to diffuse in water. Gel thickness was 0.9 mm.	[59]
HEMA	AA, AM, NVP	Ketotifen fumarate	They tested multiple functional monomers combinations and obtained a 8-fold reduction in diffusivity.	[121], [132]
Nelfilcon A formulation with modified PVA* macromer	AM, NVP, DEAEM*	Hyaluronic acid	The imprinted lenses had a reduced hyaluronic acid diffusivity of a 1.6-fold.	[120]
HEMA	AA	Timolol	Influence of the M/T (6, 8, 12, 16, 32). With M/T=6 and 8, longest release duration (>1 day) was achieved. Gel thickness was 0.2 mm	[129]
HEMA, NVP/DMA*	Zinc, methacrylate, zinc nitrate hexahydrate, 1VI*, 4VI*, HEAA	Acetazolamide, ethoxzolamide	PHEMA zinc methacrylate imprinted hydrogel was opaque and not suitable for contact lenses use. The NVP-co-DMA imprinted with 4VI, HEAA and zinc nitrate, was transparent and had a 2-fold increment in drug loading. The release duration was 9 hours for acetazolamide and one week for ethoxzolamide. Gel thickness 0.9 mm.	[133], [134]
Betacon macromere/TRIS/DMA	AA	Hydropropyl methylcellulose	The imprinted lenses were able to release for 50 days and at a constant rate of 16 μg/day.	[125]

Principal monomer	Functional monomers	Drugs (template molecules)	Comments	Reference
HEMA	MAA	Prednisolone acetate	Different M/T were tested and M/T=4 revealed the best loading capacity (about 2-fold increment) and 48 hours of release duration.	[124]
HEMA	AA/AM/NVP	Ketotifen fumarate	*In vivo* study on rabbit. The imprinted lenses showed a 50-fold increase in mean residence time in the cornea, compared with the eye drops.	[135]
HEMA	DEAEM	Dicoflenac sodium salt	They tested two *in vitro* methods: sink conditions, and physiological flow rate. Different M/T were tested and M/T=10.5 revealed the best for the release duration, which gave a 3-fold increase. The loading capacity increased of a 5-fold, regardless of the M/T.	[136]
HEMA/TRIS	AA	Ciprofloxacin	Imprinted gels extended the release to 3-14 days.	[137]

* *n,n*-diethylacrylamide (DEAA); *n,n* -dimethylacrylamide (DMMA); *n*-(3-aminopropyl) methacrylamide (APMA); 2-(diethylamino) ethyl methacrylate (DEAEM); 1-vinylimidazonle (1VI); 4-vinylimidazole (4VI); *n*-hydroxyethyl acrylamide (HEAA).

Recently, a new approach has been studied to molecularly imprint the contact lenses without modifying the polymer composition. Yanez *et al.* imprinted drug cavities in fully polymerized gel, forcing the penetration of the drug into the matrix under super critical carbon dioxide (CO_2) pressure [138] (more details about the definition of super critical fluids (SCFs) can be found in Chapter 6). In this study, flurbiprofen, a nonsteroidal anti-inflammatory drug, was loaded into the contact lenses under super critical fluid conditions, and it is subsequently extracted and reloaded, repeating this cycle 3 times. Similar to the previously described molecular imprinting technique, the application of sequential flurbiprofen impregnation and extraction steps resulted in the rearrangement of some polymeric regions of the SCLs, creating effective and specific cavities, with the ability to chemically and structurally recognize the drug. After the 3 cycles of treatments, the loading capacity increased 450% and the release duration increased about 3-fold, but the amount released represented only 6% of the loaded drug, being this a strong drawback. In a similar study, Costa *et al.* increased timolol [139] and flurbiprofen [140] loading capacity of commercial contact lenses using impregnation by supercritical fluid technique.

1.4.3 Interaction between drug and matrix

Hydrogen bond, host-guest interactions, and electrostatic interactions between the drug and the matrix, can promote the loading and the controlled release of the drug [141-149].

Thanks to these interactions, the partitioning of the drug into the hydrogel can be increased, and hydrogels able to maximize the adsorption of the drug can be designed.

Sato *et al.* fabricated two types of PHEMA hydrogels: one containing cationic functional groups to deliver anionic drugs and the other containing anionic functional groups to deliver cationic drugs, see Figure 1.12.

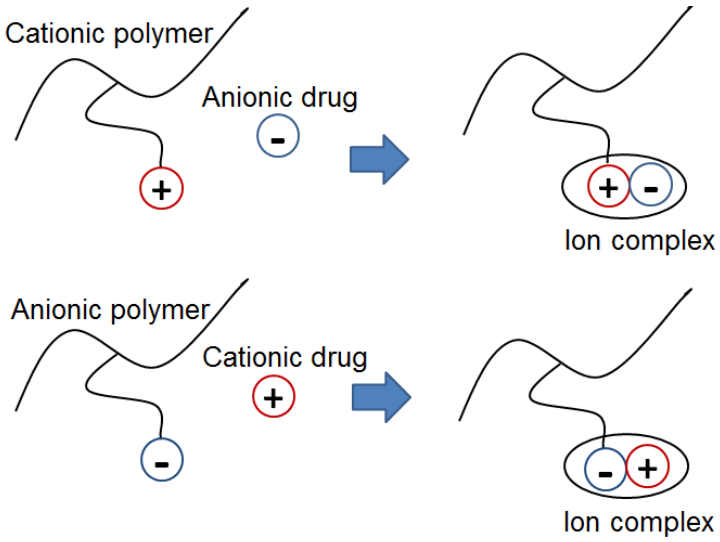

Figure 1.12 Uptake process of drugs by hydrogels with ionic groups.

In the first case, PHEMA lenses were synthetized by incorporating the cationic chains of methacrylamine propyltrimethylammonium chloride (MAPTAC) into the gel, in order to deliver the anionic anti-inflamatory drug azulene. The drug release experiments were performed in saline solution, and the hydrogels released azulene for about 8 hours. In the second case, PHEMA hydrogel was synthetized by incorporating the anionic chains of MAA and methacryloyloxyethyl phosphate (MOEP). The cationic vasoconstrictor, naphazoline, was tested and its uptake was reported to be proportional to the fraction of the anionic ligands in the hydrogel [145].

Yamazaki *et al.* explored the drug interaction and release of the antibiotic ofloxacin from the anionic silicone hydrogels, whose composition was MAA and 2-methacryloyloxyethyl hydrogen succinic acid, and 3-methacryloxypropyl tris(trimethylsiloxy)silane. This study reports an increase in the drug-hydrogel ionic interactions, and an increase in the drug release duration, probably due to the reduction in transport of water, which is required for the solvation of the drug [149].

In vivo studies on rabbits were performed by Xu *et al.*, who synthetized a PHEMA hydrogel incorporating NVP. The uptake and drug release of the puerarin, an anti-oxidant drug with anti-inflammatory power that is used to alleviate glaucoma, was explored. The presence of NVP increased the drug uptake due to the interaction of the OH groups of the drug and the carbonyl group of PVP. The *in vivo* test showed a 6-fold increase in the residence time of the drug in the rabbit tears, compared to eye drops instillation [150].

In a more recent *in vivo* study performed on rabbits by Kakisu *et al.*, the release of two antibiotics (gatifloxacin and moxifloxacin), whose activity has been proved against *S. aureus*, was tested from a PHEMA lens containing the anionic MAA. The complementary *in vitro* experiments showed that the ionic lens increased the uptake of both antibiotics in a proportional way to the amount of MMA incorporated in the matrix, and presented an extended release of 2-3 days. The *in vivo* study results reported higher drugs concentrations in the rabbit cornea, aqueous humor, and crystalline lens in the case of loaded SCLs compared to eye drops instillation [151].

All the studies previously presented in this section incorporate ionic molecules before the polymerization occurs, which may lead to changes in the structure and in the SCL properties, such as transmittance and tensile modulus. For this reason, a different approach was proposed by Bergani and Chauhan [152], based on the incorporation of ionic surfactants. Adequate surfactants can be loaded into the polymerized hydrogel and interact with the drugs, thus increasing the partitioning and decreasing the drug diffusion. Cationic surfactant, benzyldimenthylhexadecylammonium chloride (CAC) and subsequently dexthametasone phosphate were loaded into PHEMA hydrogel and commercial lenses (1-Day Acuvue®). From the results, the authors concluded that the release duration increased by 100-fold in the PHEMA lens and 10-fold in the commercial lenses, without interfering with the lenses properties [152].

Table 1.6 reports different studies focused on ionic interactions between drug and the matrix.

Table 1.6: Summary of studies with ionic interactions used in drug delivery for contact lenses. Adapted from [130].

Principal monomer	Functional monomers	Drugs	Comments	Reference
PHEMA	MAA - anionic MOEP - anionic MAPTAC – cationic	Azulene - anionic	Extended release of 8 hours of azulene, thanks to the incorporation of MAPTAC, addition of the anionic MAA and MOEP to prevent swelling of the lens due to the cationic monomer	[146]
PHEMA	NVP MA	Puerarin	In this case the interactionis between the group OH- of the drug and the carbonyl group of PVP. The best extended release achieved was with 5% MA and no NVP, the 80% of drug released in the first 2-3 hours, the rest over next 8 hours. The presence of NVP would lead to higher drug uptake and release rate.	[150]
PHEMA	MOEP - anionic MAA - anionic	Naphazoline - cationic	Extended release of 3 and 9 hours of naphazoline, in the case of the incorporation of MAA and MOEP respectively	[145]
PHEMA	MAA – anionic MOESA – anionic MAPTAC –cationic MPTS – sylis group	Ofloxacin - cationic	The best extended release achieved was of 70 hours, in the case of the incorporation of 10% MAA and 15% MPTS*	[149]
PHEMA	MAA – anionic MAPTAC –cationic	Gatifloxacin – cationic Moxifloxacin - cationic	Extended release during 24 hours unsing MAA. *In vivo* experiments revealed higher bioavailability of the drug released by the lenses than the eye drops.	[151]
PHEMA	CAC – cationic surfactant	Dexathamethasone phosphate- anionic	Increasing the percentage of CAC increased th release duration, 20% of CAC would result in a 5 days release predicted duration	[152]

*MPTS: (3-mercaptopropyl)trimethoxysilane

1.4.4 Nanostructures

Colloidal carriers have been used and exploited for extended drug delivery in ocular, oral, intravenous, and transdermal applications [2, 153]. Recent studies focused on the applications of colloidal carriers, such as liposomes, and nanoparticles, to ophthalmic drug delivery, through their incorporation into the matrix of the contact lenses. In order to maintain the transparency of the gel, the dimensions of the colloidal structures have to be adequate (<415 nm [154]) and the particles must be homogeneously distributed into the matrix. Nanostructures can increase the drug partitioning in the hydrogel matrix, thus reducing the effective diffusivity. The drug must first migrate through the particle, penetrate the particle surface to reach the hydrogel matrix, and finally diffuse through and outside the gel. For this reason, colloidal carriers are expected to increase drug release durations.

Liposomes are composite structures usually made of phospholipids. Thanks to their good biocompatibility, low toxicity and capacity to incorporate hydrophilic and

hydrophobic drugs, have received widespread attention as carrier systems for therapeutically active compounds [155]. Gulsen *et al.* achieved drug controlled release through the dispersion of dimyristoylphosphatidylcholine (DMPC) liposomes into PHEMA hydrogel, studying lidocaine, a common local anesthetic. The drug was released with an initial burst, which corresponded to 15-30% of the drug, due to the free drug, followed by a sustained release over 6 days. The transparency of the PHEMA lens was affected by the presence of the liposomes, decreasing from 90% of the pure PHEMA gel to 80%. [156]. Danion *et al.* proposed the immobilization of liposomes on the surface of commercial contact lenses, and obtained a prolonged release of carboxyfluorescein along more than 10 days [157]. In a very similar study, the same group studied the release of levofloxacin drug from commercial contact lenses with surface immobilized liposomes, obtaining a 30 hours drug release in the case of 2 liposomes layers, and 5 days in the case of 5 or 10 layers of liposomes. In this study the antibacterial activity of the drug was successfully verified after the drug release, but the oxygen permeability decreased [158]. The liposome immobilization process has the disadvantage of being complex and very time consuming. However, because of the technique's success in prolonging release times the investigation of the effect of liposome layers on the LVF release from PHEMA hydrogels was attempted and is reported in Chapter 5 of this thesis. In the experiments reported in this chapter, a layer of liposomes will be adsorbed on the surface of PHEMA, avoiding the long lasting immobilization process proposed by Danion [158].

Jung and Chauhan studied the control release of timolol from PHEMA hydrogels by covalently attaching timolol to propoxylated glyceryl triacrylate (PGT) nanoparticles (3.5 nm size). The nanoparticles were added to the polymerizing medium resulting in particle dispersion in the hydrogel matrix. The particle laden hydrogels released timolol for 30 days at room temperature; increasing the temperature led to a decrease of the drug release times, while changing the gel thickness had no effect on the release profiles. Those facts proved that the drug release processes were controlled by the particles and thermally activated [159]. In a similar study Jung *et al.* embedded the same timolol nanoparticles into silicone hydrogels, suitable for extended wear, and into silicone commercial contact lenses, by soaking the contact lenses into a nanoparticles solution [160]. The drug release results confirmed those obtained from the previous study; however, it was verified that nanoparticle incorporation origins reduction in ion

and oxygen permeabilities of the hydrogel, and an undesired increase in tensile modulus [160]. *In vivo* preliminary tests on beagles were successfully conducted [160].

Gulsen and Chauhan proposed delivering lidocaine using nanoparticles obtained through a microemulsion of hexadecane oil and Brij 97 surfactant, and the addition of silica shells to stabilize the structures. The drug release profiles presented a 7-8 days sustained drug release, with an initial burst release of 50% of the total drug; the burst was due to the not-encapsulated drug. Furthermore the samples were 1 mm thick i.e. much thicker than the commercial contact lenses [161]. In a similar study, lidocaine release was studied with the incorporation of microemulsion of canola oil into the polymerizing mixture. The microemulsion was stabilized by a nonionic surfactant and emulsifier, tween 80, often used in foods and cosmetics, and silica shells were added, to further prolong the drug release. The obtained hydrogel was opaque, likely due to the destabilization of the microemulsion during polymerization. The transparency loss was minimized by using Brij 97 as surfactant, but the drug release profiles obtained presented a burst and a release for few days [162].

More studies on the incorporation of drug loaded nanoparticles into hydrogel matrix were done by Ferreira *et al.* [163]. Anti-inflamatory flurbiprofen silicone coated nanoparticles, were prepared and incorporated, together with the surfactant Brij 35, into PHEMA -co-methacrylic acid hydrogels. This method resulted in an undesirable burst release of the drug, followed by 8 days of controlled release [163]. A mathematical model confirmed that this was the expected pattern of release [163].

Chapter 6, presents the results obtained through the investigation on the production of nanoparticles containing LVF, for ophthalmologic drug release use.

All previous approaches consisted in two-step based methods: preparation and incorporation of nanostructures, which may represent a drawback, being a time consuming process. To avoid these steps Kapoor *et al.* presented two studies in which the non-ionic surfactant (Brij 97, Brij 98, Brij 78) and the drug (different drugs were tested, Cyclosporine A, dexamethasone, dexamethasone acetate) were added straight into the polymerization solution. The surfactant self-assembled into 50-100nm size surfactant aggregates (see Figure 1.13), and permitted a 5-fold increase of the drug

release times compared to pure PHEMA gels, due to the higher partitioning of the drug into the particles than in the matrix [164, 165].

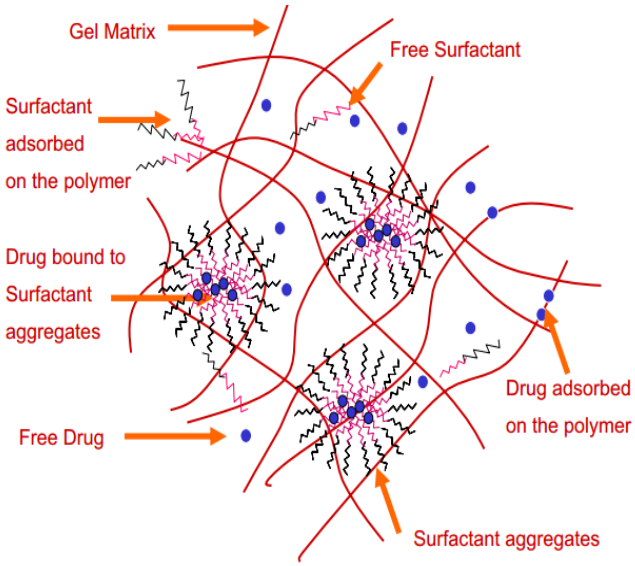

Figure 1.13 Representation of the microstructure of the surfactant-laden gels, [164]

To avoid premature drug release in contact lens storage solution, Kim *et al.* presented an innovative work using nano-diamonds as drug delivery vehicles. Nano-diamonds-embedded PHEMA contact lens were tested, and were able to perform a triggered release, eluting timolol only in the presence of lysozyme, an enzyme present in the tear fluid [166].

Table 1.7 presents recent studies of the potential of nanostructures in the ophthalmic drug delivery research world.

Table 1.7 Summary of studies with nanostructures used in drug delivery for contact lenses. Adapted from [130]

Principal monomer	Nano structure	Drugs	Comments	Reference
pHEMA	DMPC liposomes	Lidocaine	Incorporation of liposomes in the gel, initial burst followed by a sustained release over 6 days. Loss of 10% of transparency of the gel.	[156]
Hioxifilcon B	PEG*-biotinylated lipids	Carboxy-fluorescein dye	Liposomes layer on hydrogel, initial burst followed by a sustained release over 10 days.	[157]
pHEMA-MAA	Rod like silica shell cross-linked MPEG-b-PCL* micelles	Dexamethasone acetate	The effect of the presence of the silica shell was studied, even though it would improve the release profiles. This system would release the 60 % of drug within 8 hours.	[167]

Principal monomer	Nano structure	Drugs	Comments	Reference
pHEMA	Brij 98 micelles	Cyclosporine A	Different % of surfactants were tested, the 2% showed a 7-8 days of drug controlled release, while the 8% 16 days.	[165]
pHEMA	Brij 97, Brij 98, Brij 78 and Brij 700 micelles	Cyclosporine A, dexamethasone (DMS), dexamethasone acetate (DMSA)	Brij 78 seems most promising surfactant. Gels showed promising results for the drug CyA*, but not for DMS and DMSA.	[164]
pHEMA	Hexadecane micro emulsion stabilized with silica shell	Lidocaine	Strong burst (50% of drug) release within the first hours. 80% of drug was released by day 5.	[161]
pHEMA	Brij 35 stabilized with silica shell	Lidocaine	Burst release (35% of drug) within the first hours. 80% of drug was released by day 4.	[162]
pHEMA-co-MAA	Silicone nanoparticles	Flurbiprofen	Initial burst and a sustained drug release along 8 days, release profiles were fitted to a mathematical model.	[163]
pHEMA	Cross linked PGT nanoparticles	Timolol	The hydrogels released the drug within 3-4 days, and the process was temperature sensitive.	[159]
pHEMA	cross-linking PEI*-coated nanodiamonds	Timolol	The drug release is triggered by the presence of the enzyme in the eyes. The researchers verified the bioactivity of the drug after the release.	[166]

* Polyethylene glycol (PEG); polyethylenimine (PEI); cyanuric acid (CyA); polycaprolactone (PCL).

1.4.5 Hydrophobic interactions

Recently Chauhan *et al.* have demonstrated that vitamin E nano-barriers can be created inside silicone hydrogels [63, 67, 69, 168-171]. The drug release duration scales as h^2/D_{eff}, where h is the thickness of the gel and D_{eff} the effective diffusivity of the drug in the gel. Since increasing the thickness would decrease the ion and oxygen permeability, Chauhan *et al.* used the presence of the vitamin E nano-barriers to force the drug molecules to diffuse around the barriers, and so increase their path, increasing subsequently the drug release duration times [63, 67, 69, 168-171] (see Figure 1.14). Chauhan studies were performed on commercial silicone contact lenses, where vitamin E aggregates would form thanks to the biphasic structure of these materials. Moreover, this antioxidant molecule was chosen because it has a minimal impact on the oxygen permeability of the lenses.

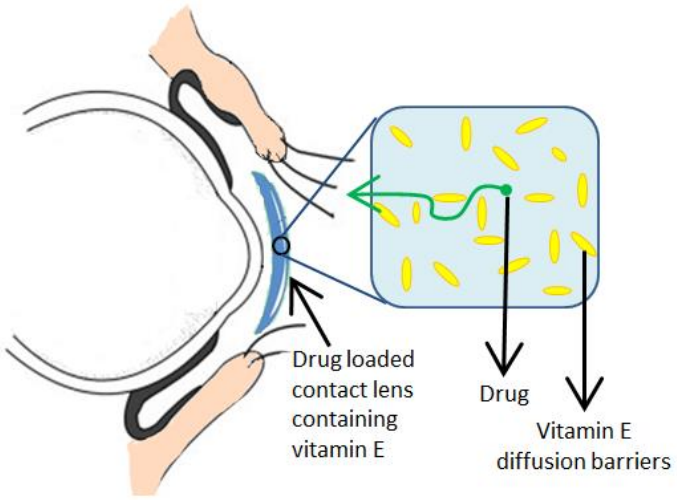

Figure 1.14 Schematic representation of the drug diffusion mechanism into vitamin E loaded contact lenses. Adapted from [18]

Because vitamin E is hydrophobic, it facilitates the steady release of hydrophilic drugs through nano-barriers. The first study published by Chauhan *et al.* focused on release of hydrophilic drugs, namely, timolol, dexamethasone phosphate, and the antifungal fluconazole. Each drug had a slightly different release time due to differences in molecular weight and partitioning in the matrix, however, the release time of all three increased 5- and 40-fold, for 10 and 40% of vitamin E respectively [69, 170]. Subsequent studies verified that vitamin E nano-barriers also decrease the effective diffusivity of hydrophobic drugs, such as dexamethasone and cyclosporine. However, due to the fact that the drug diffuses through the vitamin E aggregates, hydrophobic drug's release duration increase is smaller compared to the one obtained in the case of the hydrophilic drugs aggregate [168, 169]. Amphiphilic drugs were investigated in another study where it was hypothesized the adsorption of the drugs (anesthetics) on the nano-barriers [63]. Recently, silicone contact lenses containing vitamin E were proposed to control the release of cysteamine for the treatment of cystinosis [67]. *In vivo* studies were performed to test the efficacy of vitamin E loaded lenses impregnated with timolol on glaucoma affected beagles. The efficacy and safety of the contact lenses were proved along 4 days [171].

Table 1.8 presents some results from the most successful studies performed by Chauhan group on drug delivery by silicone contact lenses loaded with vitamin E.

Table 1.8 Summary of studies with vitamin E loaded (20% w/w) silicone hydrogels. Adapted from [130].

Drug	Drug character	Commercial contact lens	Release duration (sink conditions)	Release time ratio (20% vit E/ control)	Reference
Timolol	Hydrophilic	Acuvue Oasys	~ 24 h	~ 20	[69, 170]
Fluconazole	Hydrophilic	Acuvue Oasys	~ 70 h	~ 24	[170]
Dexamethasone phosphate	Hydrophilic	Acuvue Oasys	~540 h	~ 30	[170]
Dexamethasone	Hydrophobic	Acuvue Oasys	~ 96 h	~ 14	[168]
Cyclosporine A	Hydrophobic	Acuvue Oasys	> 50 days	~ 7	[169]
Lidocaine	Amphiphilic	O_2 Optix	~ 4 h	~2.2	[63]
Tetracaine	Amphiphilic	O_2 Optix	~ 10 h	~3	[63]
Bupivacaine	Amphiphilic	O_2 Optix	~ 8 h	~2.2	[63]
Cysteamine	Hydrophilic	Acuvue Oasys	~3 h	~ 28	[67]

In this thesis, the vitamin E incorporation approach will be investigated on the release of LVF and CHX drugs from commercial contact lenses. The studies were performed at the University of Florida, under the supervision of Professor Anuj Chauhan. The results are shown in Chapter 4.

Cyclodextrins (CDs) are "host" hydrophobic molecules that represent a cavity for "guest" drug molecules, and have recently been investigated as drug delivery promoters [143, 144]. Dos Santos *et al.* investigated the potential of CDs in the drug eluting contact lenses field [142]. PHEMA gels were synthetized and β-cyclodextrin (β -CD) was attached, without interfering in the network formation, and without altering the matrix structure. The presence of β-CDs increased the uptake of dicloflenac by 1300%, and permitted a drug release for up to 2 weeks, against the 1 day of the control [142]. In a similar study, Xu *et al.* incorporated β-CDs in PHEMA hydrogels to tailor release profiles of puerarin, which complexes with β -CDs. A 40% increase in the drug uptake of the lenses was described together with an increase in the release time from 1 to 10 hours, without altering of the hydrogel properties. *In vivo* experiments on rabbits were conducted, showing that puerarin loaded contact lenses permitted a measurable drug concentration in tears for about 4 hours against the 30 minutes obtained by eye drop instillations [148].

1.4.6 Multilayer contact lenses

In the approach made by Ciolino *et al.*, a poly(lactic-co-glycolic) acid (PLGA), which is a biodegradable polymer well known for its biocompatibility and its ability to control drug-release kinetics [172], was used to create films containing drugs. These films were then sandwiched between PHEMA layers (see Figure 1.15). This method allows to decrease or eliminate the burst effect and to obtain a continuous zero-order kinetics of drug release [172].

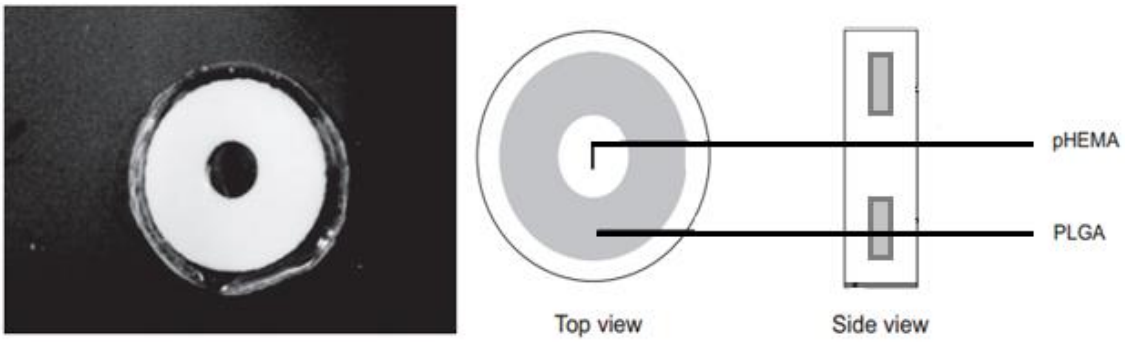

Figure 1.15 Photograph on the left, and schematic design of the PHEMA hydrogel coating the drug containing PLGA film, the central aperture has Ø 5 mm [173]

Ciprofloxacin, fluorescein and econazole, the latter being active against *Candida albicans* fungi, were tested and release times of one month were obtained [173, 174]. The main drawbacks of this approach are the opacity of the inner PLGA film, and the necessity of a central aperture on the contact lenses, which can be uncomfortable for the patient. Recently, *in vivo* studies on rabbits were performed testing PLGA sandwiched lenses eluting latanoprost, a drug active against glaucoma. The results showed how the contact lens appeared safe in both cell culture and animal studies [175].

1.5 References

1. D. Ghate and H.F. Edelhauser, *Ocular drug delivery.* Expert Opin Drug Deliv, 2006. **3**(2): p. 275-87.
2. R. Gaudana, H.K. Ananthula, A. Parenky and A.K. Mitra, *Ocular drug delivery.* AAPS J, 2010. **12**(3): p. 348-60.
3. S.S. Chrai, M.C. Makoid, S.P. Eriksen and J.R. Robinson, *Drop size and initial dosing frequency problems of topically applied ophthalmic drugs.* J Pharm Sci, 1974. **63**(3): p. 333-8.
4. M.H. Friedlaender, D. Breshears, B. Amoozgar, H. Sheardown and M. Senchyna, *The dilution of benzalkonium chloride (BAK) in the tear film.* Adv Ther, 2006. **23**(6): p. 835-41.
5. C.L. Bourlais, L. Acar, H. Zia, P.A. Sado, T. Needham and R. Leverge, *Ophthalmic drug delivery systems--recent advances.* Prog Retin Eye Res, 1998. **17**(1): p. 33-58.
6. J. Larke, *Tears*, in *The eye in contact lens wear*, L. Larke, Editor. 1995, Butterworth Heinemann, Oxford: Boston. p. 30.
7. N. Yokoi and A. Komuro, *Non-invasive methods of assessing the tear film.* Exp Eye Res, 2004. **78**(3): p. 399-407.
8. H. Zhu and A. Chauhan, *A mathematical model for ocular tear and solute balance.* Curr Eye Res, 2005. **30**(10): p. 841-54.
9. A. Urtti, *Challenges and obstacles of ocular pharmacokinetics and drug delivery.* Adv Drug Deliv Rev, 2006. **58**(11): p. 1131-5.
10. L. Salminen, *Review: systemic absorption of topically applied ocular drugs in humans.* J Ocul Pharmacol, 1990. **6**(3): p. 243-9.
11. M.R. Prausnitz and J.S. Noonan, *Permeability of cornea, sclera, and conjunctiva: a literature analysis for drug delivery to the eye.* J Pharm Sci, 1998. **87**(12): p. 1479-88.
12. M.A. Watsky, M.M. Jablonski and H.F. Edelhauser, *Comparison of conjunctival and corneal surface areas in rabbit and human.* Curr Eye Res, 1988. **7**(5): p. 483-6.
13. A.B. Trawick, *Potential systemic and ocular side effects associated with topical administration of timolol maleate.* J Am Optom Assoc, 1985. **56**(2): p. 108-12.

14. A.A. Al-Kinani, G. Calabrese, A. Vangala, D. Naughton and R.C. Alany, *Nanotechnology in ophtalmic drug delivery*, in *Patenting Nanomedicines*, S. E.B., Editor. 2012, Springer-Verlag: Berlin Heidelberg. p. 277-303.
15. N. Kuno and S. Fujii, *Recent Advances in Ocular Drug Delivery Systems.* Polymers, 2011. **3**: p. 193-221.
16. N. Efron and C. Maldonado-Codina, *Development of Contact Lenses from a Biomaterial Point of View – Materials, Manufacture, and Clinical Application*, in *Comprehensive Biomaterials*, P. Ducheyne, Editor. 2011, Elsevier Science: Amsterdam. p. 517-541.
17. S. Anderson, *Health Management Systems*, in *Professional Practice for Foundation Doctors*, J. McKimm, K. Forrest, and A. Byrne, Editors. 2011, SAGE: Exeter.
18. August 2015]; Available from: http://caleblookeye.wikispaces.com/Internal+Structure+of+the+Eye.
19. N.A. McNamara, K.A. Polse, R.J. Brand, A.D. Graham, J.S. Chan and C.D. McKenney, *Tear mixing under a soft contact lens: effects of lens diameter.* Am J Ophthalmol, 1999. **127**(6): p. 659-665.
20. J.L. Creech, A. Chauhan and C.J. Radke, *Dispersive mixing in the posterior tear film under a soft contact lens.* Ind Eng Chem Res, 2001. **40**(14): p. 3015-3026.
21. A.S. Phillips, L, *Contact Lenses*. 1997, London: Butterworth-Heinemann.
22. N. Pritchard, L. Jones, K. Dumbleton and D. Fonn, *Epithelial inclusions in association with mucin ball development in high-oxygen permeability hydrogel lenses.* Optometry Vision Sci, 2000. **77**(2): p. 68-72.
23. N. Pritchard, D. Fonn and D. Brazeau, *Discontinuation of contact lens wear: a survey.* Int Contact Lens Clin, 1999. **26**(6): p. 157-162.
24. G. Young, J. Veys, N. Pritchard and S. Coleman, *A multi-centre study of lapsed contact lens wearers.* Ophthalmic Physiol Opt, 2002. **22**(6): p. 516-27.
25. N. Efron, *Contact Lens Practice*. 2nd ed. 2010, China: Butterworth-Heinemann.
26. J.E. Walsh, L.V. Koehler, D.P. Fleming and J.P. Bergmanson, *Novel method for determining hydrogel and silicone hydrogel contact lens transmission curves and their spatially specific ultraviolet radiation protection factors.* Eye Contact Lens, 2007. **33**(2): p. 58-64.

27. H.F. Mark, *Encyclopedia of Polymer Science and Technology, Concise*. 2013: Wiley.
28. C. Maldonado C, *Soft Lens Materials*, in *Contact Lens Practice*, N. Efron, Editor. 2010, Butterworth-Heinemann/Elsevier.
29. P.C. Nicolson and J. Vogt, *Soft contact lens polymers: an evolution.* Biomaterials, 2001. **22**(24): p. 3273-83.
30. J.A. Bonanno, T. Stickel, T.B. Nguyen, T., D. Carter, W.J. Benjamin and P.S. Soni, *Estimation of human corneal oxygen consumption by noninvasive measurement of tear oxygen tension while wearing hydrogel lenses.* Invest Ophthalmol Vis Sci, 2002. **43**(2): p. 371-6.
31. T.S. Koffas, A. Opdahl, C. Marmo and G.A. Somorjai, *Effect of equilibrium bulk water content on the humidity-dependent surface mechanical properties of hydrophilic contact lenses studied by atomic force microscopy.* Langmuir, 2003. **19**(8): p. 3453-3460.
32. R. Stone, *Why contact lens groups.* Contact Lens Spectr, 1988. **3**(12): p. 38-41.
33. N. Efron, N.A. Brennan, J.M. Currie, J.P. Fitzgerald and M.T. Hughes, *Determinants of the initial comfort of hydrogel contact lenses.* Am J Optom Physiol Opt, 1986. **63**(10): p. 819-823.
34. G. Young, *Evaluation of soft contact lens fitting characteristics.* Optom Vis Sci, 1996. **73**(4): p. 247-254.
35. F.J. Montes Ruiz-Cabello, M.A. Rodríguez-Valverde, A. Marmur and M.A. Cabrerizo-Vílchez, *Comparison of Sessile Drop and Captive Bubble Methods on Rough Homogeneous Surfaces: A Numerical Study.* Langmuir, 2011. **27**(15): p. 9638-9643.
36. R.J. Good, *Contact angle, wetting, and adhesion: a critical review.* Journal of Adhesion Science and Technology, 1992. **6**(12): p. 1269-1302.
37. P.L. Kaufman, A. Alm and F.H. Adler, *Adler's Physiology of the Eye: Clinical Application*. 2003: Mosby.
38. A.S. Bruce and N.A. Brennan, *Corneal Pathophysiology with Contact-Lens Wear.* Survey of Ophthalmology, 1990. **35**(1): p. 25-58.
39. D.M. Harvitt and J.A. Bonanno, *Re-evaluation of the oxygen diffusion model for predicting minimum contact lens Dk/t values needed to avoid corneal anoxia.* Optom Vis Sci, 1999. **76**(10): p. 712-719.

40. P.B. Morgan and N. Efron, *The oxygen performance of contemporary hydrogel contact lenses.* Cont Lens Anterior Eye, 1998. **21**(1): p. 3-6.
41. E.B. Papas, C.M. Vajdic, R. Austen and B.A. Holden, *High-oxygen-transmissibility soft contact lenses do not induce limbal hyperaemia.* Curr Eye Res, 1997. **16**(9): p. 942-8.
42. M. Millodot, *Effect of Soft Lenses on Corneal Sensitivity.* Acta Ophthalmologica, 1974. **52**(5): p. 603-608.
43. D. Austin and R.V. Kumar, *Ionic conductivity in hydrogels for contact lens applications.* Ionics, 2005. **11**(3-4): p. 262-268.
44. B. Tighe, *Silicone hydrogel materials—How do they work?*, in *Silicone Hydrogels: The Rebirth of Continuous Wear Contact Lenses*, D. Sweeney, Editor. 2000, Butterworth-Heinemann/BCLA: Oxford. p. 1-21.
45. J. Pozuelo, V. Compan, J.M. Gonzalez-Meijome, M. Gonzalez and S. Molla, *Oxygen and ionic transport in hydrogel and silicone-hydrogel contact lens materials: An experimental and theoretical study.* J Membrane Sci, 2014. **452**: p. 62-72.
46. C. Cerretani, C.C. Peng, A. Chauhan and C.J. Radke, *Aqueous salt transport through soft contact lenses: An osmotic-withdrawal mechanism for prevention of adherence.* Contact Lens Anterior Eye, 2012. **35**(6): p. 260-265.
47. P.C. Nicolson, R.C. Baron, P. Chabrecek, J. Court, A. Domschke, H.J. Griesser, A. Ho, J. Hopken, B.G. Laycock and Q. Liu, *Extended wear ophthalmic lens*. 1998, Patent number: US5760100 A.
48. C.E. Soltys-Robitaille, D.M. Ammon, Jr., P.L. Valint, Jr. and G.L. Grobe, 3rd, *The relationship between contact lens surface charge and in-vitro protein deposition levels.* Biomaterials, 2001. **22**(24): p. 3257-60.
49. L.N. Subbaraman, R. Borazjani, H. Zhu, Z. Zhao, L. Jones and M.D. Willcox, *Influence of protein deposition on bacterial adhesion to contact lenses.* Optom Vis Sci, 2011. **88**(8): p. 959-66.
50. J.L. Andreassi, *Psychophysiology: Human Behavior & Physiological Response*. 2013: Taylor & Francis.
51. A.C. Rennie, P.L. Dickrell and W.G. Sawyer, *Friction coefficient of soft contact lenses: measurements and modeling.* Tribol. Lett., 2005. **18**(4): p. 499-504.

52. S.H. Kim, C. Marmo and G.A. Somorjai, *Surface friction studies of hydrogel contact lenses using AFM: Non-crosslinked polymers at the surface.* Abstr Pap Am Chem Soc, 2001. **221**: p. U353-U353.
53. G. Hung, F. Hsu and L. Stark, *Dynamics of the human eyeblink.* Am J Optom Physiol Opt, 1977. **54**(10): p. 678-90.
54. N.A. Peppas, P. Bures, W. Leobandung and H. Ichikawa, *Hydrogels in pharmaceutical formulations.* Eur J Pharm Biopharm, 2000. **50**(1): p. 27-46.
55. C. Maldonado-Codina and N. Efron, *Hydrogel lenses - materials and manufacture. A review.* Optom Practice, 2003. **4**: p. 101-115.
56. J.F. Kuntzler, *Hydrogels*, in *Encyclopedia of Polymer Science and Technology, Concise*, H.F. Mark, Editor. 2007, Wiley. p. 557-562.
57. J. Jacob, *A - Biomaterials: Contact Lenses*, in *Biomaterials Science (Third Edition)*, B.D.R.S.H.J.S.E. Lemons, Editor. 2013, Academic Press. p. 909-917.
58. I. Tranoudis and N. Efron, *Water properties of soft contact lens materials.* Cont Lens Anterior Eye. **27**(4): p. 193-208.
59. P. Andrade-Vivero, E. Fernandez-Gabriel, C. Alvarez-Lorenzo and A. Concheiro, *Improving the loading and release of NSAIDs from pHEMA hydrogels by copolymerization with functionalized monomers.* J Pharm Sci, 2007. **96**(4): p. 802-13.
60. S.G. Lee, G.F. Brunello, S.S. Jang and D.G. Bucknall, *Molecular dynamics simulation study of P (VP-co-HEMA) hydrogels: effect of water content on equilibrium structures and mechanical properties.* Biomaterials, 2009. **30**(30): p. 6130-41.
61. M. Roba, E.G. Duncan, G.A. Hill, N.D. Spencer and S.G.P. Tosatti, *Friction Measurements on Contact Lenses in Their Operating Environment.* Tribol. Lett., 2011. **44**(3): p. 387-397.
62. R.J. Duffey and D. Leaming, *US trends in refractive surgery: 2003 ISRS/AAO survey.* J Refract Surg, 2005. **21**(1): p. 87-91.
63. C.C. Peng, M.T. Burke and A. Chauhan, *Transport of topical anesthetics in vitamin E loaded silicone hydrogel contact lenses.* Langmuir, 2012. **28**(2): p. 1478-87.
64. R. Autrata and J. Rehurek, *Laser-assisted subepithelial keratectomy for myopia: two-year follow-up.* J Cataract Refract Surg, 2003. **29**(4): p. 661-8.

65. C.P. Herbort, A. Jauch, P. Othenin-Girard, J.J. Tritten and M. Fsadni, *Diclofenac drops to treat inflammation after cataract surgery.* Acta Ophthalmol Scand, 2000. **78**(4): p. 421-4.
66. E. Tsilou, M. Zhou, W. Gahl, P.C. Sieving and C.C. Chan, *Ophthalmic manifestations and histopathology of infantile nephropathic cystinosis: report of a case and review of the literature.* Survey of Ophthalmology, 2007. **52**(1): p. 97-105.
67. K.H. Hsu, R.C. Fentzke and A. Chauhan, *Feasibility of corneal drug delivery of cysteamine using vitamin E modified silicone hydrogel contact lenses.* Eur J Pharm Biopharm, 2013. **85**(3 Pt A): p. 531-40.
68. R.J. Casson, G. Chidlow, J.P. Wood, J.G. Crowston and I. Goldberg, *Definition of glaucoma: clinical and experimental concepts.* Clin Experiment Ophthalmol, 2012. **40**(4): p. 341-9.
69. C.C. Peng, M.T. Burke, B.E. Carbia, C. Plummer and A. Chauhan, *Extended drug delivery by contact lenses for glaucoma therapy.* J Control Release, 2012. **162**(1): p. 152-8.
70. A.L. Coleman and S. Miglior, *Risk factors for glaucoma onset and progression.* Survey of Ophthalmology, 2008. **53 Suppl1**: p. S3-10.
71. H. Janumala, P.K. Sehgal and A.B. Mandal, *Bacterial Keratitis - Causes, Symptoms and Treatment*, in *Keratitis*, M. Srinivasan, Editor. 2012, InTech: Rijeka, Croatia. p. 15-30.
72. A. Al-Mujaini, N. Al-Kharusi, A. Thakral and U.K. Wali, *Bacterial Keratitis: Perspective on Epidemiology, Clinico-Pathogenesis, Diagnosis and Treatment.* Sultan Qaboos Univ Med J, 2009. **9**(2): p. 184-95.
73. P.G.A. J. G. Bartlett, P. A. Pham, *The ABX Guide: Diagnosis & Treatment of Infectious Diseases*. 2012, Burlington.
74. M.P. Upadhyay, M. Srinivasan and J.P. Whitcher, *Microbial keratitis in the developing world: does prevention work?* Int Ophthalmol Clin, 2007. **47**(3): p. 17-25.
75. D. Bremond-Gignac, F. Chiambaretta and S. Milazzo, *A European Perspective on Topical Ophthalmic Antibiotics: Current and Evolving Options.* Ophthalmol Eye Dis, 2011. **3**: p. 29-43.

76. M.D. Willcox, *Review of resistance of ocular isolates of Pseudomonas aeruginosa and staphylococci from keratitis to ciprofloxacin, gentamicin and cephalosporins.* Clin Exp Optom, 2011. **94**(2): p. 161-8.
77. M. Daniell, R. Mills and N. Morlet, *Microbial keratitis: what's the preferred initial therapy?* Br J Ophthalmol, 2003. **87**(9): p. 1167.
78. *http://www.oregon.gov/oha/pharmacy/therapeutics/docs/ps-2009-12-antibiotics-ophthalmic.pdf*.
79. R. Watanabe, T. Nakazawa, S. Yokokura, A. Kubota, H. Kubota and K. Nishida, *Fluoroquinolone antibacterial eye drops: effects on normal human corneal epithelium, stroma, and endothelium.* Clin Ophthalmol, 2010. **4**: p. 1181-7.
80. J.E.C. Lin and D. Welty, *Ocular pharmacokinetics of moxifloxacin after topical treatment of animals and humans.* Survey of Ophthalmology, 2006. **51**(5): p. 530-530.
81. J.J. Dajcs, B.A. Thibodeaux, M.E. Marquart, D.O. Girgis, M. Traidej and R.J. O'Callaghan, *Effectiveness of ciprofloxacin, levofloxacin, or moxifloxacin for treatment of experimental Staphylococcus aureus keratitis.* Antimicrob. Agents Chemother., 2004. **48**(6): p. 1948-52.
82. R.P. Kowalski, E.G. Romanowski, F.S. Mah, R.M.Q. Shanks and Y.J. Gordon, *Topical levofloxacin 1.5% overcomes in vitro resistance in rabbit keratitis models.* Acta Ophthalmologica, 2010. **88**(4): p. 120-125.
83. R.P. Kowalski, A.N. Pandya, L.M. Karenchak, E.G. Romanowski, R.C. Husted, D.C. Ritterband, M.K. Shah and Y.J. Gordon, *An in vitro resistance study of levofloxacin, ciprofloxacin, and ofloxacin using keratitis isolates of Staphylococcus aureus and Pseudomonas aeruginosa1.* Ophthalmology, 2001. **108**(10): p. 1826-1829.
84. H.R. Koch, S.C. Kulus, M. Roessler, A. Ropo and K. Geldsetzer, *Corneal penetration of fluoroquinolones: Aqueous humor concentrations after topical application of levofloxacin 0.5% and ofloxacin 0.3% eyedrops.* J Cataract Refract Surg, 2005. **31**(7): p. 1377-1385.
85. M. Rahman, G. Johnson, R. Husain, S. Howlader and D. Minassian, *Randomised trial of 0.2% chlorhexidine gluconate and 2.5% natamycin for fungal keratitis in Bangladesh.* Br J Ophthalmol, 1998. **82**(8): p. 919-25.

86. A.A. Dunlop, E.D. Wright, S.A. Howlader, I. Nazrul, R. Husain, K. McClellan and F.A. Billson, *Suppurative corneal ulceration in Bangladesh. A study of 142 cases examining the microbiological diagnosis, clinical and epidemiological features of bacterial and fungal keratitis.* Aust N Z J Ophthalmol, 1994. **22**(2): p. 105-10.
87. C.M. Phan, L. Subbaraman and L. Jones, *Contact lenses for antifungal ocular drug delivery: a review.* Expert Opin Drug Deliv, 2014. **11**(4): p. 537-46.
88. S.T. Awwad, W.M. Petroll, J.P. McCulley and H.D. Cavanagh, *Updates in Acanthamoeba keratitis.* Eye Contact Lens, 2007. **33**(1): p. 1-8.
89. R. Kumar and D. Lloyd, *Recent Advances in the Treatment of Acanthamoeba Keratitis.* Clin Infect Dis, 2002. **35**(4): p. 434-441.
90. B. Clarke, A. Sinha, D.N. Parmar and E. Sykakis, *Advances in the Diagnosis and Treatment of Acanthamoeba Keratitis.* J Ophthalmol, 2012. **2012**: p. 6.
91. M. Elder, J.G. Dart, S. Kilvington, D.V. Seal, J. Hay and C.M. Kirkness, *Chemotherapy for acanthamoeba keratitis.* The Lancet, 1995. **345**(8952): p. 791-793.
92. W. Mathers, *Use of higher medication concentrations in the treatment of acanthamoeba keratitis.* Arch Opthalmol (Chic.), 2006. **124**(6): p. 923-923.
93. B.D. Cookson, M.C. Bolton and J.H. Platt, *Chlorhexidine resistance in methicillin-resistant Staphylococcus aureus or just an elevated MIC? An in vitro and in vivo assessment.* Antimicrob Agents Chemother, 1991. **35**(10): p. 1997-2002.
94. A. Lambert, J.B. Regnouf-de-Vains and M.F. Ruiz-López, *Structure of levofloxacin in hydrophilic and hydrophobic media: Relationship to its antibacterial properties.* Chem Phys Lett, 2007. **442**(4–6): p. 281-284.
95. N.S. Gokhale, *Medical management approach to infectious keratitis.* Indian J Ophthalmol, 2008. **56**(3): p. 215-20.
96. K. Akahane, M. Kato and S. Takayama, *Involvement of inhibitory and excitatory neurotransmitters in levofloxacin- and ciprofloxacin-induced convulsions in mice.* Antimicrob Agents Chemother, 1993. **37**(9): p. 1764-70.
97. B.M. Lomaestro, *Fluoroquinolone-induced renal failure.* Drug Saf, 2000. **22**(6): p. 479-85.

98. M.T. Schwartz and J.F. Calvert, *Potential neurologic toxicity related to ciprofloxacin.* DICP, 1990. **24**(2): p. 138-40.
99. D.M. Foulkes, *Some Toxicological Observations on Chlorhexidine.* Journal of Periodontal Research, 1973: p. 55-57.
100. P.Y. Zeng, A. Rao, T.S. Wiedmann and W. Bowles, *Solubility Properties of Chlorhexidine Salts.* Drug Development and Industrial Pharmacy, 2009. **35**(2): p. 172-176.
101. M.M.A.N. Rudolph, *Ocular Toxicity of Intraoperatively Used Drugs and Solutions*. 1995, Amsterdam: Kugler.
102. *http://www.ekhuft.nhs.uk/staff/clinical/antimicrobial-guidelines/eye-guidelines/infective-keratitis/*.
103. D.V. Seal, *Acanthamoeba keratitis update-incidence, molecular epidemiology and new drugs for treatment.* Eye (Lond), 2003. **17**(8): p. 893-905.
104. P. Kosrirukvongs, D. Wanachiwanawin and G.S. Visvesvara, *Treatment of Acanthamoeba keratitis with chlorhexidine1.* Ophthalmology, 1999. **106**(4): p. 798-802.
105. D. Seal, J. Hay, C. Kirkness, A. Morrell, A. Booth, A. Tullo, A. Ridgway and M. Armstrong, *Successful medical therapy of Acanthamoeba keratitis with topical chlorhexidine and propamidine.* Eye (Lond), 1996. **10 (Pt 4)**: p. 413-21.
106. O. Wichterle and D. Lim, *Hydrophilic Gels for Biological Use.* Nature, 1960. **185**(4706): p. 117-118.
107. S.R. Waltman and H.E. Kaufman, *Use of hydrophilic contact lenses to increase ocular penetration of topical drugs.* Invest Ophthalmol, 1970. **9**(4): p. 250-5.
108. J.S. Hillman, J.B. Marsters and A. Broad, *Pilocarpine delivery by hydrophilic lens in the management of acute glaucoma.* Trans Ophthalmol Soc U K, 1975. **95**(1): p. 79-84.
109. M.R. Jain and V. Batra, *Steroid penetration in human aqueous with 'Sauflon 70' lenses.* Indian J Ophthalmol, 1979. **27**(2): p. 26-31.
110. M.R. Jain, *Drug delivery through soft contact lenses.* Br J Ophthalmol, 1988. **72**(2): p. 150-4.
111. E.M. Hehl, R. Beck, K. Luthard, R. Guthoff and B. Drewelow, *Improved penetration of aminoglycosides and fluorozuinolones into the aqueous humour of*

patients by means of Acuvue contact lenses. Eur J Clin Pharmacol, 1999. **55**(4): p. 317-23.

112. C.C.C. Li, A. , *Ocular transport model for ophthalmic delivery of timolol through p-HEMA contact lenses.* J Drug Del Sci Tech, 2007. **17**(1): p. 69-79.
113. J. Kim and A. Chauhan, *Dexamethasone transport and ocular delivery from poly(hydroxyethyl methacrylate) gels.* Int J Pharm, 2008. **353**(1-2): p. 205-22.
114. C.C. Karlgard, N.S. Wong, L.W. Jones and C. Moresoli, *In vitro uptake and release studies of ocular pharmaceutical agents by silicon-containing and p-HEMA hydrogel contact lens materials.* Int J Pharm, 2003. **257**(1-2): p. 141-51.
115. P.D. Martin, G.R. Jones, F. Stringer and I.D. Wilson, *Comparison of normal and reversed-phase solid phase extraction methods for extraction of beta-blockers from plasma using molecularly imprinted polymers.* Analyst, 2003. **128**(4): p. 345-50.
116. M.E. Byrne, K. Park and N.A. Peppas, *Molecular imprinting within hydrogels.* Adv Drug Deliv Rev, 2002. **54**(1): p. 149-61.
117. C. Alvarez-Lorenzo and A. Concheiro, *Molecularly imprinted materials as advanced excipients for drug delivery systems.* Biotechnol Annu Rev, 2006. **12**: p. 225-68.
118. M.E. Byrne and V. Salian, *Molecular imprinting within hydrogels II: progress and analysis of the field.* Int J Pharm, 2008. **364**(2): p. 188-212.
119. D.R. Kryscio and N.A. Peppas, *Critical review and perspective of macromolecularly imprinted polymers.* Acta Biomater, 2012. **8**(2): p. 461-73.
120. M. Ali and M.E. Byrne, *Controlled release of high molecular weight hyaluronic Acid from molecularly imprinted hydrogel contact lenses.* Pharm Res, 2009. **26**(3): p. 714-26.
121. M. Ali, S. Horikawa, S. Venkatesh, J. Saha, J.W. Hong and M.E. Byrne, *Zero-order therapeutic release from imprinted hydrogel contact lenses within in vitro physiological ocular tear flow.* J Control Release, 2007. **124**(3): p. 154-62.
122. C. Alvarez-Lorenzo, F. Yanez, R. Barreiro-Iglesias and A. Concheiro, *Imprinted soft contact lenses as norfloxacin delivery systems.* J Control Release, 2006. **113**(3): p. 236-44.

123. H. Hiratani and C. Alvarez-Lorenzo, *Timolol uptake and release by imprinted soft contact lenses made of N,N-diethylacrylamide and methacrylic acid.* J Control Release, 2002. **83**(2): p. 223-230.

124. B. Malaekeh-Nikouei, F.A. Ghaeni, V.S. Motamedshariaty and S.A. Mohajeri, *Controlled release of prednisolone acetate from molecularly imprinted hydrogel contact lenses.* J Appl Polym Sci, 2012. **126**(1): p. 387-394.

125. C.J. White, M.K. McBride, K.M. Pate, A. Tieppo and M.E. Byrne, *Extended release of high molecular weight hydroxypropyl methylcellulose from molecularly imprinted, extended wear silicone hydrogel contact lenses.* Biomaterials, 2011. **32**(24): p. 5698-705.

126. H. Hiratani, Y. Mizutani and C. Alvarez-Lorenzo, *Controlling drug release from imprinted hydrogels by modifying the characteristics of the imprinted cavities.* Macromol Biosci, 2005. **5**(8): p. 728-33.

127. H. Hiratani and C. Alvarez-Lorenzo, *The nature of backbone monomers determines the performance of imprinted soft contact lenses as timolol drug delivery systems.* Biomaterials, 2004. **25**(6): p. 1105-13.

128. H. Hiratani, A. Fujiwara, Y. Tamiya, Y. Mizutani and C. Alvarez-Lorenzo, *Ocular release of timolol from molecularly imprinted soft contact lenses.* Biomaterials, 2005. **26**(11): p. 1293-8.

129. F. Yañez, A. Chauhan, A. Concheiro and C. Alvarez-Lorenzo, *Timolol-imprinted soft contact lenses: Influence of the template: Functional monomer ratio and the hydrogel thickness.* J Appl Polym Sci, 2011. **122**(2): p. 1333-1340.

130. L.C. Bengani, K.H. Hsu, S. Gause and A. Chauhan, *Contact lenses as a platform for ocular drug delivery.* Expert Opin Drug Deliv, 2013. **10**(11): p. 1483-1496.

131. C. Alvarez-Lorenzo, H. Hiratani, J.L. Gomez-Amoza, R. Martinez-Pacheco, C. Souto and A. Concheiro, *Soft contact lenses capable of sustained delivery of timolol.* J Pharm Sci, 2002. **91**(10): p. 2182-92.

132. S. Venkatesh, J. Saha, S. Pass and M.E. Byrne, *Transport and structural analysis of molecular imprinted hydrogels for controlled drug delivery.* Eur J Pharm Biopharm, 2008. **69**(3): p. 852-60.

133. A. Ribeiro, F. Veiga, D. Santos, J.J. Torres-Labandeira, A. Concheiro and C. Alvarez-Lorenzo, *Bioinspired Imprinted PHEMA-Hydrogels for Ocular Delivery*

of Carbonic Anhydrase Inhibitor Drugs. Biomacromolecules, 2011. **12**(3): p. 701-709.

134. A. Ribeiro, F. Veiga, D. Santos, J.J. Torres-Labandeira, A. Concheiro and C. Alvarez-Lorenzo, *Receptor-based biomimetic NVP/DMA contact lenses for loading/eluting carbonic anhydrase inhibitors.* J Membr Sci, 2011. **383**(1–2): p. 60-69.
135. A. Tieppo, C.J. White, A.C. Paine, M.L. Voyles, M.K. McBride and M.E. Byrne, *Sustained in vivo release from imprinted therapeutic contact lenses.* J Control Release, 2012. **157**(3): p. 391-7.
136. A. Tieppo, K.M. Pate and M.E. Byrne, *In vitro controlled release of an anti-inflammatory from daily disposable therapeutic contact lenses under physiological ocular tear flow.* Eur J Pharm Biopharm, 2012. **81**(1): p. 170-177.
137. A. Hui, H. Sheardown and L. Jones, *Acetic and Acrylic Acid Molecular Imprinted Model Silicone Hydrogel Materials for Ciprofloxacin-HCl Delivery.* Materials, 2012. **5**(1): p. 85-107.
138. F. Yanez, L. Martikainen, M.E. Braga, C. Alvarez-Lorenzo, A. Concheiro, C.M. Duarte, M.H. Gil and H.C. de Sousa, *Supercritical fluid-assisted preparation of imprinted contact lenses for drug delivery.* Acta Biomater, 2011. **7**(3): p. 1019-30.
139. V.P. Costa, M.E.M. Braga, C.M.M. Duarte, C. Alvarez-Lorenzo, A. Concheiro, M.H. Gil and H.C. de Sousa, *Anti-glaucoma drug-loaded contact lenses prepared using supercritical solvent impregnation.* J Supercrit Fluids, 2010. **53**(1-3): p. 165-173.
140. V.P. Costa, M.E.M. Braga, J.P. Guerra, A.R.C. Duarte, C.M.M. Duarte, E.O.B. Leite, M.H. Gil and H.C. de Sousa, *Development of therapeutic contact lenses using a supercritical solvent impregnation method.* J Supercrit Fluids, 2010. **52**(3): p. 306-316.
141. L. Zhang, F.X. Gu, J.M. Chan, A.Z. Wang, R.S. Langer and O.C. Farokhzad, *Nanoparticles in medicine: therapeutic applications and developments.* Clin Pharmacol Ther, 2008. **83**(5): p. 761-9.
142. J.F.R. dos Santos, C. Alvarez-Lorenzo, M. Silva, L. Balsa, J. Couceiro, J.J. Torres-Labandeira and A. Concheiro, *Soft contact lenses functionalized with pendant cyclodextrins for controlled drug delivery.* Biomaterials, 2009. **30**(7): p. 1348-1355.

143. T.R. Thatiparti, A.J. Shoffstall and H.A. von Recum, *Cyclodextrin-based device coatings for affinity-based release of antibiotics.* Biomaterials, 2010. **31**(8): p. 2335-2347.

144. T.R. Thatiparti and H.A. von Recum, *Cyclodextrin Complexation for Affinity-Based Antibiotic Delivery.* Macromol Biosci, 2010. **10**(1): p. 82-90.

145. T. Sato, R. Uchida, H. Tanigawa, K. Uno and A. Murakami, *Application of polymer gels containing side-chain phosphate groups to drug-delivery contact lenses.* J Appl Polym Sci, 2005. **98**(2): p. 731-735.

146. R. Uchida, T. Sato, H. Tanigawa and K. Uno, *Azulene incorporation and release by hydrogel containing methacrylamide propyltrimenthylammonium chloride, and its application to soft contact lens.* J Control Release, 2003. **92**(3): p. 259-264.

147. V. Dulong, D. Le Cerf, L. Picton and G. Muller, *Carboxymethylpullulan hydrogels with a ionic and/or amphiphilic behavior: Swelling properties and entrapment of cationic and/or hydrophobic molecules.* Colloids and Surfaces a-Physicochemical and Engineering Aspects, 2006. **274**(1-3): p. 163-169.

148. J. Xu, X. Li and F. Sun, *Cyclodextrin-containing hydrogels for contact lenses as a platform for drug incorporation and release.* Acta Biomater, 2010. **6**(2): p. 486-93.

149. Y. Yamazaki, T. Matsunaga, K. Syohji, T. Arakawa and T. Sato, *Effect of anionic/siloxy groups on the release of ofloxacin from soft contact lenses.* J Appl Polym Sci, 2013. **127**(6): p. 5022-5027.

150. J.K. Xu, X.S. Li and F.Q. Sun, *Preparation and Evaluation of a Contact Lens Vehicle for Puerarin Delivery.* J Biomater Sci-Polym Ed, 2010. **21**(3): p. 271-288.

151. K. Kakisu, T. Matsunaga, S. Kobayakawa, T. Sato and T. Tochikubo, *Development and efficacy of a drug-releasing soft contact lens.* Invest Ophthalmol Vis Sci, 2013. **54**(4): p. 2551-61.

152. L.C. Bengani and A. Chauhan, *Extended delivery of an anionic drug by contact lens loaded with a cationic surfactant.* Biomaterials, 2013. **34**(11): p. 2814-2821.

153. G. Tiwari, R. Tiwari, B. Sriwastawa, L. Bhati, S. Pandey, P. Pandey and S.K. Bannerjee, *Drug delivery systems: An updated review.* Int J Pharm Investig, 2012. **2**(1): p. 2-11.

154. N. Vogel, R.A. Belisle, B. Hatton, T.-S. Wong and J. Aizenberg, *Transparency and damage tolerance of patternable omniphobic lubricated surfaces based on inverse colloidal monolayers.* Nat Commun, 2013. **4**.

155. M.S. Mufamadi, V. Pillay, Y.E. Choonara, G. Modi, D. Naidoo and V.M.K. Ndesendo, *A Review on Composite Liposomal Technologies for Specialized Drug Delivery.* J Drug Deliv, 2011. **2011**: p. 939851-70.

156. D. Gulsen, C.C. Li and A. Chauhan, *Dispersion of DMPC liposomes in contact lenses for ophthalmic drug delivery.* Curr Eye Res, 2005. **30**(12): p. 1071-1080.

157. A. Danion, H. Brochu, Y. Martin and P. Vermette, *Fabrication and characterization of contact lenses bearing surface-immobilized layers of intact liposomes.* J. Biomed. Mater. Res. A., 2007. **82**(1): p. 41-51.

158. A. Danion, I. Arsenault and P. Vermette, *Antibacterial activity of contact lenses bearing surface-immobilized layers of intact liposomes loaded with levofloxacin.* J Pharm Sci, 2007. **96**(9): p. 2350-63.

159. H.J. Jung and A. Chauhan, *Temperature sensitive contact lenses for triggered ophthalmic drug delivery.* Biomaterials, 2012. **33**(7): p. 2289-2300.

160. H.J. Jung, M. Abou-Jaoude, B.E. Carbia, C. Plummer and A. Chauhan, *Glaucoma therapy by extended release of timolol from nanoparticle loaded silicone-hydrogel contact lenses.* J. Control. Release, 2013. **165**(1): p. 82-89.

161. D. Gulsen and A. Chauhan, *Ophthalmic Drug Delivery through Contact Lenses.* Invest Ophth Vis Sci, 2004. **45**(7): p. 2342-2347.

162. D. Gulsen and A. Chauhan, *Dispersion of microemulsion drops in HEMA hydrogel: a potential ophthalmic drug delivery vehicle.* Int J Pharm, 2005. **292**(1-2): p. 95-117.

163. J.A. Ferreira, P. Oliveira, P.M. Silva, A. Carreira, H. Gil and J.N. Murta, *Sustained Drug Release from Contact Lenses.* Cmes-Computer Modeling in Engineering & Sciences, 2010. **60**(2): p. 151-179.

164. Y. Kapoor, J.C. Thomas, G. Tan, V.T. John and A. Chauhan, *Surfactant-laden soft contact lenses for extended delivery of ophthalmic drugs.* Biomaterials, 2009. **30**(5): p. 867-878.

165. Y. Kapoor and A. Chauhan, *Drug and surfactant transport in Cyclosporine A and Brij 98 laden p-HEMA hydrogels.* J Colloid Interface Sci, 2008. **322**(2): p. 624-633.

166. J. Kim, Y.S. Chun, S.K. Lee and D.S. Lim, *Improved electrode durability using a boron-doped diamond catalyst support for proton exchange membrane fuel cells.* Rsc Advances, 2015. **5**(2): p. 1103-1108.
167. C.H. Lu, R.B. Yoganathan, M. Kociolek and C. Allen, *Hydrogel containing silica shell cross-linked micelles for ocular drug delivery.* J Pharm Sci, 2013. **102**(2): p. 627-637.
168. J. Kim, C.C. Peng and A. Chauhan, *Extended release of dexamethasone from silicone-hydrogel contact lenses containing vitamin E.* J Control Release, 2010. **148**(1): p. 110-6.
169. C.C. Peng and A. Chauhan, *Extended cyclosporine delivery by silicone-hydrogel contact lenses.* J Control Release, 2011. **154**(3): p. 267-74.
170. C.C. Peng, J. Kim and A. Chauhan, *Extended delivery of hydrophilic drugs from silicone-hydrogel contact lenses containing vitamin E diffusion barriers.* Biomaterials, 2010. **31**(14): p. 4032-47.
171. C.C. Peng, A. Ben-Shlomo, E.O. Mackay, C.E. Plummer and A. Chauhan, *Drug Delivery by Contact Lens in Spontaneously Glaucomatous Dogs.* Curr Eye Res, 2012. **37**(3): p. 204-211.
172. R.A. Jain, *The manufacturing techniques of various drug loaded biodegradable poly(lactide-co-glycolide) (PLGA) devices.* Biomaterials, 2000. **21**(23): p. 2475-2490.
173. J.B. Ciolino, T.R. Hoare, N.G. Iwata, I. Behlau, C.H. Dohlman, R. Langer and D.S. Kohane, *A Drug-Eluting Contact Lens.* Invest Ophthalmol Vis Sci, 2009. **50**(7): p. 3346-3352.
174. J.B. Ciolino, S.P. Hudson, A.N. Mobbs, T.R. Hoare, N.G. Iwata, G.R. Fink and D.S. Kohane, *A Prototype Antifungal Contact Lens.* Invest Ophthalmol Vis Sci, 2011. **52**(9): p. 6286-6291.
175. J.B. Ciolino, C.F. Stefanescu, A.E. Ross, B. Salvador-Culla, P. Cortez, E.M. Ford, K.A. Wymbs, S.L. Sprague, D.R. Mascoop, S.S. Rudina, S.A. Trauger, F. Cade, and D.S. Kohane, *In vivo performance of a drug-eluting contact lens to treat glaucoma for a month.* Biomaterials, 2014. **35**(1): p. 432-439.

2 Comparison of two hydrogel formulations for drug release in ophthalmic lenses

The following results were partially published in the peer-reviewed international Journal of Biomedical Materials Research: Part B - Applied Biomaterials. August 2014. 102 (6): 1170–1180.
doi: 10.1002/jbm.b.33099

Table of contents

2.1 Introduction

In this chapter the potential of two hydrogel formulations as ophthalmic drug delivery vehicles will be reported. A conventional hydrogel and a silicone hydrogel were prepared in our laboratories and loaded with the two drugs of study, the antibiotic levofloxacin and the antiseptic chlorhexidine, whose release was thereafter investigated.

As previously described in the first chapter, section 1.2, conventional SCLs are often PHEMA based, which is biocompatible and has adequate optical, swelling and mechanical properties. However, they present low oxygen permeability. To increase the oxygen permeability, silicon-containing hydrogel contact lens materials were introduced and led to a new generation of contact lenses. Optimization of these biomaterials, namely of its hydrophilicity and self-lubricant properties has been pursued by many researchers. In particular, they may be improved through the addition of a small amount of specific compounds, such as vinylpyrrolidone in the monomeric (NVP) or polymeric form (PVP). In this work, the conventional hydrogel formulation chosen was HEMA/PVP, while the silicone hydrogel was obtained by adding TRIS, a hydrophobic monomer containing silicone (3- tris(trimethylsilyloxy)silylpropyl 2-methylprop-2-enoate), to PHEMA and NVP.

The first step was the characterization of the two hydrogels as SCL materials by studying important properties such as, swelling kinetics, ion permeability, transmittance, friction coefficient, elasticity, wettability and surface morphology/topography. Then, the release profiles of both drugs from the two hydrogels were obtained. The drug loading/release performances depend on the pair drug/polymeric formulation. Thus, a systematic study under varying drug loading conditions was performed to understand the interaction between the drug and the matrix and to develop optimized drug delivery systems.

The drug loading was performed by soaking. Loading the hydrogel with the drug is a crucial step in the preparation of drug-loaded contact lenses and different loading methods have been used [1-9]. Soaking the lenses in drug solutions still remains the most simple and inexpensive method of loading, and the one which involves fewer risks for the integrity of the drug molecules.

The release profiles of the two drugs of interest from the PHEMA based hydrogel and the silicone hydrogel, were obtained in static sink conditions (varying time of loading, loading solution concentration, degree of crosslinking of the silicone hydrogel, surface crosslinking of the silicone hydrogel) and under dynamic conditions. Typically, drug release experiments are conducted in infinite sink conditions that are defined as the conditions where the volume of medium is at least greater than ten times that required to form a saturated solution of a drug substance. However, the human eye has a small tear volume (around 7 µL [7, 10]) and, under normal physiological conditions, has a tear turnover rate that varies between 1 and 4 µL/min [11], consequently, infinite sink conditions may do not adequately describe drug release kinetics on the eye. Still, for simplicity reasons, infinite sink conditions are generally used to compare different systems and predict their relative efficacy. Previous studies performed on drug loaded thin films, showed zero-order release profiles under dynamic conditions using a microfluidic device [12-14]. Those results demonstrated that the release time of the drug under physiological flow conditions would provide a more linear and sustained release profile than those obtained in sink conditions, highlighting the importance of the simulation of local conditions to effectively tailor drug delivery devices.

For these reasons and to predict the *in vivo* performance of the drug eluting contact lenses, a mathematical model, which takes into account the eye hydrodynamic mechanisms, was developed and applied to the data obtained in sink conditions. Furthermore, a novel microfluidic cell was developed to simulate the physiological ocular tear flow conditions (temperature, tear volume and flow rate) in the drug release tests.

To better interpret the different release profiles, interactions between the drugs and the polymers were investigated using Raman spectroscopy, under the supervision of Professor Luis Santos from IST. Furthermore, the minimal inhibitory concentration (MIC) of chlorhexidine with respect to *Staphylococcus aureus* was determined, while the MICs of levofloxacin for that species and for *Pseudomonas aeruginosa* were taken from a previous work [15]. Microbiological assays were done to determine the toxicity of chlorhexidine towards *Acanthamoeba castelanii* thank to the collaboration with Professor António Pedro Alves de Matos, from the Curry Cabral Hospital, Lisbon.

2.2 Experimental part

2.2.1 Materials

2-Hydroxyethyl methacrylate (HEMA), ethylene glycol dimethacrylate (EGDMA), 2,2′-azobis(2-methylpropionitrile) (AIBN), 3-tris(trimethylsilyloxy)silylpropyl 2-methylprop-2-enoate (TRIS), levofloxacin (LVF), phosphoric acid, triethylamine, dichloromethane, and glutaraldehyde (GTA) (25 wt%) were all purchased from Sigma-Aldrich. Poly(vinylpyrrolidone) (PVP K30, Kollidon® 30) was kindly provided by BASF. N-Vinyl pyrrolidone (NVP) and sodium chloride were obtained from Merck, chlorhexidine diacetate monohydrate (CHX), from AppliChem, carbon tetrachloride, from Riedel-de Haën, acetonitrile, from Fisher Scientific, dimethyldichlorosilane, from Fluka, and sulfuric acid (96%) from Panreac. Muller Hinton broth solution was purchased from Becton, Dickinson and Company. A Millipore Milli-Q water purification system was used to prepare distilled and deionized (DD) water.

2.2.2 Hydrogels preparation

Two types of hydrogels were prepared: a conventional HEMA based, HEMA/PVP (98/2, w/w) and a silicone based: TRIS /NVP/HEMA (40/40/20, w/w/w). In the first case, an appropriate amount of the crosslinker EGDMA was dissolved in HEMA (hydrophilic monomer) to obtain a concentration of 80 mM. Then, the mixture was degassed by ultra-sounds (5 min) and bubbled with a gentle stream of nitrogen (15 min) before the addition of AIBN (initiator), final concentration 10 mM, and PVP (hydrophilic additive), final concentration of 0.02 g/mL. The solution was magnetically stirred for about two hours to obtain complete dissolution of PVP. In the case of TRIS/NVP/HEMA hydrogel, TRIS (silicone monomer), NVP (hydrophilic additive), HEMA and EGDMA were added to prepare a mixture with concentrations of 0.94 M, 3.58 M, 1.53 M and 30 mM, respectively. Samples with a higher amount of crosslinker (300 mM) were also prepared. The mixture was then degassed by ultra-sounds (5 min) and bubbled with a gentle stream of nitrogen (15 min) before the final addition of AIBN to obtain a concentration of 15 mM. The final mixture was magnetically stirred for about 10 min, to obtain a homogeneous solution. Both mixtures were injected into a mould consisting of two silanized glass plates separated by a spacer of polyurethane or

teflon. The glass plates were silanized according to the procedure described by Vasquez et al [16], in order to facilitate the hydrogel removal from the mould. Briefly, the glasses were incubated in a 2% solution of dimethyldichlorosilane in carbon tetrachloride for one hour and then rinsed with dichloromethane and dried with nitrogen. In the case of HEMA/PVP, the polymerization reaction was performed at 50 °C for 14 hours, followed by 24 hours at 70°C, while in the case of TRIS/NVP/HEMA hydrogel it occurred at 60 °C for 24 hours. The obtained hydrogel sheets were washed over 5 days, with DD water renewed 3 times a day, to remove unreacted monomers and to facilitate the cutting of the samples used in the study. The hydrated samples (0.30- 0.35 mm in thickness) were cut, namely 50×10 mm^2 and 10 x10 mm^2 respectively for the experiments under static and dynamic conditions and were then dried in an oven at 40 °C overnight.

In the case of TRIS/NVP/HEMA, some samples were submitted to surface crosslinking using the method described by Wu [8]. A crosslinking solution (40 mL) containing 4 wt% GTA was prepared by mixing DD water, GTA solution (25 wt%), and sulfuric acid solution (10 vol%). GTA solution (25 wt%), and sulfuric acid solution (10 vol%) were added in equal volumes. After heating the solution in a water bath at 37 °C for 5 min, dry hydrogel samples were immersed into the crosslinking solution for 30 s. The solution adsorbed on the sample surfaces was blotted off and the resulting samples were allowed to react overnight in a desiccator, at room temperature. The samples were washed by immersion in water which was renewed twice during 24 h. Finally, they were dried at 40 °C during 24 h.

2.2.3 Hydrogels characterization

2.2.3.1 Swelling kinetics

Swelling kinetics assays were performed by placing dried samples of each composition, (three replicates each) in 13 mL of DD water at three different temperatures namely: 4, 22 and 35 °C, being 35°C the mean temperature of the human cornea in the eye [17, 18]. The samples were weighed at various times after careful wiping of their surface with absorbent paper. Swelling capacity, *SC*, was estimated as the relative weight gain during the hydration:

$$SC = \frac{W_t - W_0}{W_0} \times 100$$ **Equation 2.1**

where W_0 is the weight of the dry sample and W_t is the weight at time t. When equilibrium is achieved, the constant weight value, W_∞, allows the calculation of the equilibrium water content, *EWC*, which is defined by:

$$EWC = \frac{W_\infty - W_0}{W_\infty} \times 100$$ **Equation 2.2**

From the value of *EWC*, the oxygen permeability, Dk, (in barrer), at 35 °C, may be estimated for traditional PHEMA hydrogels using the empirical Equation 2.3[19]:

$$Dk = 1.67e^{0.0397\mathrm{EWC}}$$ **Equation 2.3.**

The oxygen transmissibility corresponds to the ratio Dk/h, were h represents the thickness of the sample.

2.2.3.2 Ionic permeability

The ionic permeability of the hydrogels was measured using a home-made PMMA horizontal diffusion cell. The fully hydrated hydrogel was mounted in the cell, and 24 mL of NaCl solution (130 mM) and 32 mL of DD water were placed into the donor and the receiver compartments, respectively. The experiment was performed at 35 °C in triplicate. The conductivity of the fluid in the receiving chamber was determined as a function of time for a minimum of 10 hours, using a conductivity meter (Cond 340i/SET, WTW). The conductivity data (in µS/cm) were converted into NaCl concentration (in mg/mL) through a calibration curve previously obtained. The rate of ion transport (F) corresponds to the slope of the linear regression applied to the concentration versus time data. Solving the diffusion equation under the pseudo-steady state conditions leads to the determination of the ionic permeability (also referred as the ionoflux diffusion coefficient, D_{ion}):

$$\frac{F \cdot V}{A} = D_{ion} \frac{dC}{dx}$$ **Equation 2.4**

where *V* is the volume of the receiver solution, A is the cross-sectional area of the hydrogel sample and *dC/dx* represents the initial NaCl concentration gradient across the hydrogel.

2.2.3.3 Transmittance

Optical clarity studies were carried out by measuring the percent transmittance of visible light (wavelength range from 400 to 700 nm) through swollen lenses. Fully hydrated hydrogel samples were cut properly and mounted on one side of the outer surface of a quartz cuvette. The cuvette was placed in the spectrophotometer and the transmittance values were measured using a UV-Vis Beckmam DU-70 spectrophotometer. The tests were done in triplicate before and after drug loading.

2.2.3.4 Friction coefficient

Tribology experiments were run on a CSM microtribometer using saline solution (130 mM) as the lubricant. Polymethylmethacrylate semi-spheres, with a curvature radius of 2 mm, were used as the counterbody. The experiments were done in triplicate, at room temperature. The normal force applied was 20 mN and the sliding velocity, 0.7 cm/s. The data were analyzed with the software TriboX.

2.2.3.5 Mechanical properties

The Young's modulus was determined from the slope of linear dependence of the stress-strain curves obtained during tensile tests performed on swollen hydrogels. The tests were made at room temperature, making sure that the samples were kept well hydrated at all times during the experiment. The samples were carefully suspended in a vertical support and submitted to increasing tension by placing hanged weights on its

lower extremity. The produced elongation was monitored with a cathetometer. Five separate samples were tested for each hydrogel formulation.

2.2.3.6 Wettability

The wettability of the dry hydrogels was determined through the measurement of DD water contact angles by the sessile drop method. Drops of 4–6 μL were generated with a micrometric syringe and deposited on the substrate surface, inside a chamber previously saturated with water. The hydrated hydrogels were characterized by measuring the contact angles of captive air bubbles lying underneath the substrates immersed in water. Drop and bubble images were acquired using a video camera (JAI CV-A50) attached to a microscope (Wild M3Z) which is connected to a frame grabber (Data Translation DT3155). The image acquisition and analysis were performed using the ADSA-P software (Axisymmetric Drop Shape Analysis Profile). The measurements were done at room temperature and five to eight drops were measured on each hydrogel formulation.

2.2.3.7 Surface topography

The topography of hydrogels HEMA/PVP and TRIS/NVP/HEMA was assessed by atomic force microscopy (AFM). A Nanosurf Easyscan 2 AFM was used in contact mode, at room temperature, with a gold coated PPP-CONTSCAuD Nanosensor cantilever (force constant 0.06 N/m). All observations were conducted in an aqueous environment with swollen samples. The average roughness was determined from at least five regions in the AFM images.

2.2.4 Drug loading

The dry hydrogel samples were loaded with the drugs by soaking in drug solution (2.6 mL/cm^2 of surface area). In the case of static sink conditions HEMA/PVP and TRIS/NVP/HEMA were respectively drug loaded by soaking in solutions of LVF and CHX with concentration of 5 mg/mL, for 14 or 36 hours at 4 °C. In the case of CHX, concentrations of 1.5 and 2.5 mg/mL were also used. In the case of the physiological tear flow conditions, HEMA/PVP hydrogels were loaded with LVF by soaking in solutions of 5 mg/mL of LVF. The loaded samples were rinsed with DD water and dried

with absorbent paper in order to remove drug residues deposited on the lens surface during the loading process. Levofloxacin was dissolved in a saline solution (130 mM), while chlorhexidine was dissolved in simple DD water due to its limited solubility in saline solution. The soaking process was protected from light.

2.2.5 Drug release experiments

Drug release studies were conducted through two different *in vitro* methods: 1) static sink conditions, defined as the experimental conditions when the volume of medium is at least greater than three times the one required to form a saturated solution of the drug substance; 2) dynamic conditions, under physiological flow conditions using a microfluidic device. All the experiments, including the controls, were performed in triplicate.

2.2.5.1 Static sink conditions

Drug release experiments were carried out for 24 hours to determine drug release profiles. The loaded samples were immersed in 13 mL of saline solution (130 mM) in closed vessels, at 35 °C, under stirring (150 rpm). These conditions were chosen to simulate the lachrymal fluid and to ensure that the concentration of chlorhexidine remained below its solubility limit. At pre-determined time intervals, 1 mL aliquots of the supernatant were collected and replaced by the same volume of fresh NaCl solution.

The concentration of LVF was determined using a high performance liquid chromatograph, at a wavelength of 290 nm, with a Jasco UV-VIS detector and a C-18 column Nova-Pak Watters. The mobile phase, consisting of water, acetonitrile, phosphoric acid and triethylamine (86/14/0.6/0.3 in volume), was introduced into the column at a flow rate of 1 mL/min and a pressure of 14 MPa, according to the method described by Wong *et al.* [20] In the case of CHX, spectrophotometry UV-Vis at a wavelength of 255 nm was used.

2.2.5.2 *Physiological tear flow conditions*

A microfluidic system dedicated to drug release testing of loaded contact lenses under simulated quasi-physiological tear conditions was conceived and built during the present dissertation work, in collaboration with Professor José Mata from IST. Figure 2.1 shows the experimental setup and a schematic representation of the microfluidic cell; more details are reported in Appendix B.

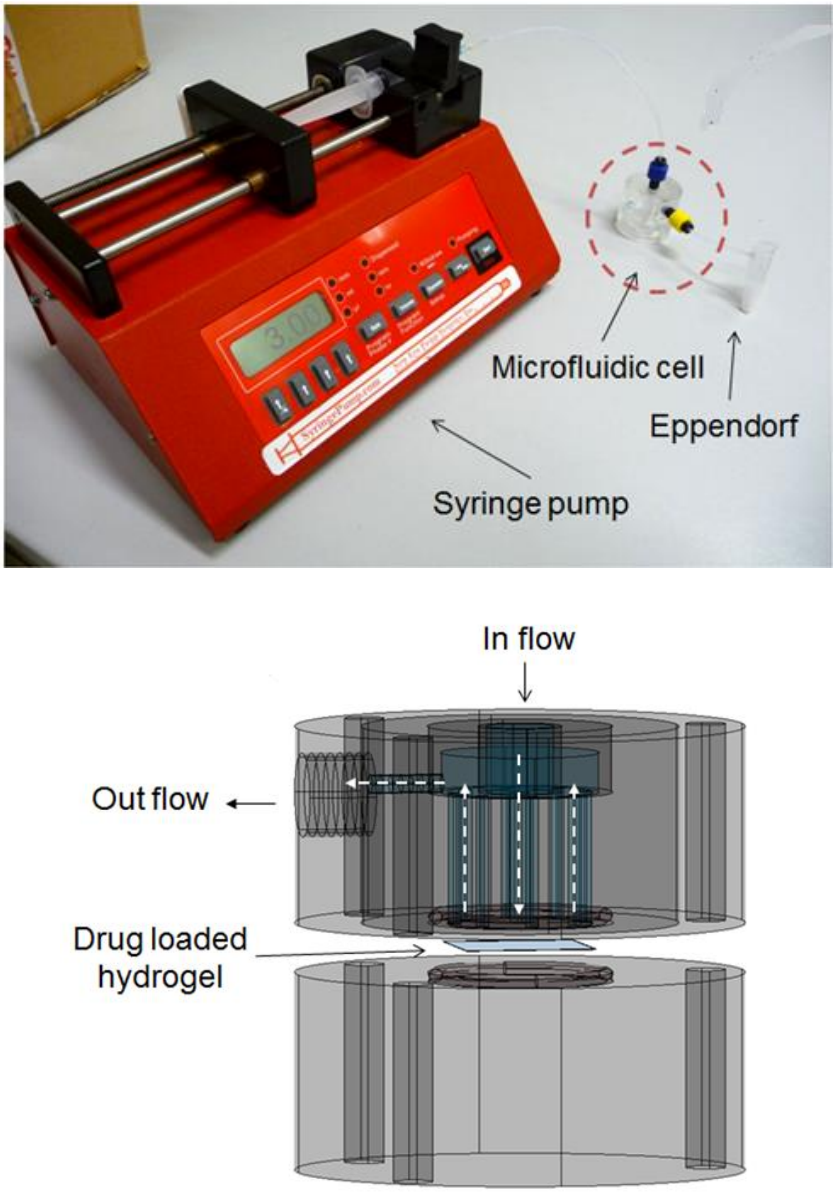

Figure 2.1: On the top, experimental setup during the experiment under physiological tear flow conditions. On the bottom, the microfluidic cell representation.

The microfluidic device is made of PMMA. The experiments were carried out at the temperature of 35 °C and the saline solution (130 mM) was pumped by a syringe pump, N-300, from New Era Pump Iystems, Inc, through the device. The cell possesses a central channel through which the saline solution is admitted to a chamber where the drug-loaded lens is placed, and 8 surrounding parallel channels for solution exit. This geometry allows the saline solution to flow radially over the lens. The volume of the chamber (45 μL) was chosen due to design limitations. It has been assessed that after 6 hours of contact lens wear the turnover rate of tears could be 2.82 ± 1.45 μL/min [11]. This value depends on several factors, such as the type of lens or the tolerance of the user, but may be used as an average value. Therefore, the syringe pump was set to pump at the physiological flow rate of 3 μL/min. The device was designed to mimic the flow rate of tears but it does not intend to fully reproduce the eye conditions. In the human eye, the presence of contact lenses makes the tear flow a complicated phenomenon with significant differences in the pre-lens and post-lens regions. The tear film is influenced by the evaporation between blinks. It was assumed that even though this factor may affect drug concentration, it will not affect tear flow rate [21].

The hydrogels were cut in order to fit into the microfluidic cell. The ratio area of the sample volume of loading solution was maintained the same in the case of the static release experiments. The loading lasted for 14 hours at 4 °C temperature. The protocol for the preparation of the drug solution is the same as described before. Samples were collected at regular time intervals. Control tests were performed in sink conditions.

The concentration of LVF was determined following the procedure described in the end of the previous section.

2.2.6 Raman and FTIR spectroscopic analyses

Raman spectra were collected in the range 200–1800 cm^{-1}, using a LabRAM HR Evolution Confocal Microscope (Horiba Scientific) with 532 nm excitation. The light was focused with a 100×, NA = 0.9, WD = 0.21 mm objective. The laser power on the sample without any neutral density filters was ≈ 10 mW. The Raman signal was detected with a Peltier-cooled (-70˚C) Horiba Synapse CCD detector with 1024 x 256 pixels. Spectra were acquired using 5 s of signal collection time and 10 accumulations.

Labspec 6 software (Horiba Scientific) was used to analyze all spectra through background subtraction and peak fitting.

ATR-FTIR spectra were recorded with a Thermo Electron, model Nicolet 5700, FTIR spectrometer, at 4 cm^{-1} resolution, with an average of 128 scans per spectrum.

2.2.7 Determination of the antimicrobial drug activity

The minimum inhibitory concentration of chlorhexidine for *S. aureus* was estimated by agar diffusion tests. All the microbiological tests showed in the present thesis were performed at CiiEM, Instituto Superior de Ciências da Saúde Egas Moniz, thanks to the collaboration with Professor Maria Guilhermina Moutinho. A culture of this microorganism was inoculated and a solution with final optical bacterial density of 1 McFarland was prepared by dilution with distilled, sterilized water. A volume of 350 μL of this suspension was added to 50 mL of Muller Hinton broth solution. The inoculated medium was poured in square plates, where, after solidification, several paper discs were carefully placed. Each disc was impregnated with 15 μL solution of defined concentration (between 12.5 and 250 μg/mL). Sterile water-loaded discs were used as negative controls. After overnight incubation at 37 ° C, the diameter of the inhibition halos was measured with an electronic caliper. The assays were repeated 3 times in duplicate. MICs correspond to the minimum concentration tested, which led to the observation of growth inhibition zones.

A. castellanii was grown in PYG medium (Peptone 1,5% + Yeast extract 0,5% + Glucose 1% in distilled H_2O) under axenic conditions in plastic petri dishes at 28ºC. For evaluating the effects of chlorhexidine on the amoebae, the PYG medium was removed and replaced by several concentrations of chlorhexidine in saline (25, 30, 40 50 and 100 μM). The cells were filmed with a Moticam 5.0 digital camera on a Motic AE2000 inverted microscope equipped with a 20x phase contrast objective. The camera was controlled by Motic ImagePlus 2.0 software. The movies were made at room temperature for up to 3 hours. In some cases several consecutive movies involving a period of 24 hours were made. Death of the cells was evaluated as a stop of all intracellular movement. The movies were observed with VLC software under acceleration of up to 100%. Ten second clips produced with Avidemix software are

provided as supplementary material. The clips were accelerated 10 times to allow easy evaluation of the movement of the cells.

2.3 Results and Discussion

2.3.1 Hydrogel characterization

Two types of hydrogels were studied: HEMA/PVP, a conventional hydrogel, and TRIS/NVP/HEMA, a silicone hydrogel. Besides the presence of the silicone monomer (TRIS), a significant difference between the compositions of both hydrogels concerns the amount of crosslinking agent which is about three times more concentrated in HEMA/PVP. In general, increasing the crosslink density within a hydrogel network improves its mechanical properties, but decreases the water-induced swelling capacity of the hydrogel.

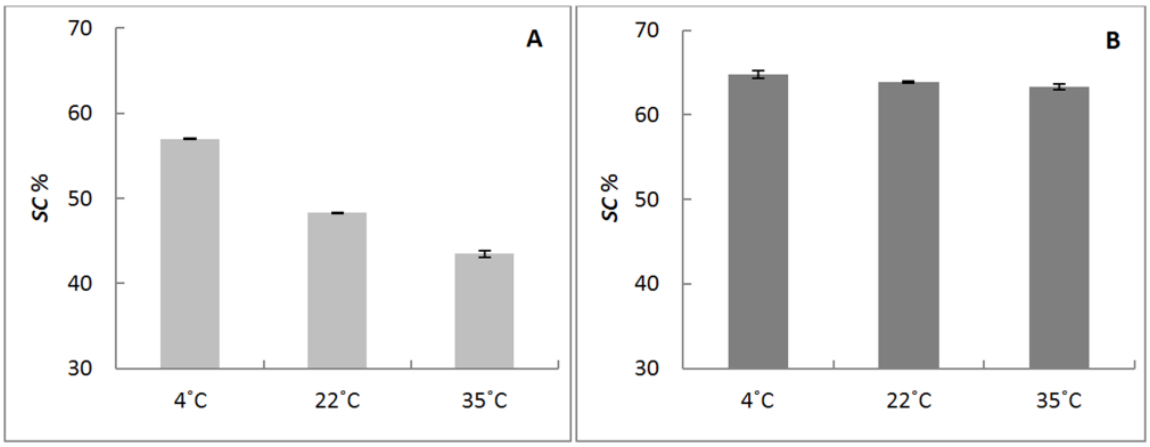

Figure 2.2: Temperature dependence of the swelling capacity (SC) of HEMA/PVP (A) and TRIS/NVP/HEMA (B) hydrogels. The error bars are ± SD

The temperature dependence of the swelling capacity of both hydrogels is shown in Figure 2.2. Both hydrogels reach the swelling equilibrium within 3 hours. In each case, the swelling capacity decreases as the temperature increases which is the typical behavior of negative thermosensitive hydrogels [22]. However, while the swelling

capacity of HEMA/PVP varies significantly with the temperature, for TRIS/NVP/HEMA this variation is quite small. Since the maximum value was achieved at 4 °C, we decided to use this temperature in the loading process. The swelling capacity of TRIS/NVP/HEMA hydrogel is higher than that of HEMA/PVP in spite of the presence of TRIS, a hydrophobic component. This may be caused by the presence of the wetting agent NVP, which represents 40% of this silicone hydrogel formulation. Furthermore the fact that the crosslinking degree is lower in TRIS/NVP/HEMA, compared to HEMA/PVP, shall be another determinant factor for the swelling capacity.

Table 2.1 presents other hydrogel properties which are important for their performance as contact lens materials.

Table 2.1: Hydrogel Properties: Ionic Permeability, Dion, Oxygen transmissibility, DK/h, Transmittance, T%, Friction Coefficient, μ, Young's Modulus, E, Average Roughness, Ra, and Water Contact Angle, Θ_W

	HEMA/PVP	TRIS/NVP/HEMA
D_{ion} (cm^2/s)	$8 \times 10^{-8} \pm 2\times10^{-8}$	$5\times10^{-7}\pm2\times10^{-8}$
Dk/h (Barrer/mm)	15.88±0.03[a]	---[b]
T (%)	97±2	97.6±0.5
μ	0.26±0.02	0.29±0.03
E (MPa)	1.4±0.1	2.7±0.4
R_a(nm)	11±1	5±1
Θ_w(°) dry hydrogel	69±7	90±4
Θ_w(°)hydrated hydrogel	40±3	35±5

a: calculated from equation 1.5
b: value non calculated for experimental limitation

The hydrogels have ionic permeability values above the minimum acceptable value, $2.5 \times 10^{-8} cm^2/s$ [23].The higher swelling capacity of TRIS/NVP/HEMA hydrogel explains why its ionic permeability is larger than that of HEMA/PVP, assuming that no specific affinity exists between the polymeric matrix and the ions. The oxygen transmissibility of HEMA/PVP estimated from the capacity of water absorption is higher than the minimum required (D_K/h= 5.0 barrer/mm) [24]. For TRIS/NVP/HEMA hydrogel, it is not possible to calculate the oxygen permeability using Equation 1.5 because silicone-containing hydrogels are known to carry oxygen mainly via the

silicone molecules [25]. Taking into consideration that, as previously referred, these hydrogels have higher oxygen permeability than the PHEMA based ones, we may conclude that both materials present adequate oxygen permeability values.

Both hydrogels present values of transparency over 90%, matching the transmittance characteristics of soft contact lenses [25]. Drug loading did not affect the transparency (data not shown). The friction coefficients of both materials are very similar and lie within the range of the typical values for soft contact lens materials [9]. TRIS/NVP/HEMA hydrogel is stiffer than the HEMA/PVP which may be attributed to the presence of the silicone monomer that surpasses the effect of its lower crosslink density.

Dry samples of TRIS/NVP/HEMA are more hydrophobic than those of HEMA/PVP which is expected from the known hydrophobicity of the siloxane groups present in the TRIS monomer. However, an inversion in the wettability of the hydrated samples is observed suggesting that hydroxyl groups in HEMA are now exposed at the water interface. A similar behavior was reported by Li and Chin [26] who demonstrated that the surface of a PHEMA based polymer containing TRIS may rearrange in response to a polar environment. In contact with air, the siloxane groups of the TRIS monomer concentrate at the surface to minimize the surface energy. However, if air is substituted by water, the dynamic motion of the hydrophilic functionalities might occur and the surface becomes hydrophilic in order to keep a low interfacial energy.

The AFM images of the surface of the hydrogels are presented in Figure 2.2. The most significant difference between both surfaces is the nanoporous structure observed on the image of TRIS/NVP/HEMA surface. The presence of nanopores in this surface is consistent with the higher swelling capacity demonstrated by this polymer and does not imply an increase in the roughness; on the contrary, the roughness of the TRIS/NVP/HEMA surface is lower than that of HEMA/PVP (see Table 2.1).

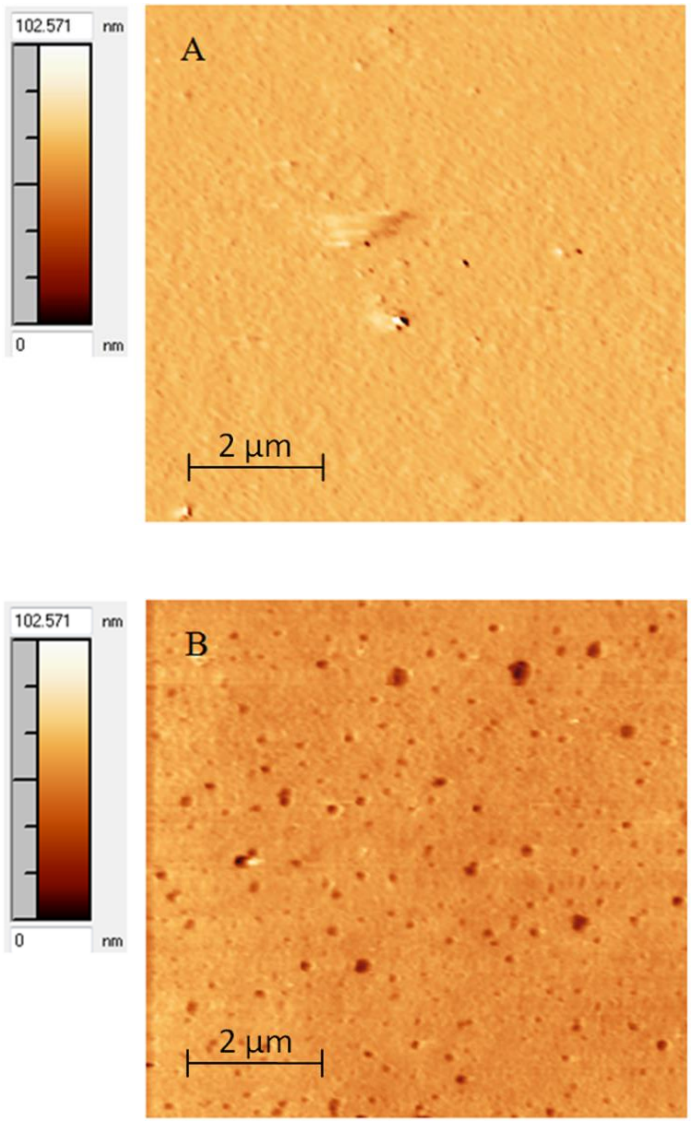

Figure 2.3 AFM images of the surface of HEMA/PVP (A) and TRIS/NVP/HEMA (B).

2.3.2 Levofloxacin release in static sink conditions

The cumulative release profiles of LVF from HEMA/PVP and TRIS/NVP/HEMA hydrogels previously loaded for 14 hours and 36 hours, obtained in static sink conditions, are compared in Figure 2.4. The drug loading time does not influence the drug release profiles of TRIS/NVP/HEMA indicating that equilibrium was achieved after 14 hours of soaking. In contrast, for HEMA/PVP a longer loading time led to an increased amount of drug released, despite the fact that the swelling equilibrium was

achieved within 3 hours. This means that the amount of drug loaded in the hydrogel depends not only on the swelling, but mainly on the drug diffusion.

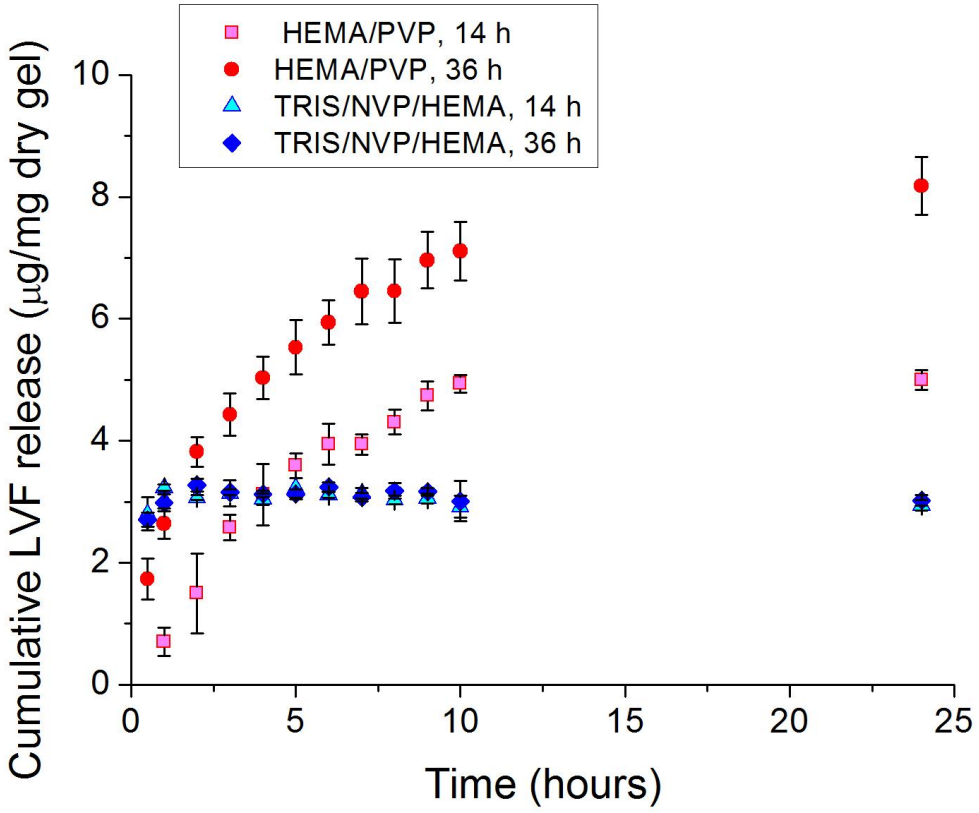

Figure 2.4: Cumulative release profiles of levofloxacin from HEMA/PVP and from TRIS/NVP/HEMA hydrogels, previously loaded for 14 hours and 36 hours with [LVF] 5 mg/mL, obtained in static sink conditions. The error bars correspond to ± standard deviation.

The release of LVF from TRIS/NVP/HEMA was complete in less than 2 hours, showing an initial burst which is typical of drug accumulation near the surface of the sample. HEMA/PVP led to controlled release curves along the time of study (at least 10 hours) and the achieved cumulative concentrations were higher than in the case of TRIS/NVP/HEMA. The higher crosslinking degree of the HEMA/PVP may be responsible for the slower release, while its lower water content may justify a higher affinity for levofloxacin, a moderately lipophilic drug.

2.3.3 Chlorhexidine release in static sink conditions

Figure 2.5 shows the cumulative release profiles of CHX from HEMA/PVP and TRIS/NVP/HEMA hydrogels previously loaded for 14 hours and 36 hours, obtained in static sink conditions. Both materials presented controlled releases along the time of study, but the initial burst is much higher in the case of TRIS/NVP/HEMA. For this hydrogel, longer loading times resulted in higher drug released amounts, while the loading time had a negligible effect in the case of HEMA/PVP. It is interesting to notice that this behavior is opposite to the one previously described for levofloxacin.

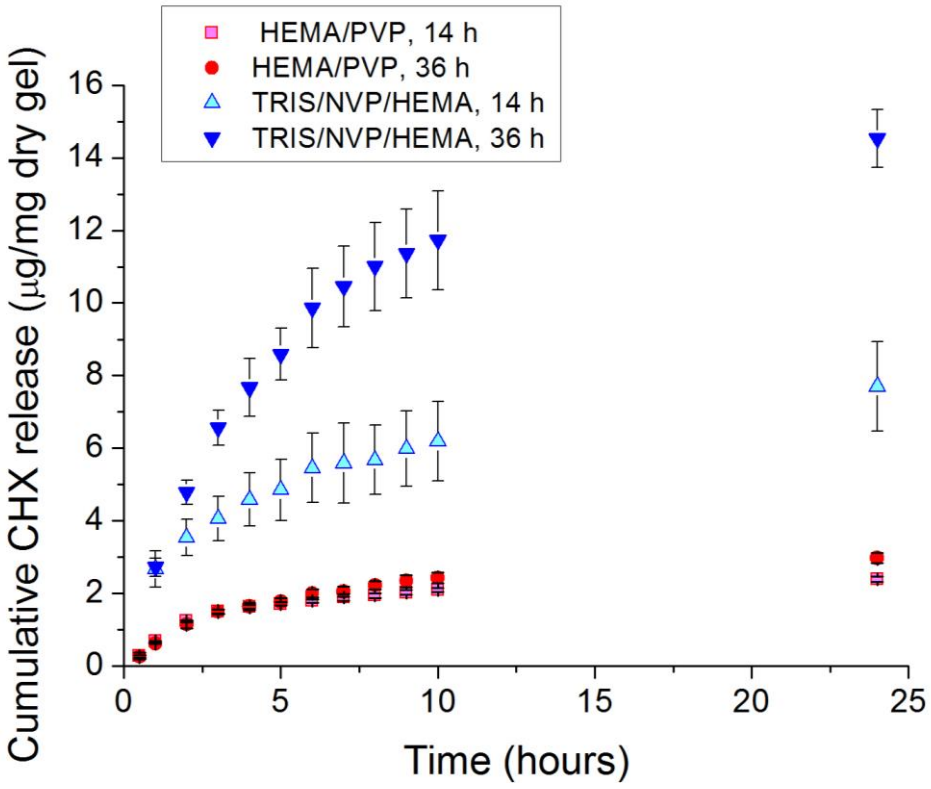

Figure 2.5: Cumulative release profiles of chlorhexidine from HEMA/PVP and from TRIS/NVP/HEMA hydrogels, previously loaded for 14 hours and 36 hours with [CHX] 5 mg/mL obtained in static sink conditions. The error bars correspond to ± standard deviation.

The amount of CHX released per time unit was always larger from TRIS/NVP/HEMA than from HEMA/PVP. Since CHX is a hydrophilic drug, it is expected to diffuse preferentially into the network of the hydrogel with lower crosslinking density, and greater water content. These results are in agreement with those of Hirachi et al [27], who claimed that water-induced swelling has an enhancing effect upon the CHX release

rate, based on their observations of higher release rates of CHX from hydrophilic resins with greater water contents. However, we must point out that the enhanced CHX release from TRIS/NVP/HEMA with respect to HEMA/PVP cannot be exclusively attributed to an increase of ≈ 8 % in the swelling capacity. A possible explanation could be a stereochemical effect. In fact, while water is able to diffuse inside both polymeric matrices, the bulkier CHX molecule diffuses more easily within the more open structure of TRIS/NVP/HEMA.

Cumulative release of CHX from TRIS/NVP/HEMA, loaded with 5 mg/mL drug solution attained high values, as shown in Figure 2.5. To test the effect of the drug concentration, other experiments were done using 2.5 and 1.5 mg/mL solutions. The results for a loading time of 14 hours are compared in Figure 2.6. As it was expected, the mass released decreased with the decrease in concentration, in a nearly linear way.

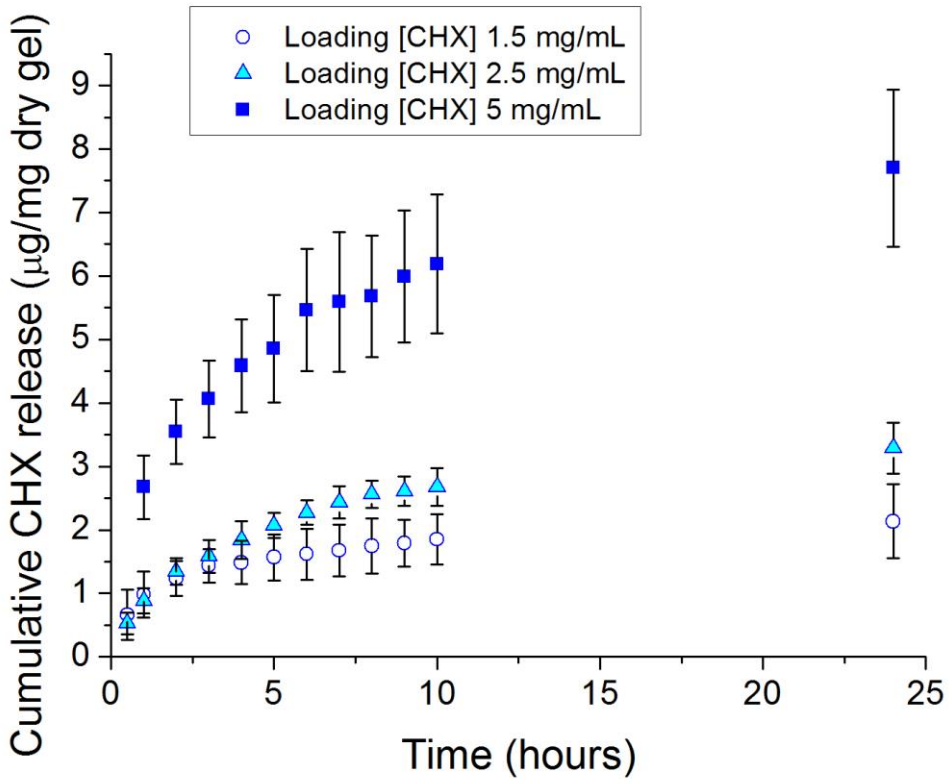

Figure 2.6: Cumulative release profiles of chlorhexidine from TRIS/NVP/HEMA hydrogels loaded for 14 hours with solutions of concentrations: 5mg/mL, 2.5 mg/mL and 1.5mg/mL obtained in static sink conditions. The error bars correspond to ± standard deviation.

The effect of the crosslinking degree of TRIS/NVP/HEMA hydrogels in the drug release was investigated by increasing the concentration of the crosslinker EGDMA ten times. The comparison of the drug release profiles obtained with two loading times is shown in Figure 2.7.

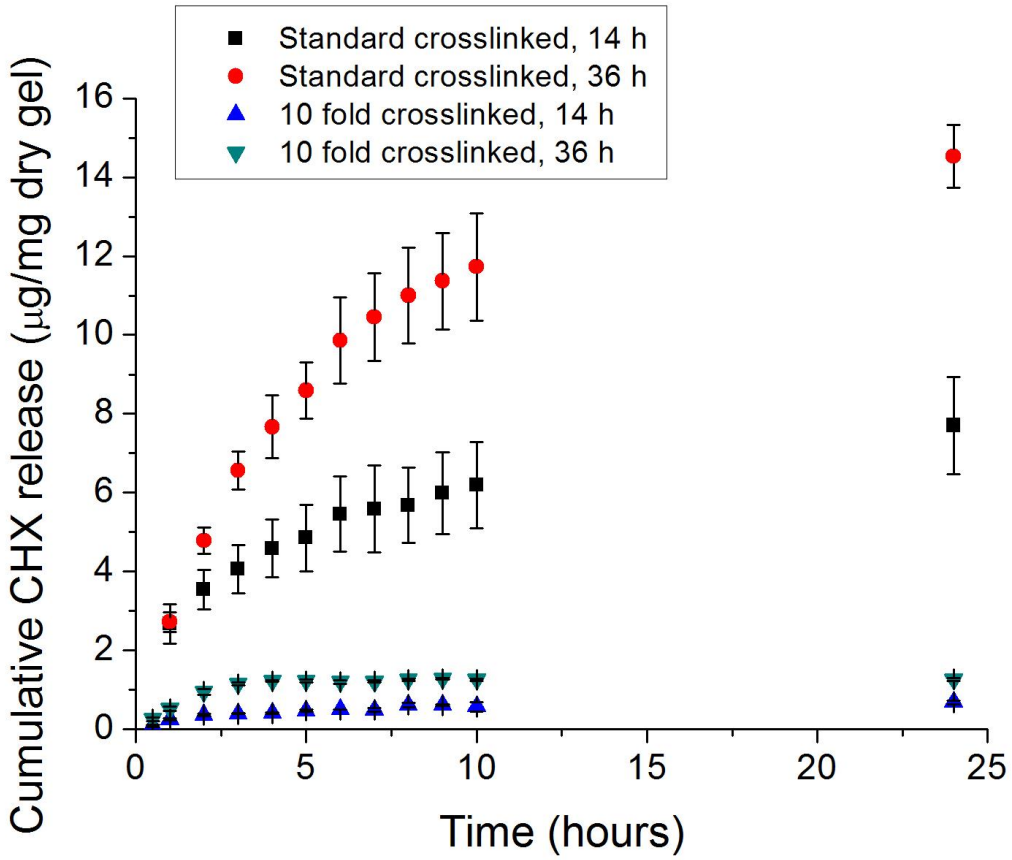

Figure 2.7: Cumulative release profiles of chlorhexidine from TRIS/NVP/HEMA hydrogels with different crosslinking degrees, standard and 10-fold, loaded during 14 hours and 36 hours, obtained in static sink conditions. The error bars correspond to ± standard deviation.

When the crosslinking degree of the hydrogel increased, the amount of drug released was significantly reduced and reached even lower values than those obtained with HEMA/PVP (see Figure 2.5). These results confirm the importance of the mesh size in the release of chlorhexidine, since a higher crosslinked network implies a reduction in the water content and a stereochemical hindrance to the drug diffusion. The influence of the time of loading on the drug release is negligible for the samples with higher crosslinking degree, compared to that in the less crosslinked ones.

Finally, crosslinking of the TRIS/NVP/HEMA hydrogel surface was attempted in order to generate a surface barrier that could retard the drug release. The results obtained (not shown) do not reveal any variation of the drug release profile. Since the surface crosslinking was done before the drug loading due to the need of washing to remove the glutaraldehyde in excess, the surface barrier may have the undesired effect of hindering the drug loading of the hydrogel.

2.3.4 Study of the interaction between drugs and hydrogels

The differences observed in the release of levofloxacin and chlorhexidine from both hydrogels were further investigated in terms of eventual interactions between the drugs and the polymers. In fact, transport of drugs through hydrogels depends not only on the characteristics of the polymer and the drugs but also on the interactions established between them which may enhance the drug loading and/or hinder the drug diffusion. FTIR and Raman spectroscopy are adequate techniques to study the hydrogen bonding and electrostatic interactions between drug/proteins and hydrogels. Hydrogen bonding may be detected by the shifts towards lower wavenumbers in the stretching vibration of the carbonyl group, while electrostatic interactions are responsible by the presence of carboxylate anion, the ionized form of the carbonyl group [28, 29].

The Raman spectra of HEMA/PVP and TRIS/NVP/HEMA hydrogels shown in Figure 2.8 present the typical peaks of the polymer components [30, 31]. Differences between the spectra obtained before and after drug loading will be analyzed. FTIR spectroscopy was also applied but the spectra (not shown) did not reveal any effect of the presence of the drug.

The spectrum of LVF shows two intense peaks at 1613 cm^{-1} and 1437 cm^{-1}. When comparing the spectra of both hydrogels (Figure 2.8A and 2.8B), before and after drug loading, the most intense peak of levofloxacin can be clearly identified in both cases, although shifted to 1620 and 1617 cm^{-1}, for the HEMA/PVP (Figure 2.8A) and TRIS/NVP/HEMA (Figure 2.8A) hydrogels, respectively. This peak was found to present higher intensity in HEMA/PVP which is in agreement with the increased amount of drug released by this hydrogel (see Figure 2.4). Furthermore, an increase of the small peak at ≈1395 cm^{-1} and the presence of a small feature at ≈1550 cm^{-1} in the

levofloxacin loaded HEMA/PVP hydrogel may be attributed to the presence of the carboxylate anion, indicating the existence of electrostatic interactions between the drug and the hydrogel [32]. In the case of the levofloxacin loaded TRIS/NVP/HEMA hydrogel, only an incipient peak at ≈1550 cm^{-1} may be detected which confirms the lower affinity of levofloxacin towards this hydrogel inferred from the cumulative release profiles in Figure 2.4.

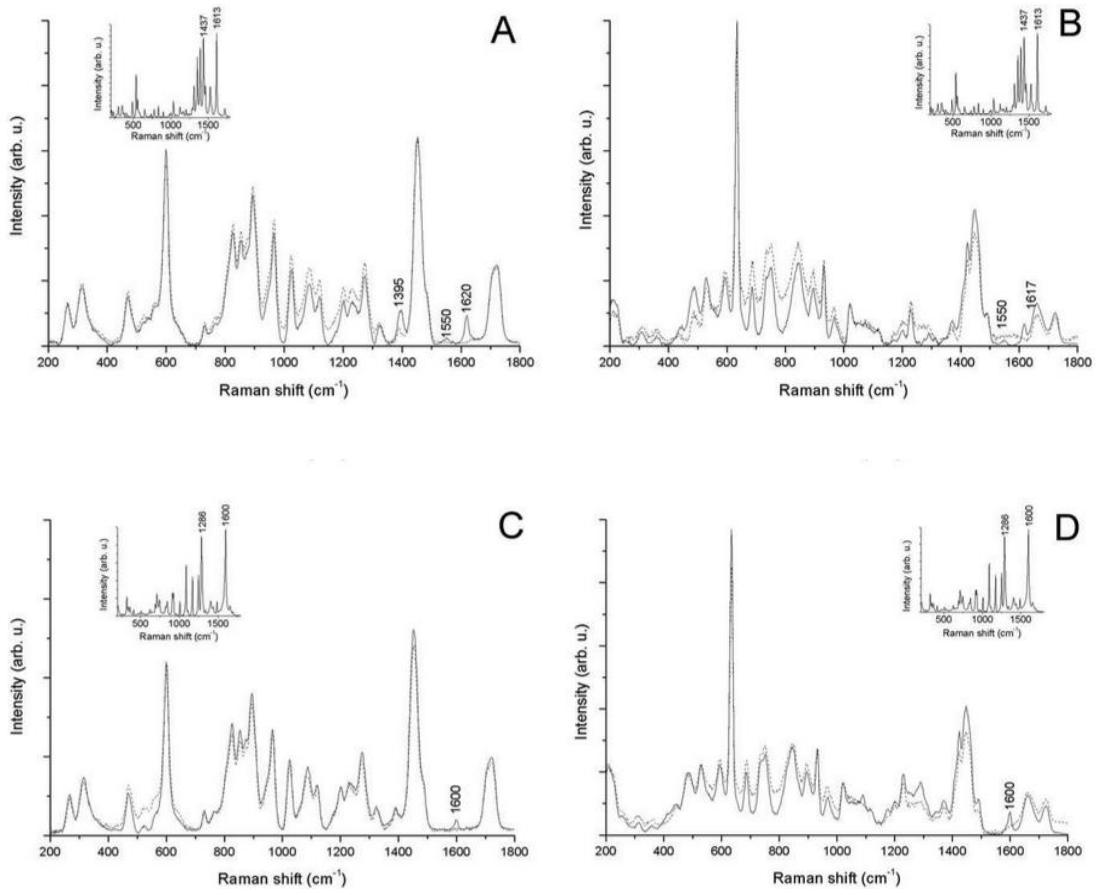

Figure 2.8: Raman spectra of HEMA/PVP (A,C) and TRIS/NVP/HEMA (B,D) hydrogels: dashed lines refer to the hydrogels before drug loading and full lines to the hydrogels after drug loading. (A) HEMA/PVP and LVF; (B) TRIS/NVP/HEMA and LVF; (C) HEMA/PVP and CHX; (D) TRIS/NVP/HEMA and CHX. The inserts represent the spectra of the pure drugs: (A,B) LVF; (C,D) CHX.

The spectrum of CHX shows two intense peaks at 1600 cm^{-1} and 1286 cm^{-1}. Analysis of the spectra of both hydrogels (Figure 2.8C and 2.8D), before and after loading with CHX, shows these two peaks in the drug loaded TRIS/NVP/HEMA hydrogel (Figure 2.8D) and only a small peak at 1600 cm^{-1} (the most intense peak of chlorhexidine) in HEMA/PVP (Figure 2.8C). This comparison is consistent with the higher amount of CHX released from the TRIS/NVP/HEMA hydrogel, observed in the cumulative release profiles of Figure 2.5. In contrast with the LVF loaded hydrogels, the carboxylate anion peaks are not observed in the spectra of the CHX loaded hydrogels, which suggests that electrostatic interactions between the drug and the polymers are not important. Moreover, no shifts of the peaks characteristic of the hydrogels were produced by the presence of the drug which rules out the existence of significant hydrogen bonding. This seems to confirm that the higher loading of CHX in the TRIS/NVP/HEMA hydrogel should not be related with its special affinity to the drug.

2.3.5 Microbiological tests

The MIC of chlorhexidine for *S. aureus* was determined to be 25 μg/ml, see Figure 2.9.

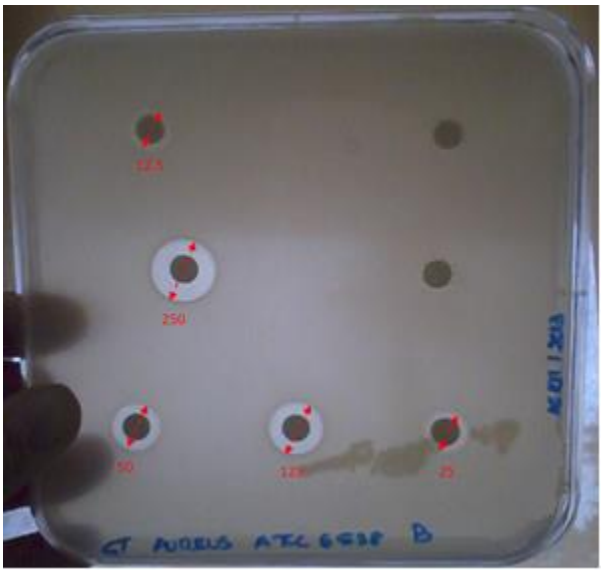

Figure 2.9: Minimum inhibitory concentrations test on CHX against *S. aureus.* The numbers represent the CHX concentration in μg/mL. The halos are evidenced.

In the case of *A. castelanii*, the cells exposed to 30 μg/ml of the drug cannot survive for more than 24 h. Beginning at 1 hour of exposure, many cells show rapid movements with emission of large irregular pseudopods. They can recover from this "stress" response with time and return to a normal morphology. Cells exposed to 40 μg/ml show stop of all intracellular activity within 1 hour of exposure. Exposure to 50 μg/ml leads to stop of all intracellular activity within 10 min for most cells. Exposure to 100 μg/ml leads to rapid burst of most cells. Encysted cells were present in all preparations and in most cases intracystic movements also stopped according to the pattern described, although more slowly. No encystment of cells was observed upon exposure to the drug.

2.3.6 Estimation of the *in vivo* efficacy of the studied systems through mathematical modelling

The experimental data of the release curves relative to 14 hours of drug loading were fitted to various kinetic models: zero order, first order, Higuchi and Korsmeyer-Peppas [33, 34], in order to find which one gives the best description of the cumulative release profiles from the hydrogels.

Before continuing, a brief introduction to these models will be given.

Zero order model

Slow and controlled drug delivery from dosage forms that do not disaggregate, are described by the following equation [35]:

$$M_t = M_0 + k_0 \cdot t \qquad \textbf{Equation 2.5}$$

where M is the amount of drug in the solution at time zero (often equal to zero), M_t is the amount of drug released at time t, k_0 is the zero order release rate constant. In this case the drug release takes place at a constant rate, and is not dependent on the concentrations of the components involved in the process.

Examples that reflect this diffusion model are some transdermal systems, and matrix tablets with low soluble drugs in coated forms [35].

First order model

The first order model describes a drug release in which the release kinetic is directly proportional to the drug concentrations.

The equation that describes this model is the following [35]:

$$\log M_t = \log M_0 - \frac{k_1 \cdot t}{2.303} \qquad \textbf{Equation 2.6}$$

where k_1 is the first order release rate constant.

The first order model describes the drug release from pharmaceutical dosage forms, containing water-soluble drugs in porous matrices [35]

Higuchi model

This model was developed by Higuchi in 1961 and is based on the following equation [35]:

$$M_t = k_H \cdot t^{\frac{1}{2}} \qquad \textbf{Equation 2.7}$$

where k_H is the Higuchi release rate constant.

This model describes the dissolution of the drugs from some transdermal systems and from matrix tablets with water soluble drugs [35]

Korsmeyer-Peppas model

Kormeyer and Peppas in 1983 developed this simplified model to describe Fickian and non-Fickian release of drug from swelled and non-swelled polymeric delivery systems [35].

The model equation is [35]:

$$q = \frac{M_t}{M_\infty} = k_{KP} \cdot t^n \qquad \textbf{Equation 2.8}$$

where $q = M_t/M_\infty$ is the fraction of drug released at the time t, k_{KP} is the release rate constant, and n is the diffusion exponent, which indicates the type of drug transport

mechanism through the polymer. This model equation fits the curve of the cumulative release over time for the first 60% of drug released [35].

Based on the Korsmeyer-Peppas model, values of the n exponent equal to or less than 0.5 define the Fickian or quasi-Fickian diffusion, while an anomalous mechanism of drug release is described by values of $0.5<n<1$. The diffusion coefficient is equal to 1 in the case of zero order release.

The mathematical expression that best described levofloxacin and chlorhexidine release from HEMA/PVP and TRIS/NVP/HEMA was Korsmeyer-Peppas, as it can be concluded by the coefficients of determination presented in Table 2.2.

Table 2.2: Coefficients of determination, R^2, resulting from the fittings of the drug release profiles ([drug] 5 mg/mL and 14 hours loading) to the Zero Order, First Order, Higuchi and Korsmeyer-Peppas models.

Drug/hydrogel system	Zero Order	First Order	Higuchi	Peppas-Krosmeyer
LVF from HEMA/PVP	0.3275	0.9057	0,9416	0.980
LVF from TRIS/NVP/HEMA	-0,853	0.8504	0,9145	---[a]
CHX from HEMA/PVP	0.2198	0.8364	0.9037	0.924
CHX from TRIS/NVP/HEMA	0.3164	0.8941	0.9315	0.995

a: value not calculated

Table 2.3 reports the values of the diffusional exponent, *n*, and coefficient of determination, R^2, obtained from the fittings of the drug release profiles (for the section of curve corresponding to $M_t/M_\infty<0.6$), plotting the logarithm of the cumulative percentage of drug released over the logarithm of the time.

Table 2.3: Diffusional exponents, *n*, and coefficients of determination, R^2, resulting from the fittings of the drug release profiles (14 hours loading) to the Korsmeyer–Peppas Model.

	n	R^2
LVF from HEMA/PVP (5 mg mL^{-1})	0.50	0.980
LVF from TRIS/NVP/HEMA (5 mg mL^{-1})	---[a]	---[a]
CHX from HEMA/PVP (5 mg mL^{-1})	0.49	0.924
CHX from TRIS/NVP/HEMA (1.5 mg mL^{-1})	0.42	0.978
CHX from TRIS/NVP/HEMA (2.5 mg mL^{-1})	0.48	0.994
CHX from TRIS/NVP/HEMA (5 mg mL^{-1})	0.35	0.995

a: value not calculated

The values of *n* are found to be ≤ 0.5 which are consistent with processes mostly controlled by Fickian or quasi-Fickian drug diffusion in the water containing hydrogel network. The release curve of levofloxacin from TRIS/NVP/HEMA did not have enough data to permit a proper fitting.

In order to extrapolate the results obtained from the static sink release experiments to the *in vivo* conditions, a simplified mathematical model, which mimics the physiological conditions of the eye, was developed and applied to the drug release experimental data obtained in sink conditions.

It is assumed that the amount of drug delivered by a drug-loaded, commercial sized, lens to the lachrymal fluid (M_t) during a given time interval (Δt) can be estimated by:

$$M_t = \dot{q} \cdot m_l \Delta t \qquad \textbf{Equation 2.9}$$

where $\dot{q}$ is the drug release rate per unit mass of dry gel, (the derivative of the cumulative mass, q, in order to the time), and m_l is the dry mass of the lens. Assuming a renewal rate of the lachrymal fluid of 3 μL/min, that is the case for contact lenses wearers [11], and a total tear volume in the eye (V_t) of ≈7 μL at each instant [7, 10], the volume fraction of renovated fluid in each minute, R_r, corresponds to 0.43. Thus, the drug concentration in the lachrymal fluid at a given time, *t*, (in min) after the lens application may be obtained from:

$$[Drug]_t = \frac{M_t}{V_t} + (1 - R_r)[Drug]_{t-1}$$ **Equation 2.10**

As a first approximation, the tear volume is considered a homogeneous mixture although it is known that the drug in the PoLTF is not perfectly mixed with the remaining fluid [36]. The dry masses of the gels were 66 mg and 36 mg, in the case of HEMA/PVP and TRIS/NVP/HEMA respectively, which correspond to lenses with diameter of 14 mm.

Figure 2.10 shows the estimated LVF concentration profile in the eye, obtained by the application of HEMA/PVP hydrogel, loaded for 14 hours with a 5 mg/mL LVF solution. For comparative purposes, the figure also shows the estimated antibiotic concentration in the eye over time, as a result of the application of commercial levofloxacin eye drops (QUIXIN® 5 mg/mL) and the minimum inhibitory concentrations of *S. aureus* and *P. aeruginosa*, previously estimated [15] ($MIC_{S.\ aureus}$ = 16 μg/mL and $MIC_{P.\ aeruginosa}$ = 62 μg/mL).

The eye drops profile results in a saw shape like curve, assuming that only the 5% of the instillation remained in the eye, after the application of the recommended dosage (1-2 drops every hour). According to our model, when using the drug loaded PHEMA based lenses, the LVF concentration in the tear fluid remains well above both MICs for about 7.5 hours. Furthermore, the initial burst of drug release is in the same order of magnitude of the maximum concentration for each eye drops application.

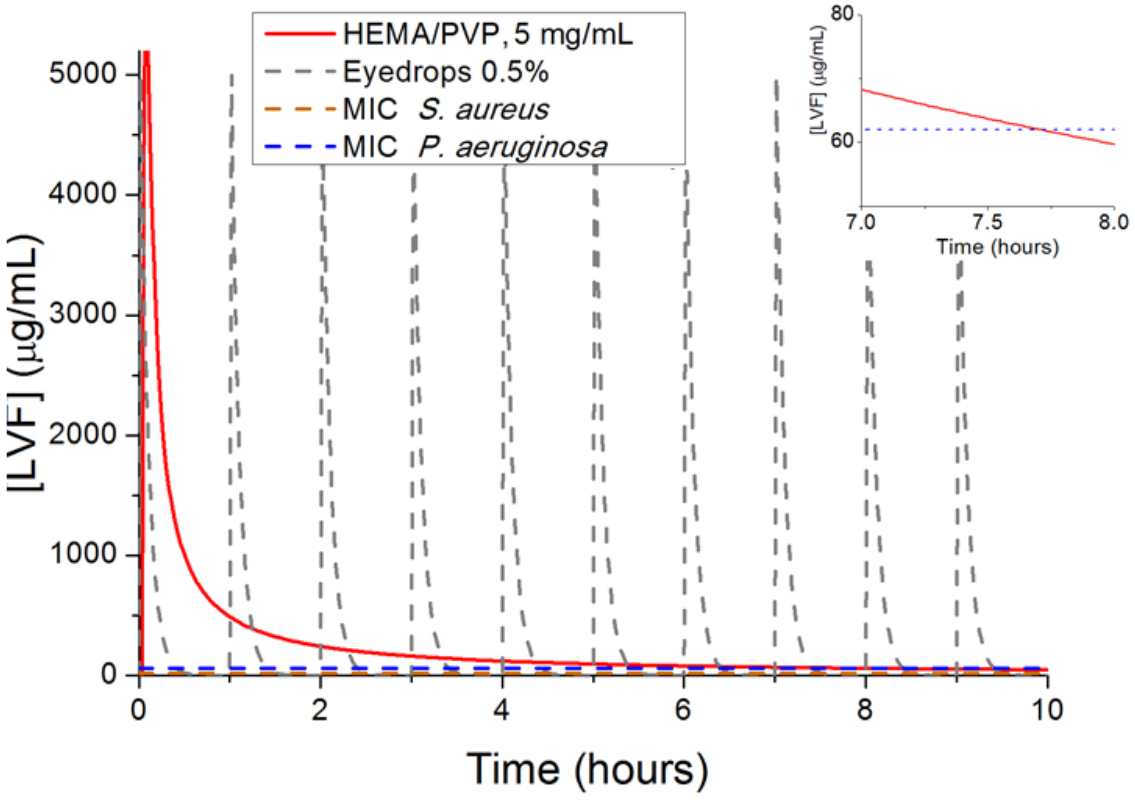

Figure 2.10: Estimation of the LVF concentration in the eye, following the application of drug loaded HEMA/PVP lenses loaded for 14 hours. The antibiotic concentration in the eye resultant from the application of commercial eyedrops and the MICs of S. *aureus* and P. *aeruginosa* are included. The enlargement on the right top of the figure shows the crossing line of the concentration profile with the P. *aeruginosa* MIC.

Figure 2.11 shows the estimated CHX concentration profiles in the eye, obtained by the application of TRIS/NVP/HEMA hydrogel, loaded for 14 hours with respectively 1.5 mg/mL, 2.5 mg/mL and 5 mg/mL CHX solution, and of HEMA/PVP hydrogel loaded for 14 hours with 5 mg/mL of CHX. For comparative purposes, the figure also shows the estimated CHX concentration in the eye over time, as a result of the application of 0.2% CHX eye drops along 12 hours, and the minimum inhibitory concentrations of *S. aureus* ($MIC_{S.\ aureus}$ = 25 µg/mL) and the maximum concentration (600 µg/mL) used in patients with very severe eye diseases, which may be considered as a toxicity limit [37].

The toxicity of chlorhexidine towards *A. castelanii* is not included for the sake of clarity but, as explained in section 2.3.5, cell death occurs for concentrations above 40 µg/mL.

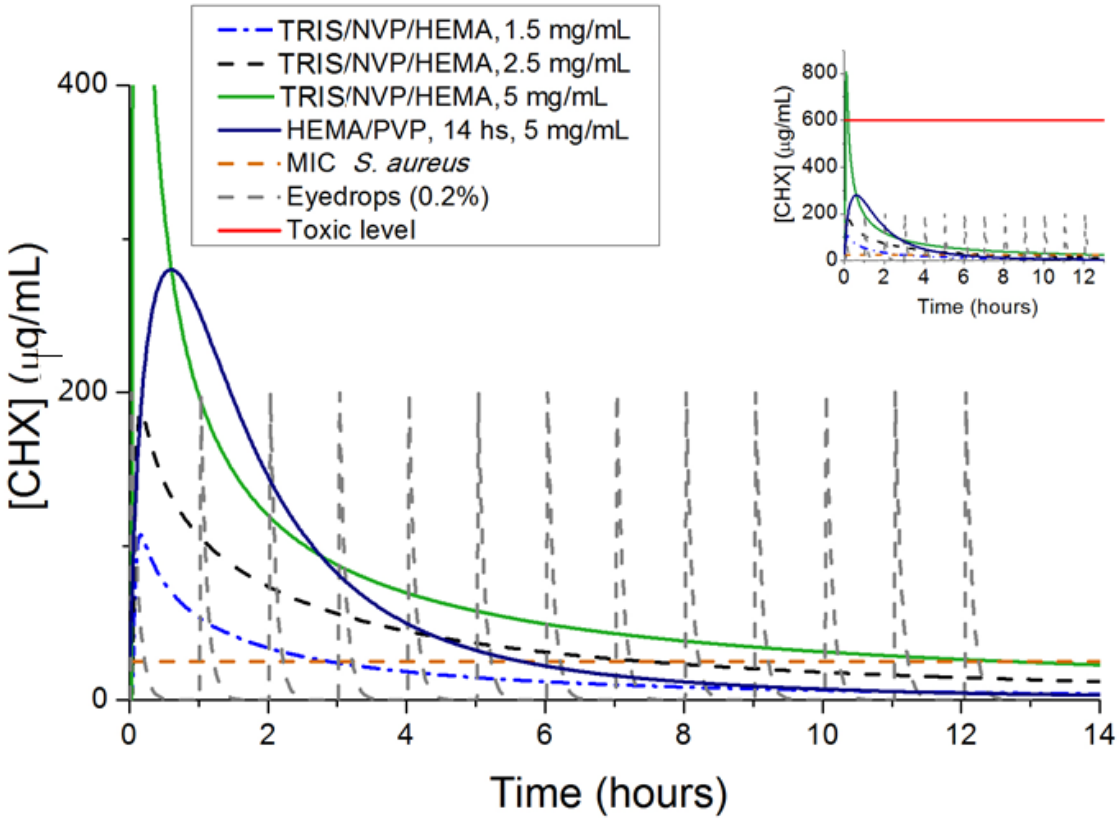

Figure 2.11: Estimation of the chlorhexidine concentration in the eye, following the application of drug loaded TRIS/NVP/HEMA lenses loaded for 14 hours respectively in: 5 mg/mL, 2.5 mg/mL and 1.5 mg/mL, and HEMA/PVP lens: 5 mg/mL. The concentration in the eye resultant from the application of 0.2% CHX eye drops, the toxicity limit and the MIC of S. *aureus* are included. The insert represents the same figure with a major scale on the y axis.

The CHX concentration profiles referred respectively to TRIS/NVP/HEMA loaded with 1.5 mg/mL, 2.5 mg/mL and 5 mg/mL result to be higher than the $MIC_{S.\ aureus}$ along 3, 7 and 13 hours. The TRIS/NVP/HEMA, 5 mg/mL, system presents an initial burst that overcomes the toxicity limit, as it is shown in the insert in Figure 2.10. The concentration profiles from HEMA/PVP (5 mg/mL) results to be higher than the $MIC_{S.\ aureus}$ along 5.5 hours.

It may be concluded that in both LVF and CHX cases, the hydrogels under study have a successful potential as therapeutic SCLs materials. The burst effect evidenced in every concentration profile is a consequence of the fact that the developed mathematical model is applied to the data obtained in static sink conditions. For this reason a further

investigation using a microfluidic cell was performed, with the attempt to further approximate to the *in vivo* conditions.

2.3.7 Release studies under dynamic conditions

The static sink model represents the fastest release condition with the highest possible driving force and, for this reason, it is not consistent with the physiological eye conditions. It is expected that in *in vivo* conditions, the drug release rates would be slowed down due to the small tear volume (7 μL) and to the physiological tear flow rates encountered in the eye.

In order to predict in a more accurate way the *in vivo* drug concentration profiles, a microfluidic device was built to simulate the hydrodynamic conditions of the eye. The cumulative release profile of LVF from HEMA/PVP hydrogels previously loaded for 14 hours in 5 mg/mL of LVF solutions is shown in Figure 2.12.

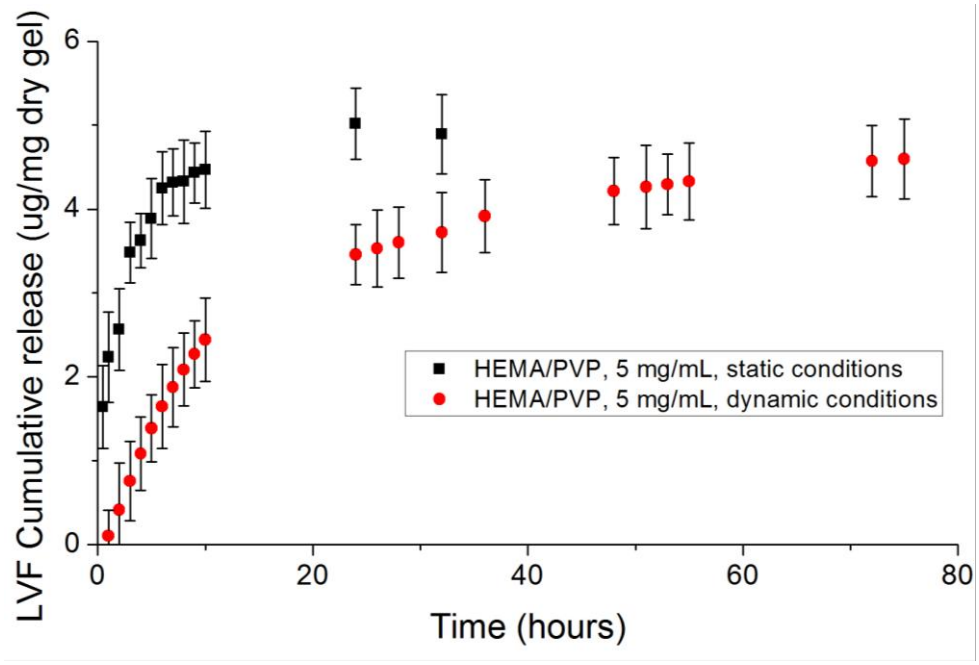

Figure 2.12 Cumulative release profiles of levofloxacin from HEMA/PVP hydrogels, under static sink and dynamic conditions. Hydrogels loaded for 14 hours with [LVF] 5mg/mL.

The curve obtained in dynamic conditions is compared with the one obtained in static sink conditions. The figure shows a controlled drug release along at least 70 hours under tear flow conditions, while under static sink conditions the release time of LVF from

HEMA/PVP is much shorter (duration of 10 hours). The total amount of drug released in both static and continuous flow conditions tends to similar values.

The obtained results demonstrate that LVF was released at much lower rates in flow conditions than under static sink conditions. The profiles obtained in static sink conditions present an initial burst, which does not exist in continuous flow conditions. As Tieppo *et al.* proposed [12], the boundary layer effects caused by the low physiological renovation rates and the small cell volume used in the microfluidic cells are determinant and lead to the decrease of the local diffusion concentration driving forces which consequently causes the decrease in the release rates.

For a better understanding of the effect of the dynamic condition of release on the drug release kinetics, the previously described simplified mathematical model (Equation 2.10), using the conditions of the microfluidic cell (flow rate= 3μL/min and release volume= 45 μL), was applied to the time derivative of the experimental data of cumulative release presented in Figure 2.12.

Figure 2.13 compares the estimated LVF concentrations in the eye obtained using the drug release rates, respectively, under static and dynamic release conditions. These concentration profiles are compared to the MICs of *S. aureus* and *P. aeruginosa*.

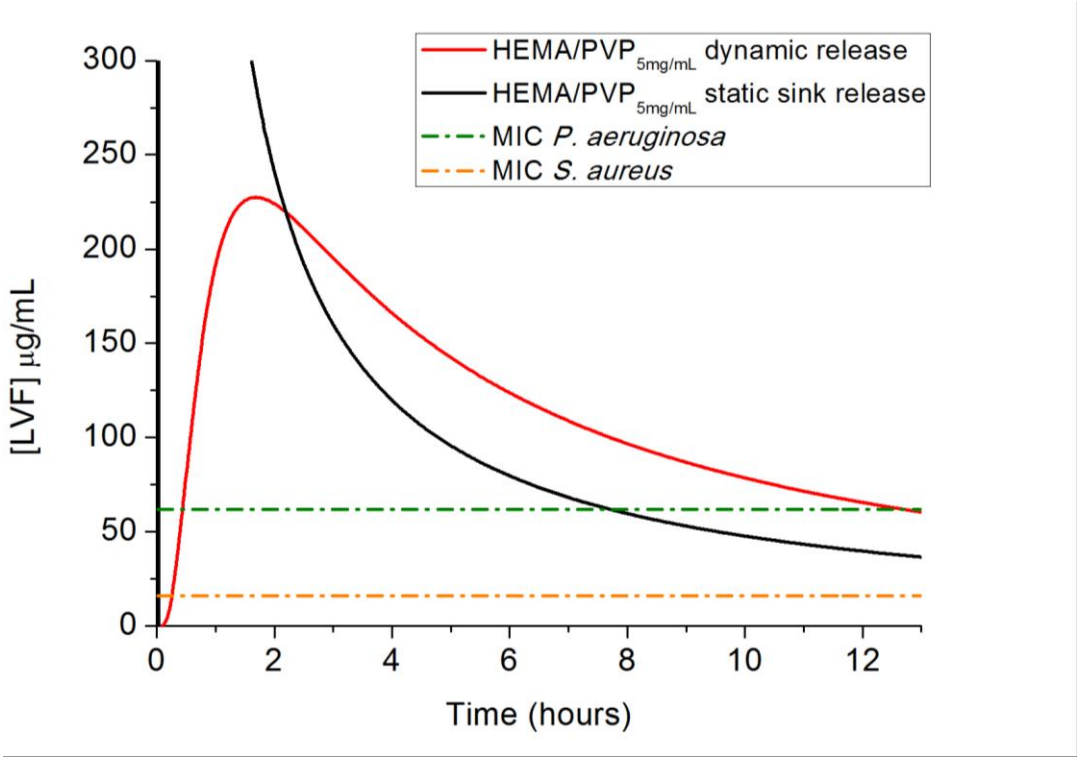

Figure 2.13: Estimation of the LVF concentration through the mathematical model applied to the experimental data obtained by the release experiment under dynamic and sink conditions. The LVF concentrations are compared with the MICs of *S. aureus* and *P. aeruginosa*.

The curves presented in Figure 2.13 confirm the previously described assumption, namely that the small release volume (in the case of the microfluidic cell 45 µL) and the low renovation rate allow a more sustained drug release, slowing down the release rates. The efficacy duration against the *S. aureus* and *P. aeruginosa* are prolonged to 13 hours, in the case of dynamic release conditions, against the 7.5 hours for the case of static release conditions. It is believed that this efficacy duration can further be extended by increasing the drug upload of the hydrogel, without risking to exceed eventual toxic level, thanks to the fact that, as it can be seen in Figure 2.12, the physiological conditions largely decrease the burst, previously evidenced in Figures 2.9 and 2.10.

2.4 Conclusions

Two types of hydrogels, HEMA/PVP (98/2 w/w) and TRIS /NVP/HEMA (40/40/20, w/w/w), were prepared, characterized and tested for drug release in therapeutic lenses. Both hydrogels revealed adequate properties to be used as ophthalmic materials. Loading with levofloxacin and chlorhexidine was done by soaking in the drug solutions. The *in vitro* tests, under static and dynamic conditions, show that the hydrodynamic conditions strongly determine the release profiles.

In static sink conditions, the levofloxacin (5 mg/mL) loaded HEMA/PVP hydrogel leads to controlled drug release keeping the drug concentration well above the MICs of the *S. aureus* and *P. aeruginosa* for 7.5 hours, as predicted by a simple mathematical model. For chlorhexidine, the TRIS/NVP/HEMA hydrogel loaded with 1.5mg/mL, 2.5 mg/mL and 5 mg/mL, kept the concentration in the eye above the MIC of the *S. aureus* for 3, 7 and 13 hour, respectively, although for the higher [CHX] concentration (5 mg/mL), the toxic level is overcome in the first hour. HEMA/PVP loaded with a solution of [CHX] 5 mg/mL maintained a therapeutic level higher than the MIC for only 5.5 hours.

Under dynamic conditions, using a small release volume (45 μL) and physiological flow rate conditions (3 μL/min),the drugs are released in a more sustained way, without initial burst, reaching a total release time superior to 70 hours in the case of LVF from HEMA/PVP hydrogels. Application of the simplified mathematical model to these experimental data, led to concentrations of LVF above the MICs of *S. aureus* and *P. aeruginosa* for at least 13 hours

The differences between the results obtained under static and dynamic conditions are expected taking into consideration that a small release volume and the presence of physiological flow rate in the dynamic approach cause a lower driving force for release, and avoid the burst effect.

Anyway, the results of the mathematical model applied to the profiles obtained in static sink conditions, as well as the results obtained from the use of the microfluidic cell simulating the physiological tear flow condition, suggest that both hydrogels may be useful to produce therapeutic daily disposable contact lenses, since they are able to

maintain levofloxacin and/or chlorhexidine concentrations in the eye above the minimum inhibitory concentrations of the pathological agents for several hours. The efficacy time of the hydrogels against the microorganisms of study can be increased by increasing the loading concentration of LVF and CHX.

The microfluidic device, under adequate conditions of flow rate and cell volume, was confirmed to be a proper tool for the study of the drug release from SCLs. Although sink conditions are useful for comparative studies, it is imperative to take in consideration the dynamic release experiments when characterizing the release performances of SCLs with respect to the MICs of the pathological species.

2.5 References

1. C. Alvarez-Lorenzo, H. Hiratani and A. Concheiro, *Contact lenses for drug delivery.* Am. J. Drug. Deliv., 2006. **4**(3): p. 131-151.
2. V.P. Costa, M.E.M. Braga, J.P. Guerra, A.R.C. Duarte, C.M.M. Duarte, E.O.B. Leite, M.H. Gil and H.C. de Sousa, *Development of therapeutic contact lenses using a supercritical solvent impregnation method.* J Supercrit Fluids, 2010. **52**(3): p. 306-316.
3. A. Danion, H. Brochu, Y. Martin and P. Vermette, *Fabrication and characterization of contact lenses bearing surface-immobilized layers of intact liposomes.* J. Biomed. Mater. Res. A., 2007. **82**(1): p. 41-51.
4. D. Gulsen and A. Chauhan, *Ophthalmic Drug Delivery through Contact Lenses.* Invest Ophth Vis Sci, 2004. **45**(7): p. 2342-2347.
5. H. Hiratani and C. Alvarez-Lorenzo, *Timolol uptake and release by imprinted soft contact lenses made of N,N-diethylacrylamide and methacrylic acid.* J Control Release, 2002. **83**(2): p. 223-230.
6. H.J. Jung, M. Abou-Jaoude, B.E. Carbia, C. Plummer and A. Chauhan, *Glaucoma therapy by extended release of timolol from nanoparticle loaded silicone-hydrogel contact lenses.* J. Control. Release, 2013. **165**(1): p. 82-89.
7. Y. Kapoor, J.C. Thomas, G. Tan, V.T. John and A. Chauhan, *Surfactant-laden soft contact lenses for extended delivery of ophthalmic drugs.* Biomaterials, 2009. **30**(5): p. 867-878.
8. L. Wu and C.S. Brazel, *Surface crosslinking for delayed release of proxyphylline from PHEMA hydrogels.* Int J Pharm, 2008. **349**(1-2): p. 1-10.
9. F. Yañez, A. Concheiro and C. Alvarez-Lorenzo, *Macromolecule release and smoothness of semi-interpenetrating PVP–pHEMA networks for comfortable soft contact lenses.* Eur J Pharm Biopharm, 2008. **69**(3): p. 1094-1103.
10. C. White, A. Tieppo and M. Byrne, *Controlled drug release from contact lenses: a comprehensive review from 1965-present.* J Drug Deliv Sci Tec, 2011. **21**(5): p. 369-384.
11. M.J. Glasson, F. Stapleton, L. Keay and M.D. Willcox, *The effect of short term contact lens wear on the tear film and ocular surface characteristics of tolerant and intolerant wearers.* Cont Lens Anterior Eye, 2006. **29**(1): p. 41-7; quiz 49.

12. A. Tieppo, K.M. Pate and M.E. Byrne, *In vitro controlled release of an anti-inflammatory from daily disposable therapeutic contact lenses under physiological ocular tear flow.* Eur J Pharm Biopharm, 2012. **81**(1): p. 170-177.
13. M. Ali, S. Horikawa, S. Venkatesh, J. Saha, J.W. Hong and M.E. Byrne, *Zero-order therapeutic release from imprinted hydrogel contact lenses within in vitro physiological ocular tear flow.* J Control Release, 2007. **124**(3): p. 154-62.
14. C.J. White, M.K. McBride, K.M. Pate, A. Tieppo and M.E. Byrne, *Extended release of high molecular weight hydroxypropyl methylcellulose from molecularly imprinted, extended wear silicone hydrogel contact lenses.* Biomaterials, 2011. **32**(24): p. 5698-705.
15. R.P. Galante, P, M. Moutinho, A. Fernandes, J. Mata, A. Matos, R. Colaço, B. Saramago and A. Serro, *About the effect of eye blinking on drug release from pHEMA-based hydrogels: an in vitro study.* J Biomater Sci Polym, 2015. **26**(4): p. 235-51.
16. R. Vazquez, R. Nogueira, M. Orfao, J.L. Mata and B. Saramago, *Stability of triglyceride liquid films on hydrophilic and hydrophobic glasses.* J Colloid Interface Sci, 2006. **299**(1): p. 274-82.
17. D. de Ortueta, T. Magnago and S. Arba-Mosquera, *Thermodynamic measurement after cooling the cornea with intact epithelium and lid manipulation.* J Optom, 2015. **8**(3): p. 170-3.
18. M. Sniegowski, M. Erlanger, R. Velez-Montoya and J.L. Olson, *Difference in ocular surface temperature by infrared thermography in phakic and pseudophakic patients.* Clinical Ophthalmology (Auckland, N.Z.), 2015. **9**: p. 461-466.
19. P.C. Nicolson and J. Vogt, *Soft contact lens polymers: an evolution.* Biomaterials, 2001. **22**(24): p. 3273-83.
20. F.A. Wong, S.J. Juzwin and S.C. Flor, *Rapid stereospecific high-performance liquid chromatographic determination of levofloxacin in human plasma and urine.* J Pharm Biomed Anal, 1997. **15**(6): p. 765-71.
21. R.D. Schoenwald, *Ocular pharmacokinetics*, in *Textbook of Ocular Pharmacology*, K.K. T.J. Zimmerman, M. and e.a. Sharir, Editors. 1997, Lippincott-Raven: Philadelphia.
22. E. Ruel-Gariépy and J.-C. Leroux, *In situ-forming hydrogels—review of temperature-sensitive systems.* Eur J Pharm Biopharm, 2004. **58**(2): p. 409-426.

23. P.C. Nicolson, R.C. Baron, P. Chabrecek, J. Court, A. Domschke, H.J. Griesser, A. Ho, J. Hopken, B.G. Laycock and Q. Liu, *Extended wear ophthalmic lens*. 1998, Google Patents.
24. N.A. Brennan, *Beyond flux: total corneal oxygen consumption as an index of corneal oxygenation during contact lens wear.* Optom Vis Sci, 2005. **82**(6): p. 467-72.
25. N. Efron and C. Maldonado-Codina, *Development of Contact Lenses from a Biomaterial Point of View – Materials, Manufacture, and Clinical Application*, in *Comprehensive Biomaterials*, D. Editor-in-Chief: Paul, Editor. 2011, Elsevier: Oxford. p. 517-541.
26. L. Li and Z. Xin, *Surface-hydrophilic and protein-resistant tris(trimethylsiloxy)-3-methacryloxypropylsilane-containing polymer by the introduction of phosphorylcholine groups.* Colloid Surface A, 2011. **384**(1–3): p. 713-719.
27. N. Hiraishi, C.K.Y. Yiu, N.M. King, F.R. Tay and D.H. Pashley, *Chlorhexidine release and water sorption characteristics of chlorhexidine-incorporated hydrophobic/hydrophilic resins.* Dent Mater, 2008. **24**(10): p. 1391-1399.
28. M.T. Am Ende and N.A. Peppas, *FTIR spectroscopic investigation and modeling of solute/polymer interactions in the hydrated state.* J Biomater Sci Polym Ed, 1999. **10**(12): p. 1289-302.
29. N.B. Colthup, L.H. Daly and S.E. Wiberley, *Introduction to infrared and Raman spectroscopy*. 1990: Academic Press.
30. A. Bertoluzza, P. Monti, J.V. Garcia-Ramos, R. Simoni, R. Caramazza and A. Calzavara, *Applications of Raman spectroscopy to the ophthalmological field : Raman spectra of soft contact lenses made of poly-2-hydroxyethylmethacrylate (PHEMA).* J Mol Struct, 1986. **143**(0): p. 469-472.
31. L. Hu, C. Zhang, Y. Chen and Y. Hu, *Synthesis and silicon gradient distribution of emulsifier-free TRIS-containing acrylate copolymer.* Colloid Surface A, 2010. **370**(1–3): p. 72-78.
32. B. Schrader, *Infrared and Raman Spectroscopy*. 1995: Wiley-VCH Verlag GmbH. 215.
33. N.A. Peppas, P. Bures, W. Leobandung and H. Ichikawa, *Hydrogels in pharmaceutical formulations.* Eur J Pharm Biopharm, 2000. **50**(1): p. 27-46.

34. L. Serra, J. Domenech and N.A. Peppas, *Drug transport mechanisms and release kinetics from molecularly designed poly(acrylic acid-g-ethylene glycol) hydrogels.* Biomaterials, 2006. **27**(31): p. 5440-5451.

35. S. Dash, P.N. Murthy, L. Nath and P. Chowdhury, *Kinetic Modeling on Drug Release from Controlled Drug Delivery Systems.* Acta Poloniae Pharmaceutica, 2010. **67**(3): p. 217-223.

36. N.A. McNamara, K.A. Polse, R.J. Brand, A.D. Graham, J.S. Chan and C.D. McKenney, *Tear mixing under a soft contact lens: effects of lens diameter.* Am J Ophthalmol, 1999. **127**(6): p. 659-665.

37. W. Mathers, *Use of higher medication concentrations in the treatment of acanthamoeba keratitis.* Arch Opthalmol (Chic.), 2006. **124**(6): p. 923-923.

3 Effect of plasma treatment on the hydrogels drug release performance

The following results were published in the peer-reviewed international Journal of Biomedical Materials Research: Part B Applied Biomaterials. July 2015.103(5):1059-68.
doi:10.1002/jbm.b.33287

Table of contents

3.1 Introduction

Plasma technology has been used to treat silicone contact lenses in order to enhance patient comfort through the improvement of wettability [1]. Other potential applications of plasma treatments are disinfection and sterilization of medical devices which are sensitive to radiation, temperature and chemicals [2]. Thus, when applied to contact lenses, plasma treatment may have the advantage of providing simultaneous sterilization and surface modification.

Plasma treatments of silicone contact lenses have relied on the techniques of plasma modification where the lenses are finished by plasma oxidation [3, 4] and by plasma deposition where a thin layer is deposited on the lens surface by plasma polymerization [5]. Several authors [6-11] investigated the modifications in the chemistry, topography, wettability and biocompatibility of the lens surface caused by plasma treatments but a large part of this research is described in technical notes and patents. The effect of the plasma on the lens surface depends on the processing conditions, namely, gas, power, pressure, and time. In general, plasma treatments in moderate conditions increase the wettability of the polymer surface, without significantly affecting other important characteristics of the lenses, such as oxygen and ion permeability [12].

One well known effect of plasma treatments of polymers is the formation of a cross-linked surface layer [13]. The restriction to the molecular chains mobility in this layer, which results from the generated tri-dimensional network, may act as a barrier to the drug release from polymers. The use of plasma treatments for sustained drug release has been the focus of interest of researchers in the last few years. Kuzuya *et al*. reported the effect of argon and oxygen plasma on the drug release from tablets [14, 15]. Hagiwara studied the effects of plasma treatment on the drug release profile of poly(ethylene-co-vinyl acetate) (EVA) polymer used in the manufacture of drug eluting stents [16].

To the best of our knowledge, the effect of plasma treatment on the performance of drug loaded contact lenses has never been investigated before. The objective of the present chapter is to assess the effect of nitrogen plasma treatment on the two drug-loaded polymeric formulations studied in Chapter 2: the PHEMA based hydrogel (HEMA/PVP) and the silicone based hydrogel (TRIS/NVP/HEMA). The PHEMA

based hydrogel loaded with levofloxacin, and the silicone based hydrogel loaded with chlorhexidine were shown to be suitable materials for the preparation of daily disposable therapeutic contact lenses. In this chapter, the modifications of the surface properties by the plasma treatment were assed using scanning electron microscopy (SEM), atomic force microscopy (AFM), contact angle measurements and friction coefficients determination. The effect of plasma on the optical properties was evaluated by transmittance and refractive index measurements. Alterations in the drug release profiles and possible losses of the drugs activities induced by the plasma treatment were evaluated. These studies were done under different plasma processing conditions, namely, power and time of irradiation.

3.2 Experimental part

3.2.1 Materials

The materials used are the same as reported in section 2.2.1 of Chapter 2

3.2.2 Hydrogels preparation

The protocol followed is the same as reported in section 2.2.1 of Chapter 2.

3.2.3 Drug loading

Before plasma treatment the hydrogel samples were drug loaded. The dry hydrogel samples were loaded with the drugs (HEMA/PVP with levofloxacin and TRIS/NVP/HEMA with chlorhexidine) by soaking in the drug solution (2.6 mL/cm^2 of surface area), with a concentration of 10 mg/mL and 5 mg/mL, respectively, for 14 hours at 4 °C. Levofloxacin was dissolved in a saline solution (130 mM NaCl), while chlorhexidine was dissolved in simple DD water due to its limited solubility in saline solution. The soaking process was protected from light. The loaded samples were rinsed with DD water, blotted with absorbent paper and dried overnight before plasma treatment or release experiments, in the case of the control samples.

3.2.4 Plasma treatments

The nitrogen plasma treatments were performed under the supervision of Professor Virginia Chu using the Electrotech Delta PECVD system located at the INESC Microsistemas e Nanotecnologias. The flux of N_2 was 2000 sccm and the process pressure was 20 Pa. RF power (13.56 MHz) was applied to the gas showerhead which also acts as the powered electrode. The polymer pieces were mounted on a 150 mm diameter silicon wafer which sat on the grounded counterelectrode, kept at ambient temperature during the plasma treatment. Three RF powers (100, 200 and 300 W) and three plasma treatment times (10, 25 and 35 s) were tested.

3.2.5 Hydrogel characterization

Section 2.3.1 reported a detailed characterization of HEMA/PVP and TRIS/NVP/HEMA. Here, we focused on the effect of plasma treatment on the properties which are more susceptible of being modified by the surface plasma.

3.2.5.1 Swelling capacity

The equilibrium water content (EWC) of HEMA/PVP and TRIS/NVP/HEMA hydrogels after plasma treatment of 200 W with a duration of 10 s, was measured following the protocol presented in Chapter 2, section 2.2.3.1.

3.2.5.2 Transmittance and refractive index

The transmittance of visible light through hydrated hydrogel samples after plasma treatment, was measured in the wavelength range of 400 to 700 nm, using a UV-Vis Beckmam DU-70 spectrophotometer, following the experimental protocol described in 2.2.3.3.

The refractive index of the dry and hydrated samples was determined with a spectral ellipsometer, which measures the relative changes in amplitude and phase of the polarized incident light before and after reflection on the surface of the samples. The experiments were performed thanks to the collaboration with Professor Luis Santos

from IST. The measurements were carried out on a UVISEL model from HORIBA Jobin-Yvon, with an angle of incidence of 70°, in the wavelength range of 300 to 850 nm. Modeling was done with the Deltapsi software from the supplier. The experimental data were modeled with a Cauchy transparent model, in order to extract the optical constants and the layer thicknesses. The tests were done in triplicate and the excess of water in the hydrated sample surfaces was removed.

3.2.5.3 Wettability

The wettability of both dry and hydrated hydrogels was determined through the measurement of DD water contact angles by the sessile drop and the captive air bubble methods, respectively. For the dry samples the experimental procedure was described in 2.2.3.6.The hydrated hydrogels were characterized by measuring the contact angles of air bubbles, of volume 4-6 μL, lying underneath the substrates immersed in water. The same equipment and software, as in the case of the dry samples characterization, was used for the image acquisition and analysis. The measurements were done at 20 ºC at least in triplicate.

3.2.5.4 Surface topography/microstructure

The surface of the hydrogels was observed using a scanning electron microscope (SEM) Hitachi S2400 (15 KeV). The swollen samples were cracked in liquid nitrogen, kept at -80°C for 4 hours and then freeze-dried overnight. Prior to the SEM analysis the hydrogels were coated with a thin gold film (thickness 30 nm).

The freeze-dried samples were analyzed at nanoscale with a Veeco DI CP-II atomic force microscope. Rectangular shaped silicon cantilevers with a tip curvature of 8 nm and nominal spring constants of 0.9 N/m were used for contact mode imaging in air. Surface roughness (Ra) values and respective standard deviations correspond to five 10 x10 μm^2 scans, taken on different areas using a normal load of 50 nN.

3.2.5.5 Friction coefficient

Tribology experiments were run at room temperature on a CSM microtribometer using semi-spheres of PMMA, with a curvature radius of 2 mm, as the counterbody, and saline solution (130 m NaCl), as the lubricant. The normal force applied was 20 mN and the sliding velocity was 0.7 cm/s. The data were analyzed with the software TriboX. A minimum of three measurements were done on the samples of each type.

3.2.6 Drug release experiments

Drug release was monitored for 32 h, at 35 °C. The loaded samples, plasma treated and control, were immersed in the saline solution (2.6 mL/cm^2 of surface area), in closed vessels, under stirring (150 rpm). At pre-determined time intervals, aliquots (~ 8% of total volume) of the supernatant were collected and replaced by the same volume of fresh NaCl solution.

The concentrations in the supernatant of LVF and CHX were respectively measured following the protocol previously described in Section 2.2.5.1. A minimum of three samples was used for each release profile.

The drug loading was determined using the same conditions as in drug release, except that the samples were immersed in the saline solutions until no further release was detected. The LVF content of HEMA/PVP lenses was determined to be 15 ±1 μg/mg dry gel, whereas the CHX content in TRIS/NVP/HEMA lenses was 11.3 ±0.7 μg/mg dry gel.

3.2.7 Determination of the antimicrobial activity of the drugs

To assess the effect of plasma on the activity of the released drugs, microbiological tests were carried out with solutions resulting from the release tests. The growth inhibition halos of *S. aureus* and *P. aeruginosa* produced by the processed drugs were compared with those of freshly prepared drug solutions with the same drug concentration.

Cultures of *S. aureus* and *P. aeruginosa* were inoculated and a solution with final optical bacterial density of 1 McFarland was prepared by dilution with distilled and

sterilized water. A volume of 350 µL of this suspension was added to 50 mL of Muller Hinton broth solution (Becton, Dickinson and Company). The inoculated medium was poured into square plates and allowed to solidify. Paper discs impregnated with 15 µL of levofloxacin and chlorhexidine solutions (the latter only for *S. aureus*) obtained by the release tests of plasma treated hydrogels, were carefully placed on the plates to determine the growth inhibition diameters. For control, paper disks were impregnated with 15 µL of drug solution (same concentration) prepared with non-processed drug. The dimensions of the halos were measured with an electronic caliper, after overnight incubation at 37 °C. The assays were repeated twice in triplicate.

3.3 Results and Discussion

3.3.1 Hydrogel characterization

The transmittance of both hydrogels before and after plasma treatment is represented as a function of time and power of treatment in Figure 3.1 A and Figure 3.1 B, respectively. For both hydrogels, the values of transparency steadily decrease when the power and time of the plasma treatment increase. This effect is more pronounced in the case of TRIS/NVP/HEMA. However, up to 200W and 10 s, both hydrogels keep their transparency close to 90%, matching the transmittance characteristics required for soft contact lenses [1].

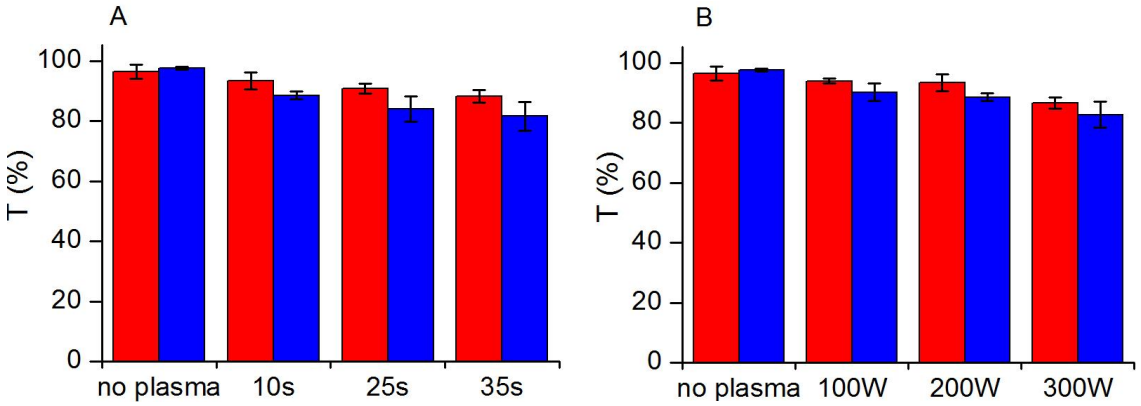

Figure 3.1: Plasma treatment effect on transmittance: time dependence (at 200 W) (A) and power dependence (for 10 s) (B) of HEMA/PVP (red) and TRIS/NVP/HEMA (blue) hydrogels.

The experimental results of the ellipsometric data of dry and hydrated samples of HEMA/PVP and TRIS/NVP/HEMA hydrogels, before and after the plasma treatment, are presented in Figure 3.2.

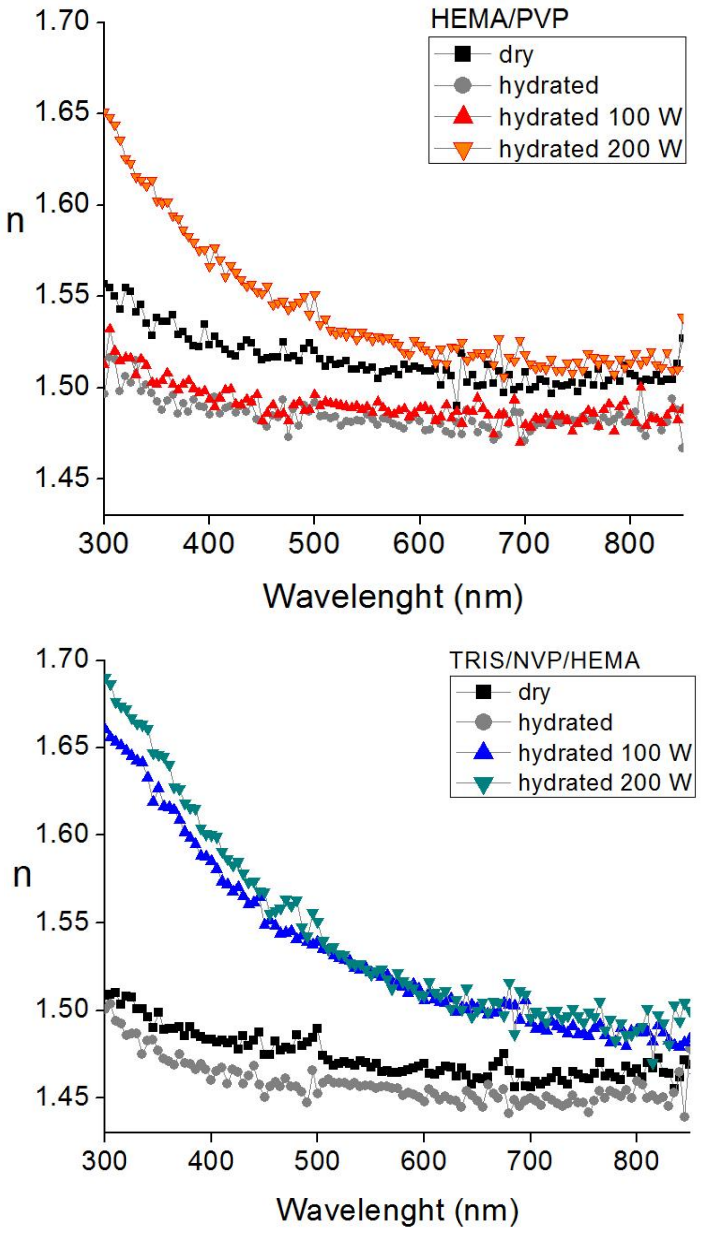

Figure 3.2 Refractive indices of dry and fully hydrated samples of HEMA/PVP and TRIS/NVP/HEMA hydrogels submitted to plasma treatment (10 s) with different powers, as a function of the wavelength.

The resulting refractive indices show a normal dispersion behavior in the visible region, i.e. the refractive index decreases with increasing of the wavelength, with no absorption. The refractive index decreases with hydration. This is in agreement with other authors, who measured the refractive indices of commercial contact lenses (conventional and silicone based) by refractometry [17] and found the values to be inversely correlated with the equilibrium water content of the materials.

The refractive index increases with plasma treatment, more significantly, for the TRIS samples. In the case of HEMA/PVP, the 100 W-treatment hardly affects the refractive index. The refractive indices increased with increasing plasma power, going upon treatment with 200 W, for HEMA/PVP samples, from 1.49 to 1.57 (at 400 nm) and from 1.48 to 1.51 (at 800 nm) and, in the case of TRIS/NVP/HEMA samples, from 1.46 to 1.60 (at 400 nm) and from 1.46 to 1.48 (at 800 nm). This can be expected, since the refractive index is determined by the interaction of light with the electrons of the constituent atoms and plasma treatments may induce an increase in either electron density or polarizability, thus promoting an increase in the refractive index. In general, the refractive indices of hydrated commercial contact lenses vary in the range of 1.38–1.44, but other materials with high refractive indices (above 1.5) have been used to assist in decreasing lens thickness and are described in several patents [18, 19]. To the best of our knowledge, the increase of the refractive index after the plasma treatment was never reported.

Application of the Cauchy transparent model to the experimental data led to thicknesses of the hydrogel layer affected by the plasma treatment varying in the range of 50–80 nm, irrespective of the power of the treatment. It is important to stress that the results of ellipsometry were not affected by the elapsed time between the plasma irradiation and the measurements: reproducible results were obtained 1 day and several weeks after the treatment.

The water contact angles measured on the dry samples before and after the plasma treatment (200 W, 10s) are shown in Figure 3.3 A.

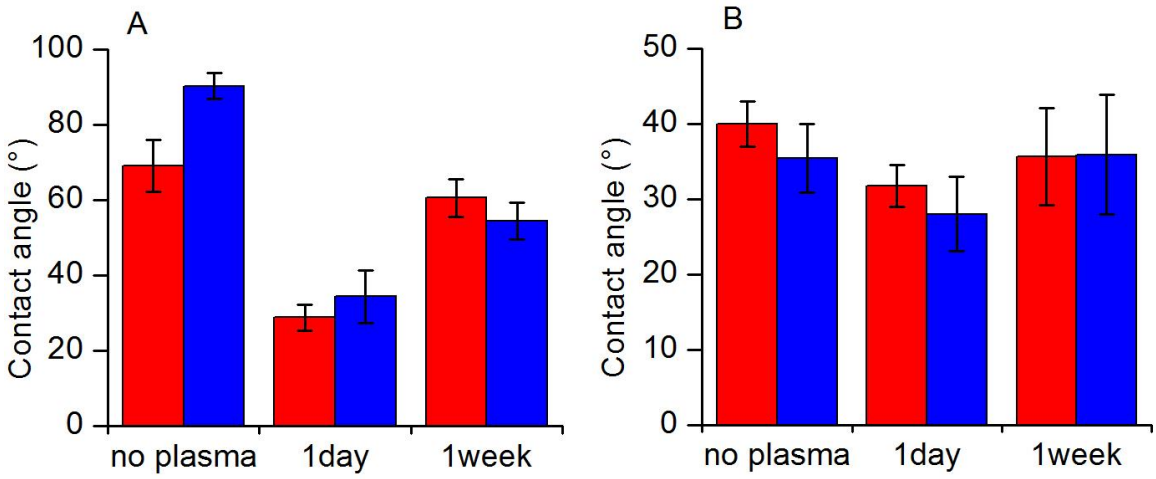

Figure 3.3: Effect of plasma treatment (200 W, 10 s) on the water contact angle on dry samples (A) and on fully hydrated samples (B) of HEMA/ PVP (red) and TRIS/NVP/HEMA (blue).

The wettability of both hydrogels was strongly modified by the plasma treatment, as expected. In fact, several authors [8, 20] reported the increase in the wettability of contact lens materials due to the formation of hydrophilic chemical groups such as polar groups on the plasma irradiated surface. The contact angles decreased 62% for TRIS/NVP/HEMA and 58% in the case of HEMA/PVP. One week after the treatment, the contact angles increased again, but did not return to the initial values, and remained unchanged one month after the treatment (results not shown). This means that the effect of plasma treatment on the chemical composition of the surface is partially reversible. The partial reversibility of the wettability contrasts with the stability of the refractive index demonstrated by the ellipsometric analysis.

The effect of plasma irradiation time upon the water contact angles on the dry samples was assessed through the comparison of samples treated at 200 W during 10 s and 35 s (data not shown). While for HEMA/PVP, no effect could be identified, for TRIS/NVP/HEMA, a lower contact angle (26° vs 34°) was achieved with the longer period of treatment. One week after the treatment, the effect of irradiation time vanished and both TRIS/NVP/HEMA samples presented approximately the same contact angle (54°).

The decrease of the contact angles of HEMA-based materials after plasma treatment has been observed by other researchers and described in numerous patents [21, 22]. This behavior may be rationalized by the incorporation of N-containing radicals at the polymer surface. X-ray photoelectron analysis of the nitrogen-plasma treated samples revealed an increase in the total percentage of nitrogen atoms and FTIR spectra showed a weak band which could be attributed to N-H bond in amines and amides [20]. However, after exposure to air, part of the nitrogen containing groups are rapidly replaced by oxygen containing groups, probably due to the reaction of imine to carbonyl groups [23]. Other authors [24] claimed that oxygen is incorporated in the surface of HEMA based materials by plasma treatment with an inert gas (argon) due to the cleavage of ester bonds and formation of -O-O- bonds. With time, these polar groups in contact with air, a hydrophobic environment, rearrange into a more stable, lower energy state, which explains the observed re-hydrophobization.

The behavior of hydrated samples shown in Figure 3.3 B is diverse. As seen in chapter 2, section 2.3.1, without any plasma treatment, both hydrogels in contact with water are more hydrophilic than the dry samples, because the HEMA hydroxyl groups rotate and become exposed at the water interface. This effect is more significant for the TRIS/NVP/HEMA which is more hydrophobic in contact with air due to the concentration at the interface of hydrophobic siloxane groups of the TRIS monomer. After plasma irradiation, the wettability of both hydrated hydrogels increased moderately (~20%). One week after the treatment, the wettability of both hydrated materials, kept in water, decreased and the contact angles reached values similar to those obtained on the non-treated samples.

The surface topography of both hydrogels submitted to plasma treatment of increasing power can be observed in the SEM images shown in Figure: 3.4 and Figure 3.5. The non-treated samples of both materials have homogeneous, smooth surfaces, while the topography of the plasma-treated ones differs from one hydrogel to the other.

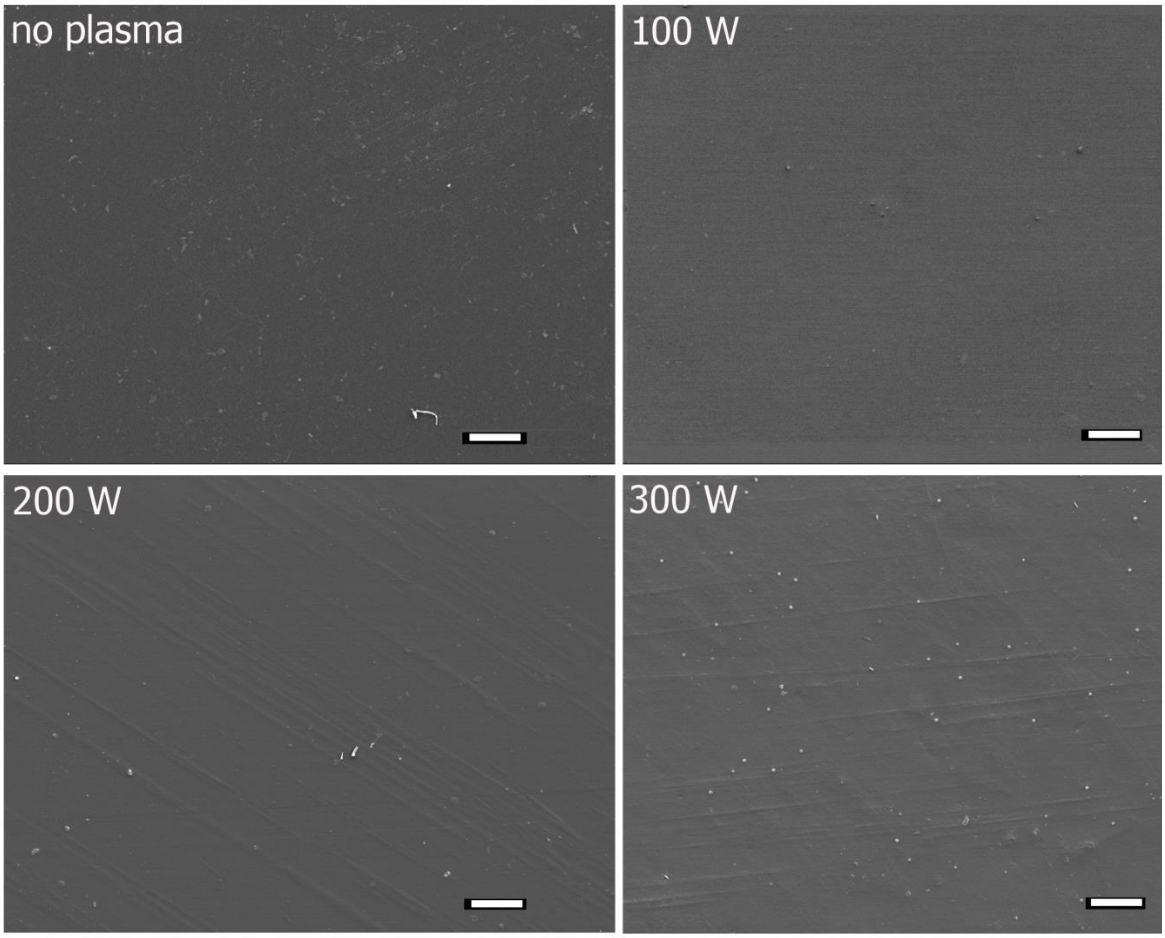

Figure: 3.4 SEM images of HEMA/PVP samples before and after 10 s of plasma treatments with different powers: 100, 200, and 300 W. The bars correspond to 10 μm.

The surface of HEMA/PVP presents significant changes only after the 300 W-treatment. In contrast, the surface-treated TRIS/NVP/HEMA samples exhibit a pattern of grooves whose number and depth increase with the power of the treatment. In addition, after the 300 W-treatment, the TRIS/NVP/HEMA sample also presents numerous micropores. The presence of grooves with different orientations and pores on plasma-treated silicone hydrogel contact lenses surfaces was previously reported by other authors [9, 25].

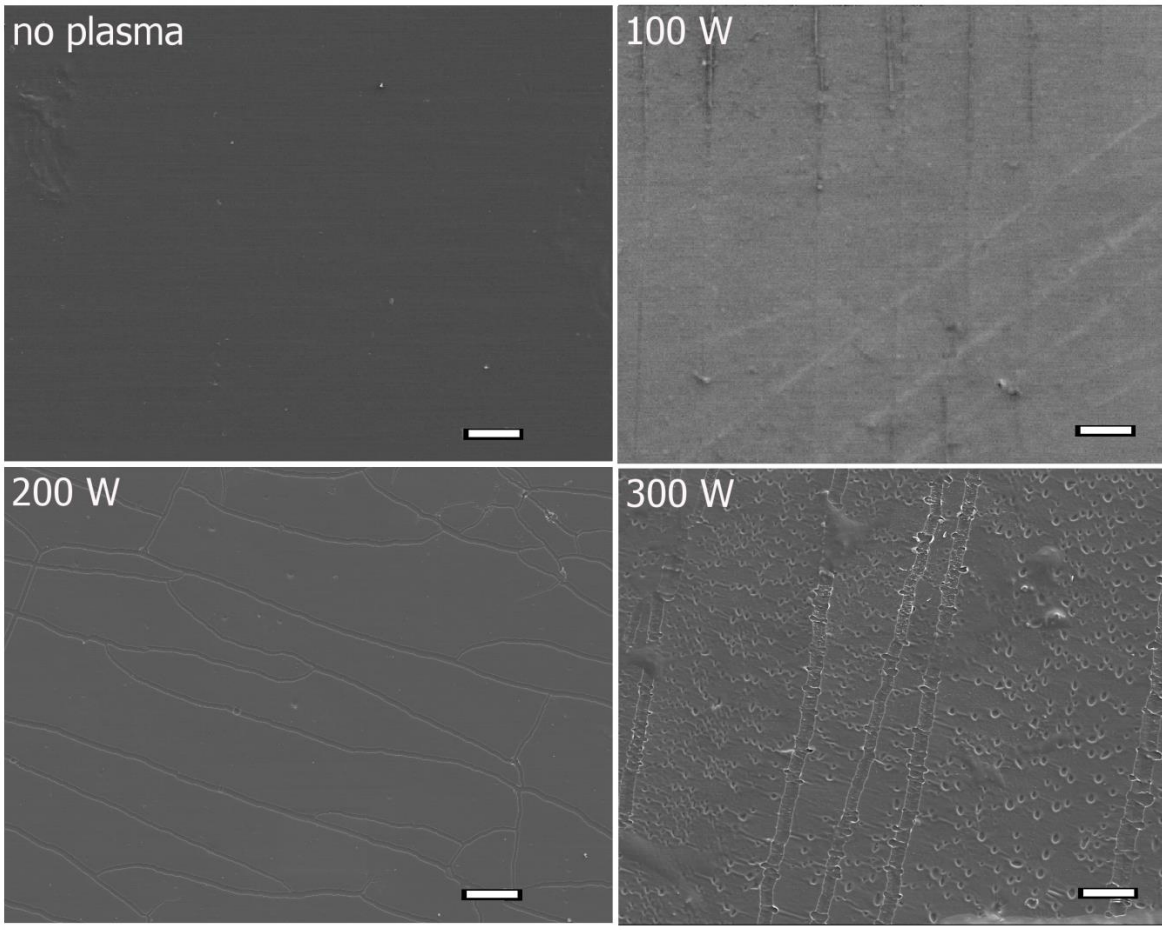

Figure 3.5: SEM images of TRIS/NVP/HEMA samples before and after 10 s of plasma treatments with different powers: 100, 200, and 300 W. The bars correspond to 10 µm.

To determine the changes induced by the plasma treatment at nanoscale, the samples treated with 200 and 300 W (10 s) were analyzed with AFM. In

Figure 3.6 images of the treated samples are compared with the non-treated ones.

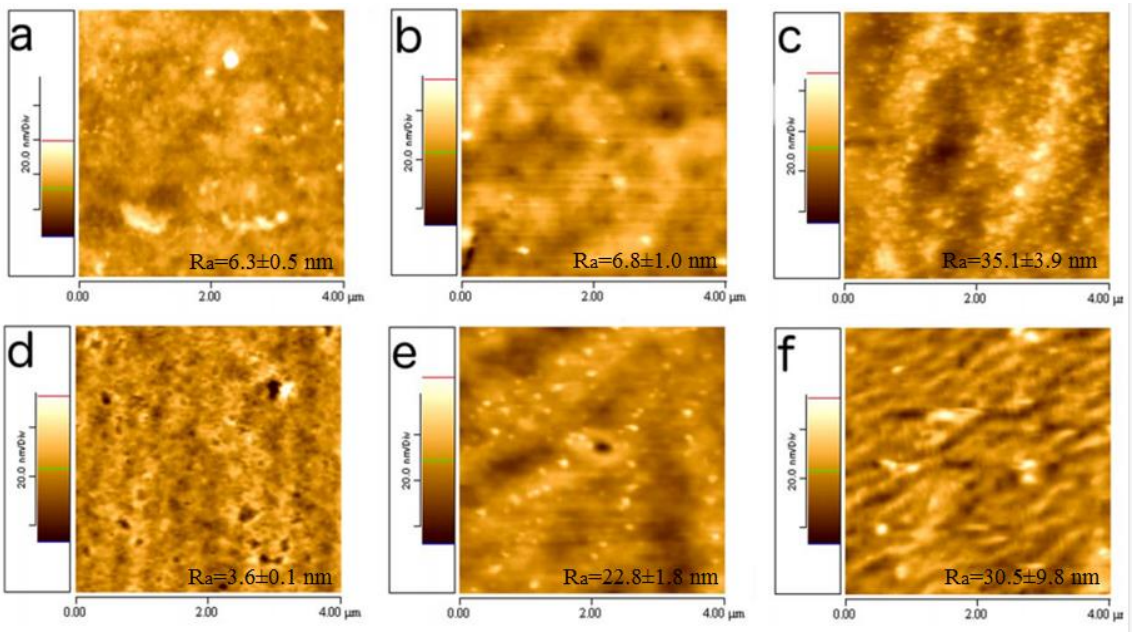

Figure 3.6: AFM images of HEMA/PVP (a, b, c) and TRIS/NVP/HEMA (d, e, f) samples before (a, d) and after the plasma treatment with 200 W (b, e) and 300 W (c, f). Roughness values are reported.

Analysis of the AFM images shows that after the 200-W treatment, a compaction of the surface of both samples may be observed and, in the case of the TRIS/NVP/HEMA sample, the nanoporosity is significantly reduced. In contrast, the 300-W treatment led to heterogeneous, irregular surfaces.

The changes in the surface morphology do not seem to affect the friction coefficients of the irradiated TRIS/NVP/HEMA samples (200 W, 10 s). The friction coefficients obtained before treatment, 0.41 ± 0.05, and after treatment, 0.47 ± 0.05, are similar. The same results were obtained for the HEMA/PVP samples: 0.49 ± 0.02 before treatment and 0.46 ± 0.04 after treatment.

These results are not surprising since several reports in the literature on friction of polymers after plasma treatment [26] suggest that plasma can either increase or decrease friction. Crosslinking is generally pointed out as a factor of shear strength increment and consequent lowering of friction, whereas the increase in the surface roughness (see Figure 3,6) may be associated to greater friction. Our observations suggest that, in

lubricated conditions, friction is not affected by the surface modifications caused by plasma treatment.

3.3.2 Drug release

The cumulative release profiles of levofloxacin from drug-loaded (10 mg/mL) HEMA/PVP hydrogels before and after plasma treatment are shown in Figure 3.7 and Figure 3.8. The effects of both power and time of irradiation were investigated.

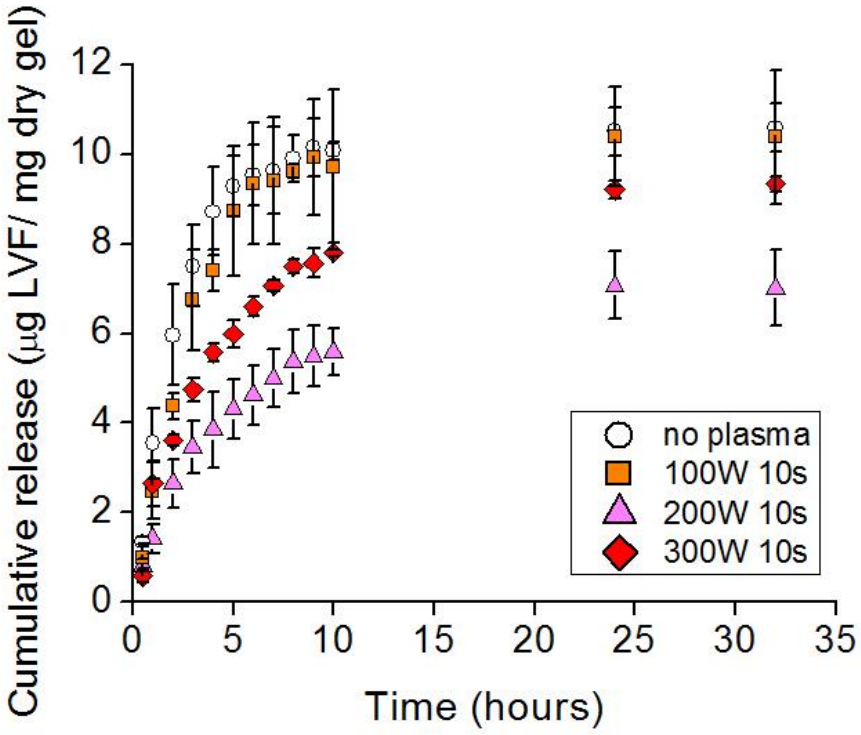

Figure 3.7 Effect of the power (irradiation time of 10 s) on the cumulative release profiles of levofloxacin from HEMA/PVP hydrogels.

Figure 3.7 shows that plasma treatment of HEMA/PVP hydrogels, for 10 s, with power of 100 W hardly affected the levofloxacin release profile, while 200 W significantly decreased the rate and the amount of drug released. However, increasing the power to 300 W did not have a stronger effect, but led to an intermediate profile, probably due to a non-uniform crosslinked barrier, as observed in the SEM and AFM images.

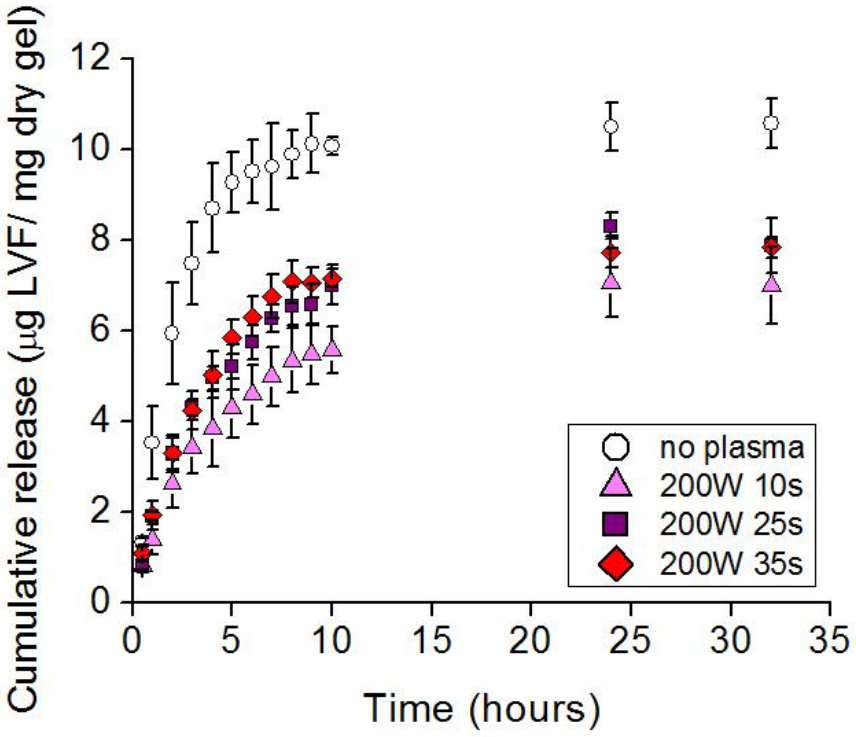

Figure 3.8: Effect of the irradiation time (power of 200 W) on the cumulative release profiles of levofloxacin from HEMA/PVP hydrogels.

The effect of plasma irradiation time shown in Figure 3.8 is more ambiguous. The resulting profiles are almost superimposed, although the 10 s irradiation time seems to lead to the lowest profile.

The cumulative release profiles of chlorhexidine from drug-loaded (5 mg/mL) TRIS/NVP/HEMA hydrogels before and after plasma treatment are shown in Figure 3.9 and Figure 3.10. The effects of both power and time of irradiation were investigated. In this case the results are clearer. The plasma treatment condition of 200 W and 10 s (Figure 3.9) is the only condition tested that affected the drug release profile. Lower (100 W) and higher (300 W) powers appear to be insufficient and too aggressive, respectively, to form a crosslinked layer on the top of the hydrogel surface. The effect of the plasma irradiation time presented in Figure 3.10 indicates that a period of 35 s for a 200 W treatment is too long and the drug release is similar ($p=0.667$) to that obtained without any treatment. The disruption of the crosslinked barrier initially formed should be the

cause of this behavior. To further understand the effect of plasma treatment on the drug release, the hydration of both materials after 200 W (10 s) treatment, was determined. The EWC values of the treated materials (200 W and 10 s) decreased approximately 35% in both cases: from 48% to 31% for HEMA/PVP and from 64% to 42% for TRIS/NVP/HEMA. This reduction in the water content might have impact on the correspondent drug release profiles. Overall, the effect of the plasma treatment on the release profiles is consistent with the SEM and AFM observations. The fact that the 100W-treatment had very little effect on the surface topography of both hydrogels is in agreement with the fact that the release profiles obtained with the materials submitted to this plasma condition are very similar to those resulting from non-treated samples. The disruption of the surface of TRIS/NVP/HEMA by 300 W-plasma justifies the similarity observed between the release profiles obtained with the 300 W plasma- treated sample and the non-treated one. However, the same power (300 W) plasma had a milder effect on the HEMA/PVP surface which explains the intermediate release profile in Figure 3.8.

We should stress that the modification of the release profiles may have both favorable and unfavorable consequences. Lowering of the release rate could be useful to reduce the usual initial burst which is typical of drug accumulation near the surface of the sample, but the significant amount of drug kept inside the hydrogels means a reduction in the release process efficiency.

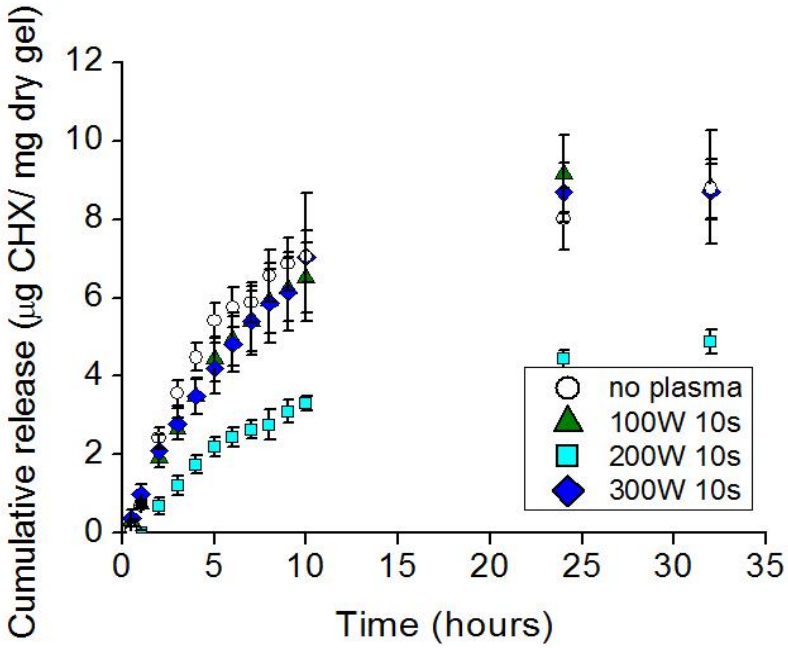

Figure 3.9: Effect of the power (irradiation time of 10 s) on the cumulative release profiles of chlorhexidine from TRIS/NVP/HEMA hydrogels.

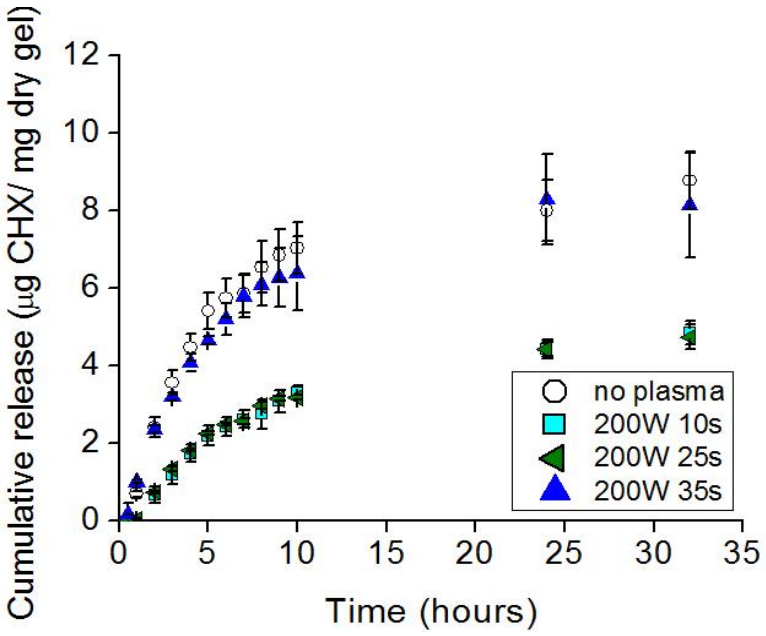

Figure 3.10: Effect of the irradiation time (power of 200 W) on the cumulative release profiles of chlorhexidine from TRIS/NVP/HEMA hydrogels.

Finally, the results of the microbiological tests indicate that the antibiotic activity of both levofloxacin and chlorhexidine released from HEMA/PVP and TRIS/NVP/HEMA

hydrogels submitted to plasma treatment (200 W and 10 s) is maintained. This is probably due to the small depth of the plasma effect on the hydrogel (~50-80 nm, from ellipsometry data).

3.4 Conclusions

In the present chapter, the effect of nitrogen plasma treatment on the performance of two types of polymers, previously investigated as drug releasing contact lens materials, was investigated. The PHEMA based hydrogel was loaded with levofloxacin and the silicone based hydrogel was loaded with chlorhexidine. It was demonstrated that, depending on the processing parameters, plasma may have a beneficial effect on the surface and optical properties of those contact lens materials. If moderate conditions (200 W and 10 s) were used, the surfaces became more hydrophilic (although they recover hydrophobicity with time), the refractive index of the hydrogels increased which may be an advantage allowing for the design of thinner, low-weight lenses, while roughness and transmittance were not much affected. For higher power and/or longer times, the treatment became aggressive and the surfaces were damaged. It is clear from the comparison of the behavior of both hydrogels, that the properties of the silicone based hydrogel were more affected by the plasma treatment.

From the point of view of drug delivery, the plasma treatment may have pros and cons. Moderate power (200 W) plasma treatments led to a reduction of the initial release rate, which may be considered an advantage, but the considerable decrease of the total amount of drug released is certainly a disadvantage. For lower (100 W) and higher powers (300 W), the release profiles were scarcely affected because the samples surfaces were, respectively, hardly modified and disrupted. For 200 W-treatment, the superficial nature of the treatment did not lead to any significant loss of the antimicrobial activity of the drugs.

It is important to stress that our conclusions refer to the polymeric formulations tested and to the only nitrogen plasma treatment used. Different polymers and other plasma conditions may have other effects. However, since the polymers investigated are the basic components of contact lenses, and nitrogen plasma is widely used in the lens

treatment, the obtained results should be relevant for the contact lens manufacturers and researchers.

3.5 References

1. N. Efron and C. Maldonado-Codina, *Development of Contact Lenses from a Biomaterial Point of View – Materials, Manufacture, and Clinical Application*, in *Comprehensive Biomaterials*, P. Ducheyne, Editor. 2011, Elsevier Science: Amsterdam. p. 517-541.
2. M.L. Burts, I. Alexeff, E.T. Meek and J.A. McCullers, *Use of atmospheric non-thermal plasma as a disinfectant for objects contaminated with methicillin-resistant Staphylococcus aureus.* Am J Infect Control, 2009. **37**(9): p. 729-33.
3. B. Tighe, *Silicone hydrogel materials—How do they work?*, in *Silicone Hydrogels: The Rebirth of Continuous Wear Contact Lenses*, D. Sweeney, Editor. 2000, Butterworth-Heinemann/BCLA: Oxford. p. 1-21.
4. S. Yin, Y. Wang, L. Ren, L. Zhao, H. Chen and J. Qu, *Surface Hydrophilicity Improvement of RGP Contact Lens Material by Oxygen Plasma Treatment.* Mater Sci Forum, 2009. **610-613**: p. 1268-1272.
5. C.M. Weikart, Y. Matsuzawa, L. Winterton and H.K. Yasuda, *Evaluation of plasma polymer-coated contact lenses by electrochemical impedance spectroscopy.* J Biomed Mater Res, 2001. **54**(4): p. 597-607.
6. D.W. Fakes, M.C. Davies, A. Brown and J.M. Newton, *The surface analysis of a plasma modified contact lens surface by SSIMS.* Surface Interface Anal, 1988. **13**(4): p. 233-236.
7. D.W. Fakes, J.M. Newton, J.F. Watts and M.J. Edgell, *Surface modification of a contact lens co-polymer by plasma-discharge treatments.* Surface Interface Anal, 1987. **10**(8): p. 416-423.
8. S.S. Hyung, S.S. Jang, Y.S. Kwon and K.C. Mah, *Surface Modification of Rigid Gas Permeable Contact Lens Treated by Using a Low-Temperature Plasma in Air.* J Korean Phys Soc, 2009. **55**(6): p. 2436-2440.
9. A. Lopez-Alemany, V. Compan and M.F. Refojo, *Porous structure of Purevision versus Focus Night&Day and conventional hydrogel contact lenses.* J Biomed Mater Res, 2002. **63**(3): p. 319-25.
10. D.I. McBriar, *The plasma treatment of contact lenses*. 1990, PhD thesis, Durham University.

11. Y. Wang, X. Qian, X. Zhang, W. Xia, L. Zhong, Z. Sun and J. Xia, *Plasma surface modification of rigid contact lenses decreases bacterial adhesion.* Eye Contact Lens, 2013. **39**(6): p. 376-80.
12. M. Boselli, V. Colombo, E. Ghedini, M. Gherardi, R. Laurita, F. Rotundo, P. Sanibondi, A. Stancampiano, M. Minelli and M.G. De Angelis. *Comparing the effects of different atmospheric pressure non-equilibrium plasma sources on polylactide oxygen permeability*. in *Plasma Science (ICOPS), 2012 Abstracts IEEE International Conference on*. 2012.
13. S. Tajima and K. Komvopoulos, *Effect of reactive species on surface crosslinking of plasma-treated polymers investigated by surface force microscopy.* Appl Phys Lett, 2006. **89**(12): p. 124102 1-3.
14. M. Kuzuya, K. Ito, S. Kondo and Y. Makita, *A new drug delivery system using plasma-irradiated pharmaceutical aids. VIII. Delayed-release of theophylline from double-compressed tablet composed of eudragit as wall material.* Chem Pharm Bull (Tokyo), 2001. **49**(12): p. 1586-92.
15. M. Kuzuya, S.I. Kondo and Y. Sasai, *Addendum - Recent advances in plasma techniques for biomedical and drug engineering.* Pure Appl Chem, 2005. **77**(4): p. 667.
16. K. Hagiwara, T. Hasebe and A. Hotta, *Effects of plasma treatments on the controlled drug release from poly(ethylene-co-vinyl acetate).* Surf Coat Tech, 2013. **216**(0): p. 318-323.
17. J.M. Gonzalez-Meijome, M. Lira, A. Lopez-Alemany, J.B. Almeida, M.A. Parafita and M.F. Refojo, *Refractive index and equilibrium water content of conventional and silicone hydrogel contact lenses.* Ophthalmic Physiol Opt, 2006. **26**(1): p. 57-64.
18. H. Neidlinger, E. Cichacz and W.E. Meyers, *High refractive index oxygen permeable contact lens system and method*. Apr 2, 2013, US 8408697 B2
19. J. Salamone, J. Kunzler, R. Ozark and D. Seelye, *High refractive index polymeric siloxysilane compositions*. 16 June, 2005, US 20050131189 A1
20. S. Paulussen, D. Vangeneugden, O. Goossens and E. Dekempeneer, *Antimicrobial Coatings Obtained in an Atmospheric Pressure Dielectric Barrier Glow Discharge.* Mater Res Soc, 2002. **724**: p. 17-84.

21. P.L. Valint, G.L. Grobe, D.M. Ammon and M.J. Moorehead, *Plasma surface treatment of silicone hydrogel contact lenses*. 2001, Patent number: US6193369 B1.
22. S. Rastogi, M.J. Moorehead, W.J. Appleton, G.L. Grobe and P. Trotto, *Plasma treatment of contact lens and IOL*. 2007, Patent number: US7250197 B2.
23. L.J. Gerenser, *XPS studies of in-situ plasma-modified surfaces* in *Plasma Surface Modification of Polymers: Relevance to Adhesion* M. Strobel, C.S. Lyons, and K.L. Mittal, Editors. 1994, VSP, 1994: Utrecht, The Netherlands p. 43-64.
24. G. Tan, R. Chen, C. Ning, L. Zhang, X. Ruan and J. Liao, *Effects of argon plasma treatment on surface characteristic of photopolymerization PEGDA–HEMA hydrogels.* J Appl Polym Sci, 2012. **124**(1): p. 459-465.
25. M. Lira, L. Santos, J. Azeredo, E. Yebra-Pimentel and M.E. Oliveira, *Comparative study of silicone-hydrogel contact lenses surfaces before and after wear using atomic force microscopy.* J Biomed Mater Res B Appl Biomater, 2008. **85**(2): p. 361-7.
26. A. Bismarck, W. Brostow, R. Chiu, H.E. Hagg Lobland and K.K.C. Ho, *Effects of surface plasma treatment on tribology of thermoplastic polymers.* Polym Eng Sci, 2008. **48**(10): p. 1971-1976.

4 Controlled drug release from vitamin E loaded commercial silicon lenses

The following results were accepted for publication in the peer-reviewed international Journal of Pharmaceutical Sciences. November 2015.

Table of contents

4.1 Introduction

In the present chapter the incorporation of vitamin E into SCLs will be investigated as an approach for controlled drug delivery. Most part of the experiments here reported were performed at the University of Florida in Gainesville, Florida, USA, under the supervision of Professor Anuj Chauhan.

Section 1.4 of this thesis describes the different strategies investigated by researchers along the last decades to overcome the disadvantages of eye drops therapy through the design of therapeutic SCLs. It is well known that commercial contact lenses loaded by soaking release the drugs for only a few hours [1-5] and so various researchers have proposed novel approaches to increase the release durations. Chauhan and coworkers have proposed creation of diffusion barriers by incorporation of vitamin E, to increase the release duration of several ophthalmic drugs [6-12]. Previous studies have shown that vitamin E is not released from the contact lenses due to the negligible solubility in water or phosphate buffered saline making it a viable candidate as diffusion barrier [11]. Vitamin E has no irritant effect on the eye and its benefits, for example over cataracts and keratocyte apoptosis after surgery, was shown in previous research studies on animals [13-16]. Additionally it has been demonstrated that vitamin E has a positive effect after topical application, due to strong antioxidant properties [17]. Considering the benefits of vitamin E incorporation, we focused on this approach for extended delivery of our drugs of study: levofloxacin (LVF) and chlorhexidine (CHX). Even though LVX is a common ophthalmic drug, and CHX revealed to present benefits against fungal keratitis, there are very few prior studies focusing on transport of these drugs in commercial contact lenses. To our knowledge, only one previous study performed by Danion *et al.* [18] focused on the extended delivery of LVF from commercial soft contact lenses, while no work was done on the delivery of CHX. In that study [18], the commercial contact lenses (Hioxifilcon B), loaded by soaking in a LVF solution of 5 mg/mL and coated with a liposome layer, yielded a sustained drug release for 48 hours.

Although several researchers have proposed vitamin E loaded contact lenses for delivery of ophthalmic drugs [6-12], the present study has many new aspects not explored previously. Firstly, in addition to designing the lenses for extended delivery of antibiotics,

we are interested in understanding how the properties of the control lenses impact the relative benefits in drug transport achieved by vitamin E loading. To achieve our goal, we compare two different types of commercial contact lenses (ACUVUE® TrueEye™ and ACUVUE OASYS®), both with and without vitamin E. We also show that the release durations from the control lenses chosen in this study are significantly longer than some of the ones reported in literature from other drug loaded SCLs [1-4].

Finally, another useful contribution of this work is the characterization of the vitamin E loaded lenses focusing on some properties that are critical to the performance of contact lenses. This aspect is important because there is the risk that, with the efforts to improve the drug release properties of the contact lenses, other properties may be compromised. Besides assessing the drug release profiles, the vitamin E loaded contact lenses were characterized for ion permeability, wettability and transmittance. These are important properties of the lenses that have to be controlled. In particular, as described in Chapter 1, ion permeability was described in the seminal patent [19] as an essential feature to maintain lens motion during wear. Since it is known that vitamin E incorporation will reduce the ion permeability due to the diffusion barrier effect, it is critical to ensure that the level of permeability is still adequate for *in vivo* applications. Similarly, it is also important to ensure that incorporation of the hydrophobic vitamin E does not reduce the wettability of the lenses, a critical property which greatly determines its comfort. The maintenance of optical such as the transmittance is essential to ensure a clear vision

In the last section of this chapter, the combination of the *in vitro* experiments with a mathematical model will be presented. In this way the authors aim to achieve optimal design in terms of the loading of both drug and vitamin E, such that extended release is achieved while ensuring *in vivo* concentrations within the therapeutic window.

4.2 Experimental part

4.2.1 Materials

Two brands of commercial silicone contact lenses were used in this study: ACUVUE® OASYS (Johnson&Johnson Vision Care, Inc., Jacksonville, FL, USA), diopter -6.5,

Senofilcon A, 38% H_2O and 1-DAY ACUVUE® TrueEye (Johnson&Johnson Vision Care, Inc., Jacksonville, FL, USA), diopter -8, Narafilcon A, 46% H_2O. Levofloxacin (≥98%), vitamin E ((±)-α-Tocopherol, ≥96%), and Ethanol (≥99.5%) were purchased from Sigma-Aldrich Chemicals (St. Louis, MO, USA). Chlorhexidine diacetate hydrate (≥ 98%) , Phosphate-Buffered Saline (PBS) and Sodium Chloride (≥99.9%) were obtained, respectively, from Acros Organics (Gent, Belgium), Corning (Manassas, VA, USA) and Fisher Chemical (Failawn, NJ, USA). All chemicals were used as received. Distilled and Milli-Q deionized water (DD) was used for all preparations.

4.2.2 Vitamin E loading into lenses

Lenses with a range of vitamin E loadings (5-20 w/w fraction), were prepared by soaking in solutions with various concentrations of vitamin E (20-42 mg vitamin E/mL solution), according to the procedure previously described [8, 9, 11, 12]. This range of vitamin E fractions was chosen because it was demonstrated that for vitamin E fractions higher than 20% in weight, the ion permeability and the oxygen permeability were negatively affected [8].

Briefly, vitamin E was dissolved in ethanol by vortexing for a few seconds followed by magnetic stirring for a few minutes. Previously air dried contact lenses were soaked in 3 mL of the solution for 3 hours at room temperature to load the vitamin E. After the 3 hours of loading, lenses were withdrawn from the ethanol solutions, gently blotted and dried overnight in air. All the samples were dried in the same conditions, namely at 20±1 ºC and for 14 hours. The dried lenses were weighted and mass of vitamin E loaded in the lenses was determined by subtracting the dry weight of the lenses before vitamin E loading.

In order to verify any eventual change of the hydrogel structure caused by soaking into ethanol, the contact lenses equilibrium water content (EWC) was measured before and after the 3 hours of ethanol exposure, as:

$$EWC = \frac{W_\infty - W_0}{W_\infty}\ x\ 100 \qquad \textbf{Equation 4.1}$$

where W_∞ is the constant weight value and W_0 is the weight of the dry sample.

4.2.3 Soft contact lens characterization

4.2.3.1 Ion permeability

The ion permeability of the lenses, kD, was defined as the product of the diffusivity, D, and the ion partition coefficient, k. A previously described method [20] was followed to calculate the ion permeability for both the lenses without and with 20% of vitamin E. Lenses were soaked in 0.75 M NaCl solution overnight to achieve equilibrium and then soaked into 36mL of well-stirred (300 rpm) DD water. The NaCl concentration of the aqueous medium was monitored periodically by measuring the conductivity using a Con 110 series sensor (OAKTON®), and then related to NaCl concentration through a calibration curve. The tests were done in triplicate. The partition coefficient of NaCl was determined from the total mass of salt released by the lens, which yielded the equilibrium concentration in the lens at the end of the loading experiment.

$$k = \frac{C_{gel}}{C_{sol}} = \frac{M_{gel}}{V_{gel}C_{sol}} \qquad \textbf{Equation 4.2}$$

where M_{gel} is the mass of salt released into the DD water, V_{gel} the volume of the lens and C_{sol} the concentration of salt in the loading solution. The diffusion coefficient for a diffusion control transport in sink conditions was calculated by plotting the fraction release (f) as a function of √t. A linear plot is an indication of a diffusion controlled release [8] and the molecular diffusivity was calculated by equating the slope to $2/\sqrt{\pi}\sqrt{(D_{eff}/\hbar^2)}$ (details presented in section 4.3.3.1).

4.2.3.2 Transmittance

Optical studies were carried out by measuring the percent transmittance of visible light (wavelength range from 400 to 700 nm) through hydrated contact lenses without and with 20% of vitamin E. The samples were directly mounted on the outer surface of a quartz cuvette, which was then placed in a spectrophotometer (UV–vis Beckmam DU-70). The tests were done in triplicate.

4.2.3.3 Wettability

The wettability of the hydrated contact lenses, without and with 20% of vitamin E, was characterized by measuring the water contact angles through the captive bubble method. In the captive bubble method the contact angle was measured by placing a bubble of air onto the lens surface with an inverted syringe, while the lens was immersed in the liquid. The bubble images were acquired using a video camera (JAI CV-A50) attached to a microscope (Wild M3Z) which was connected to a frame grabber (Data Translation DT3155). The image analysis was performed using the ADSA-P software (Axisymmetric Drop Shape Analysis Profile). The measurements were performed over 8 samples, at room temperature and in DD water.

4.2.4 Drug loading and drug release experiments

Drug loading was achieved by soaking the previously dried lenses in 3 mL of PBS-drug solution of 5 mg/mL for 7 days, at room temperature. Due to the limited solubility of CHX in saline, this drug was dissolved in DD water. A set of ACUVUE® OASYS contact lenses, loaded with a 25 mg/mL LVF solution for14 days, was prepared for the tests described in section 4.3.3.2. Both drug solutions were protected from light to minimize the drug degradation. After loading, the lenses were taken out from the solutions, blotted with absorbent paper and dried overnight at room temperature.

The drugs were loaded into the vitamin E loaded lenses following the same procedure as described above for loading drugs into control lenses, except that the loading duration was increased (up to three weeks) to account for the expected attenuation in drug diffusion. Specifically, it was ensured that the loading durations were longer than the release durations measured subsequently. It was demonstrated in previous work [7, 8, 10] that the release profiles are not affected by the soaking time if it exceeds the time needed for equilibrium between the soaking solution and the immersed lens. All data reported here correspond to equilibrium drug uptake during the loading step, thus comparison with control lenses is possible.

The drug loaded contact lenses were immersed in 3 mL PBS, which was determined to represent sink conditions. The samples were kept at room temperature and protected from light. At pre-determined time intervals, the absorbance spectra of the aqueous

solutions was measured over the wavelength range of 220-265 nm for chlorhexidine, and 265-305 nm in the case of levofloxacin using a UV-vis spectrophotometer (Thermospectronic Genesys 10 UV), after the measurements the samples were replaced in the release volume. The experiments were conducted till there was no increase in the drug concentration in three successive measurements. The tests were done in triplicate. In all drug release experiments, the magnitude of the supernatant solution absorbance increased with time, but the shape of the spectra remained unchanged suggesting that the drugs were stable during the entire experiments, when protected from visible light. Similar experiments conducted under normal light exposure showed significant drug degradation for chlorhexidine. In a few experiments, the lenses were subjected to a second cycle of release to test the validity of the sink assumption. The data showed negligible release of both drugs in the second release cycle proving that the release conditions for the first cycle can be considered as sink.

4.3 Results and discussion

4.3.1 Vitamin E loadings in the lenses

During the soaking, the mass of vitamin E absorbed by the lens was approximately equal to the product of the concentration of vitamin E in the solution and the volume of the solution absorbed by the lens. Subsequent drying of the lenses leads to vitamin E super-saturation in the matrix hydrogel that results in the phase separation and formation of vitamin E aggregates [9]. The vitamin E loaded lenses were transparent for all loadings, suggesting that the size of the aggregates did not exceed the wavelength of the visible light (400-700 nm).Vitamin E was loaded at different concentrations into 1-DAY ACUVUE® TrueEye™ and ACUVUE OASYS®. Figure 4.1 shows the linear dependency between the concentration of vitamin E in the loading solutions and the vitamin E loaded mass in the lenses. Both contact lenses present a comparable vitamin E loading capacity. These results are in agreement with previous studies on vitamin E loadings in various commercial lenses [7].

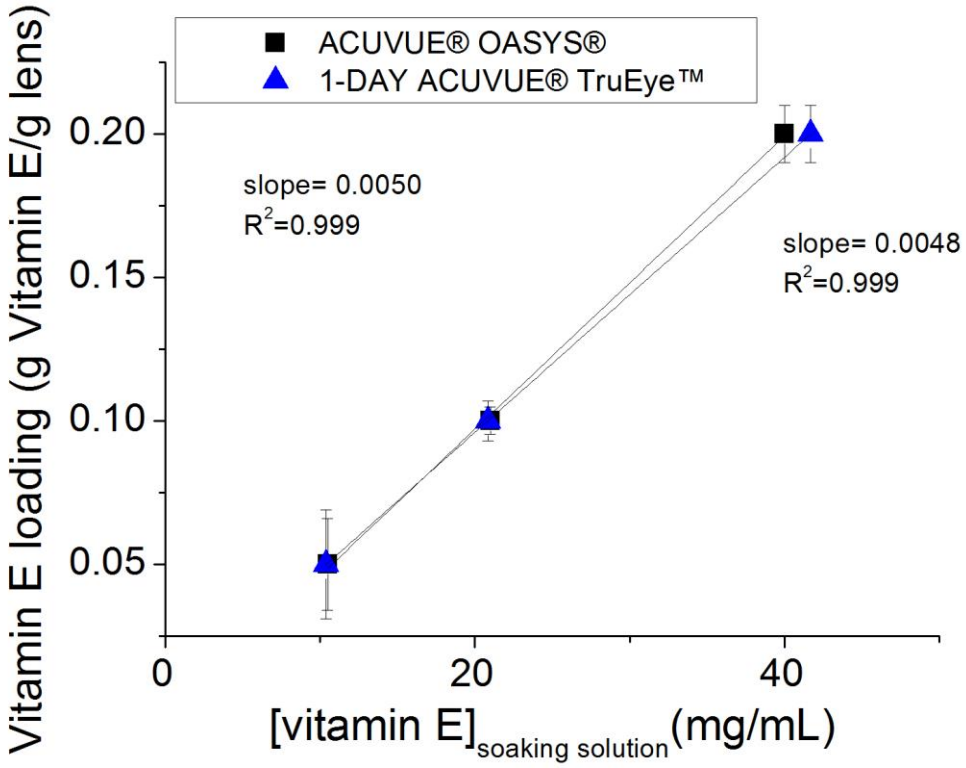

Figure 4.1: Correlation of vitamin E loading and concentration of soaking solution for 1-DAY ACUVUE® TrueEye™ and ACUVUE OASYS® lenses.

The study of the swelling of the lenses before and after the exposure to ethanol showed no particular change into the measured EWC.

4.3.2 Contact lens characterization

The effect of vitamin E in some properties, such as oxygen permeability, refractive index and power of the lens was previously investigated by the group of Chauhan. Vitamin E loadings below 20% have a negligible effect on the oxygen permeability of silicon based lenses [11], while the refractive index of the hydrogel with 20% of vitamin E loading increased by 4% [10]. The power of the SCL depends on the geometry of the lens and the refractive index. Peng *et al.* [8] measured the wet diameter of lenses loaded with 40% of

vitamin E and verified an increase relative to the dimension of the non-loaded lens lower than 8%, that in the application perspective can likely be tolerated.

In this work, the lens characterization was restricted to the samples loaded with the highest amount of vitamin E (20%) to assess the maximum possible impact on the properties of the SCLs. Ion partition coefficient (k), diffusivity (D) and permeability (kD) are listed in Table 1.

Table 4.1: Effect of vitamin E incorporation on partition coefficient (k), diffusivity (D) and permeability (kD) of salt in SCLs.

	Partition coefficient, k	Diffusivity, D (10^{-7} cm^2/s)	Permeability, kD (10^{-7} cm^2/s)
1-DAY ACUVUE® TrueEye™	0.3 ±0.2	3.3 ± 0.2	1.1± 0.6
ACUVUE® OASYS®	0.3 ±0.1	26.0 ± 0.1	8.1± 0.3
1-DAY ACUVUE® TrueEye™ _Vit E	0.3 ±0.1	2.0±0.1	0.7± 0.4
ACUVUE® OASYS®_Vit E	0.3 ±0.1	2.7 ± 0.1	0.8 ± 0.3

The measured salt partition coefficient values were in the range of the ones measured in previous works [20, 21]. Even though the incorporation of 20% of vitamin E reduced the ion permeabilities values, the measured kD were still above the minimum acceptable value for SCLs (2.5 x 10^{-8} cm^2s^{-1} [19]). It was noted that the ion permeability was measured using DD water as the release medium, while the *in vivo* environment has about 150 mM salt. Previous studies have however shown that the ion permeability was not affected by the ionic strength of the release medium within the salt concentrations investigated [20].

Both commercial contact lenses, with and without vitamin E, had over 90% transparency matching the transmittance characteristics of soft contact lenses [11]. 1-DAY ACUVUE® TrueEye™ presented a transmittance of above 95%, while ACUVUE® OASYS®, presented 97.5%. In both cases, the presence of 20% in weight of vitamin E caused a decrease in the transmittance by about 5%. While the vitamin E did not reduce significantly the visible transmittance, it absorbed a considerable fraction of the UVB radiation which is an unintended additional benefit [22].

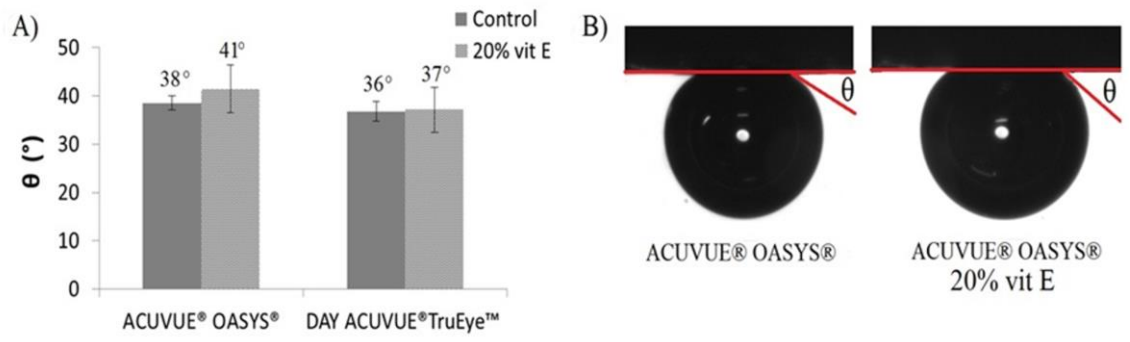

Figure 4.2: Effect of vitamin E incorporation on the wettability A) contact angle values measured for both contact lenses with and without vitamin E. B) representative bubble profiles in the case of ACUVUE® OASYS®, for control and vitamin E loaded lenses.

Figure 4.2 shows that the presence of vitamin E did not significantly alter the wettability of the lens surface for both ACUVUE® OASYS® and 1-DAY ACUVUE® TrueEye™. The contact angles were comparable to those reported in a previous study on silicone contact lenses [23].

4.3.3 Drug release

At room temperature and under perfect sink condition, ACUVUE® TrueEye™ released 90% of the loaded drug in 32 hours (see Figure 4.3-A). With the inclusion of 20% of vitamin, the drug release duration (for 90% release) increased to 100 hours. The mass of drug released was slightly impacted by vitamin E incorporation. At room temperature and under perfect sink condition, the release duration (for 90% release) of OASYS® was about 8 hours which is inadequate for extended drug delivery (see Figure 4.3-B). Comparison with Figure 4.3-A shows that the total amount of drug released from the lens was smaller than the one released from ACUVUE® TrueEye™. Incorporation of 20% vitamin E increased the drug release duration to 50 hours, with a small reduction in the mass of drug released. The effect of vitamin E incorporation on drug release duration was more significant for the ACUVUE OASYS® compared to the ACUVUE® TrueEye™ lenses.

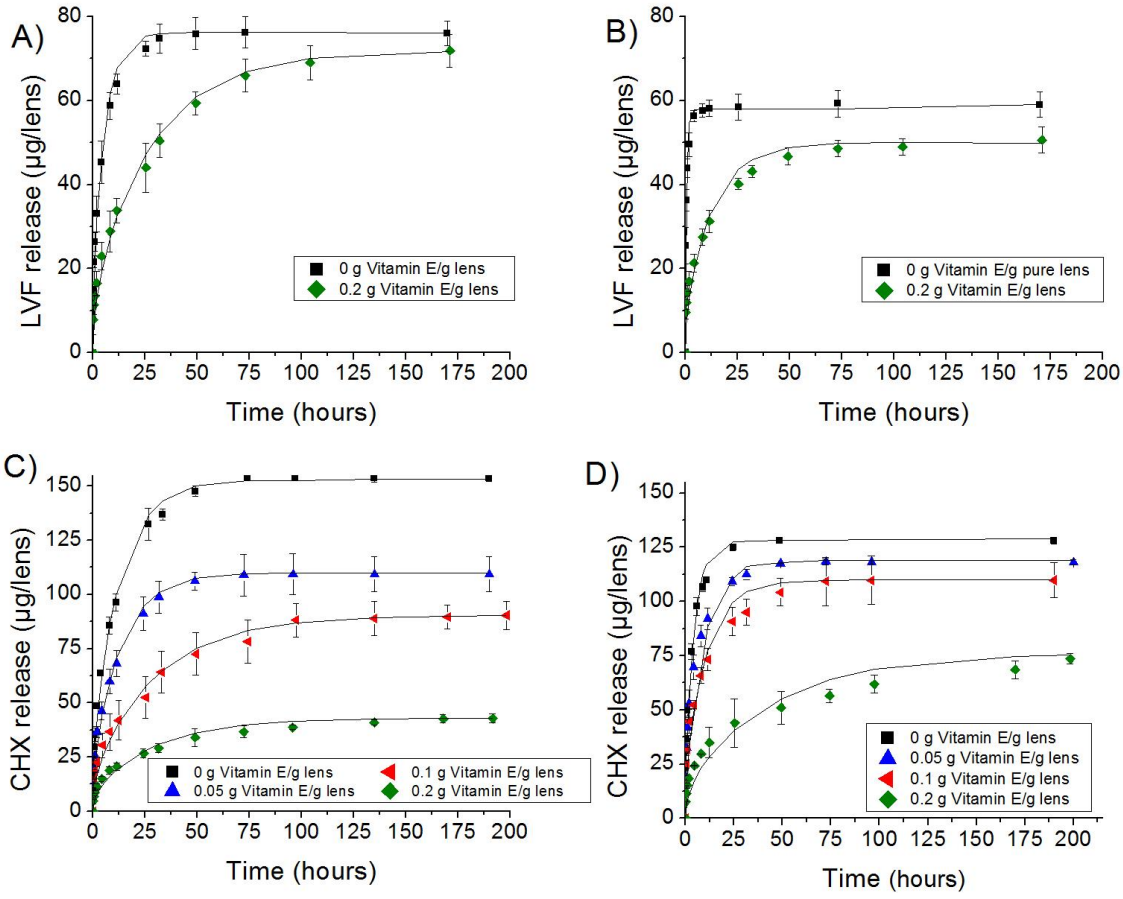

Figure 4.3: Experimental data and diffusion model fits for cumulative release of levofloxacin, from A) 1-DAY ACUVUE® TrueEye™ lenses, B) ACUVUE OASYS® lenses, and of chlorhexidine C) 1-DAY ACUVUE® TrueEye™ lenses, D) ACUVUE OASYS® lenses.

In the case of chlorhexidine, different concentrations of vitamin E were tested, see Figure 4.3-C. The release duration increased from 50 hours for the control, to 100 and 130 hours with 10 and 20% vitamin E, respectively. Also, the mass of drug released was influenced by the presence of vitamin E: it decreased from 150 µg for the control to 109 µg, 90 µg, and 42 µg for 5, 10 and 20% vitamin E, respectively.

Figure 4.3-D shows that ACUVUE OASYS® lenses without vitamin E released 90% of the loaded chlorhexidine in 18 hours, while lenses with 5, 10 and 20% vitamin E released the drug in 49, 70, and 170 hours, respectively. The presence of vitamin E caused a decrease in the drug released which was proportional to the percentage of loaded vitamin E: the mass released decreases from 130 µg for the control to 118 µg,

109 µg, and 75 µg with 5%, 10% and 20% of vitamin E, respectively. In comparison with 1-DAY ACUVUE® TrueEye™, the ACUVUE OASYS® lenses loaded less drug, which further decreased with vitamin E loading.

The partition coefficients of both drugs in the two types of commercial lenses were calculated from the starting concentration in the lens (obtained from the total drug released) and the drug concentration in the loading solution, through Equation 4.2. The masses of drugs released from the lenses and the partition coefficients are listed in Table 2 for both drugs and the two lenses.

Table 4.2: Mass of loaded drug and partition coefficient (k) of LVF and CHX in lenses soaked in drug-PBS solution (5 mg/mL)

Contact lenses	Partition coefficient, k	Total drug release amount (µg)
1-DAY ACUVUE® TrueEye™ LVF	0.74 ±0.11	76 ± 4
ACUVUE® OASYS® LVF	0.58 ±0.09	59 ± 3
1-DAY ACUVUE® TrueEye™ CHX	1.48 ±0.15	154 ± 4
ACUVUE® OASYS® CHX	1.3 ±0.1	128±5

The partition coefficient of levofloxacin was less than one for both drugs, with a slightly higher value for 1-DAY ACUVUE® TrueEye™ compared to the ACUVUE OASYS®. The silicone fraction in the ACUVUE OASYS® is likely higher than that for 1-DAY ACUVUE® TrueEye™ because of the requirement of higher oxygen permeability. The higher silicone fraction reduces the water content for ACUVUE OASYS® to 38% compared to 46% for 1-DAY ACUVUE® TrueEye™. Since levofloxacin is highly hydrophilic, a lower partition coefficient for ACUVUE® OASYS® is expected. The release duration of levofloxacin was about 4-fold longer in the ACUVUE® TrueEye™ lenses compared to ACUVUE OASYS®, but the relative increase in release duration due to vitamin E incorporation was much higher for the OASYS. In the presence of 20% of vitamin E, the release times of LVF from 1-DAY ACUVUE® TrueEye™ and ACUVUE OASYS® exhibited a 3 and 6-fold increase to 100 hours and 50 hours, respectively. The 100-hours release duration from 1-DAY ACUVUE® TRueEye™ would be sufficient for the initial critical period of the keratitis treatment but may not be clinically relevant because this lens is approved as a daily wear lens. The 2-day release

from the OASYS was also encouraging, as it was a significant improvement over the control lens and could be further increased by higher loadings of vitamin E.

The increased release times were due to the presence of the vitamin E aggregates, which acted as a diffusion barrier forcing the drug to diffuse around the vitamin E barriers in the lenses [10]. The mass of drug released in the lenses was not significantly affected by vitamin E incorporation because of the negligible interaction between the drug and the vitamin E barriers. The slight decrease could be attributed to the vitamin E solubilized in the lens that decreased the water content [24]. The drug transport in a silicone hydrogel is complex due to the bi-continuous microstructure, constituted by silicone and hydrophilic content [24]. The release durations of any drug will depend on the diffusivities and partition coefficients of the drug in the silicone and the hydrophilic phases, which, in turn, are related with the microstructure of the material. The diffusivity of both drugs and salt are significantly lower in the TrueEye™ lenses compared to the OASYS® but the relative reduction in the diffusivities with vitamin E incorporation is much larger for the OASYS®. The water content of the TrueEye™ and the OASYS® lenses are 38 and 46%, respectively while the oxygen Dk for both lenses is about 100 (cm^2/sec) (mL of O_2/mL) (mm Hg) [25]. Thus the water content and oxygen permeability for both lenses are comparable, while the ion permeability is significantly lower for the TrueEye™ lens compared to the OASYS®. The lower ion permeability could potentially be due to higher tortuosity but that is likely because the oxygen Dk are comparable. We hypothesize that the lower ion permeability as well as the lower diffusivity of hydrophilic drugs in the TrueEye™ lenses can be attributed to a fraction of the hydrogel trapped as a discontinuous phase rather than the continuous microstructure. The drugs and the ions in the discontinuous hydrogel phase must diffuse through a silicone barrier, which lowers the average diffusivity. This hypothesis is also consistent with the comparable oxygen Dk for both lenses in spite of a 20% higher water content for the TrueEye™. The relative increase in the drug release duration with vitamin E incorporation was much higher for OASYS suggesting that the barrier effect of vitamin E was more effective. The increase in release duration of the drugs due to incorporation of diffusion barriers will depend on the number, aspect ratio and orientation of the barriers. Our method of barrier incorporation relied on the interaction of the vitamin E with the silicone-hydrogel microstructure and thus the shapes of the barriers could vary across contact lenses. Due to limited data on the

detailed microstructure of any of the contact lenses, it was difficult to clearly understand the differences on the effect of vitamin E incorporation in various types of lenses.

In contrast with levofloxacin, the partition coefficient of chlorhexidine was larger than one for both lenses. The mass of drug released as well as the release durations were larger for ACUVUE® TrueEye™ compared to ACUVUE OASYS®. Incorporation of vitamin E increased the release durations in both lenses but the effect was much more significant in ACUVUE OASYS®. In the presence of 20% of vitamin E, the release duration from ACUVUE® TrueEye™ and ACUVUE OASYS®, exhibited a 2.5 and 10-fold increase to 130 hours and 170 hours, respectively. The release duration of 170 hours from the vitamin E loaded OASYS lenses was very encouraging because this lens is approved for extended wear.

In the case of chlorhexidine, for both ACUVUE® TrueEye™ and ACUVUE OASYS® lenses, the presence of vitamin E caused a significant decrease in the amount of released drug. This was an unexpected result because prior studies with several hydrophobic, hydrophilic and amphiphilic drugs show only a minimal impact of vitamin E incorporation on the drug partition coefficient [7, 9]. It could be hypothesized that the significant decrease in mass released was due to the increased release durations which may prevent equilibrium uptake during the loading. However, increase of the drug loading duration to three weeks did not have any effect on the results. Another potential explanation could be related to the degradation of the drug, but this was also proven to be incorrect because the spectra of the eluting drug matched the pure drug. It was hypothesized that the drug chlorhexidine preferred to partition in the same manner as vitamin E and this competition reduced its partition coefficient with increasing vitamin E loading. This hypothesis is plausible but needs further exploration. From the clinical design perspective, the reduction in the partition coefficient was not critical because the mass of drug loaded in the lens can be increased by choosing a higher drug concentration in the loading solution.

Comparison of the two drugs showed that the release duration of chlorhexidine was longer, likely due to the absorption of the drug on the polymer, as evidenced from the higher partition coefficient. Also, the presence of vitamin E in the lenses had a higher impact on chlorhexidine transport.

4.3.3.1 Transport mechanism and model

Previous studies on drug transport of drugs in vitamin E loaded silicone-hydrogel contact lenses have shown that the drug transport is diffusion-controlled for both control and the vitamin E loaded gels and the effective diffusivity decreased with vitamin E incorporation [8, 9, 11]. For a diffusion control transport in sink conditions, the fraction release (f) at short times is given by the following equation [11]:

$$f = \frac{2\sqrt{t\,D_{eff}}}{\sqrt{\pi}}\frac{A_{surface}}{V_{gel}} = \frac{2}{\sqrt{\pi}}\sqrt{\frac{t\,D_{eff}}{\hbar^2}} \qquad \textbf{Equation 4.3}$$

where D_{eff} is the effective diffusivity, $A_{surface}$ is the total area of the lens, V_{gel} is the total volume of the gel, and h is the mean thickness of the gel, defined as $V_{gel}/ A_{surface}$. The validity of the above equation is typically explored by plotting the fraction release (f) as a function of √t. A linear plot is an indication of a diffusion controlled release [8] and the drug diffusivity can be calculated by equating the slope to $2/\sqrt{\pi}\ \sqrt{(D_{eff}/\hbar^2)}$. Note that, only the data for fractional release of less than about 0.7 were fitted. In each case discussed above, the short time release scaled as √t suggesting that the drug transportwas diffusion controlled even after incorporation of vitamin E.

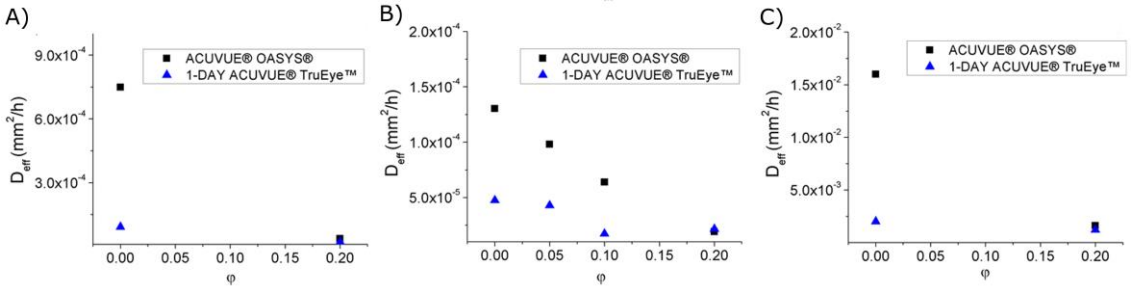

Figure 4.4: Fitted D_{eff} diffusivity for contact lenses with different vitamin E volume fraction (ϕ) in the case of (A) levofloxacin (B), chlorhexidine, and (C) sodium chloride.

Figure 4.4 shows the calculated diffusivities for ACUVUE®TrueEye™ and ACUVUE® OASYS plotted as functions of the vitamin E loading: Figure 4.4-A shows the results for levofloxacin and Figure 4.4-B for chlorhexidine, while Figure 4.4-C shows the results for the ion diffusivity (NaCl). In all cases the diffusivity decreased significantly

as the amount of vitamin E in the lens increased, and this is due to the barrier effect of the vitamin E in the lens.

In the case of chlorhexidine and 1-DAY ACUVUE® TrueEye™ the increase of vitamin E above 10% did not seem to affect further the release kinetic, presenting the same time of total release. The diffusion coefficients calculated for the levofloxacin release were much higher than those obtained for chlorhexidine.

The ion diffusivity values, shown in Figure 4.4-C, decreased, respectively, ten and two times in the presence of 20 % of vitamin E, for ACUVUE® OASYS and ACUVUE®TrueEye™. ACUVUE® OASYS. The approach to obtain the diffusivity by fitting the short time data was useful but it only provided information about the early stages of the release. Due to the complicated microstructure of the vitamin E loaded silicone hydrogel lens, it was conceivable that the long-time diffusivity was different from the short-time or that transport was controlled by some other mechanism. In order to explore this fact, the release data were fitted to the following model that is based on one-dimensional diffusion through a uniform thickness film.

$$\frac{\partial C}{\partial t} = D_{eff}\frac{\partial^2 C}{\partial y^2} \qquad \textbf{Equation 4.4}$$

where C(y,t) is the concentration of the drug in the lens, y is the spatial coordinate, where y=0 is the center of the lens, and t is time. The boundary conditions for the drugs release experiments are:

$$\frac{\partial C}{\partial y}(y = 0, \mathrm{t}) = 0$$
$$C(y = ħ, \mathrm{t}) = 0 \qquad \textbf{Equation 4.5}$$
$$C(y, t = 0) = Ci$$

The first boundary condition assumes symmetry at the center of the lens, the second boundary condition is based on the sink assumption. The third condition imposes the

known initial concentration C_i as the initial condition. Finally, the continuity of flux at the lens boundary and a well-mixed assumption for the fluid yields the following equation:

$$-2D_{eff}A_{surface}\frac{\partial C}{\partial y}(t, y = \hbar) = V_f\frac{dC_f}{dt} \qquad \textbf{Equation 4.6}$$

where V_f and C_f are, respectively, the volume and the concentration of the release medium. The above set of equations can be solved analytically to determine C(y,t) and C_f(t). The fractional release (f) can then be computed as $f(t) = \frac{V_f C_f}{V_{gel} C_i}$. The fitted data for the cumulative release profiles are plotted in Figure 4.3 as solid lines. The good fits between the experimental data and the model results suggested the validity of the diffusion model. The values of the diffusivities obtained from fitting the entire data were in good agreement with the values obtained from fitting just the short-time data further proving that the transport is diffusion limited with constant and uniform diffusivity. This in turn suggests that the distribution of the vitamin E aggregates in the lens is uniform.

4.3.3.2 Designing contact lens for therapeutic release

Currently, levofloxacin is delivered through a 5 mg/ml solution (QUIXIN®): 1-2 drops every 2 hours on days 1-2, followed by 1-2 drops, every 4 hours on days 3-7 [26]. Taking into consideration that less than 5% of the dose is absorbed by the cornea [27], and assuming 25 µL as the eye drop volume, this posology delivers 0.05-0.1 mg per day in the first two days, followed by 0.025-0.051 mg for the next five days. One may estimate that the therapeutic needs of the cornea are about 2.1-4.2 µg/hour, for the first two days, and, then 1.0-2.1 µg/hour for the next three days. Levofloxacin's toxicity studies revealed a high tolerance of the ocular cells at short duration exposure and to drug concentration below the 30 mg/mL [28].

The mass of levofloxacin loaded in the ACUVUE® OASYS contact lenses by soaking in 5mg/mL was almost 60 µg, which is clearly not sufficient to satisfy the therapeutic needs of the cornea during the total release duration of 3 days. Based on the target release of about 4 µg/hour for the first two days, the contact lens should contain at least 300 µg of drug. Assuming that the partition coefficient is independent on the

concentration, the lens was predicted to load the desired mass of 300 μg by soaking the lens in a solution of 25 mg/mL. To confirm this prediction, the cumulative release profiles from both control and vitamin E loaded contact lenses soaked in 25 mg/mL solution were determined and are presented in Figure 5A. The data show that, as expected, the mass of drug loaded in the lens reached the desired target, which confirms that the partition coefficient is indeed independent on the concentration even at 25 mg/mL. The kinetics of the release are the same of Figure 4.3-B, while the amount of drug released increases up to 300 μg, 5 times more than the drug released by the lenses soaked in 5 mg/mL solution.

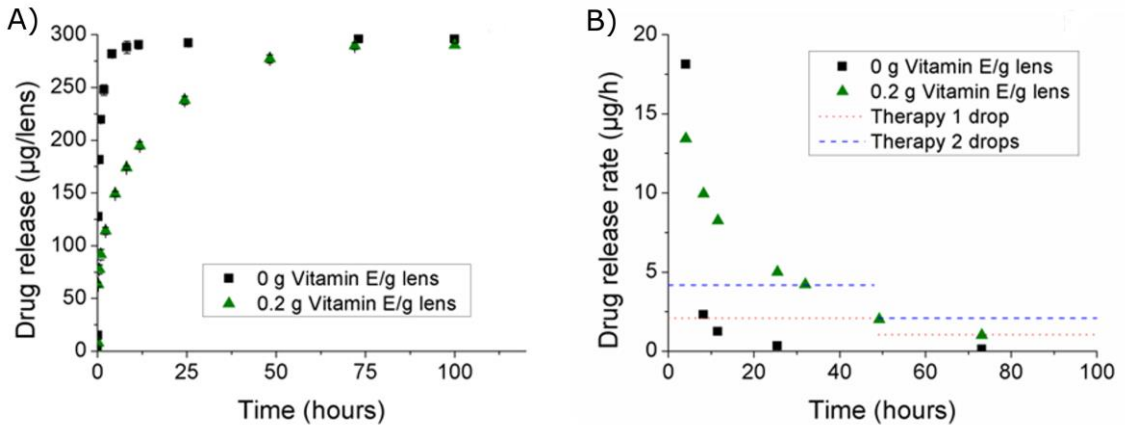

Figure 4.5: A) Cumulative levofloxacin release from vitamin E loaded ACUVUE® OASYS® lenses(drug loading: 25 mg/ml LVF/PBS solution, 14 days) B) Hourly average release rate (ST bars lower than 10%). Drug release rates referring to QUIXIN® eye drops therapy (one and two drops per instillation) are reported as dotted and dashed lines.

The release data were re-plotted in Figure 5B with the hourly drug release (mass of drug released at each hour) plotted as a function of time. The figure also contains the drug release rates resulting from the instillation of one and two drops at each dose. Since the release rates from the contact lenses are diffusion controlled, the released masses per hour were expected to decrease with time [29]. An optimally designed contact lens should release drug at rates that lie within the therapeutic window at all times, i.e., the release in the first hour of the wear should approach the upper limit, while that in the last hour should approach the lower limit of the therapeutic window. The data also shows that the lens without vitamin E could not maintain the desired delivery rates after

the first few hours, while the vitamin E loaded lens maintained drug concentrations within the desired window for about 3 days. By adjusting the drug loading concentrations, the duration of the therapeutic effect of ACUVUE® OASYS contact lenses loaded with LVF should be further increased.

The therapeutic values of chlorhexidine eye drops for the fungal keratitis were much lower, between 1.8 and 0.7 μg/hour, according to the work of Minassian et al [30]. The average release rate of chlorhexidine from ACUVUE® OASYS lenses largely exceeded those, but the drug loading can be decreased in order to reach the ideal release profile, and a 7 days therapeutic contact lens should be easily obtained.

4.4 Conclusions

The results reported here prove that vitamin E loading in commercial silicone contact lens can provide extended release of levofloxacin and chlorhexidine. The increase in duration occurs due to the presence of the vitamin E nano aggregates, which have a barrier effect for the drug release. This effect is more significant for ACUVUE® OASYS compared to the ACUVUE®TrueEye™ which shows that the size of the vitamin E barriers depend on the contact lens. The barrier effect is more significant for levofloxacin compared to chlorhexidine, which is contrary to some of the previous reports showing similar barrier effect for many hydrophilic drugs. The differences are likely caused by surface adsorption of chlorhexidine on the vitamin E barriers, followed by surface diffusion. This study also proves that incorporation of vitamin E does not impact the surface wettability which is a critical requirement for contact lenses. It is also shown that the short time diffusivity agrees also fits the entire release data suggesting that vitamin E aggregates are uniformly distributed in the lens. The comparison between the drug release rate from the levofloxacin loaded lenses and the eye drops suggests that a contact lens may cover the most acute phase of the bacterial keratitis avoiding the annoying instillation of eye drops, during, at least, the first 3 days. The results here are very encouraging but it must be stressed that *in vivo* tests are needed to assess their safety and efficacy and to fully determine the advantages of levofloxacin and chlorhexidine release from silicon contact lenses for the cure of bacterial and fungal

keratitis. Also the feasibility of integrating vitamin E loading procedures into industrial scale manufacturing must be explored.

4.5 References

1. A. Hui, A. Boone and L. Jones, *Uptake and release of ciprofloxacin-HCl from conventional and silicone hydrogel contact lens materials.* Eye Contact Lens, 2008. **34**(5): p. 266-71.
2. A. Boone, A. Hui and L. Jones, *Uptake and release of dexamethasone phosphate from silicone hydrogel and group I, II, and IV hydrogel contact lenses.* Eye Contact Lens, 2009. **35**(5): p. 260-7.
3. C.C.S. Karlgard, N.S. Wong, L.W. Jones and C. Moresoli, *In vitro uptake and release studies of ocular pharmaceutical agents by silicon-containing and p-HEMA hydrogel contact lens materials.* Int J Pharm, 2003. **257**(1–2): p. 141-151.
4. K. Kakisu, T. Matsunaga, S. Kobayakawa, T. Sato and T. Tochikubo, *Development and efficacy of a drug-releasing soft contact lens.* Invest Ophthalmol Vis Sci, 2013. **54**(4): p. 2551-61.
5. P. Paradiso, R. Galante, L. Santos, A.P. Alves de Matos, R. Colaco, A.P. Serro and B. Saramago, *Comparison of two hydrogel formulations for drug release in ophthalmic lenses.* J Biomed Mater Res B Appl Biomater, 2014.
6. K.H. Hsu, R.C. Fentzke and A. Chauhan, *Feasibility of corneal drug delivery of cysteamine using vitamin E modified silicone hydrogel contact lenses.* Eur J Pharm Biopharm, 2013. **85**(3 Pt A): p. 531-40.
7. J. Kim, C.C. Peng and A. Chauhan, *Extended release of dexamethasone from silicone-hydrogel contact lenses containing vitamin E.* J Control Release, 2010. **148**(1): p. 110-6.
8. C.C. Peng, M.T. Burke, B.E. Carbia, C. Plummer and A. Chauhan, *Extended drug delivery by contact lenses for glaucoma therapy.* J Control Release, 2012. **162**(1): p. 152-8.
9. C.C. Peng, M.T. Burke and A. Chauhan, *Transport of topical anesthetics in vitamin E loaded silicone hydrogel contact lenses.* Langmuir, 2012. **28**(2): p. 1478-87.
10. C.C. Peng and A. Chauhan, *Extended cyclosporine delivery by silicone-hydrogel contact lenses.* J Control Release, 2011. **154**(3): p. 267-74.

11. C.C. Peng, J. Kim and A. Chauhan, *Extended delivery of hydrophilic drugs from silicone-hydrogel contact lenses containing vitamin E diffusion barriers.* Biomaterials, 2010. **31**(14): p. 4032-47.
12. C.C. Peng, A. Ben-Shlomo, E.O. Mackay, C.E. Plummer and A. Chauhan, *Drug Delivery by Contact Lens in Spontaneously Glaucomatous Dogs.* Curr Eye Res, 2012. **37**(3): p. 204-211.
13. T. Yilmaz, O. Aydemir, I.H. Ozercan and B. Ustundag, *Effects of vitamin e, pentoxifylline and aprotinin on light-induced retinal injury.* Ophthalmologica, 2007. **221**(3): p. 159-66.
14. K. Bilgihan, U. Adiguzel, C. Sezer, G. Akyol and B. Hasanreisoglu, *Effects of topical vitamin E on keratocyte apoptosis after traditional photorefractive keratectomy.* Ophthalmologica, 2001. **215**(3): p. 192-6.
15. M. Kojima, Y.B. Shui, H. Murano and K. Sasaki, *Inhibition of steroid-induced cataract in rat eyes by administration of vitamin-E ophthalmic solution.* Ophthalmic Res, 1996. **28 Suppl 2**: p. 64-71.
16. M. Nagata, M. Kojima and K. Sasaki, *Effect of vitamin E eye drops on naphthalene-induced cataract in rats.* J Ocul Pharmacol Ther, 1999. **15**(4): p. 345-50.
17. T. Yilmaz, S. Celebi and A.S. Kukner, *The protective effects of melatonin, vitamin E and octreotide on retinal edema during ischemia-reperfusion in the guinea pig retina.* Eur J Ophthalmol, 2002. **12**(6): p. 443-9.
18. A. Danion, I. Arsenault and P. Vermette, *Antibacterial activity of contact lenses bearing surface-immobilized layers of intact liposomes loaded with levofloxacin.* J Pharm Sci, 2007. **96**(9): p. 2350-63.
19. P.C. Nicolson, R.C. Baron, P. Chabrecek, J. Court, A. Domschke, H.J. Griesser, A. Ho, J. Hopken, B.G. Laycock and Q. Liu, *Extended wear ophthalmic lens*. 1998, Patent number: US5760100 A.
20. C.-C. Peng and A. Chauhan, *Ion transport in silicone hydrogel contact lenses.* J Membr Sci, 2012. **399–400**(0): p. 95-105.
21. L. Guan, M.E.G. Jiménez, C. Walowski, A. Boushehri, J.M. Prausnitz and C.J. Radke, *Permeability and partition coefficient of aqueous sodium chloride in soft contact lenses.* J Appl Polym Sci, 2011. **122**(3): p. 1457-1471.

22. N. Khettab, M.C. Amory, G. Briand, B. Bousquet, A. Combre, P. Forlot and M. Barey, *Photoprotective effect of vitamins A and E on polyamine and oxygenated free radical metabolism in hairless mouse epidermis.* Biochimie, 1988. **70**(12): p. 1709-13.
23. C. Maldonado-Codina and P.B. Morgan, *In vitro water wettability of silicone hydrogel contact lenses determined using the sessile drop and captive bubble techniques.* J Biomed Mater Res A, 2007. **83**(2): p. 496-502.
24. A. Chauhan and J. Kim, *Contact lenses for extended release of bioactive agents containing diffusion attenuators*. 2010, Google Patents.
25. http://contactlensupdate.com/compendium/contact_lens/search/advanced/results. [cited 2015 31-07].
26. N.S. Gokhale, *Medical management approach to infectious keratitis.* Indian J Ophthalmol, 2008. **56**(3): p. 215-20.
27. C.L. Bourlais, L. Acar, H. Zia, P.A. Sado, T. Needham and R. Leverge, *Ophthalmic drug delivery systems--recent advances.* Prog Retin Eye Res, 1998. **17**(1): p. 33-58.
28. L. Clark, P. Bezwada, K. Hosoi, T. Ikuse, S. Adams, G.S. Schultz and O. OfBrien, *Comprehensive Evaluation of Ocular Toxicity of Topical Levofloxacin in Rabbit and Primate Models.* J Toxicol Cutaneous Ocul Toxicol, 2004. **23** (1): p. 1-18.
29. E. Mathiowitz, *Encyclopedia of controlled drug delivery* Vol. 1. 1999, New York.
30. M. Rahman, G. Johnson, R. Husain, S. Howlader and D. Minassian, *Randomised trial of 0.2% chlorhexidine gluconate and 2.5% natamycin for fungal keratitis in Bangladesh.* Br J Ophthalmol, 1998. **82**(8): p. 919-25.

5 Liposome based coatings on a hydrogel contact lenses material to control drug release

The presented results were submitted in the peer-reviewed international Journal of Biomedical Materials Research Part B: Applied Biomaterials

Table of contents

5.1 Introduction

Liposomes are spherical self-closed structures, composed of curved phospholipid bilayers. Their size varies from around 20 nm up to several micrometers and they may be composed of one concentric bilayer, as in the case of the unilamellar liposomes, or several concentric bilayers, each membrane having a thickness of around 4 nm, in the case of multilamellar liposomes.

Figure 5.1 shows different types of liposomes.

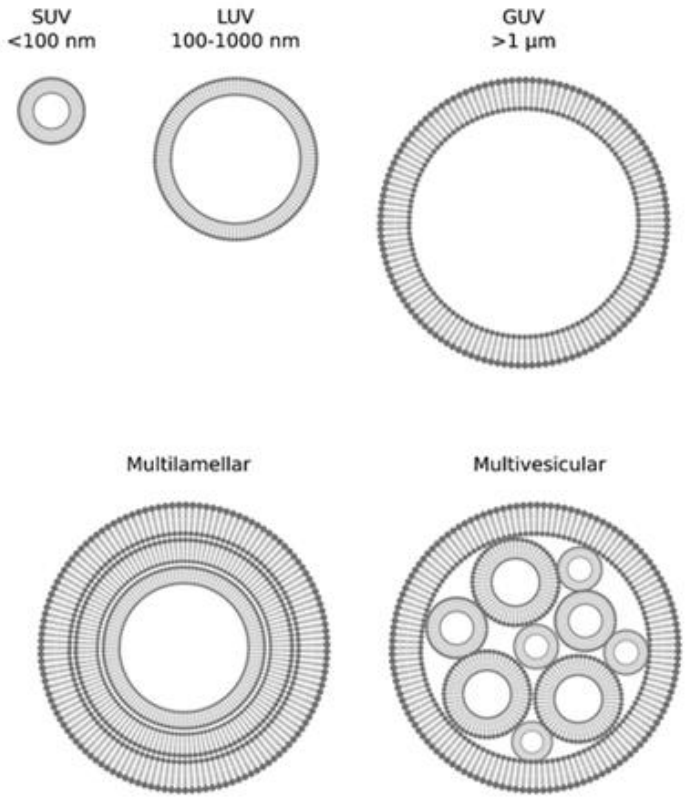

Figure 5.1: A schematic representation of different liposome types, with respective dimensions and structure [1]; small unilamellar vescicle (SUV), large unilamellar vescicle (LUV), giant unilamellar vescicle (GUV), multilamellar vesicle and multivesicular vesicle.

Liposomes are biocompatible structures that are characterized by their capacity to incorporate hydrophilic and hydrophobic drugs due to the amphiphilic character of the

phospholipids [2, 3]. For these reasons, these arrangements have received widespread attention as carrier systems for therapeutically active compounds [4].In recent years, researchers presented studies in which the presence of liposomes, dispersed in the hydrogel matrix [5], or immobilized on the contact lens surface [6, 7], permitted a prolonged ophthalmic drug release from SCLs.

According to Skirtach *et al.* [8], polyelectrolyte films showed the capacity of incorporation of nano and micro carriers, such as liposomes or polymeric capsules. Volodkin *et al.* proposed biocoatings for implant materials consisting in liposomes incorporated in polyelectrolyte coatings [9, 10] assembled using the layer-by-layer (LbL) technique, first proposed by Decher in 1991 [11]. These coatings were designed to preserve the biocompatibility of the implant and to release, in a controlled way, agents that are able to reduce inflammatory response upon implantation.

As far as the authors know, all the studies presented in the literature which investigate coatings with liposomes to control the drug release from SCLs materials, use drug loaded liposomes. None of them focus on the use of bare liposomes immobilized on the surface of drug loaded SCL hydrogels to act as barriers to the drug release. Furthermore, the biotribological effect of the eyelid blinking on the stability of the liposome coatings and, consequently on their ability to control drug release also was never investigated.

In this chapter a coating formed by polyelectrolyte layers over which is adsorbed a layer of liposomes was used to try to control the release of LVF from a HEMA/PVP material previously loaded with the drug. Two lipid compositions were used for the liposomes preparation: 1,2-dimyristoyl-sn-glycero-3-phosphocholine (DMPC) and DMPC+cholesterol (DMPC+CHOL). The presence of cholesterol in the liposome formulation is known to improve the viscoelastic properties of the liposomes, as described in Serro *et al.* [12]. Through this protocol, the long immobilization process proposed by Danion *et al.* [7] was avoided.

The formation of the polyelectrolyte bilayer and of the lipid barrier was followed *ex situ* with a Quartz Crystal Microbalance with Dissipation (QCM-D). The coatings morphologies were analyzed by atomic force microscopy (AFM). Confocal fluorescence microscopy studies were performed to investigate the stability of the lipid coating, namely if the liposomes remain intact upon adsorption or if they rupture with

the consequent formation of a lipid bilayer. These last experiments were performed at the Natural and Medical Sciences Institute (NMI) at the University of Tübingen, Germany, under the supervision of Professor Rumen Krastev.

The effect of eye blinking on the drug release was investigated using an apparatus designated Simublink, especially designed and conceived in our lab to simulate the movement of the eyelids [13]. With this apparatus the effect of repetitive load and friction cycles associated to the eyelid movement, present in *in vivo* conditions, was tested. The results were compared with those obtained in static sink conditions.

In order to study the influence of the temperature on the eventual barrier effect, the LVF release profiles from the PHEMA based hydrogel were obtained in static sink conditionsat different temperatures (4, 20 and 35°C) below or above the transition temperature of the lipids (Tg).

5.2 Experimental part

5.2.1 Materials

2-Hydroxyethyl methacrylate (HEMA), ethylene glycol dimethacrylate (EGDMA), 2,2′-azobis(2-methylpropionitrile) (AIBN), levofloxacin (LVF), phosphoric acid, triethylamine, the buffer N-(2-hydroxyethyl) piperazine-N′-(2-ethanesulfonic acid) (HEPES), chloroform, dichloromethane, 5,6-carboxyfluorescein (CF) and the polyelectrolytes: polyethylenimine (PEI) with average molecular weight of 750 KDa, poly(sodium 4-styrene-sulfonate) (PSS) with average molecular weight of 70 KDa, poly(allylamine hydrochloride) (PAH) with average molecular weight of 70 KDa, were all purchased from Sigma-Aldrich. Poly(vinylpyrrolidone) (PVP K30, Kollidon® 30) was kindly provided by BASF. Octadecyl Rhodamine B Chloride (R18) was from Invitrogen (Carlsbad, CA, USA). The lipids 1,2-Dimyristoyl-sn-glycero-3-phosphocholine (DMPC), and cholesterol (CHOL) were obtained from Avanti Polar Lipids (Alabaster, AL, USA). Sodium chloride was obtained from Merck, carbon tetrachloride from Riedel-de Haën, acetonitrile from Fisher Scientific, and dimethyldichlorosilane from Fluka. Solutions of Hellmanex II 2% (Hellma GmbH) and

sodium dodecyl sulfate (SDS, Sigma-Aldrich) 3% were used to clean the QCM-D parts and the quartz crystals, respectively. The AT-cut 5 MHz piezoelectric quartz crystals (14 mm in diameter) coated with gold and supplied by Q-Sense (Gothenburg, Sweden) were used in the QCM experiments. DD water was used in all experiments.

5.2.2 Hydrogel preparation

HEMA/PVP hydrogel was prepared following the protocol reported in section 2.2.2 of Chapter 2. The hydrated samples were cut in pieces of 50×10 mm^2 and dried overnight inside an oven at 40 °C.

5.2.3 Drug loading

The dry HEMA/PVP hydrogel samples were loaded with LVF by soaking in the drug solution (2.6 mL/cm^2 of surface area), with a concentration of 5 mg/mL for 14 hours at 4 °C. Levofloxacin solution was prepared by dissolution of the drug in saline solution (130 mM NaCl). The soaking process was performed protecting the loading solution from light. The loaded samples were rinsed with DD water and blotted with absorbent paper prior to the coating. Control samples did not undergo the coating steps.

5.2.4 Liposomes production

Two types of liposomes were prepared, namely DMPC and DMPC+CHOL liposomes.

The method followed for the production of the unilamellar vescicles is described schematically in Figure 5.2. Appropriate amounts of DMPC and DMPC+CHOL (70:30 mol%) were dissolved in chloroform, and then dried under a nitrogen stream. The resulting film was kept under vacuum for at least 3 hours in order to remove all traces of organic solvent. After drying, the film was hydrated with HEPES (final concentration 5mg/mL) inside a thermostatic water bath at ≈ 10–15 °C above the temperature of the gel-to-liquid crystalline phase transition. Heating was alternated with vortex agitation for 1 hour. The obtained multilamellar vesicles (MLVs) were submitted to 5 freezing–thawing cycles, respectively, in liquid nitrogen and in a water bath at the temperature referred above. Large unilamellar vesicles were obtained from the MLVs by extrusion in a stainless steel homemade extruder, thermostated at the same temperature. The samples were passed several times through polycarbonate filters (Nucleopore,

Whatman) of decreasing pore size (600 nm, 5 times; 200 nm, 5 times; and 100 nm,10 times), under inert nitrogen atmosphere. The liposome dispersions were stored at 4 °C and were used within 2 weeks from preparation.

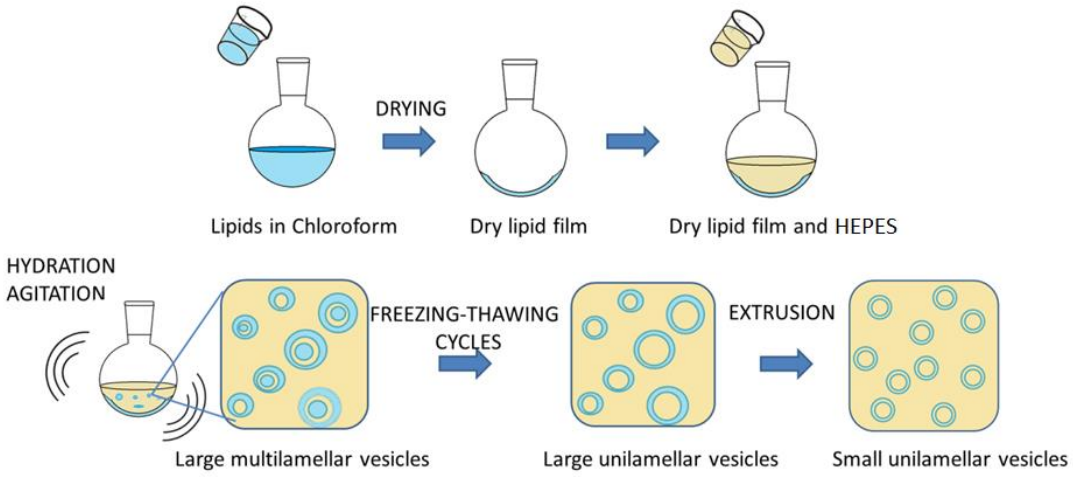

Figure 5.2 Schematic representation of the liposomes steps production.

Liposome suspension of 0.7 mg/mL was prepared for the coating on HEMA/PVP hydrogel and for the QCM-D experiments. The choice of this concentration was based on previous observations that this concentration leads to a monolayer of adsorbed liposomes on the quartz crystals [12].

Size distribution of extruded vesicles was determined to be 103±8 nm for both liposome compositions. The measurements were performed at 25 °C by dynamic light scattering (DLS) using a Spectra Physics model 127 He–Ne laser (632.8 nm, 35 mW) and a Brookhaven instrument with a BI-200SM goniometer, a BI-2030AT autocorrelator and a APD detector.

For the confocal microscopy experiments, liposomes were prepared with the hydrophobic R18-labeled lipids and the encapsulated hydrophilic CF (see Figure 5.3) following a previously established protocol [12]. The lipidic membranes were labelled with R18, by adding an appropriate amount of dye to the mixture of lipids in chloroform, to reach a final concentration of 294 μM in the final liposome suspension. To encapsulate CF inside the liposomes, the lipid film was hydrated in a solution of HEPES containing 50 μM of the dye.

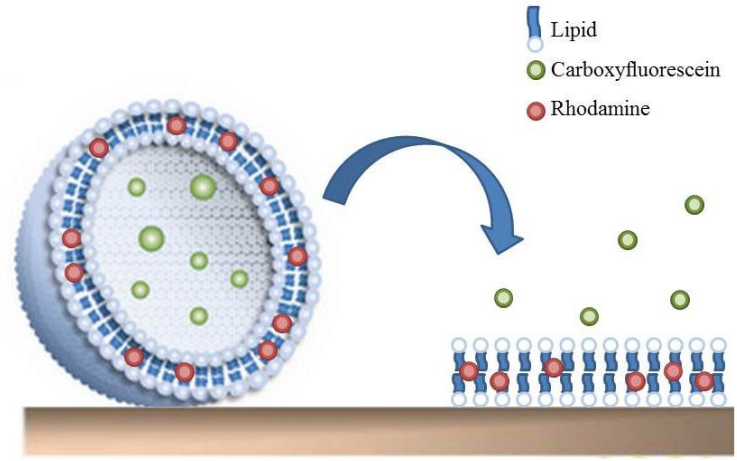

Figure 5.3 Schematic representation of the labelled liposomes. It is shown how, in the case of liposome rupture, the carboxyfluorescein is released, while the rhodamine remains in the lipid bilayer.

5.2.5 Coatings assembly

The polyelectrolyte multilayer coating on HEMA/PVP was prepared using the LbL technique of electrostatically driven sequential adsorption of polyions from their solutions [14]. Adsorption of polyelectrolytes was performed by immersion of the samples in the respective solutions: PEI solution had a concentration of 10 mg/mL and pH adjusted to 7 with hydrocloric acid, both PSS and PAH solutions had a concentration of 2 mg/mL in 0.5 M NaCl solution. All the solutions had a concentration of LVF of 5 mg/mL (except the liposome suspensions).

PEI deposition step lasted 15 minutes, PSS and PAH deposition steps lasted 6 minutes, each. Rinsing in between the steps was done for 5 minutes in water. The liposomes deposition step lasted 20 minutes. The sequence of the depositions is shown in Figure 5.4.

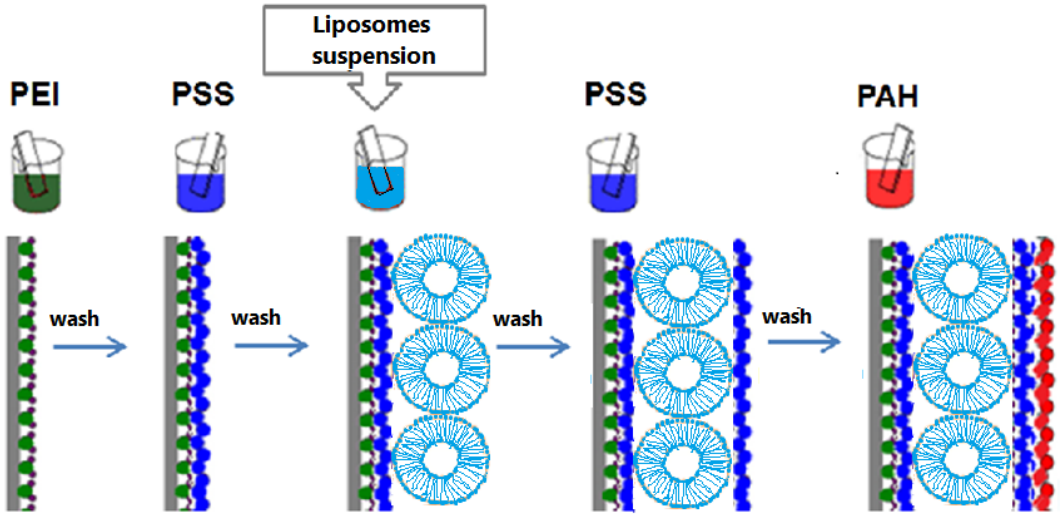

Figure 5.4 Schematic representation of the coating assembly steps

5.2.6 Coating characterization

5.2.6.1 QCM-D measurements

QCM-D measurements were performed using the quartz crystal microbalance with dissipation (QCM-D, Q-Sense model E4) as described by Rodahl et al. [15], using gold crystals. The piezoelectric crystals were excited at their fundamental resonance frequency and the third, fifth, seventh and ninth overtones were observed. The decrease in the resonance frequency, $\Delta f/n$, describes an increase of the mass adsorbed to the crystal, while the change in dissipation, ΔD, gives information on the viscoelastic properties, namely the dissipation factor, D, is related to the acoustic energy loss by the adsorbed film. In this work, the reported changes in dissipation and in the normalized frequency refer to the third overtone of the crystal fundamental resonance frequency. From the time-dependence of the frequency shift and of the dissipation change, the kinetics of the coating adsorption and the interaction between layers were investigated.

The same polyion solutions and liposome suspension, used for the coating formation on hydrogels, were used for the QCM-D experiments. DD water (baseline), PEI solution, water (rinsing), PSS solution, water (rinsing), liposome suspension, water (rinsing), PSS solution and water (rinsing) were sequentially injected into the QCM-D cells. Each

injection lasted approximately 10 minutes under a flow rate of 0.1 mL/min, followed by a pause in order to allow for the stabilization of the frequency and dissipation signals.

The experiments were performed at 35 °C and the results are averages of, at least, four independent measurements.

Prior to each experiment, all the QCM-D balance parts were washed with Hellmanex solution, abundantly rinsed with DD water and finally dried through the blow of nitrogen. The gold crystals were sonicated 5 minutes in SDS solution, abundantly rinsed with DD water and sonicated twice for 5 minutes in DD water, and finally blown dried with nitrogen. Immediately before the QCM-D experiments, the crystals were subjected twice to UV/ozone treatments (10 minutes), rinsing with DD water in between, and dried with nitrogen flow.

5.2.6.2 Surface topography

The topography of the coatings on HEMA/PVP hydrogels was investigated by AFM. Different samples were prepared for each step of the coating, namely, after the first bilayer (PEI/PSS), after the liposomes layer (PEI/PSS/DMPC or PEI/PSSDMPC+CHOL liposomes) and finally, after the second bilayer (PEI/PSS/liposomes/PSS/PAH). The samples were hydrated and a Nanosurf AFM was used in contact mode in liquid (130 mM NaCl), with a gold coated PPP-CONTSCAuD Nanosensor cantilever (force constant 0.06 N/m). All observations were conducted at 25 ºC. The average roughness was determined from at least five regions, of 5x5 μm^2, in the AFM images, avoiding zones with aggregates.

5.2.6.3 Confocal fluorescence microscopy

Fluorescence images of the coatings were collected using a confocal fluorescence Zeiss Axiovert 200M with a 63x water immersion objective (high magnification). The images were analyzed with QWin software (Leica Microsystems, Heidelberg, Germany). The fluorescence imaging of the coatings permitted to better understand the liposomes coating adherence and the interaction with the polyelectrolyte layers. Hydrogels could not be used as substrates because CF was absorbed by the matrix, overlapping the fluorescence

signal of the liposomes. Silicon oxide samples served as substrate for the coatings which were prepared following the same procedure as described in section 5.2.4. Liposomes with both compositions (DMPC and DMPC+CHOL) were tested. The coatings were imaged, before and after the deposition of the second bilayer: PEI/PSS/liposomes and PEI/PSS/liposomes/PSS/PAH.

5.2.7 Drug release

5.2.7.1 Experiments under simulated eyelid movement

The effect of the eyelid movement on the drug release performance of uncoated PHEMA based hydrogels, was studied in a previous work by our group [13], using the Simublink apparatus (see Figure 5.5), built in collaboration with professor José Mata from IST. The working principle of Simublink resides on the conversion of the rotation motion of a stepping motor into alternate linear motion. An Arduino interface (Uno+EasyDriver) controls the motor pace. The contact pressure created by the eyelid during blinking was estimated to be in the range 3.5-4.0 kPa with a blinking speed average around 12 cm/s [16]. Due to design limitations, a pressure of 16 kPa was applied on the hydrogel using a cylinder shaped counterbody of PMMA with a weight of 3.5 g. The final pressure was calculated through the following equation [17]:

$$P_{max} = \left(\frac{E^*}{2\pi R} * \frac{F_N}{L}\right) \qquad \textbf{Equation 5.1}$$

where E* is the elastic modulus depending on the Young modulus and Poisson coefficient of both materials, R is the ray of the cylinder, F_N the normal force and L the length of the contact area between the cylinder and the plane hydrogel.

A sliding velocity of 14 cm/s, making a 2 seconds pause between “blinkings” to mimic the eye conditions [16].

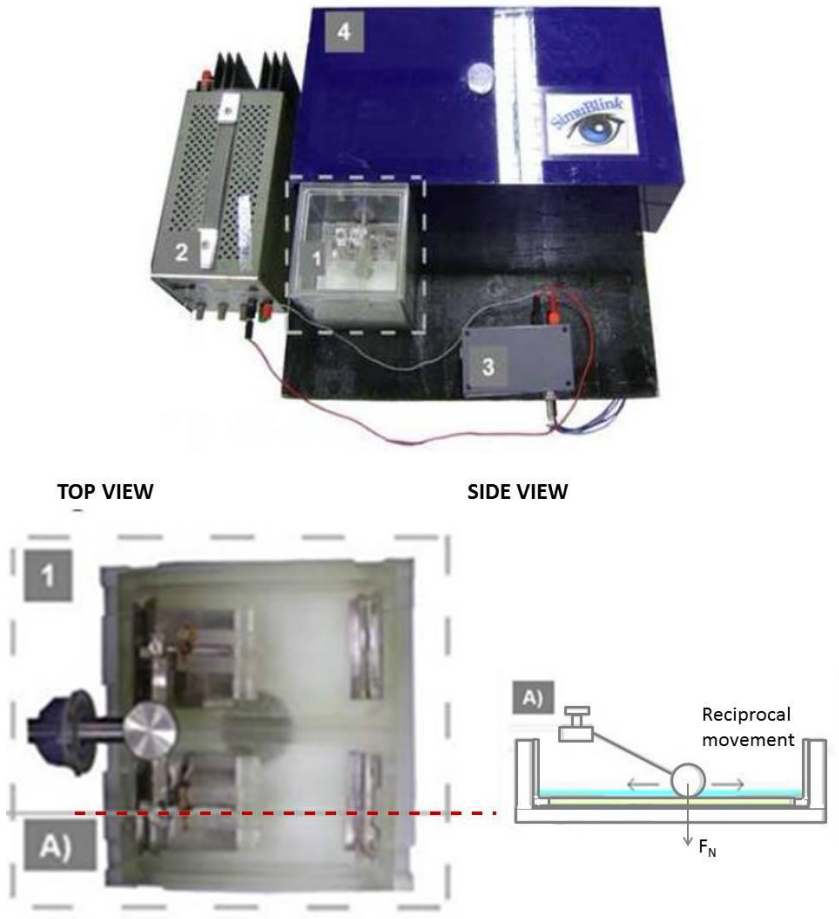

Figure 5.5 Simublink apparatus. 1) Experiment cell, 2) Power supply, 3) Arduino controller, 4) Step by step motor. In detail the top and side view (A) of the experimental cell.

Both lipid composition coatings, PEI/PSS/liposomes/PSS/PAH, with DMCP and DMPC+CHOL liposomes, were submitted to the friction experiments simulating the eyelid action. The experiments were performed not at the physiological ocular temperature of 35 ºC [18], but at 20ºC due to experimental limitations.

The experiments were done using strips of the hydrogels of 5x1 cm^2 and keeping the ratio for the supernatant volume (2.6 mL of NaCl solution/cm^2 of surface area). At pre-determined time intervals, aliquots (~ 8% of total volume) of the supernatant were collected and replaced by the same volume of fresh NaCl solution. The concentration of LVF in the supernatant was determined as described before.

The experiments were performed in triplicate.

5.2.7.2 Effect of temperature at static sink conditions

Drug release experiments in static conditions were performed on coated and non-coated samples. The previously loaded and coated samples were immersed in the saline solution (2.6 mL/cm^2 of surface area), in closed vessels, under stirring (150 rpm). At pre-determined time intervals, aliquots (~ 8% of total volume) of the supernatant were collected and replaced by the same volume of fresh NaCl solution. The concentration of LVF in the supernatant was determined using a high performance liquid chromatograph (HPLC), at the wavelength of 290 nm, with a Jasco UV-VIS detector and a C-18 column Nova-Pak Watters. The mobile phase, which consisted of DD water, acetonitrile, phosphoric acid and triethylamine (86/14/0.6/0.3 in volume), was introduced into the column at a flow rate of 1 mL/min and a pressure of 14 MPa. A minimum of three samples was used for each release profile. In the case of DMPC liposomes, the effect of temperature of release on the behavior of the lipid coating was investigated. As the gel–liquid crystalline phase transition temperature, $T_{g,}$ of DMPC is 23.7 °C [19], three different temperatures were chosen: two temperatures below $T_{g,}$ 4 °C and 20 °C, and one above, 35 °C.

The experiments were performed in triplicate.

5.3 Results and Discussion

5.3.1 Coatings characterization

5.3.1.1 QCM-D measurements

The LbL deposition, including the liposomes adsorption, was investigated using the QCM-D. The frequency and dissipation shifts obtained during deposition are shown in Figure 5.6. The polyelectrolytes deposition and the liposomes adsorption are accompanied by a decrease in the frequency signal which testifies an increase in mass of the coating. The injection of the liposome suspension causes a large shift in the resonant frequency, $\Delta f/n$~350 Hz, in both liposome compositions (Figure 5.6 A and B), and a

relative large change in dissipation, which confirms the adsorption of intact liposomes [20-22].

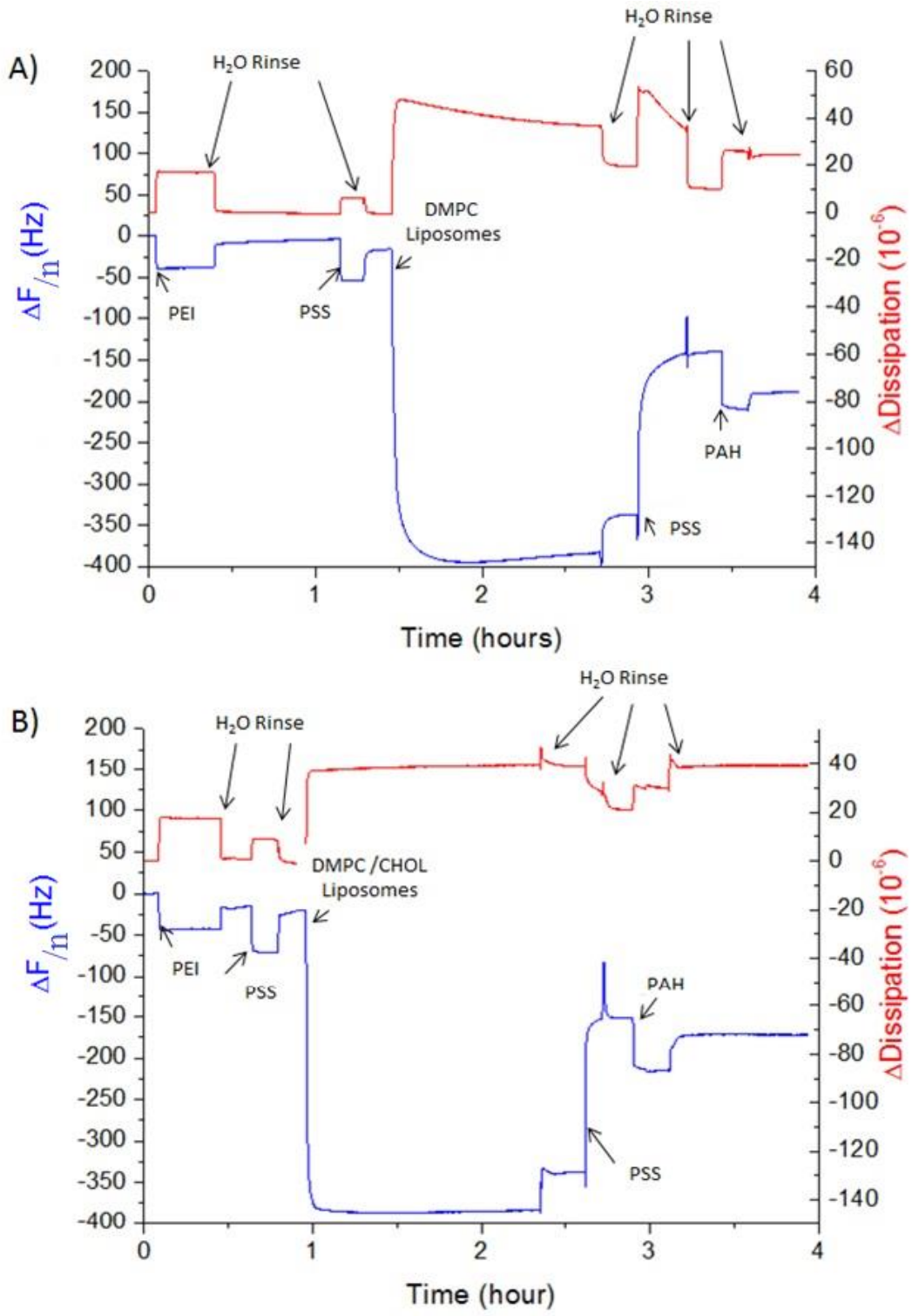

Figure 5.6: Coating assembly monitored by QCM-D: A) PEI/PSS/DMPC liposomes/PSS/PAH; B) PEI/PSS/DMPC+CHOL liposomes/PSS/PAH. The third overtone is shown.

The frequency shift corresponding to the adsorption of both DMPC and DMPC+CHOL liposomes is higher than the one described in literature on clean gold [20-22], which may be due to the presence of the polyelectrolytes underlayer. During rinsing with DD water, which follows each adsorption step (PEI, PSS and of the liposomes), there is an increase in frequency and a decrease in dissipation, which represents a compaction of the film and removal of weakly adsorbed species. After adsorption of the liposomes, during the injection of the PSS solution, the frequency strongly increases ($\Delta f/n \sim 150$ Hz) in the case of both lipids, while the dissipation increases in the case of DMPC ($\Delta D \sim 53 \times 10^{-6}$) (Figure 5.6A) and slightly decreases in the case of DMPC+CHOL ($\Delta D \sim 30 \times 10^{-6}$) (Figure 5.6B). A strong interaction between the anionic layer and the liposomes is occurring, but both dissipation and frequency values are too high to hypothesize the total rupture of the liposomes and formation of a single bilayer, which, from literature, would correspond to $\Delta f \sim 25$ Hz and $\Delta D \sim 1 \times 10^{-6}$ [23, 24]. Thus, it is plausible to assume that the strong interaction may lead to the partial rupture of the liposomes creating a heterogeneous layer where fragments of liposomes shall coexist with bilayer regions and eventually some intact liposomes. During the following rinsing step, the frequency is not affected, while the dissipation decreases in both cases, in a stronger way in the case of the DMPC lipids. After PAH adsorption, during the DD water rinse, dissipation values do not change, but the frequency increases. This behaviour may be justified by the detachment of weakly bound molecules, without any change in the viscoelastic properties.

5.3.1.2 Surface topography

Contact mode AFM images of coated HEMA/PVP samples are presented in Figure 5.7. All observations were done in an aqueous environment with swollen samples. The AFM images shown are representative of the samples, even though the adsorption of the polyelectrolyte presents heterogeneities, namely spots with aggregates. The average roughness is also reported in the figures. The roughness of the surface increases with the adsorption of the liposomes and decreases with the subsequent adsorption of the polyelectrolytes bilayer.

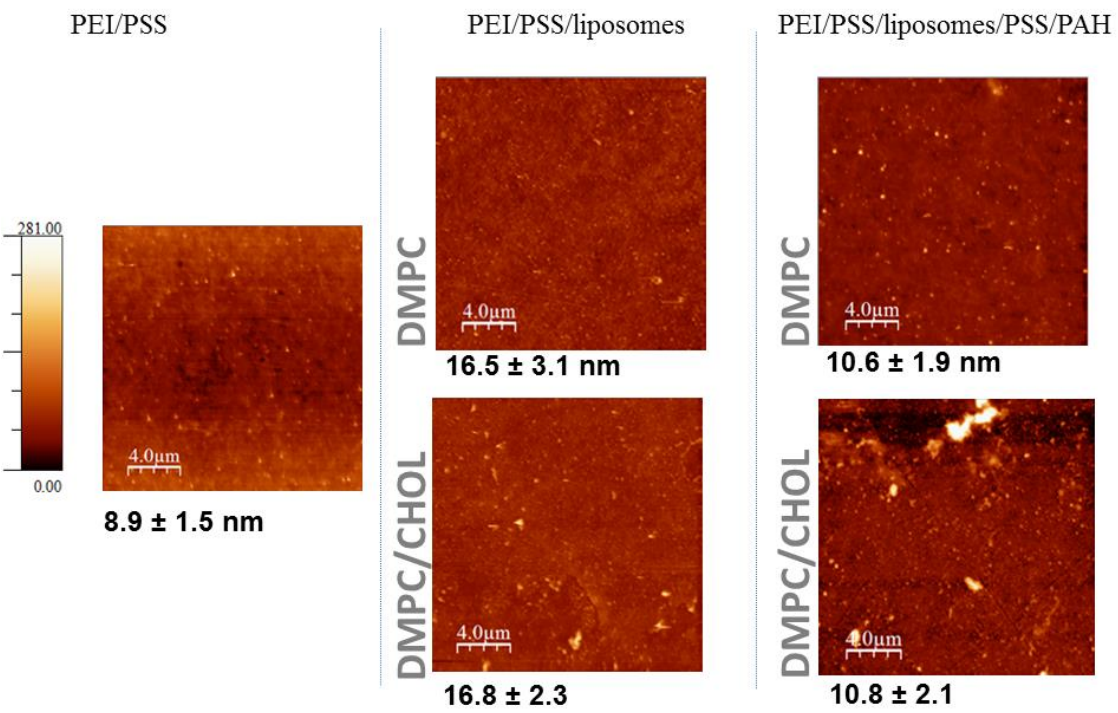

Figure 5.7: Contact-mode AFM images of HEMA/PVP after deposition of PEI/PSS, PEI/PSS/liposomes and PEI/PSS/liposomes/PSS/PAH. The mean roughness values are reported below the images.

5.3.1.3 Confocal fluorescence microscopy

Confocal fluorescence microscopy investigation was used as a mean to further investigate the stability and the structure of the DMPC and DMCP+CHOL liposomes. As described in section 5.2.4, liposomes were labelled with dyes, namely the hydrophilic CF encapsulated inside the liposomes and R18 labelling the lipid layers. Two types of samples were prepared for these measurements, representing two steps of the coating, namely, the liposomes layer before and after the PSS/PAH polyelectrolytes bilayer adsorption.

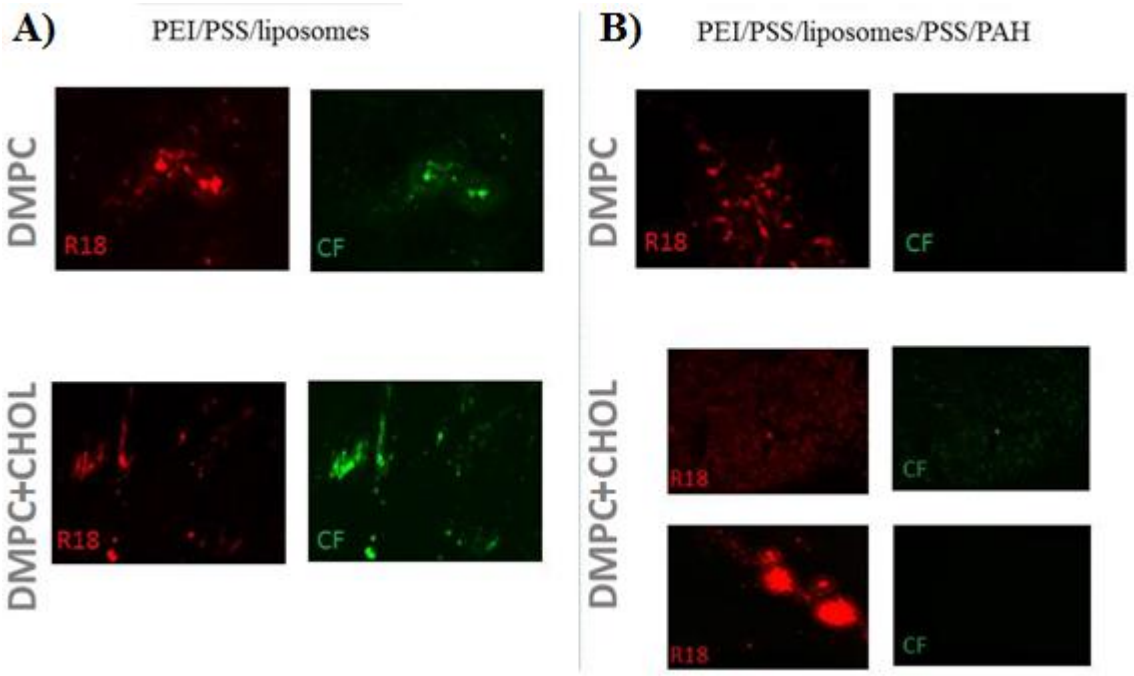

Figure 5.8: Confocal fluorescent images of DMPC and DMPC+CHOL liposome coating before (A) and after (B) the PSS/PAH polyelectrolytes bilayer adsorption. The fluorescent emission of CF (green) and of R18 (red) are reported. The images were obtained at 63x magnification.

Figure 5.8 shows the fluorescent emission of CF (obtained at 530-550 nm) and of R18 (obtained at 580-680nm) on the coated silicon samples. Figure 5.8A presents the fluorescent emissions of the adsorbed liposomes. Both fluorescent emissions of CF and R18 are visible in the figures in both DMPC and DMPC+CHOL coatings, evidencing the presence of intact liposomes. However, the signal is not homogeneous, indicating a discontinuous coating of the surface, which is in agreement with AFM observations. After the PSS/PAH polyelectrolytes bilayer adsorption (Figure 5.8B), in the case of DMPC, the fluorescent signal of the encapsulated CF is not recorded, being a sign of liposomes rupture. In the case of DMCP+CHOL, the sample presents areas where the CF signal is still emitted and other areas without signal. These observations are in agreement with the QCM-D results: the higher stiffness and viscosity of the DMPC+CHOL liposomes suggests that they are more resistant to rupture because the lipids are more densely packed, as described in Serro *et al.* [12].

5.3.2 Drug Release

Figure 5.9 compares the cumulative release curves of LVF obtained in static sink conditions with those obtained under friction conditions which attempt to simulate the eye blinking effect. The experiments were carried out at 20 ºC. At this temperature, both lipids, DMPC and DMPC+CHOL, are in the gel phase, since the T_g of DMPC is 23 ºC and of DMPC+CHOL is 30 ºC [25].

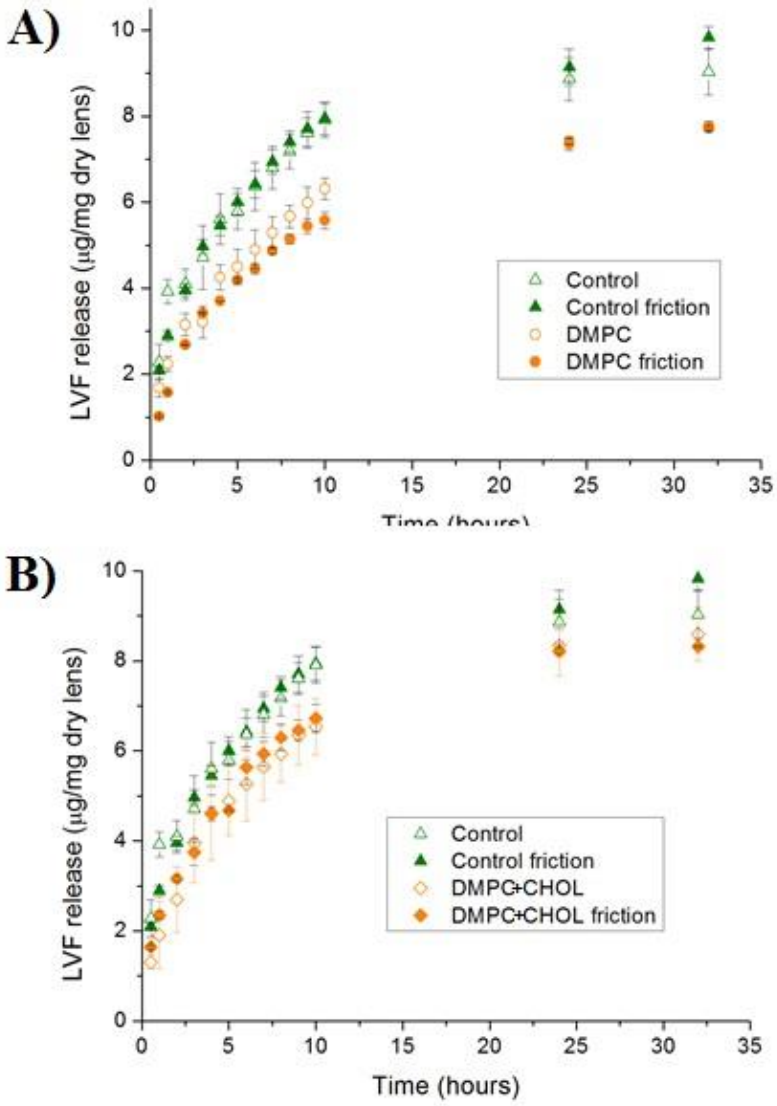

Figure 5.9: Effect of the friction on the cumulative release profiles of levofloxacin from HEMA/PVP hydrogels controls and coated samples with A) PEI/PSS/DMPC liposomes/PSS/PAH layer and B) PEI/PSS/DMPC+CHOL liposomes/PSS/PAH.

It can be seen that both coatings play a barrier effect, reducing the amount of drug released. No noticeable difference between the curves obtained with and without friction could be observed, indicating that both coatings maintain their protective effect.

In a previous work performed by our group [13], the authors concluded that friction does not influence significantly the LVF release of thermal polymerized HEMA/PVP hydrogels, which is confirmed by the data presented here.

The effect of temperature of release on the cumulative release profiles of LVF obtained in static sink condition was also investigated. The results obtained before and after the PEI/PSS/DMPC liposomes/PSS/PAH coating assembly are shown in Figure 5.10.

The effect of the presence of the coating on the release of levofloxacin is null at 4ºC, but increases with temperature, probably due to the phase transition that occurs in the DMPC bilayer at 23ºC [19]. The liquid disordered state of the bilayer at 35ºC may be responsible for the higher capacity of the lipids to decrease the drug release. However, it is important to stress that the kinetics of drug release is not much affected, in contrast to the amount of drug released that is significantly reduced. The lipid barrier seems to retain part of the LVF which, thanks to its amphiphilic character, shall have affinity to the lipid bilayers.

Increasing the temperature of release leads to an increase of the drug diffusion rate through the hydrogel. This phenomenon is recorded both in the control and in the coated samples.

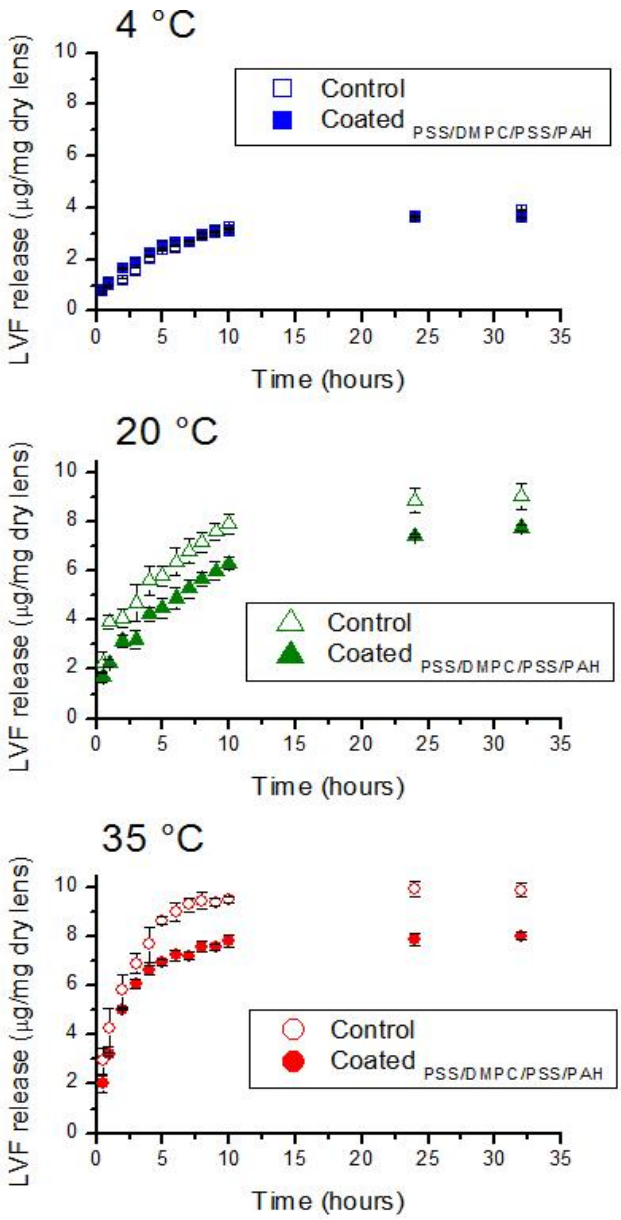

Figure 5.10: Effect of the temperature of release on the cumulative release profiles of levofloxacin from HEMA/PVP hydrogels coated with PEI/PSS/DMPC liposomes/PSS/PAH.

5.4 Conclusions

In the present chapter the effect of using liposome coatings to control the drug release from a PHEMA based hydrogel was investigated.

The PHEMA based hydrogel was first loaded with levofloxacin and subsequently coated with a polyelectrolyte coating containing liposomes. Two liposome compositions were tested, DMPC and DMPC+CHOL, which give rise to coatings with different viscoelasticity: DMPC+CHOL liposomes confer higher viscosity and stiffness to the coating. The coatings were characterized using different techniques: QCM-D, AFM and confocal fluorescence microscopy. It was demonstrated that after the intact liposomes adsorption, there is partial rupture of the liposomes caused by the interaction with the anionic polyelectrolytes. From the drug release experiments performed in the presence of friction, which simulate the eye blinking on the SCLs during wear, it was concluded that no noticeable difference is introduced by the presence of friction, both for the control and the coated samples.

Different temperatures of release were tested for the samples coated with DMPC liposomes, namely 4, 20 and 35 ºC in order to study the influence of the T_g of the lipid. The results obtained showed that the drug release rate increased for higher temperatures, due to the expected increase in drug diffusion coefficient. The presence of the coating seems to retain part of the loaded drug without changing the kinetic of release; this effect is more visible with the increase of the temperature of release.

5.5 References

1. B. Yu, R.J. Lee and L.J. Lee, *Microfluidic methods for production of liposomes.* Methods Enzymol, 2009. **465**: p. 129-41.
2. R.A. Schwendener and H. Schott, *Liposome formulations of hydrophobic drugs.* Methods Mol Biol, 2010. **605**: p. 129-38.
3. C. Jaafar-Maalej, R. Diab, V. Andrieu, A. Elaissari and H. Fessi, *Ethanol injection method for hydrophilic and lipophilic drug-loaded liposome preparation.* J Liposome Res, 2010. **20**(3): p. 228-243.
4. M.S. Mufamadi, V. Pillay, Y.E. Choonara, G. Modi, D. Naidoo and V.M.K. Ndesendo, *A Review on Composite Liposomal Technologies for Specialized Drug Delivery.* J Drug Deliv, 2011. **2011**.
5. D. Gulsen, C.C. Li and A. Chauhan, *Dispersion of DMPC liposomes in contact lenses for ophthalmic drug delivery.* Curr Eye Res, 2005. **30**(12): p. 1071-1080.
6. A. Danion, H. Brochu, Y. Martin and P. Vermette, *Fabrication and characterization of contact lenses bearing surface-immobilized layers of intact liposomes.* J. Biomed. Mater. Res. A., 2007. **82**(1): p. 41-51.
7. A. Danion, I. Arsenault and P. Vermette, *Antibacterial activity of contact lenses bearing surface-immobilized layers of intact liposomes loaded with levofloxacin.* J Pharm Sci, 2007. **96**(9): p. 2350-63.
8. A. Skirtach, D. Volodkin and H. Mohwald, *Remote and SelfInduced Release from Polyelectrolyte Multilayer Capsules*, in *Multilayer Thin Films: Sequential Assembly of Nanocomposite Materials*, G. Decher and J. Schlenoff, Editors. 2012, John Wiley & Sons: Darmstadt, Germany. p. 838-940.
9. D. Volodkin, H. Mohwald, J.-C. Voegel and V. Ball, *Coating of negatively charged liposomes by polylysine: Drug release study.* Journal of Controlled Release, 2007. **117**(1): p. 111-120.
10. D. Volodkin, Y. Arntz, P. Schaaf, H. Möhwald and J.C. Voegel, *Composite multilayered biocompatible polyelectrolyte films with intact liposomes: stability and temperature triggered dye release.* Soft Matter, 2008. **4**(1): p. 122-130.
11. G. Decher and J.D. Hong, *Buildup of Ultrathin Multilayer Films by a Self-Assembly Process: II. Consecutive Adsorption of Anionic and Cationic Bipolar*

Amphiphiles and Polyelectrolytes on Charged Surfaces. Berichte der Bunsengesellschaft für physikalische Chemie, 1991. **95**(11): p. 1430-1434.

12. A.P. Serro, A. Carapeto, G. Paiva, J.P.S. Farinha, R. Colaço and B. Saramago, *Formation of an intact liposome layer adsorbed on oxidized gold confirmed by three complementary techniques: QCM-D, AFM and confocal fluorescence microscopy.* Surf and Interface Anal, 2012. **44**(4): p. 426-433.
13. R.P. Galante, P, M. Moutinho, A. Fernandes, J. Mata, A. Matos, R. Colaço, B. Saramago and A. Serro, *About the effect of eye blinking on drug release from pHEMA-based hydrogels: an in vitro study.* J Biomater Sci Polym, 2015. **26**(4): p. 235-51.
14. *Multilayer Thin Films: Sequential Assembly of Nanocomposite Materials*. 2003: Wiley-VCH.
15. M. Rodahl, F. Höök, A. Krozer, P. Brzezinski and B. Kasemo, *Quartz crystal microbalance setup for frequency and Q ‐ factor measurements in gaseous and liquid environments.* Review of Scientific Instruments, 1995. **66**(7): p. 3924-3930.
16. A.C. Rennie, P.L. Dickrell and W.G. Sawyer, *Friction coefficient of soft contact lenses: measurements and modeling.* Tribol. Lett., 2005. **18**(4): p. 499-504.
17. R. Galante, *Influência da ação tribológica na libertação de levofloxacina a partir de materiais de lentes de contacto*, in *Biomedical Engineer* 2012, Instituto Superior Tecnico: Lisbon.
18. M. Sniegowski, M. Erlanger, R. Velez-Montoya and J.L. Olson, *Difference in ocular surface temperature by infrared thermography in phakic and pseudophakic patients.* Clinical Ophthalmology (Auckland, N.Z.), 2015. **9**: p. 461-466.
19. A.P. Serro, R. Galante, A. Kozica, P. Paradiso, A.M.P.S.G. da Silva, K.V. Luzyanin, A.C. Fernandes and B. Saramago, *Effect of tetracaine on DMPC and DMPC+cholesterol biomembrane models: Liposomes and monolayers.* Colloids Surf B, 2014. **116**(0): p. 63-71.
20. J.J. Stalgren, P.M. Claesson and T. Warnheim, *Adsorption of liposomes and emulsions studied with a quartz crystal microbalance.* Adv Colloid Interface Sci, 2001. **89-90**: p. 383-94.
21. B. Seantier, C. Breffa, O. Felix and G. Decher, *Dissipation-enhanced quartz crystal microbalance studies on the experimental parameters controlling the*

formation of supported lipid bilayers. J Phys Chem B, 2005. **109**(46): p. 21755-65.

22. T. Viitala, J.T. Hautala, J. Vuorinen and S.K. Wiedmer, *Structure of anionic phospholipid coatings on silica by dissipative quartz crystal microbalance.* Langmuir, 2007. **23**(2): p. 609-18.
23. R.P. Richter and A.R. Brisson, *Following the formation of supported lipid bilayers on mica: a study combining AFM, QCM-D, and ellipsometry.* Biophys J, 2005. **88**(5): p. 3422-33.
24. C.A. Keller, K. Glasmastar, V.P. Zhdanov and B. Kasemo, *Formation of supported membranes from vesicles.* Phys Rev Lett, 2000. **84**(23): p. 5443-6.
25. J.G. Paiva, P. Paradiso, A.P. Serro, A. Fernandes and B. Saramago, *Interaction of local and general anaesthetics with liposomal membrane models: a QCM-D and DSC study.* Colloids Surf B Biointerfaces, 2012. **95**: p. 65-74.

6 Production of antibiotic loaded nanoparticles using supercritical fluid technology

The following results were partly published in the peer-reviewed international Microscopy and Microanalysis. August 2013. 19 (4): 151-152.
doi:10.1017/S1431927613001372.

Table of contents

6.1 Introduction

During the past few decades, an important effort has been done in the research of drug delivery using nanoparticles as carriers for drug molecules [1]. Particulate systems like nanoparticles have been used as a physical approach to alter and improve the pharmaco-kinetic and pharmaco-dynamic properties of various types of drug molecules [2]. In section 1.4.4, several attempts to develop new ocular drug delivery systems by implementing nanoparticles in soft contact lenses were described. Advances in nanotechnology associated to noninvasive drug delivery techniques have been in the forefront of new ophthalmic drug delivery systems.

In the present chapter an investigation on the production of nano-composite particles containing levofloxacin (LVF), through super critical fluids (SCFs), is presented. Two excipients have been tested: chitosan and hydroxypropyl methylcellulose phthalate polymer. The experiments here presented were performed at the IST, under the supervision of Professor Miguel Rodrigues.

Chitosan is a linear polysaccharide which, thanks to its biological properties such as biocompatibility, antimicrobial activity, biodegradability, as well as mucoadhesion, anticholesterolemic, and permeation enhancement effects, has been widely used in specific applications such as antibacterial/anti-biofouling coatings and drug delivery systems.

Hydroxypropyl methylcellulose phthalate (HPMCP) was originally developed and used by the pharmaceutical industry as an enteric coating agent, for tablets and granules. Its favorable properties have led to the extension of the range of its applications into other fields, including sustained release preparations, binders and microcapsule bases, as an alternative to gelatin [3].

The feasibility of the nanoparticles for application in the ophthalmological field was tested, with the final aim of an eventual incorporation of the particles in soft contact lenses.

For the application in contact lenses, particles must comply with several constraints, such as: be biocompatible, retain the drug activity along the fabrication process, be in

the nanometer size range (<415 nm [4]) and present a compatible drug release kinetics to the purpose.

The influence of different working parameters, namely, working pressure, drug concentration and total concentration of excipient + drug in the liquid processing solution, on the characteristics of the particles was studied. The morphology of the nanoparticles was characterized by scanning electron microscope (SEM) and the size dispersion analysis was obtained with a zetasizer, The anti-microbial activity of LVF, before and after being processed by SCFs, was tested through microbiological tests. Finally, *in vitro* release studies were performed in order to obtain the drug release profiles and verify if the particles produced have interest from a therapeutic point of view.

6.2 Micronization processes with supercritical fluids

In order to better understand the nanoparticles production process here described, an overview on the different types of micronization procedures based on supercritical fluids, will be given.

Micronization through SCFs represents one of the most promising processes of nanoparticles production. The pharmaceutical field has shown a continuously increasing interest in the development of SCF techniques. This is due not only to the need of clean processes, but mostly because micronization through SCFs allows working at lower temperatures with substances with thermal sensitivity, structure instability or bioactivity, such as proteins. Furthermore, this technique avoids the use of organic solvents permitting the direct processing of an aqueous solution into nanoparticles [5], in contrast with conventional techniques for micro/nanoparticles production, namely, spray drying [6], mechanical comminution [7], solute recrystallization [8], coacervation [9], freeze-drying [10], and interfacial polymerization [11].

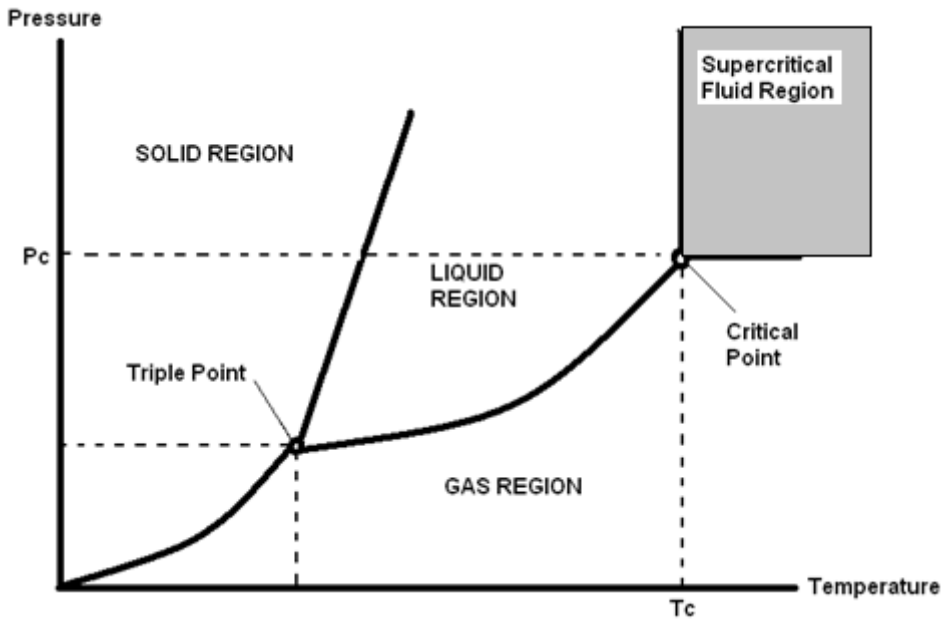

Figure 6.1: Schematic representation of an idealized phase diagram

A fluid over its critical temperature and pressure is defined as supercritical fluid, where distinct liquid and gas phases do not exist (see Figure 6.1). This phase possesses intermediate properties of liquid and gas, for example, it has some solvent power common to liquids and transport properties common to gases, such as high diffusivity, low viscosity and high compressibility. These properties are particularly interesting for micronization as will be described below. The most studied SCF-based micronization techniques are the following:

- the rapid expansion of supercritical solutions [12, 13]
- the supercritical antisolvent precipitation [14, 15]
- the particles generation from gas saturated solutions [16, 17]
- the supercritical fluids assisted atomization [18]
- the supercritical carbon dioxide assisted nebulization [19, 20]

These techniques are based on different principles and use different mechanisms to produce nano and microparticles.

In the rapid expansion of supercritical solutions (RESS) process, SCFs act as solvents in which the solute is dissolved. Solid microparticles are obtained by solute precipitation due to the fast depressurization trough the nozzle.

In supercritical antisolvent (SAS) precipitation process, the solute is dissolved in a liquid solvent, which is then injected into a high pressure vessel containing the SCF; as the liquid solvent and the SCF mix, the drug precipitates as microparticles due to the SCF presence, which acts as antisolvent.

In particles generation from gas saturated solutions (PGSS) the SCF acts as solute which leads to the substantial decrease of the substance melting temperature and viscosity, thus favoring its micronization by atomization.

The supercritical fluids assisted atomization (SAA) process is based on the solubilization of a given percentage of SCF, which acts as co-solute, in a liquid solution where the solute was previously dissolved. The solution is obtained at high pressure assuring a large contact area between liquid solution and SCF. The atomization occurs through the injection of the solution in a nozzle. Microparticles are obtained after the droplets are evaporated using warm nitrogen in co-flux with the solution.

In the supercritical carbon dioxide assisted nebulization with a Bubble Dryer® (CAN-BD), the SCF (CO_2) and the liquid solvent are mixed together into an aerosol by using a near zero volume tee and a capillary injector. The key principle is different from SAA, because the CO_2 is not solubilized in the solution but only contacts the liquid in a near zero volume tee (<1 μL) with a short residence time.

In this study, the particles were produced by super critical fluid enhanced atomization (SEA) which is a compromise between the SAA and the CAN-BD; in fact, the mixing volume between the SCF and the liquid phase is approximately 1 mL, i.e. larger than the one used in CAN-BD and smaller than in SAA.

A spray-drying setup was assembled with a coaxial SEA nozzle to enhance the atomization with a SCF (N_2). This process consists essentially in mixing the SCF with the liquid phase, and depressurizing the mixture though a nozzle with a small orifice. The significant pressure drop, together with the burst of the dissolved gas, causes the

formation of microdroplets and microbubbles that, on solidifying, creates the nanoparticles.

6.3 Experimental part

6.3.1 Materials

Chitosan of low molecular weight, 390 kDa with deacetylation degree of 88%, was gently provided by Altakitin. Glacial acetic acid was obtained from Pronalab; Hypromellose phthalate grade 50 (HP50), sodium hydroxide ≥97%, levofloxacin 98% (LVF, HPLC grade), trietilamine 99% and orthophosphoric acid 85% were supplied by Sigma Aldrich; acetonitrile (HPLC grade) from Fisher Scientific. Sodium chloride was obtained from Merck KGaA and Muller Hinton broth solution from Becton, Dickinson and Company.Nitrogen gas 99% pure was supplied by Air Liquide (Portugal). The deionized water was obtained from Millipore Milli-Q water purification system.

6.3.2 Nanoparticles production

The laboratory apparatus used for SEA is represented schematically in Figure 6.2.

The liquid solution was pumped by a LKB metering pump (model 2150) into the SEA nozzle where it was mixed with the SCF N_2. The SCF was compressed by the Newport compressor (model 46-13421-2). The nozzle flow (20 mg/min) was measured by a mass flowmeter (Rheonik, model RHM007).

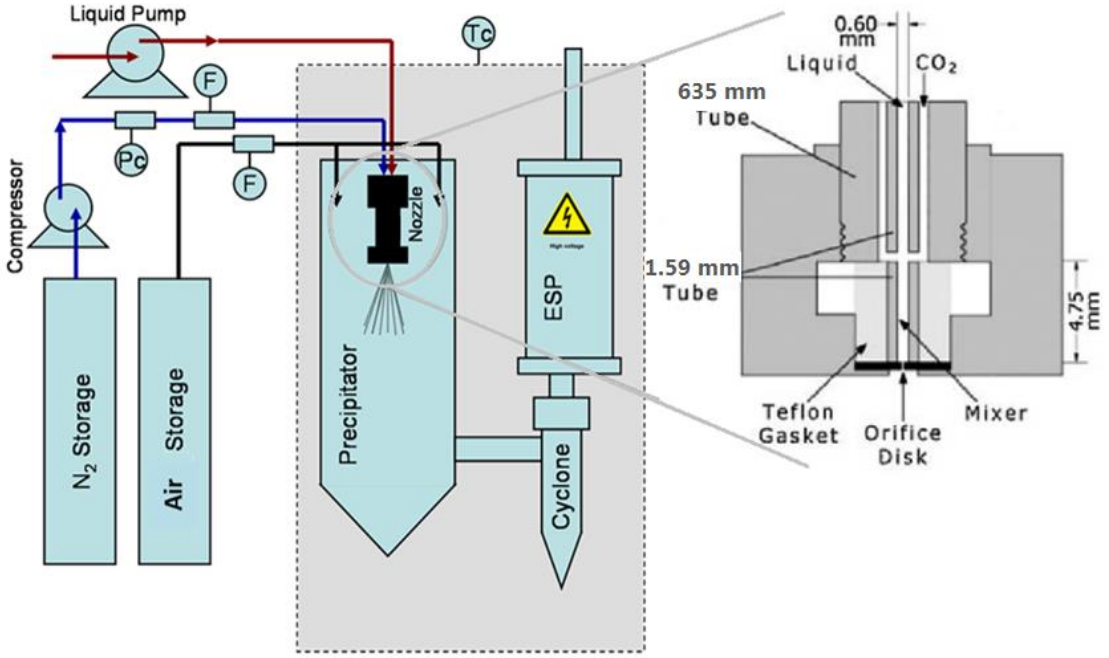

Figure 6.2 Schematic representation of the SEA experimental setup- Flow indicator (F) and temperature (TC) and pressure (PC) controller, are shown. In detail the nozzle cap.

Pressures were measured by Omega transducers (model PX603) and T-type thermocouples and Ero Electronic controllers (model LDS) were used to control the temperatures in the air chamber and in the water bath. The temperature of the nozzle was set to 50°C.

The nozzle cap, provided by Lenox Laser, presented a disk (250 µm thickness) with an orifice with a diameter of 150 µm (laser drilled).

The particles were collected in a Buchi cyclone located into an electrostatic precipitator (ESP) assembled in a single-stage tubular configuration and powered by an EMCO DX high voltage with 10 kV to 15 kV.

The optimal conditions for generating nanoparticles using the described set-up were addressed in a previous work [21]. Based on this work, 2 and 8 MPa were selected as atomization pressures and the drying temperature was set at 50 °C. All runs were carried out under a liquid flow rate of 1 mL/min.

Two different excipients have been chosen for the nanoparticles production: chitosan (CH) and HP50. Chitosan was dissolved in a solution 1% w/w acid acetic and 10% w/w LVF obtaining a total final concentration of excipient and drug equal to 10 mg/mL. The atomization pressure used for this run was 8 MPa. HP50 was dissolved in a solution containing 0.2 M of sodium hydroxide. In the case of HP50 different variables were tested, namely: working pressure, drug concentration, and final solute concentrations. The working conditions tested in HP50 particles production are shown in Table 6.1.

Table 6.1 Working condition tested in HP50 particles production.

	Pressure (MPa)	% Levofloxacin	Concentration of HP50+LVF (mg/mL)
SEA 1	8	10	5
SEA 2	2	2	5
SEA 3	2	10	5
SEA 4	2	20	5
SEA 5	2	2	10
SEA 6	2	10	10
SEA 7	2	2	20

6.3.3 Determination of the antimicrobial activity of the drugs

To assess the effect of the SEA processing on the activity of the drug, microbiological tests were carried out on processed, pure LVF. The growth inhibition halos of *S. aureus* and *P. aeruginosa* produced by the processed drug were compared with those of freshly prepared drug solutions with the same drug concentration. The concentration of the solutions was determined by HPLC.

To process the drug, a solution of 10 mg/mL of LVF in 50/50 v/v water and ethanol was prepared and subsequently processed through SEA at a pressure of 8 MPa with a flow rate of 1 mL/min.

For the microbiological tests, cultures of both microorganisms were inoculated and a solution with final optical bacterial density of 1 McFarland was prepared by dilution with distilled and sterilized water. A volume of 350 μL of this suspension was added to 50 mL of Muller Hinton broth solution. The inoculated medium was poured into round plates and allowed to solidify. Paper discs were located onto the solidified medium and were impregnated with 15 μL of LVF solution (125 mg/mL), prepared with the processed drug. For control, paper disks were impregnated with 15 μL of drug solution (same concentration) prepared with non-processed drug. The dimensions of the halos were measured with an electronic caliper, after overnight incubation at 37 °C. The assays were repeated twice in triplicate.

6.3.4 Nanoparticles characterization

The morphology of the nanoparticles was observed using a scanning electron microscope (SEM) Hitachi S2400 (15 KeV). Prior to the SEM analysis the particles were coated with a thin film of gold (thickness 30 nm). Particle size and the respective zeta potential were also determined using a Zetasizer (Nano ZS, Malvern Instruments, Malvern, UK).

6.3.5 Drug release tests

Drug release experiments were performed using a standard Dissolution Tester DT 620, from Erweka (Figure 6.3). The dissolution tester vessels were filled with 500 mL of saline solution (NaCl, 130 mM). The experimental temperature was set to 34^0C, with a continuous agitation of 50 rpm.

Figure 6.3 Picture of Dissolution Tester DT 620.

The nanoparticles were loaded in soluble gelatin pharmaceutical capsules (25 mg of NPs in each capsule). A stainless steel weight was attached on the outside of each capsule to ensure their immersion into the vessels. The drug release experiment started with the drop of one capsule into each vessel. After the dissolution of the capsules, which took around 10minutes, one capsule each vessel the drug release of the particles took place. At pre-determined time intervals, namely every 10 minutes within the first hour, and then every hour along 8 hours, 1 mL aliquots of the supernatant were collected and analysed.

The quantification of the LVF released in the collected samples, was done by high performance liquid chromatography (HPLC) using a column C18 Waters Nova-Pak, at λ=290nm and using as mobile phase water, acetonitrile, phosphoric acid and trietilamine (86:14:0,65:0,3 (v/v/v/v)).

6.4 Results and discussion

6.4.1 Antimicrobial resistance test

Figure 6.4 shows the final product of the LVF solution processed by SEA. Nanocrystals of LVF were obtained with a wide size distribution.

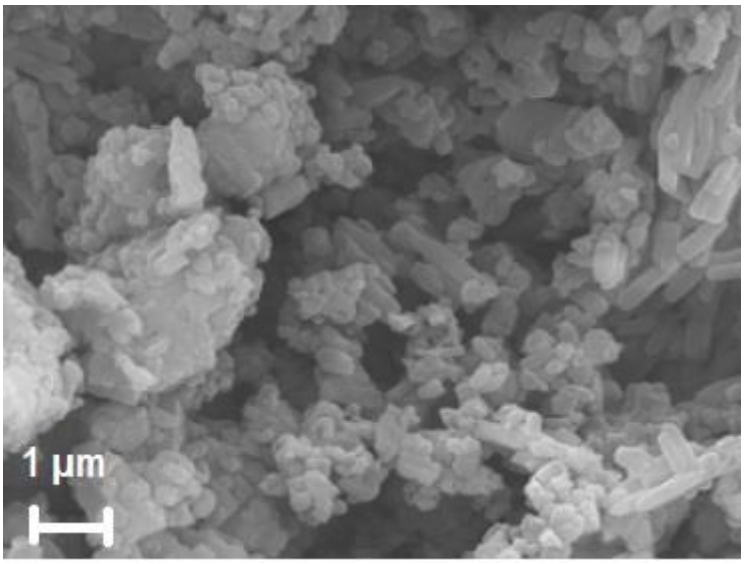

Figure 6.4 Levofloxacin nanocrystals obtained through SEA process.

The microbiological tests showed that LVF antimicrobial activity is not affected by the SEA process. After 24 hours of incubation no significant difference were registered between the inhibition halos of the discs impregnated with the processed and not processed drug.

6.4.2 Nanoparticle characterization

Figures 6.5 and Figures 6.6 to 6.12 are SEM images of chitosan and HP50 nanoparticles.

The chitosan particles, containing 10% of LVF and processed at 8 MPa, are presented in Figure 6.5. The dimensions of the particles, in the range of 1-10 µm are too big for the purpose of incorporation in contact lenses. As mentioned in section 1.4.4, to ensure hydrogel transparency the particles dimension should be smaller than 415 nm [4] and should be homogeneously distributed into the matrix. For this reason the system chitosan/levofloxacin was abandoned.

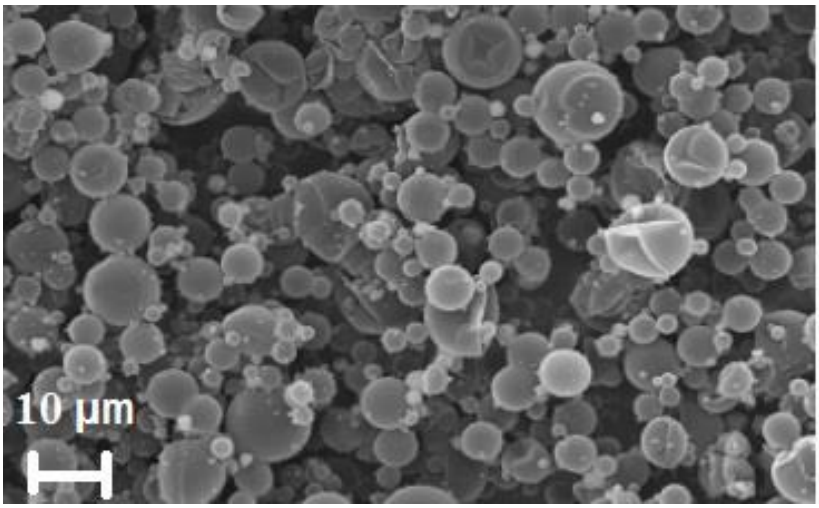

Figure 6.5 SEM image of chitosan particles processed at 8 MPa, containing 10% of LVF, and with a total solute concentration of 10 mg/mL.

Figure 6.6 presents the SEM image of the NPs production SEA 1, processed at 8 MPa, containing 10% of LVF, and with a total solute concentration of 5 mg/mL. All the particles obtained through the SEA process presented an approximately spherical shape. It can be observed that the high pressure causes the atomization of bigger particles, and the presence of capsules (hollow particles) and collapsed structuresindicated through A, B and C in the figure**.**

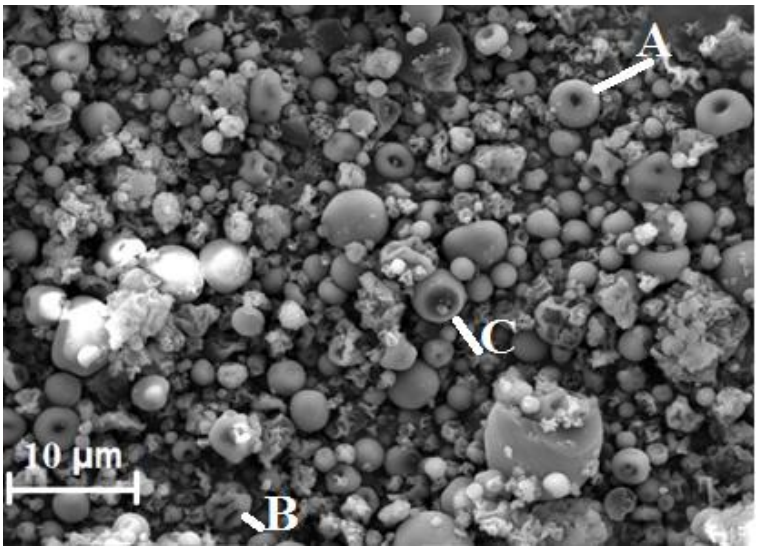

Figure 6.6: SEM image of SEA 1 HP50 particles, processed at 8 MPa, containing 10% of LVF and with a total solutes concentration of 5 mg/mL.

Figure 6.7 to Figure 6.9, represent the morphology of the three sets of particles processed at 2 MPa, with a total solute concentration of 5 mg/mL, and a LVF concentration, respectively, of 2%, 10% and 20%. The comparison of these figures does not permit any conclusions on the effect on the morphology of the percentage of LVF in the particles. The three sets of particles present a wide range of size distribution; with diameters ranging from hundreds of nm to several μm. SEA 3 presents a higher proportion of particles in the submicrometer scale.

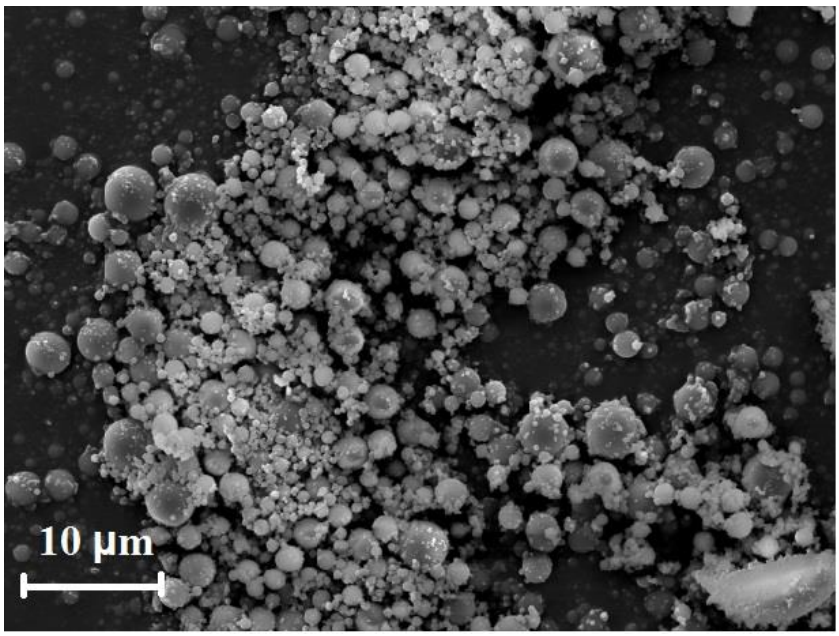

Figure 6.7: SEM image of HP50 particles, SEA 2, processed at 2 MPa, containing 2% of LVF, and with a total solute concentration of 5 mg/mL.

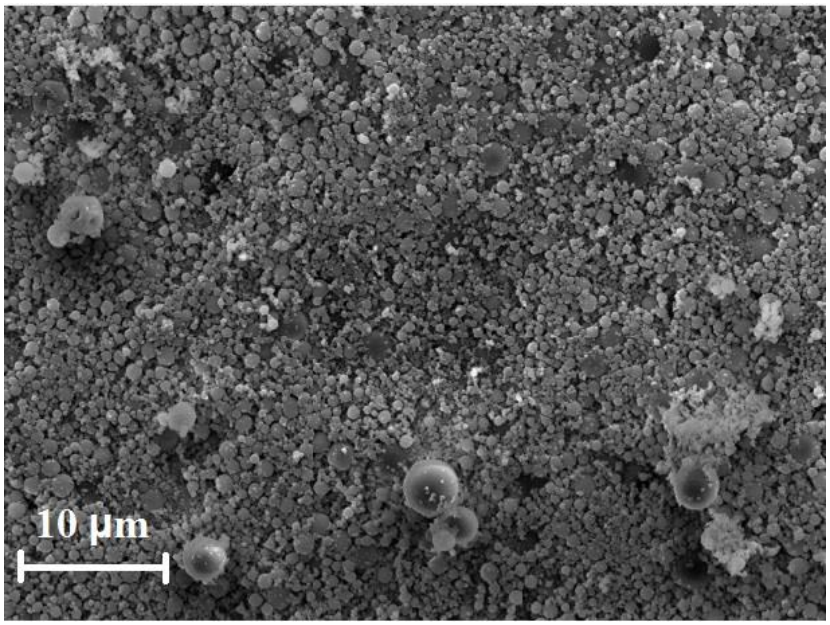

Figure 6.8 SEM image of HP50 particles, SEA 3, processed at 2 MPa, containing 10% of LVF, and with a total solute concentration of 5 mg/mL.

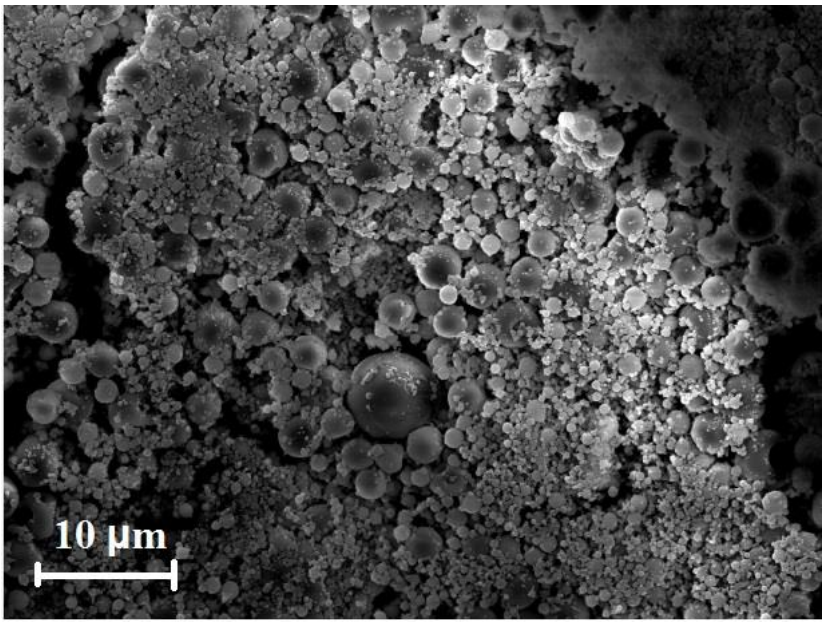

Figure 6.9 SEM image of HP50 particles, SEA 4, processed at 2 MPa, containing 20% of LVF, and with a total solute concentration of 5 mg/mL.

Figure 6.10 and Figure 6.11 show the morphology of SEA 5 and SEA 6 particles, characterized by 10 mg/mL total solute concentration. Comparing Figure 6.10 with Figure 6.7 and Figure 6.11 with Figure 6.8 shows that increasing the total concentration of the solutes in the solution, the dimension of the particles increases as well as the polydispersivity, and capsule like particles (hollows particles) start to appear. Figure 6.12 presents the morphology of SEA 7 produced with 20 mg/mL of solutes, but no further change in the morphology is noticed.

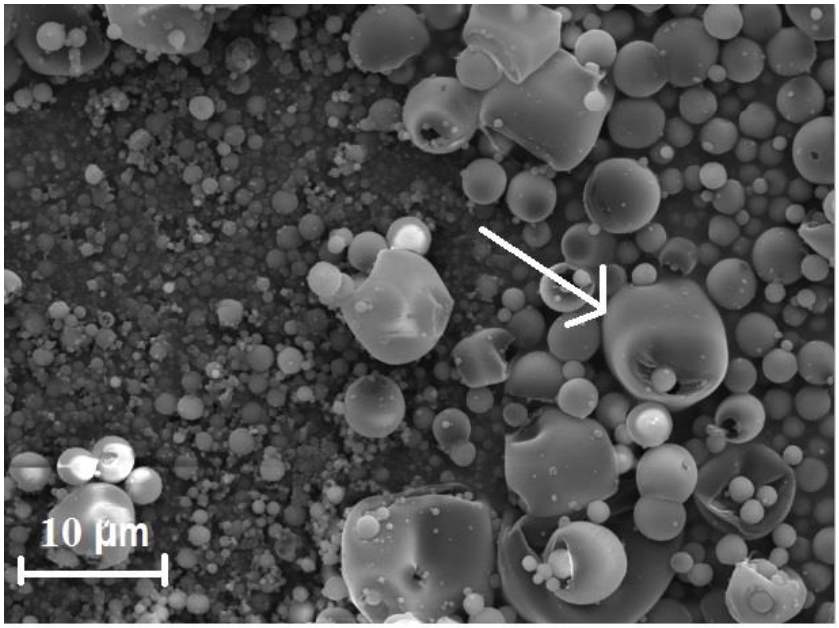

Figure 6.10 SEM image of HP50 particles, SEA 5, processed at 2 MPa, containing 2% of LVF, and with a total solute concentration of 10 mg/mL. The arrow indicates a capsule like structure.

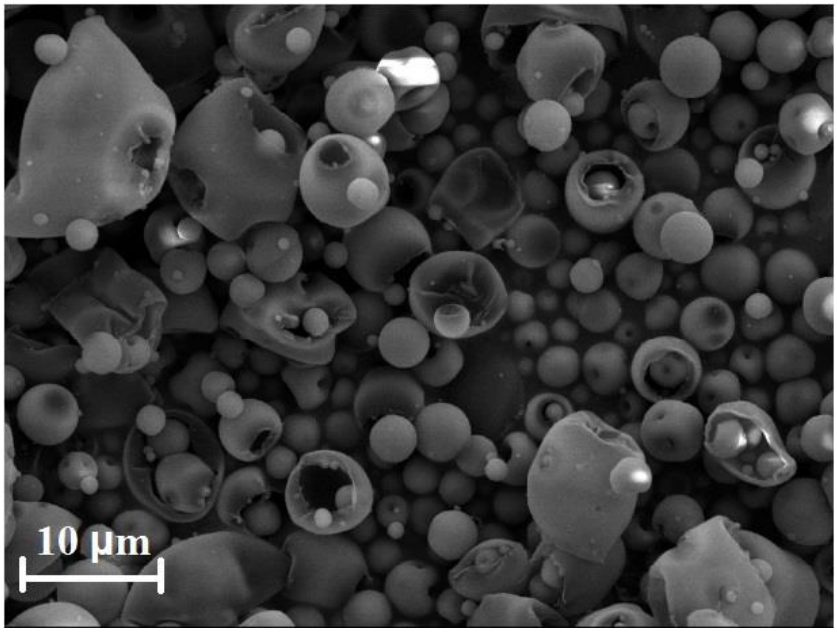

Figure 6.11 SEM image of HP50 particles, SEA 6, processed at 2 MPa, containing 10% of LVF, and with a total solute concentration of 10 mg/mL.

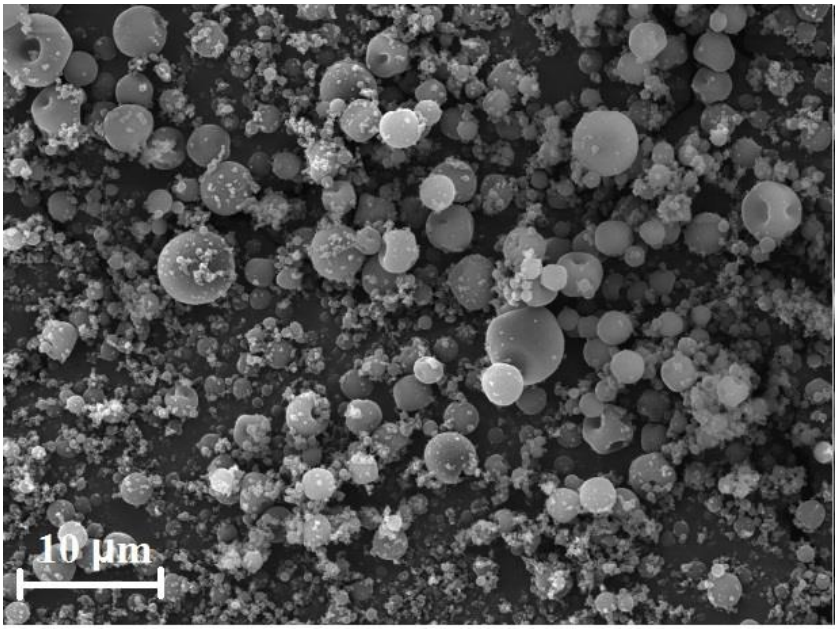

Figure 6.12 SEM image of HP50 particles, SEA 7, processed at 2 MPa, containing 2% of LVF, and with a total solute concentration of 20 mg/mL.

As an example, the zetasizer analysis was performed on the SEA 3 set of particles.

The results confirmed the wide dispersion of the particles size evidenced by the SEM image. The main intensity peak is located around 300 nm (Figures 6.13).

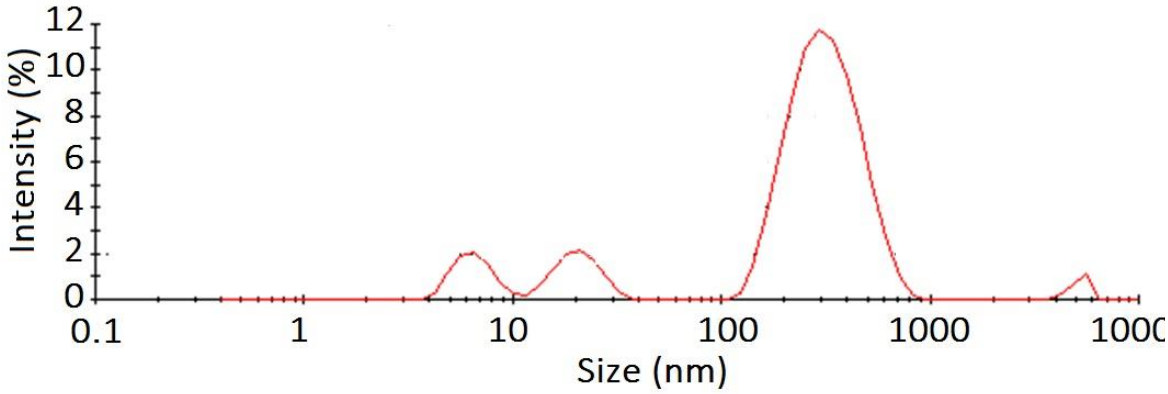

Figure 6.13: Size dispersion spectrum of SEA 3, obtained by Zetasizer.

Zeta potential measurements gave a slightly negative potential, -10 mV. Particles characterized by zeta potential values outside the limits ±30 mV (more positive than 30 mV and more negative than -30 mV) are considered stable [22]. For this reason, the obtained HP50 particles will have the tendency to flocculate or aggregate, since their zeta potential is too low and the attraction forces prevail on the repulsion forces. The aggregation could eventually be solved by a stabilizer, such as glucose [10].

Although, a significant fraction of the produced HP50 nanoparticles has not adequate size for incorporation in contact lenses, we decided to go on with the drug release studies because future optimization of the processing parameters may yield smaller nanoparticles.

6.4.3 Drug Release

Figure 6.14 reports the release curves of SEA 2, SEA 5 and SEA 7, and allows to evaluate the effect of the total solute concentration. The released amounts are presented in the form of percentages, assuming that the proportion of drug contained in the particles is the same as that used in the solutions used in their preparation. This means

that the total amount of LVF contained in the particles referred in Figure 6.14 (100%) corresponds to 2% of their mass. It can be observed that increasing the total solutes concentration of the initial solution, the time for total release decreases. The set SEA 7 (C= 20 mg/mL) releases 100% of the drug in less than 15 minutes, while the set SEA 2 (C= 5 mg/mL) reaches its plateau in a little more than 1 hour.

SEA 2 and SEA 5 do not reach 100% of drug released, as SEA 7. This could be justified by the fact that, since the concentration is higher in the case of SEA 7, the kinetics of precipitation during the atomization will increase, and this may lead to a more amorphous structure with a consequent enhanced solubility [23].

Figure 6.15 reports the effect of the percentage of LVF in the particle composition on the drug release profiles. Increasing the drug percentage of the particles, the retention time decreases: the set SEA 4 (20% of LVF) reaches the plateau after 30 minutes, against ≈ 60 minutes taken by the set of particles containing 2% and 10% of LVF. An explanation can be the access of water to inner regions of the particles: it shall increase with the increase of the drug composition of the particle. Being LVF highly soluble in water, its presence in the particles is translated as particle porosity and, consequently, implies a higher release rate.

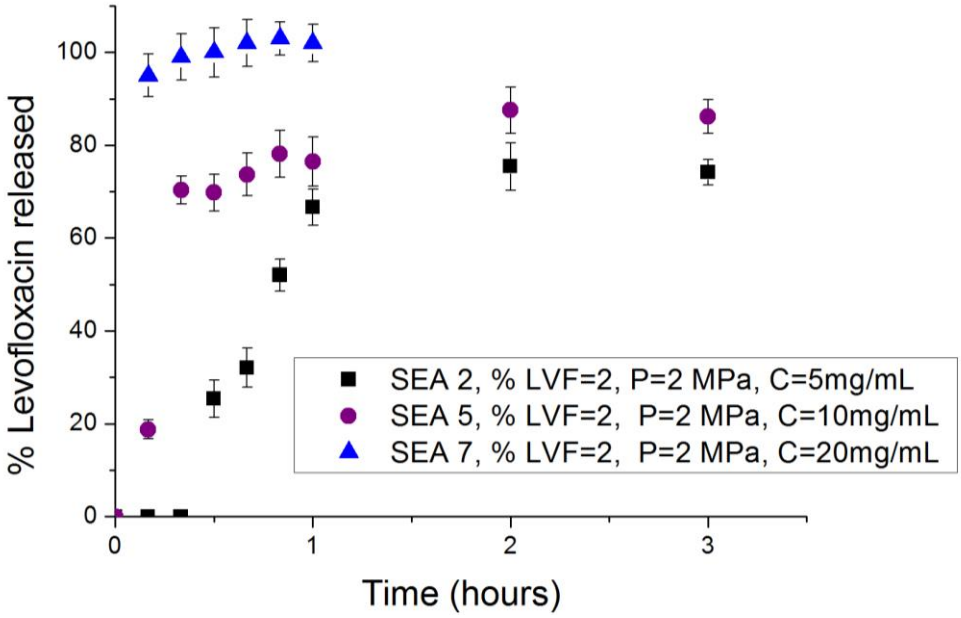

Figure 6.14 Solutes concentration effect on the drug release kinetics: profiles of percentage of levofloxacin released from HP50 NPs, sets SEA 2, SEA 5 and SEA 7.

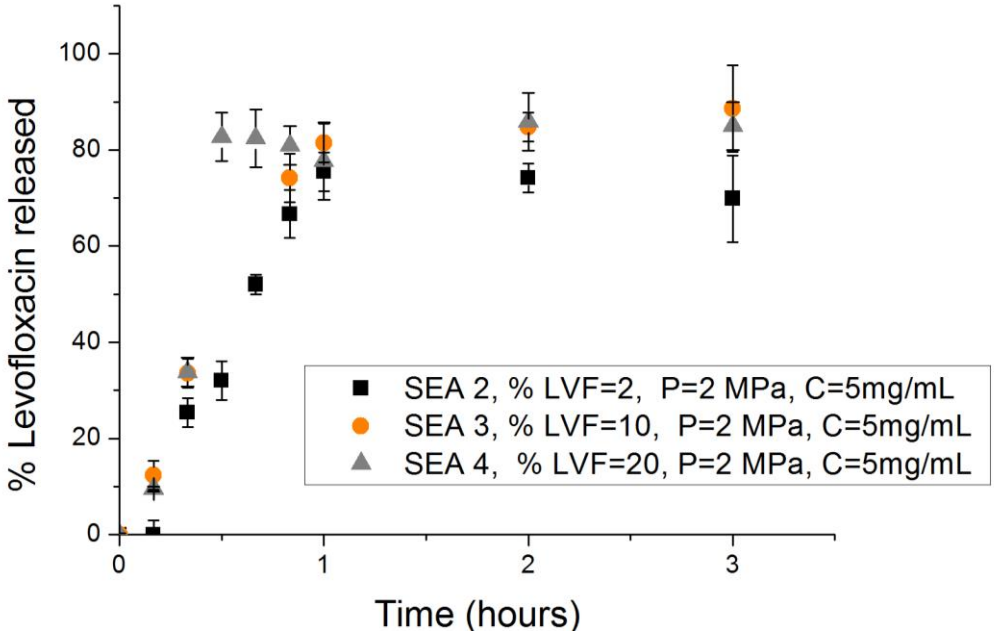

Figure 6.15 Levofloxacin % effect on the drug release kinetics: profiles of percentage of levofloxacin released from HP50 NPS, sets SEA 2, SEA 3 and SEA 4.

Figure 6.16 reports the effect of the working pressure during the NPs production process. There is a slightly decrease in the release rate in the case of the SEA 3

produced under a working pressure of 2 MPa, compared to SEA 1, produced under a working pressure of 8 MPa.

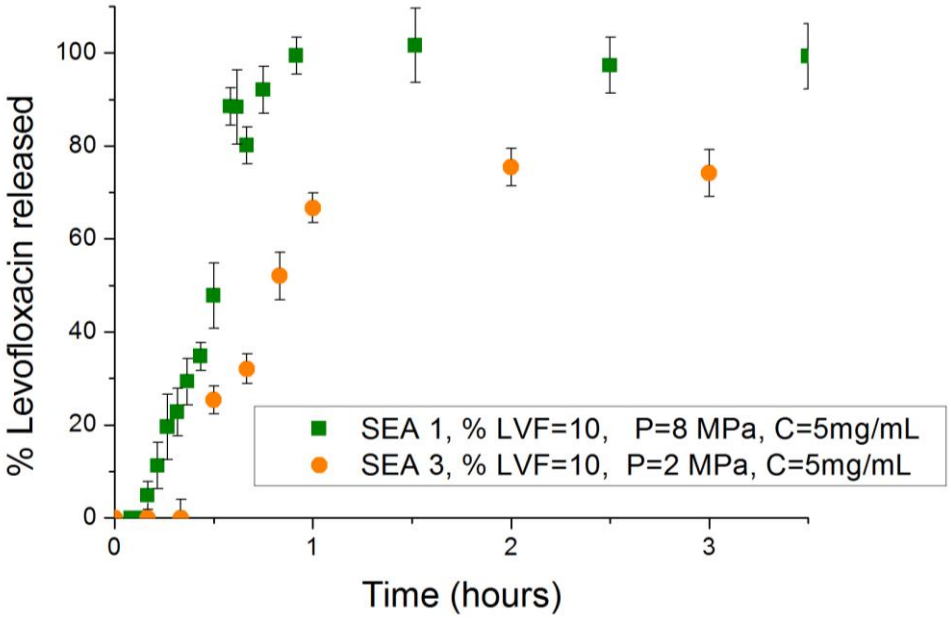

Figure 6.16 Working pressure effect on the drug release kinetics: profiles of percentage of levofloxacin released from HP50 NPS, sets SEA 1 and SEA 3.

Figure 6.17 reports the LVF release rate values obtained from the derivative of the initial linear sections of the cumulative drug release curves represented in absolute terms (mass/time) and normalized to mg of NPs. By comparison of the release rates, it is concluded that the most influencing parameter on drug release kinetics is the percentage of drug encapsulated in the particles. Namely, with the increase of the percentage of drug encapsulated in the particles the release rate increases. The working pressure and the total concentration have a smaller impact on the drug release kinetics of the particles.

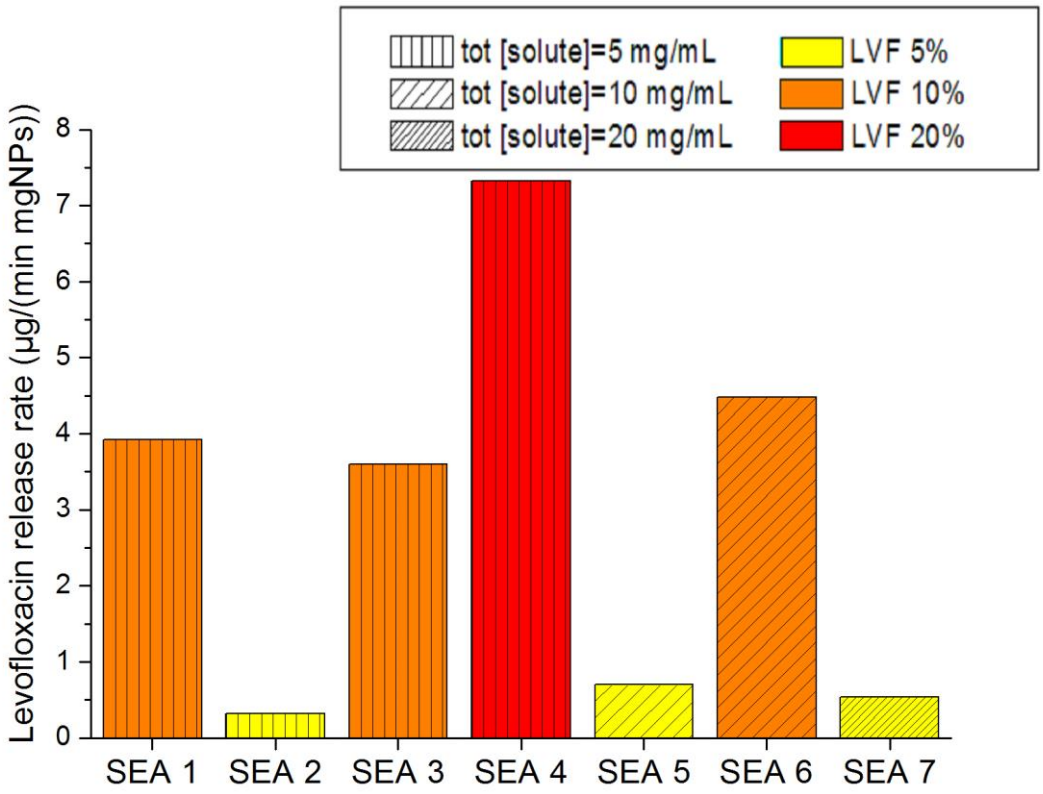

Figure 6.17: Levofloxacin release rate values in the initial period of the drug release. The legend describes the code used to identify the parameters total solutes concentration and LVF percentage. Every set of particles was processed under a working pressure of 2 MPa, except SEA 1, which was processed under 8 MPa.

It should be stressed that although the drug release profiles represented in relative terms (% levofloxacin released) may be similar, in absolute terms (mass levofloxacin released) they may be significantly different. See, for example, the case of the sets SEA 2 and SEA 3 in Figure 6.15 and Figure 6.18.

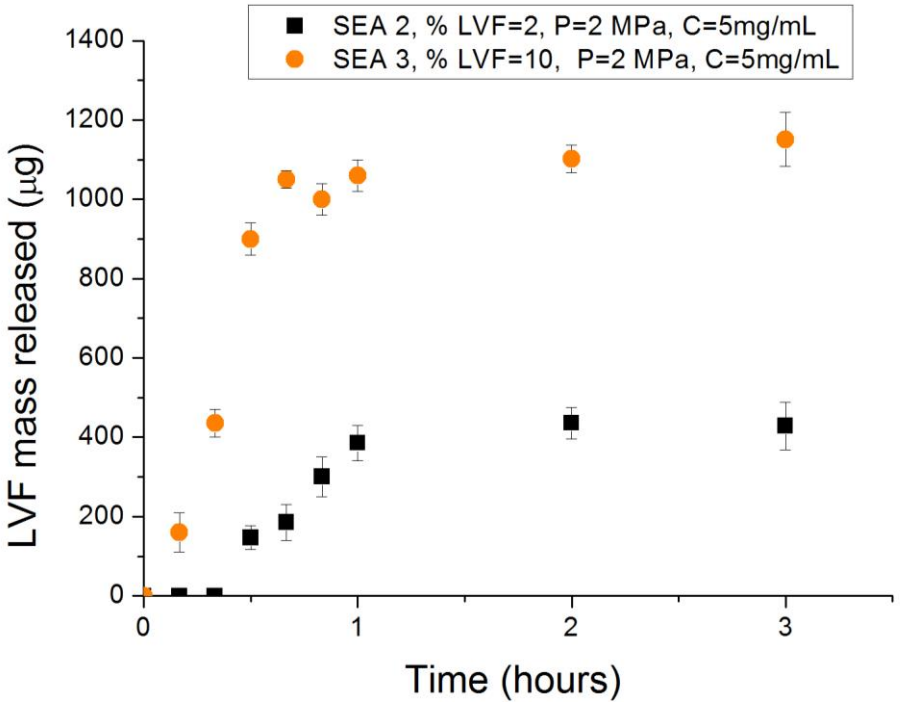

Figure 6.18 Cumulative release curve of LVF mass from HP50 NPs, sets SEA 2 and SEA 3.

6.4.4 Estimation of the *in vivo* efficacy of the studied systems

In order to investigate the therapeutic interest of the obtained particles, the simplified mathematical model, proposed in Chapter 2, section 2.3.6, will be applied, in order to anticipate the LVF concentration in the tear fluid obtained by the drug loaded particles.

The mathematical model takes into account the eye hydrodynamics: assuming a renewal rate of the lachrymal fluid of 3 μL/min, and a total tear volume in the eye (V_t) of ≈7 μL at each instant [24, 25], the volume fraction of renovated fluid in each minute, R_r, corresponds to 0.43. Thus, the drug concentration in the lachrymal fluid at a given time, t, (in minutes) may be estimated from:

$$[Drug]_t = \frac{M_t}{V_t} + (1 - R_r)[Drug]_{t-1} \qquad \textbf{Equation 6.1}$$

where M_t is the amount of drug delivered at each minute.

For this analysis two sets of particles, SEA 2 (2% of LVF) and SEA 3 (10% of LVF), were selected. This choice was due to the fact that both sets are characterized by a release duration of 1 hour, and their respective release rates values are very different between themselves, namely 0.32 µg/(min.mg NPs) for SEA 2 and 3.6 µg/(min.mg NPs) for SEA 3.

In Figure 6.19 the expected concentration curves of LVF in the tear liquid are shown, considering different amount of particles, namely: 700 µg and 250 µg in the case of SEA 2 and 35 µg and 60 µg in the case of SEA 3. These amounts were chosen to be above the minimum inhibitory concentrations of *P. aeruginosa* and of *S. Aureus*, respectively (also represented in the figure).

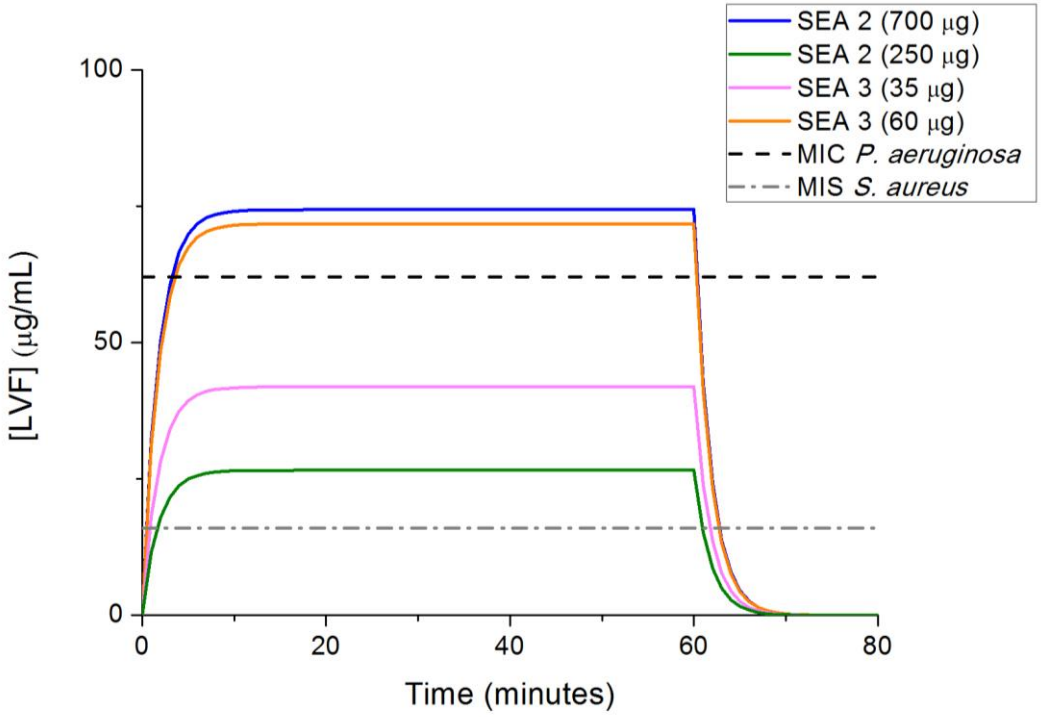

Figure 6.19: Estimated levofloxacin concentration in tear fluid for different amounts of particles–. SEA 2=2%LVF, SEA3=10%LVF

From the obtained values, we infer that in order to maintain the antibiotic concentrations above the determined minimum inhibitory concentrations of *S. aureus* and *P. aeuriginosa*, simultaneously, for one hour, it would be necessary 60 µg of SEA 3 (10% of LVF) or 700 µg of SEA 2 (2%).

Even though the mass of particles in the case of SEA 3 is reasonable and could be entrapped in a contact lens (see Figure 6.20 as an indication of amount of NPs), the release duration of one hour is far below the desired release duration of a daily contact lens. However, the curves presented in Figure 6.18 do not take into account the diffusion barrier that the SCL would represent for the LVF embedded in the particles. The hydrogel will slow down the release kinetics of the drug. Thus, in order to cover in an efficient way an entire day of therapy the lens should be loaded with an higher amount of drug loaded NPs.

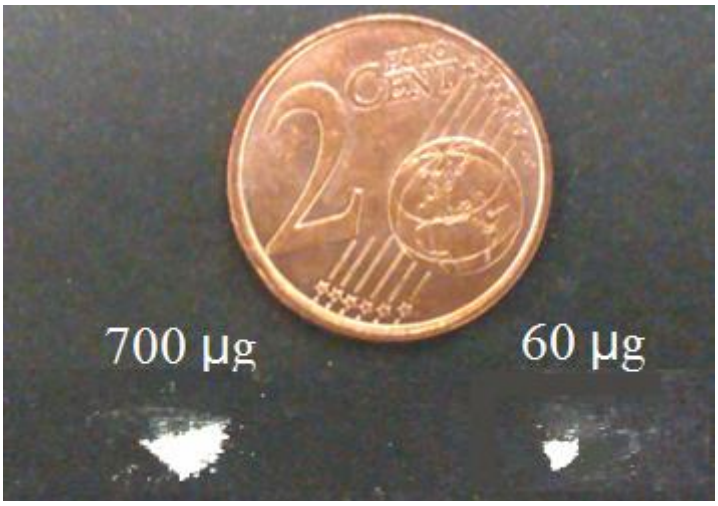

Figure 6.20: Picture of the amounts of particles of SEA 2 and SEA 3, respectively 700 µg and 60 µg, compared with a coin.

6.5 Conclusions

The purpose of this work was to produce drug loaded nanoparticles for incorporation in therapeutic SCLs. SCF technology was tested to produce LVF loaded nanoparticles. Different excipients (chitosan and HP50) and working parameters (working pressure, percentage of drug and solutes concentrations) were tested.

Although the antimicrobial activity of LVF was maintained after the process, chitosan particles presented dimensions in the range of 1-10 µm, too big for the purpose of the

study. HP50 particles presented smaller dimensions, with a wide size dispersion and a low zeta potential. The low zeta potential suggests that the particles could have problems of aggregation

Release tests were performed on seven sets of HP50 particles. The release studies of HP50 particles show in most cases a linear and controlled drug release along 1 hour.

The influence of the different working parameters on the kinetics of release was also studied. It was concluded that the drug percentage in the particles represented the most influencing factor on the release rate, namely the release rates increase with the increase of the drug percentage. However, even for the lowest drug content, the drug release was fast (~1 hour).

A simplified mathematical model was applied to predict the drug concentrations in the eye resultant of the drug release from two sets of HP50 particles. However, the performed analysis does not take into account the retarding effect that the incorporation of the particles in the hydrogels should have on the drug release. It is foreseeable that the amount of particles which should be incorporated in a SCL to efficiently cover one day of therapy for ocular keratitis should be significantly higher than that estimated here (without incorporation)..

Future perspectives may include further investigation on the working parameters and/or different excipient materials, in order to obtain nanoparticles of adequate size and zeta potential with higher drug content. Once these nanoparticles are obtained, incorporation into an hydrogel material should be made to study the influence of the hydrogel matrix on the overall release kinetics.

6.6 References

1. L. Zhang, F.X. Gu, J.M. Chan, A.Z. Wang, R.S. Langer and O.C. Farokhzad, *Nanoparticles in medicine: therapeutic applications and developments.* Clin Pharmacol Ther, 2008. **83**(5): p. 761-9.
2. W.H. De Jong and P.J.A. Borm, *Drug delivery and nanoparticles: Applications and hazards.* Int J Nanomedicine, 2008. **3**(2): p. 133-49.
3. T. Ogura, Y. Furuya and S. Matsuura, *HPMC capsules: an alternative to gelatin.* Pharm Technol Europe, 1998. **10**: p. 32-42.
4. N. Vogel, R.A. Belisle, B. Hatton, T.-S. Wong and J. Aizenberg, *Transparency and damage tolerance of patternable omniphobic lubricated surfaces based on inverse colloidal monolayers.* Nat Commun, 2013. **4**.
5. M.A. Rodrigues, L. Figueiredo, L. Padrela, A. Cadete, J. Tiago, H.A. Matos, E. Gomes de Azevedo, H.F. Florindo, L.M. Goncalves and A.J. Almeida, *Development of a novel mucosal vaccine against strangles by supercritical enhanced atomization spray-drying of Streptococcus equi extracts and evaluation in a mouse model.* Eur J Pharm Biopharm, 2012. **82**(2): p. 392-400.
6. R. Vehring, W.R. Foss and D. Lechuga-Ballesteros, *Particle formation in spray drying.* J Aerosol Sci, 2007. **38**(7): p. 728-746.
7. N. Monzawa and K. Otsuki, *Comminution and fluidization of granular fault materials: implications for fault slip behavior.* Tectonophysics, 2003. **367**(1–2): p. 127-143.
8. B. Subramaniam, S. Saim, R.A. Rajewski and V. Stella, *Methods for particle micronization and nanonization by recrystallization from organic solutions sprayed into a compressed antisolvent*. 1999, Google Patents.
9. C. Yan and W. Zhang, *Chapter 12 - Coacervation Processes,* in *Microencapsulation in the Food Industry*, A.G. Gaonkar, et al., Editors. 2014, Academic Press: San Diego. p. 125-137.
10. W. Abdelwahed, G. Degobert, S. Stainmesse and H. Fessi, *Freeze-drying of nanoparticles: Formulation, process and storage considerations.* Adv Drug Deliv Rev, 2006. **58**(15): p. 1688-1713.

11. A.V. Berezkin and Y.V. Kudryavtsev, *Linear interfacial polymerization: theory and simulations with dissipative particle dynamics.* J Chem Phys, 2014. **141**(19): p. 194906.
12. D.W. Matson, J.L. Fulton, R.C. Petersen and R.D. Smith, *Rapid expansion of supercritical fluid solutions: solute formation of powders, thin films, and fibers.* Ind Eng Chem Res, 1987. **26**(11): p. 2298-2306.
13. E. Reverchon, G. Della Porta, R. Taddeo, P. Pallado and A. Stassi, *Solubility and micronization of griseofulvin in supercritical CHF3.* Ind Eng Chem Res, 1995. **34**(11): p. 4087-4091.
14. E. Reverchon and G. Della Porta, *Production of antibiotic micro- and nano-particles by supercritical antisolvent precipitation.* Powder Tech, 1999. **106**: p. 23-29.
15. M. Rehman, B.Y. Shekunov, P. York, D. Lechuga-Ballesteros, D.P. Miller, T. Tan and P. Colthorpe, *Optimisation of powders for pulmonary delivery using supercritical fluid technology.* Eur J Pharm Sci, 2004. **22**(1): p. 1-17.
16. P. Senčar-Božič, S. Srčič, Z. Knez and J. Kerč, *Improvement of nifedipine dissolution characteristics using supercritical CO2.* Int J Pharm, 1997. **148**(2): p. 123-130.
17. J. Kerč, S. Srčič, Ž. Knez and P. Senčar-Božič, *Micronization of drugs using supercritical carbon dioxide.* Int J Pharm, 1999. **182**(1): p. 33-39.
18. E. Reverchon, *Supercritical assisted atomization to produce micro- and/or nanoparticles of controlled size and distribution.* Ind Eng Chem Res, 2002. **41**: p. 2405-2411.
19. R.E. Sievers, P.D. Milewski, D.P. Sellers, K.D. Kusek, P.G. Kleutz and B.A. Miles, *Supercritical CO2-assisted methods for the production and pulmonary administration of pharmaceuticals aerosol.* J Aerosol Sci. **29**(1): p. 1271-1272.
20. S.P. Sellers, G.S. Clark, R.E. Sievers and J.F. Carpenter, *Dry powders of stable protein formulation from aqueous solutions prepared using supercritical CO2-assisted atomization.* J Pharm Sci, 2001. **90**: p. 785-797.
21. L. Padrela, M.A. Rodrigues, S.R. Velaga, H.A. Matos and E.G. de Azevedo, *Formation of indomethacin-saccharin cocrystals using supercritical fluid technology.* Eur J Pharm Sci, 2009. **38**(1): p. 9-17.

22. W.K. Mekhamer, *The colloidal stability of raw bentonite deformed mechanically by ultrasound.* J Saudi Chem Soc, 2010. **14**(3): p. 301-306.
23. M. Kakran, N.G. Sahoo, L. Li and Z. Judeh, *Dissolution of artemisinin/polymer composite nanoparticles fabricated by evaporative precipitation of nanosuspension.* J Pharm Pharmacol, 2010. **62**(4): p. 413-21.
24. Y. Kapoor, J.C. Thomas, G. Tan, V.T. John and A. Chauhan, *Surfactant-laden soft contact lenses for extended delivery of ophthalmic drugs.* Biomaterials, 2009. **30**(5): p. 867-878.
25. C. White, A. Tieppo and M. Byrne, *Controlled drug release from contact lenses: a comprehensive review from 1965-present.* J Drug Deliv Sci Tec, 2011. **21**(5): p. 369-384.

7. Conclusions and future work

The general aim of this thesis was the investigation of the drug release behaviour of different materials for SCLs (in-house hydrogels and commercial SCLs). Different strategies were attempted to improve the drug release profiles and different conditions of release were tested. An extensive characterization of the systems was carried out in order to evaluate several properties essential for their use in SCLs production. It was conclusively shown the possibility of extended ophthalmic drug delivery by SCL hydrogel materials. For clarity reasons, the conclusions will be divided by chapters.

In chapter 2, two types of hydrogels, a conventional one (HEMA/PVP, 98/2 w/w) and a silicone based (TRIS/NVP/HEMA, 40/40/20 w/w/w) were prepared, characterized and loaded by soaking with CHX and LVF. Both hydrogels revealed adequate properties to be used as ophthalmic materials. Release studies under static sink and dynamic conditions were performed. Although sink conditions are useful for comparative studies, dynamic release method, using a microfluidic device, was confirmed to be a better tool for the prediction of release performance in the human eye. As an alternative, a simplified mathematical model was used to estimate the drug concentration in the tear film, starting from the data obtained under static sink conditions. It was concluded that the best systems, with the better performances in terms of controlled drug release, were HEMA/PVP+LVF and TRIS/NVP/HEMA+CHX. Namely, both systems released the drugs along ten hours in sink conditions, while under microdynamic conditions, the release was prolonged to about 50 hours (in the case of HEMA/PVP+LVF) , thanks to the limited release volumes.

In chapter 3, the effect of nitrogen plasma treatment on the performance of the two drug promising releasing systems, namely HEMA/PVP+LVF and TRIS/NVP/HEMA+CHX were investigated. Under the moderate conditions (200 W and 10 s), plasma may have a beneficial effect on the surface and optical properties of those contact lens materials, making the surfaces more hydrophilic and increasing the refractive index, which may be an advantage allowing for the design of thinner, low-weight lenses. However, it was concluded that plasma treatment is not the ideal strategy to control drug release, in fact, despite the fact that the moderate plasma conditions led to a minimal reduction of the initial release rate, a decrease of the total amount of drug released was verified.

In chapter 4, it was studied the effect of loading vitamin E in commercial silicone contact lenses (ACUVUE® TrueEye and ACUVUE® OASYS), on the release of LVF and CHX.

It was concluded that vitamin E provides an increase in the release duration of both drugs from the studied lenses. Results show that, with about 20% (w) of vitamin E loading, the release times of LVF from ACUVUE® TrueEye™ and from ACUVUE OASYS® exhibit a 3 and 6-fold increase, reaching 100 hours and 75 hours release respectively, while for CHX the increase is 2.5 and 10-fold, to 130 hours and 170 hours, respectively. In particular, it was demonstrated that ACUVUE OASYS® loaded with vitamin E could deliver LVF and maintain its concentrations in the tear film within the desired window for about 3 days, being this the duration of the acute phase of bacterial keratitis.

The last two chapters, 5 and 6, focused on the investigation of the potential of nanostructures to improve drug release performances.

In chapter 5, it was concluded that liposomes-based coatings on HEMA/PVP loaded with LVF presented a heterogeneous appearance and did not improve the kinetics of release, even though they demonstrated to be resistant to eye blink mechanical stress.

In chapter 6, the production of LVF containing nanoparticles by a SCF technique is described and the drug release behaviour of the nanoparticles is characterized. It was concluded that despite the fact that the produced HP50 nanoparticles containing LVF had suitable dimensions for the incorporation in hydrogels for SCLs (<415 nm), the drug release profiles was not promising enough (less than 1 hour) to be considered as an eventual strategy for controlled release. In order to embed nanoparticles inside the hydrogel, further studies should be performed to optimize the nanoparticles size and drug release performance, focusing on improving the drug encapsulation capacity

Although different approaches to improve and control the drug release from SCL materials were faced, there are still many others possibilities to explore. First of all, as we demonstrated, each pair drug/SCL material has a different behaviour, which means that it is not possible to extrapolate the conclusions from one system to the others and that the best solution for one system may not work in a different case.

Inner barriers, such as vitamin E nanoaggregates, revealed to be the most promising strategy found in this work, for this reason more drugs and commercial SCLs should be tested with the incorporation of vitamin E.

Apart of what has already been done, further future perspectives of work are suggested by the author, namely:

- to investigate the drug toxicity risks that could arise due to the small volume of the PoLTF;
- to study the drug degradation during *in vivo* wear (eventual oxidation, drug instability, etc.);
- to assess the effect of SCLs post-production steps (eg. packaging, sterilization, etc.);
- and finally, being the eye a profoundly complex system, it is mandatory to proceed in the future with *in vivo* tests, which would help to fully determine the advantages of therapeutic SCLs for drug release, and to explore their safety and efficacy.

Appendix A

Ophthalmic antibiotics with respective FDA approved indications, adapted from [1,2]

Class	Drug	Manufacturer	FDA-Approved indication(s)
Aminoglycosides	Gentamicin	Generic	Superficial ocular infections involving the conjunctiva or the cornea
	Tobramycin (Tobrex®)	Generic	Superficial ocular infections involving the conjunctiva or the cornea
	Tobramycyn ointment (Tobrex®)	Generic	Treatment of external infections of the eye and its adnexa
Fluoroquinolones	Besifloxacin (Besivance™)	Bausch & Lomb	Bacterial conjunctivitis
	Ciprofloxacin solution (ciloxan®)	Generic	Bacterial conjunctivitis Corneal ulcers
	Ciprofloxacin ointment (ciloxan®)	Alcon	Bacterial conjunctivitis
	Gatifloxacin (Zymar™)	Allergan	Bacterial conjunctivitis
	Levofloxacin 0.5% (Quixin®)	Vistakon	Bacterial conjunctivitis
	Levofloxacin 1.5% (Iquix®)	Vistakon	Corneal ulcers
	Moxifloxacin (Vigamox™)	Alcon	Bacterial conjunctivitis
	Ofloxacin (Ocuflox®)	Generic	Bacterial conjunctivitis Corneal ulcers
Macrolides	Azithromycin (AzaSite™)	Inspire	Bacterial conjunctivitis
	Erythromycin (Romycin®)	Generic	Superficial ocular infections involving the conjunctiva or cornea Forophtalmia neonatorum due to *Chlamydia trachomatis* and prophilaxis of ophtalmia neonatorum due to *Neisseria gonorrhoeae*
Other	Bacitracin	Generic	Superficial ocular infections involving the conjunctiva and the cornea
	Bacitracin/polymyxin B	Generic	Bacterial conjunctivits
	Natamycin (Natacyn®)	Alcon	Fungal blepharitis, conjunctivitis, and keratitis
	Neomycin/Polymyxin B/ Bacitracin	Generic	Bacterial conjunctivitis Superficial ocular infections
	Neomycin/Polymyxin B/Gramidicin (Neosporin®)	Generic	Bacterial conjunctivitis Superficial ocular infections
	Polymyxin B/Trimethoprim (Polytrim®)	Generic	Bacterial conjunctivitis Blepharoconjunctivitis Superficial ocular infections
	Sulfacetamide (Bleph®-10)	Generic	Bacterial conjunctivitis Superficial ocular infections Adjunctive therapy with systemic sulfonamide therapy for trachoma

References

1. *http://www.oregon.gov/oha/pharmacy/therapeutics/docs/ps-2009-12-antibiotics-ophthalmic.pdf* [June 2015]
2. Bremond-Gignac, D., F. Chiambaretta, and S. Milazzo, *A European Perspective on Topical Ophthalmic Antibiotics: Current and Evolving Options.* Ophthalmology and Eye Diseases, 2011. **3**: p. 29-43.

Appendix B

Technical drawing of the microfluidic cell

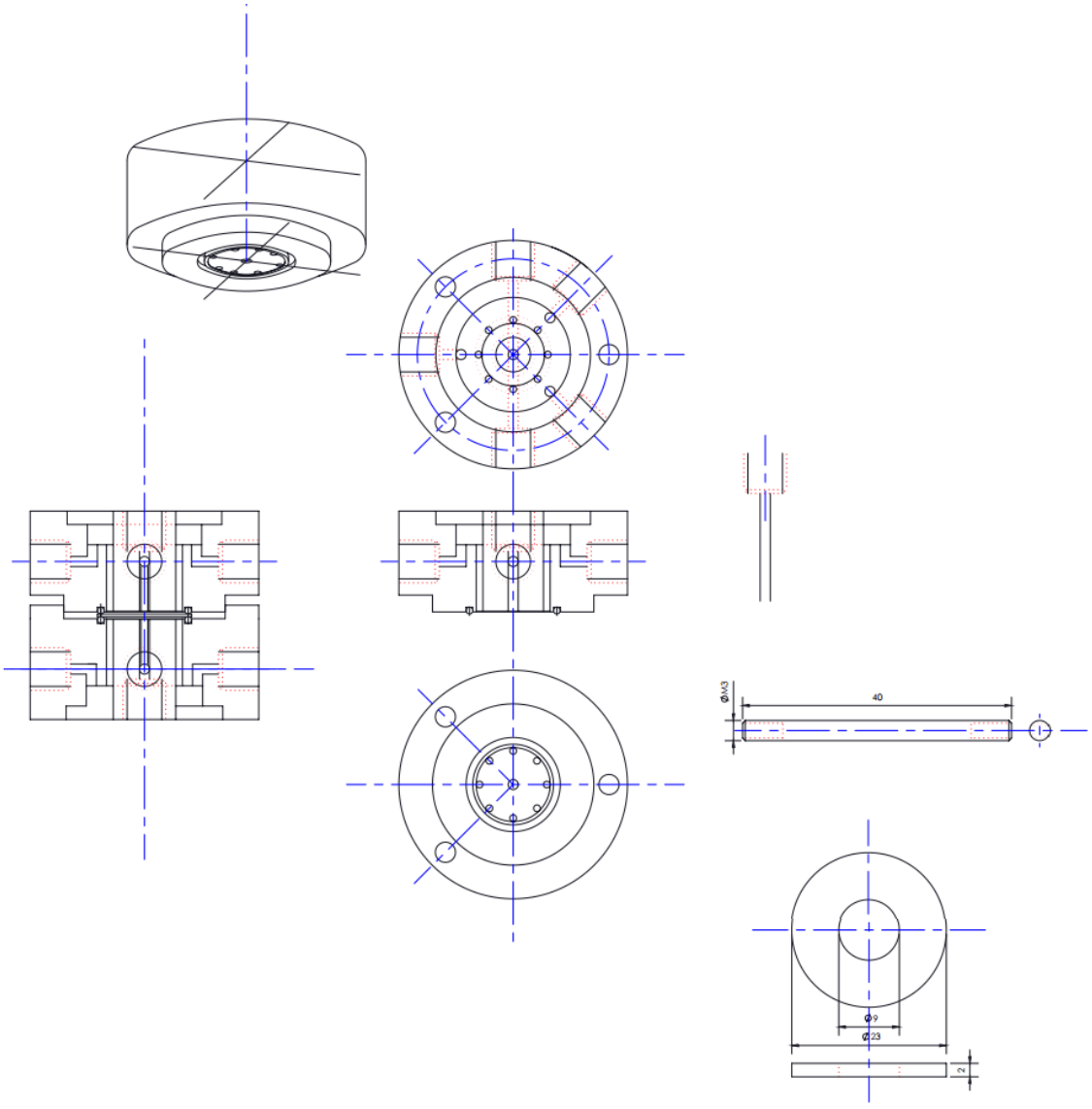

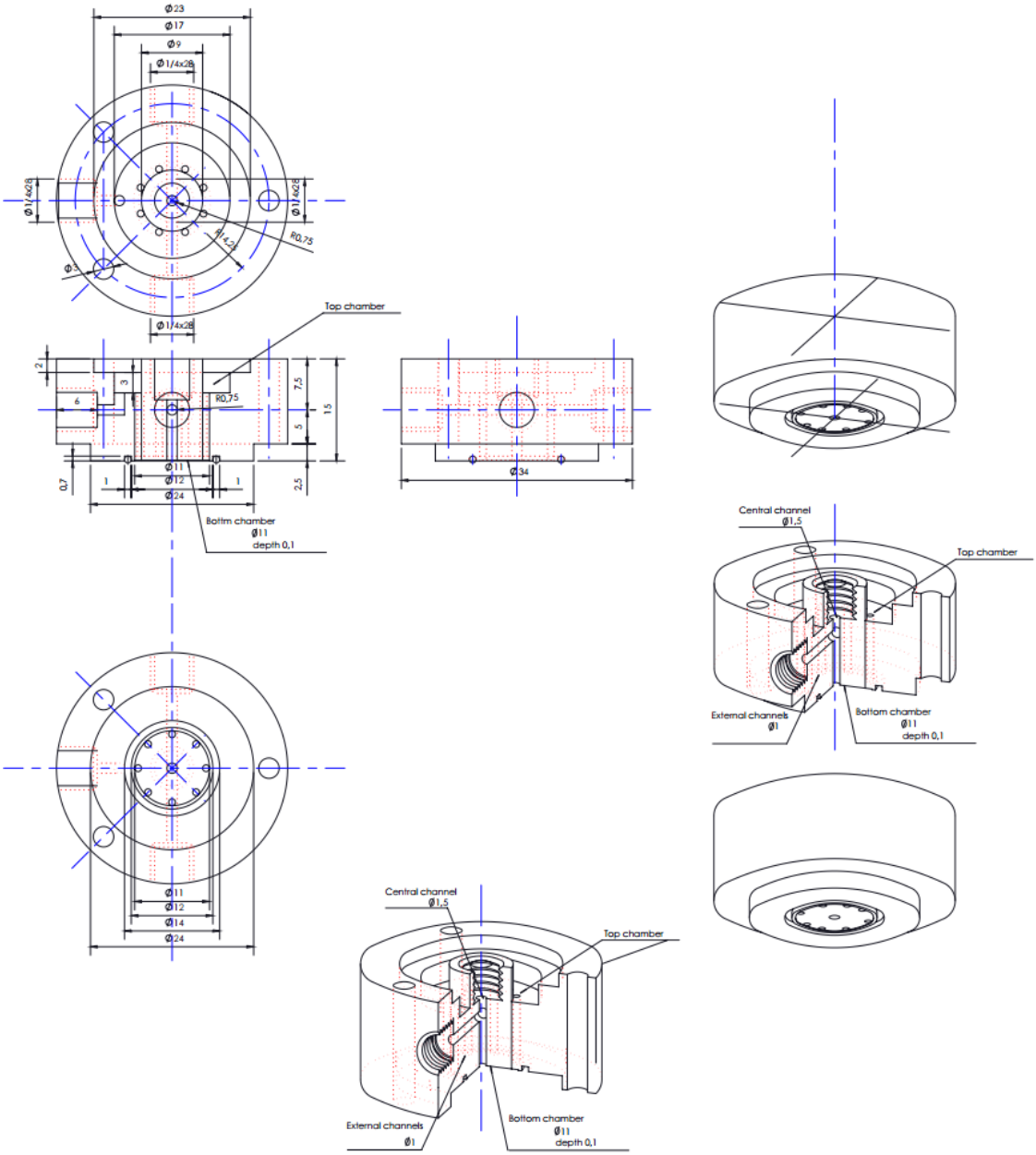
Ø23
Ø17
Ø9
Ø1/4x28
Ø1/4x28
Ø1/4x28
R0,75
Top chamber
Ø1/4x28
R0,75
Ø11
Ø12
Ø24
Bottm chamber
Ø11
depth 0,1
Ø34
Central channel
Ø1,5
Top chamber
External channels
Ø1
Bottom chamber
Ø11
depth 0,1
Ø11
Ø12
Ø14
Ø24
Central channel
Ø1,5
Top chamber
External channels
Ø1
Bottom chamber
Ø11
depth 0,1

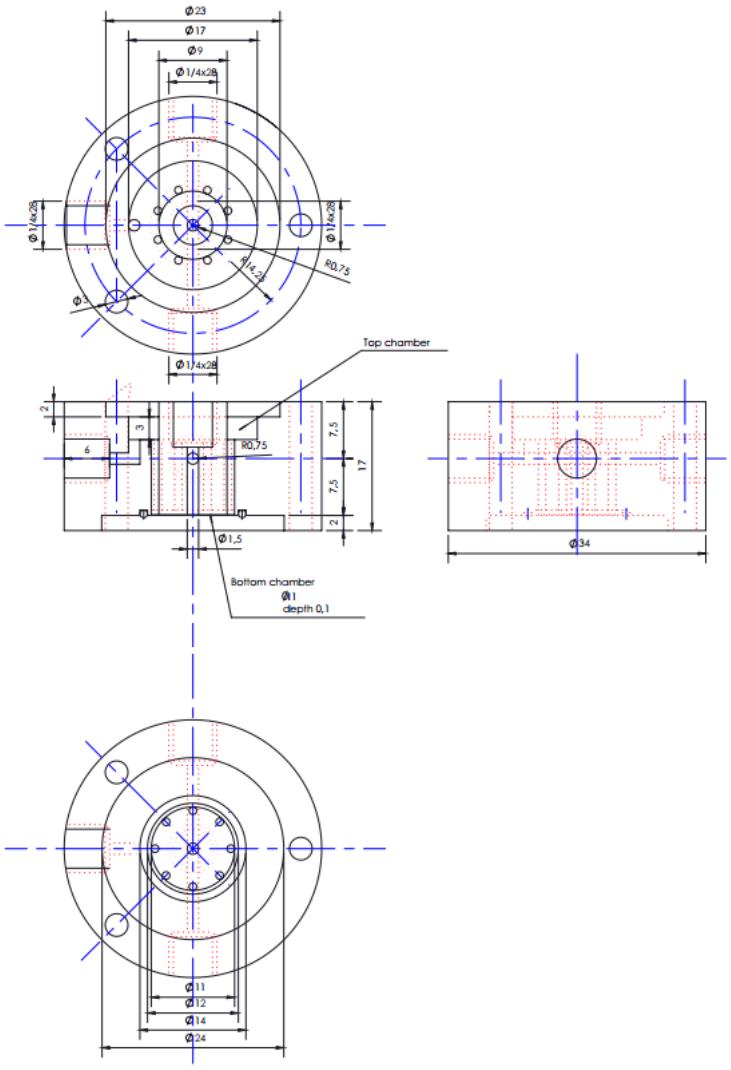
Ø23
Ø17
Ø9
Ø1/4x28
Ø1/4x28
Ø1/4x28
R0,75
Ø3
Ø1/4x28
Top chamber
2
3
6
R0,75
7,5
7,5
17
2
Ø1,5
Bottom chamber
Ø1
depth 0,1
Ø34
Ø11
Ø12
Ø14
Ø24